



Universiteit
Leiden
The Netherlands

Shear stress regulated signaling in renal epithelial cells and polycystic kidney disease

Kunnen, S.J.

Citation

Kunnen, S. J. (2018, September 27). *Shear stress regulated signaling in renal epithelial cells and polycystic kidney disease*. Retrieved from <https://hdl.handle.net/1887/66002>

Version: Not Applicable (or Unknown)

License: [Licence agreement concerning inclusion of doctoral thesis in the Institutional Repository of the University of Leiden](#)

Downloaded from: <https://hdl.handle.net/1887/66002>

Note: To cite this publication please use the final published version (if applicable).

Cover Page



Universiteit Leiden



The handle <http://hdl.handle.net/1887/66002> holds various files of this Leiden University dissertation.

Author: Kunnen, S.J.

Title: Shear stress regulated signaling in renal epithelial cells and polycystic kidney disease

Issue Date: 2018-09-27

**SHEAR STRESS REGULATED SIGNALING
IN RENAL EPITHELIAL CELLS
AND POLYCYSTIC KIDNEY DISEASE**

Steven Jeffrey Kunnen

Shear stress regulated signaling in renal epithelial cells and polycystic kidney disease

Steven Jeffrey Kunnen
Leiden University Medical Center, The Netherlands

ISBN: 978-94-9301-439-8

Layout & cover design: Steven Kunnen
Printing: Gildeprint www.gildeprint.nl

© 2018, Steven Kunnen. Copyright of the published material in chapters 2-5 lies with the publisher of the journal listed at the beginning of each chapter.

All rights reserved. No part of this thesis may be reprinted, reproduced or utilized in any form by electronic, mechanical, or other means now known or hereafter invented, including photocopying and recording in any information storage or retrieval system without prior written permission of the author.

SHEAR STRESS REGULATED SIGNALING IN RENAL EPITHELIAL CELLS AND POLYCYSTIC KIDNEY DISEASE

PROEFSCHRIFT

ter verkrijging van de graad van Doctor aan de Universiteit Leiden,
op gezag van Rector Magnificus prof.mr. C.J.J.M. Stolker,
volgens besluit van het College voor Promoties
te verdedigen op donderdag 27 september 2018
klokke 12:30 uur

door

Steven Jeffrey Kunnen

geboren te Rotterdam, Nederland
in 1984

Promotor:

Prof. dr. D.J.M. Peters

Leden promotiecommissie:

Prof. dr. P. ten Dijke

Prof. dr. R.J.M. Bindels

Prof. dr. R. Roepman

Dr. A.D. Bakker

Radboud UMC, Nijmegen

Radboud UMC, Nijmegen

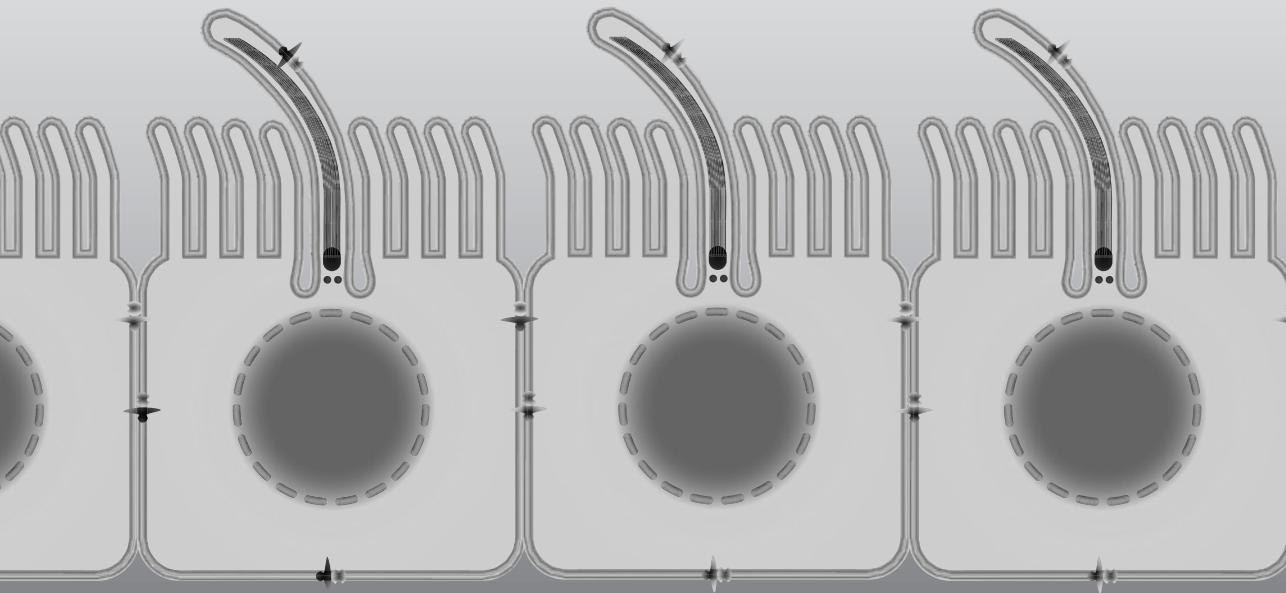
ACTA, Amsterdam

TABLE OF CONTENTS

CHAPTER 1	Introduction	7
	Shear stress and mechanotransduction	8
	Mechano-sensing complexes in the kidney	9
	Shear stress regulated signaling in the kidney	13
	Renal diseases associated to shear stress	17
	Aim and outline of this thesis	20
CHAPTER 2	Fluid shear stress-induced TGF-β/ALK5 signaling in renal epithelial cells is modulated by MEK1/2	31
CHAPTER 3	Comprehensive transcriptome analysis of fluid shear stress altered gene expression in renal epithelial cells	67
CHAPTER 4	Comparative transcriptomics of shear stress treated <i>Pkd1</i>^{-/-} cells and pre-cystic kidneys reveals pathways involved in early Polycystic Kidney Disease	97
CHAPTER 5	Inhibition of Activin signaling slows progression of Polycystic Kidney Disease in mice	133
CHAPTER 6	Summarizing discussion	163
APPENDIX	Appendices	177
	List of abbreviations	178
	Nederlandse samenvatting	180
	Curriculum vitae	184
	List of publications	185
	Dankwoord	186

CHAPTER 1

Introduction



SHEAR STRESS AND MECHANOTRANSDUCTION

Mechanotransduction is the cellular biochemical response to mechanical or physical forces, like pressure, fluid shear stress, drag force/torque, mechanical load and circumferential stretch¹. Not only is this mechanism important for hearing, touch experience and balance in animals, but cellular mechanotransduction plays a crucial role in embryonic and tissue development, as well as cell viability, cellular function and maintenance of organs²⁻⁶. A wide variety of cells types are exposed to different mechanical forces, which are detected by specialized mechano-sensors, thereby regulating the cellular response. The most well-known mechanical force is fluid shear stress on endothelial cells by blood flow^{7,8}. The first publications of mechanical shear stress responses in endothelial cells were from the early 1980s and fluid flow exposure studies in osteoblasts followed roughly 10 years later^{9,10}. Research on fluid flow in regulating ion, nutrients and water reabsorption in kidney epithelial cells was initially started in the 1960s using microperfusion techniques on renal proximal tubules¹¹⁻¹⁶. However, it took until the beginning of this century before mechanotransduction in renal epithelial cells was receiving more attention. These studies show intracellular Ca²⁺ increase and morphology changes in renal epithelial cells upon shear exposure¹⁷⁻¹⁹.

Several organs are subject to variations in fluid flow rate in response to physiological stimuli, which could be detected by mechano-sensing proteins or complexes. In kidneys, renal epithelial cells are exposed to mechanical forces due to fluid flow within the lumen of the nephron tubules (Figure 1). Urinary volume, diet and diuretics will expose the renal epithelial cells to variations in hydrodynamic forces including fluid shear stress, circumferential stretch, and drag force²⁰. Several papers describe a relatively steady flow velocity and shear stress in renal epithelial cells in a physiological range between 0.05 - 1 dyn/cm², where proximal tubular epithelial cells (PTECs) experience the highest range of shear stress^{18,21-24}. This is far lower than the shear stress experienced by endothelial cells caused by blood flow². In addition, strong oscillatory flow conditions, which are seen in the vasculature, are not expected in nephrons, because the oscillations caused by the heartbeat are almost diminished in capillaries, like the glomerulus. Furthermore, renal auto-regulation and in particular tubuloglomerular feedback (TGF) are mechanisms to regulate renal blood flow and glomerular filtration rate (GFR) during changes in renal blood pressure, thereby keeping GFR stable and oscillations small^{25,26}. Nevertheless, it is well known that high blood pressure or diabetes can cause renal hyperfiltration, resulting in a higher GFR, thereby increasing the shear stress in nephron segments. In addition, strong variations in hydrodynamic forces and shear stress are common in various kidney diseases due to tubular dilation, inflammation and obstruction, resulting in hyperfiltration in functional nephrons to compensate for lost glomeruli and tubules²⁷. Depending on the cell type and the magnitude of the hydrodynamic forces, different responses will be activated and mutations in critical components may cause or accelerate kidney diseases²⁸.

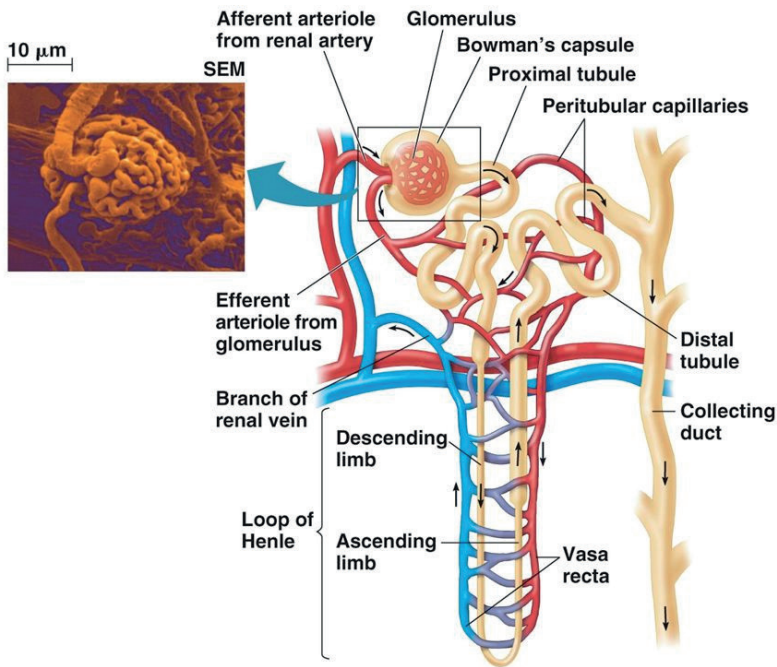


Figure 1. Structure of the nephron.

Blood enters the glomerulus from the afferent arteriole. A scanning electron microscope picture shows the glomerular structure at the top left. In the glomerulus, water, salt, nutrients and waste is filtered from the blood and is collected in the Bowman's capsule. From there the filtrate flows through the renal tubules, starting at the proximal tubule, where water, nutrient and salt molecules are reabsorbed and secreted to the efferent arterioles. Additional waste substances are excreted in the filtrate, including urea, creatinine, uric acid, potassium and hydrogen. The loop of Henle has the function to create a concentration gradient in the kidney medulla to reabsorb water from the filtrate and concentrate the filtrate. In the collecting duct the filtrate of several nephrons is collected. Image from Campbell *et al.*²⁹

MECHANO-SENSING COMPLEXES IN THE KIDNEY

Fundamental in flow-sensing are a variety of proteins, called mechano-sensors, which are located throughout the cell membrane, primary cilium/ciliary base and the cytoskeleton. These include ion channels, G-protein coupled receptors (GPCRs), adherens junction proteins, focal adhesion proteins, components of the actin cytoskeleton, but also the glycocalyx and lipid rafts can act as mechano-sensing complexes to shear stress³⁰⁻³². Activation of aforementioned sensors upon shear stress leads to alteration of cellular signaling. In the kidney, the primary cilium is the most extensively studied structure involved in flow-sensing, but it is likely that microvilli and the glycocalyx are involved as well^{21,33,34}. These cellular

structures are present in proximal tubular epithelial cells (Figure 2). In contrast, collecting duct cells are devoid of microvilli and dependent on the primary cilium, glycocalyx and other flow-sensing complexes in the cell membrane or cytoskeleton^{21,35}.

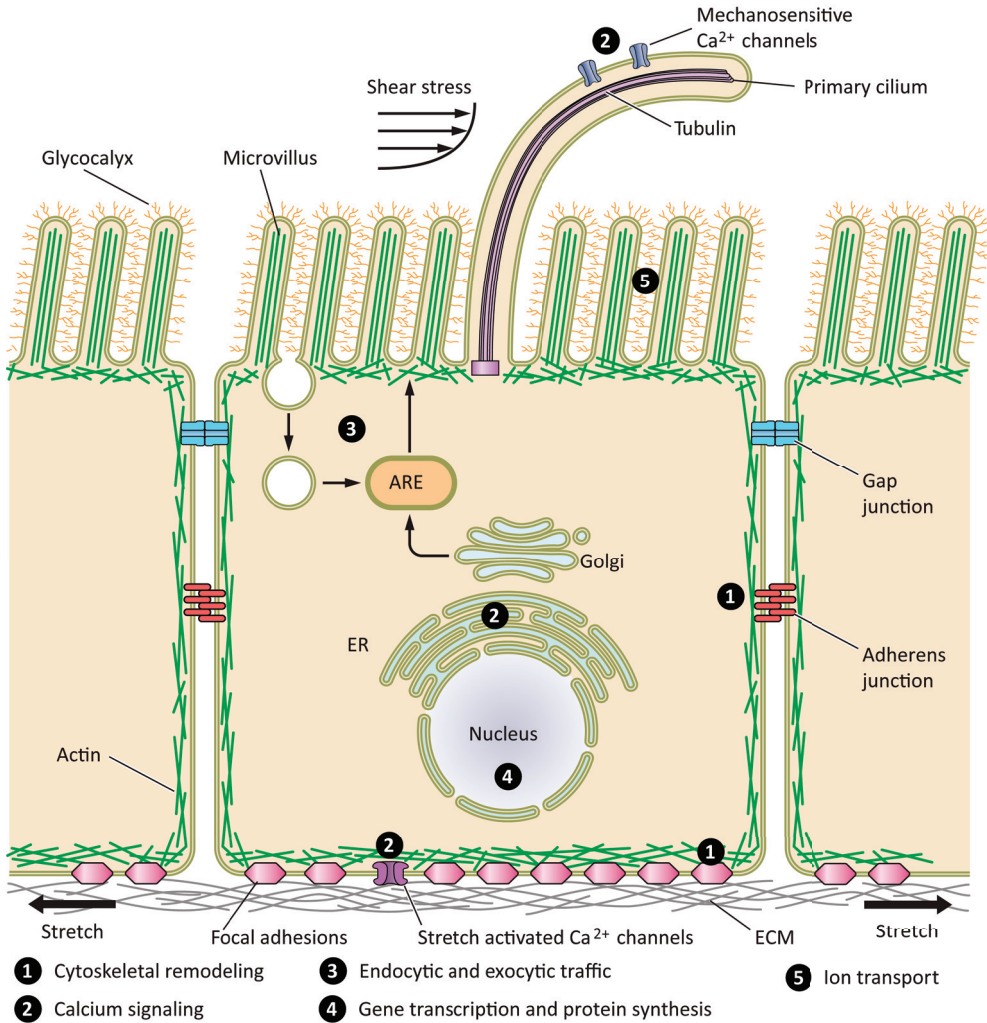


Figure 2. Mechano-sensing structures of a proximal tubular epithelial cell (PTEC).

There are 3 main structures involved in shear stress mediated mechanotransduction in PTECs: primary cilia, microvilli and the glycocalyx. Bending of cilia or microvilli by shear stress may activate mechano-sensing proteins, thereby modifying several cellular processes, including activation of Ca^{2+} and other ion transporters, cytoskeletal remodeling, endocytosis, and gene transcription. The glycocalyx may increase the frictional force of the fluid to amplify the bending of microvilli. Mechanical stretch can cause stimulation of stretch activated calcium channels and cytoskeletal reorganization, resulting in modulation of gene and protein expression. Image from Raghavan *et al.*³⁴

Primary cilia

The primary cilium is a hair-like structure that protrudes from the cell membrane of almost every cell in the body⁶. It is reabsorbed during cell division and re-assembled when the cell exits mitosis. Immotile primary cilia can act as chemical sensor or bend under fluid flow, which mediates a cellular response and are therefore called sensory cilia. In contrast, motile cilia contain motor proteins to generate cilia movement and thereby creating a fluid current, which is crucial during embryonic development for left-right asymmetry³⁶. The central axoneme of primary cilia is assembled from 9 + 0 microtubule doublets by anterograde intraflagellar transport (Figure 3). Motile cilia have a 9 + 2 axoneme, with an extra central pair of microtubules³⁷. Several proteins are involved in ciliary trafficking, including dynein, kinesin, Bardet-Biedl syndrome (BBS) proteins and intraflagellar transport (IFT) proteins. Mutations in any of the proteins can impair cilia formation and function. This can have profound effects on the development of body pattern and the physiology of multiple organ systems, which is the cause of a wide variety of human diseases, called ciliopathies^{5,38,39}.

The primary cilium plays an essential role as mechano-sensing complex upon fluid shear, which regulates cellular signaling and homeostasis. Fluid shear regulated signaling by cilia will be discussed in more detail in later paragraphs. In addition, primary cilia act as a signaling platform for growth factor signaling. Ligands in the lumen of nephron tubules can bind to their receptors, inducing cellular responses through downstream signaling pathways, for instance affecting the Wnt, hedgehog (Hh), epidermal growth factor receptor (EGFR) and transforming growth factor β (TGF- β) pathways^{37,38}. Although not exclusively, receptors involved in these pathways have been identified in the cilium of several cell types, including renal epithelial cells, suggesting that different signaling cascades are being regulated by this organelle^{37,38,40-42}. For example, TGF- β signaling is mediated via clathrin-dependent endocytosis at the ciliary pocket⁴². The ciliary pocket is membrane domain found at the base of primary cilia that may act as platform involved in vesicle trafficking and signal transduction⁴³. The aforementioned data indicate that primary cilia are essential signaling platforms that can sense and organize different environmental cues, and transmit the signals to the cell interior. Gene expression, protein activation and overall cellular physiology will be an integration of the different signals, triggered by fluid shear stress and by growth factor stimulation.

Microvilli

Proximal tubular epithelial cells have numerous (up to a few thousand) microvilli at the apical surface of the cell. Microvilli are actin filament-based protrusions of the cell membrane that increase the cell surface area and frictional force of fluid, thereby functioning in absorption, secretion, cell adhesion and mechanotransduction⁴⁴. It has been suggested that brush border microvilli in PTECs are important in mechano-sensing, since drag forces on microvilli

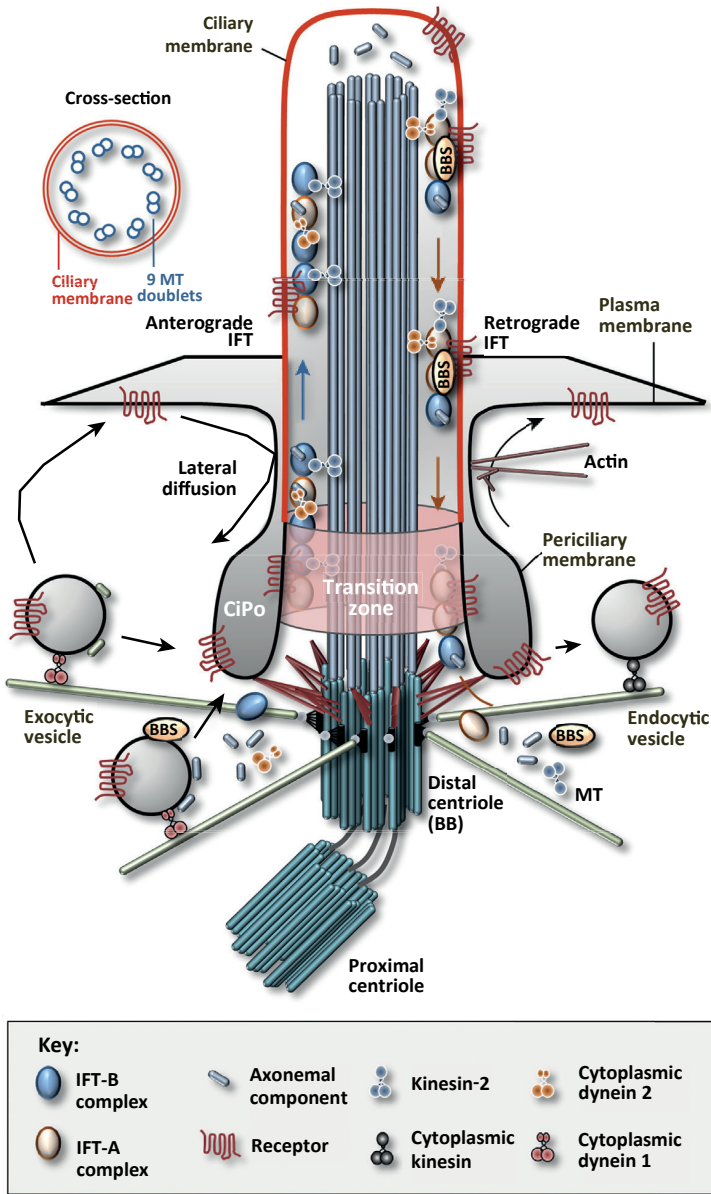


Figure 3. Primary cilium structure and assembly.

Illustration of the primary cilium structure, showing the basal body (BB), the transition zone, the ciliary pocket (CiPo) and the 9 + 0 microtubule (MT) doublets forming the axoneme. The axoneme is assembled by anterograde intraflagellar transport (IFT), executed by several IFT complexes, kinesin, and dynein. These protein complexes also play a role in transport of transmembrane receptor proteins, thereby facilitating growth factor signaling. Abbreviations: BB = basal body; BBS = the BBSome (complex of eight Bardet-Biedl syndrome proteins); CiPo = ciliary pocket; IFT = intraflagellar transport; MT = microtubules. Image from Pedersen *et al.*³⁷

are much greater than on the apical membrane of PTECs^{21,45}. Studies show that sodium transport and water reabsorption is increased upon shear stress mediated bending of microvilli in PTECs^{46,47}. There is only one known inherited disorder affecting apical microvilli assembly, called microvillus inclusion disease (MVID). It is caused by mutations in the *MYO5B* gene, which is involved in membrane trafficking of apical and basolateral proteins causing impaired microvillus assembly⁴⁸. Patients suffer from diarrhea and dehydration, likely caused by lack of water reabsorption in the intestine.

Glycocalyx

The glycocalyx is a layer of glycoproteins, glycolipids and proteoglycans at the surface of the cell and on the outside of microvilli in PTECs. It is involved in binding substances needed for uptake or as protection against harmful substances. In the kidney, the glycocalyx can act as barrier during glomerular filtration, preventing large proteins, like albumin, to pass the glomerular barrier⁴⁹. In several vascular diseases, including atherosclerosis, the glycocalyx is degraded by digesting enzymes, as well as in patients with diabetes and kidney diseases^{49,50}. The glycocalyx is known to play a fundamental role in mechanotransduction in endothelial cells due to its characteristic to increase the frictional force of fluid^{51,52}. The glycocalyx is connected to the actin cytoskeleton inside the vascular endothelial cell. It bends upon blood flow exposure and transduces this force to the cytoskeleton to activate mechano-sensors and control endothelial cell function³⁴. Shear induced nitric oxide (NO) production is dependent on heparin sulfate or hyaluronan groups in the endothelial glycocalyx⁵³. However, it has barely been studied in renal epithelial cells as shear stress sensor. One study indicates that treatment of PTECs with the glycocalyx-digesting enzyme heparinase III did not modulate shear stress induced formation of adherens and tight-junction, while microvilli disruption did⁵⁴. Nevertheless, it is likely that the glycocalyx can amplify the frictional force on the cell membrane of renal epithelial cells, as well as the bending moment of microvilli in PTECs, which may be important for other shear stress responses in the kidney.

SHEAR STRESS REGULATED SIGNALING IN THE KIDNEY

Renal epithelial cells are constantly exposed to fluid shear, which is needed to maintain cellular function and homeostasis. One of the main functions of renal epithelial cells is regulation of ion, nutrient and water reabsorption, which is regulated by fluid shear^{11-16,46,47}. Although there are fluctuations in glomerular filtration rate and shear stress, proximal tubular epithelial cells are still capable to reabsorb 65-80% of water, ions and nutrients from the nephron lumen, which is needed to maintain the glomerulotubular balance⁵⁵. The role of mechano-sensation in this process was demonstrated in a study showing increased Na⁺ and HCO₃⁻ reabsorption by shear stress in proximal tubular epithelial cells⁵⁶. In addition, several

other signaling pathways and processes are modulated by shear stress in renal epithelial cells, including mTOR, STAT6/p100, Wnt, MAPK and TGF- β signaling, as well as endocytosis, cytoskeletal reorganization and Ca²⁺ influx^{17,23,24,54,57-70}.

Calcium and cAMP signaling

One of the first responses of renal epithelial cells to the onset of fluid flow is increased intracellular Ca²⁺ levels, which modulates several signaling cascades, including cyclic AMP (cAMP) signaling^{17,66,71}. In addition, literature suggests that the ciliary polycystin1-2 complex, which is mutated in polycystic kidney disease (PKD), mediates fluid flow induced Ca²⁺ influx in kidney cells, followed by release of ryanodine receptors sensitive Ca²⁺ stores and subsequent cytosolic Ca²⁺ increase⁶⁷. In models for PKD, inactivation of the polycystin complex causes lower intracellular Ca²⁺ levels, resulting in increased cAMP signaling, which induces MAPK/ERK mediated cell proliferation and trans-epithelial fluid secretion⁷¹⁻⁷³. More recent studies showed that ciliary Ca²⁺ influx is regulated by homologous polycystin-like complexes (*Pkd1l2* and *Pkd2l1*), whereas the polycystin1-2 complex was not directly involved^{68,69}. However, the same researchers showed that fluid flow induced Ca²⁺ influx originates from the cell body after 10-20 sec of flow stimulation, which initiates a Ca²⁺ wave in the cytoplasm and propagates later into the primary cilium⁷⁰. They concluded that ciliary Ca²⁺ influx was not directly mediated by mechano-sensation of cilia. Another group showed that trans-epithelial Ca²⁺ transport is increased by fluid shear in ciliated distal convoluted and connecting tubule cells via the apical TRPV5 channel⁷⁴. They suggest that is fluid shear induced Ca²⁺ transport is mediated via increased TRPV5 and NCX1 channel expression, which is decreased upon cilia removal. However, other mechano-sensing complexes may be involved that are independent of primary cilia, since Ca²⁺ transport was lower but still present after cilia ablation. Despite numerous hypotheses about fluid shear mediated Ca²⁺ signaling and the relevance for development and disease, the mechanism how fluid shear stress regulates Ca²⁺ signaling is not entirely clear and still under debate, whereas the direct involvement of cilia and the polycystins is being criticized^{33,68-70,75,76}.

mTOR signaling

Renal epithelial cell-size is regulated by mTOR (Mechanistic Target Of Rapamycin) signaling, which is altered by primary cilia dependent shear stress sensing^{77,78}. Several upstream signals and cellular stress factors can alter mTOR signaling, including growth factors, hypoxia, osmotic stress, energy and nutrient deprivation⁷⁹. The mTOR complexes can modify several processes involved in transcription, translation, autophagy and cell volume control. mTOR signaling is also inhibited by fluid shear via LKB1-mediated AMPK activation^{59,60,77}. These signal transducers can activate autophagy and thereby control the epithelial cell volume⁸⁰. Defects in ciliogenesis decrease autophagy, showing the importance of cilia in the regulation of cell size⁷⁸. Folliculin is suggested to be required for LKB1 mediated AMPK activation,

although it still remains unclear how fluid shear bending of the cilium activates Folliculin or downstream LKB1 and AMPK⁶⁰.

TGF- β signaling

The Transforming Growth Factor- β (TGF- β) superfamily proteins are multifunctional cytokines, including TGF- β 's, activins and bone morphogenetic proteins (BMPs). TGF- β signaling modulates cell proliferation, differentiation, apoptosis, cell migration, cell adhesion and is believed to play a crucial role in fibrotic deposition⁸¹, which is a hallmark of several diseases, like polycystic kidney disease⁸². TGF- β , as well as Activin and Nodal, binds to a pair of serine/threonine kinase transmembrane receptors, that mediate the phosphorylation of SMAD2 and 3 (Figure 4). These activated SMAD proteins, p-SMAD2 and 3, form a complex with SMAD4 and can enter the nucleus. Activity of SMAD transcription factors can be modulated by several co-factors, like yes-associated protein (YAP), to regulate the transcription of various genes, including plasminogen activator inhibitor type 1 (*Pai1* or *Serpine1*), fibronectin (*Fn1*), collagen type 1 alpha 1 (*Col1a1*)^{83,84}. Canonical (SMAD2/3) TGF- β signaling can interact with the non-canonical (MAPK/ERK) TGF- β pathways at different levels⁸⁵. A direct link between TGF- β and MAPK/ERK signaling is the phosphorylation of ShcA by the activated TGF- β receptor complex⁸⁶. ShcA competes with SMAD2/3 for binding to the TGF- β receptor, and stabilizes the TGF- β receptor complexes in caveolae, where it activates MAPK/ERK signaling⁸⁷. Consequently, reduced ShcA expression results in increased levels of TGF- β receptor complexes in clathrin-coated pits, leading to enhanced SMAD2/3 activation. In addition, activated ERK1/2 can phosphorylate regulatory SMADs (R-SMAD) as well SMAD2/3 linker region, which modulate transcriptional activity of the SMAD complex^{88,89} (Figure 4).

TGF- β signaling is involved in epithelial-to-mesenchymal transition (EMT), which is important during development and tissue repair, but it contributes to fibrosis and metastasis of several cancers⁹⁰. Because of the multiple interactions between TGF- β signaling, MAPK/ERK and other cascades, the integration of these pathways is complex and biological context dependent.

In embryonic endothelial cells, shear stress mediated TGF- β /ALK5 signaling induced endothelial-to-mesenchymal transition, depending on the strength of shear and presence or absence of a cilia^{91,92}. Similarly, in renal epithelial cells fluid shear stress dynamically regulated TGF- β gene expression and SMAD3 activation, depending on the magnitude of fluid shear, *i.e.* physiological versus pathological, and depending on ERK activation and NOTCH4 expression^{23,24,47}. Moreover, several studies demonstrated that hypertension and pathological shear can induce TGF- β signaling and fibrosis, which is observed in a broad range of diseases, including renal diseases⁹³⁻⁹⁸.

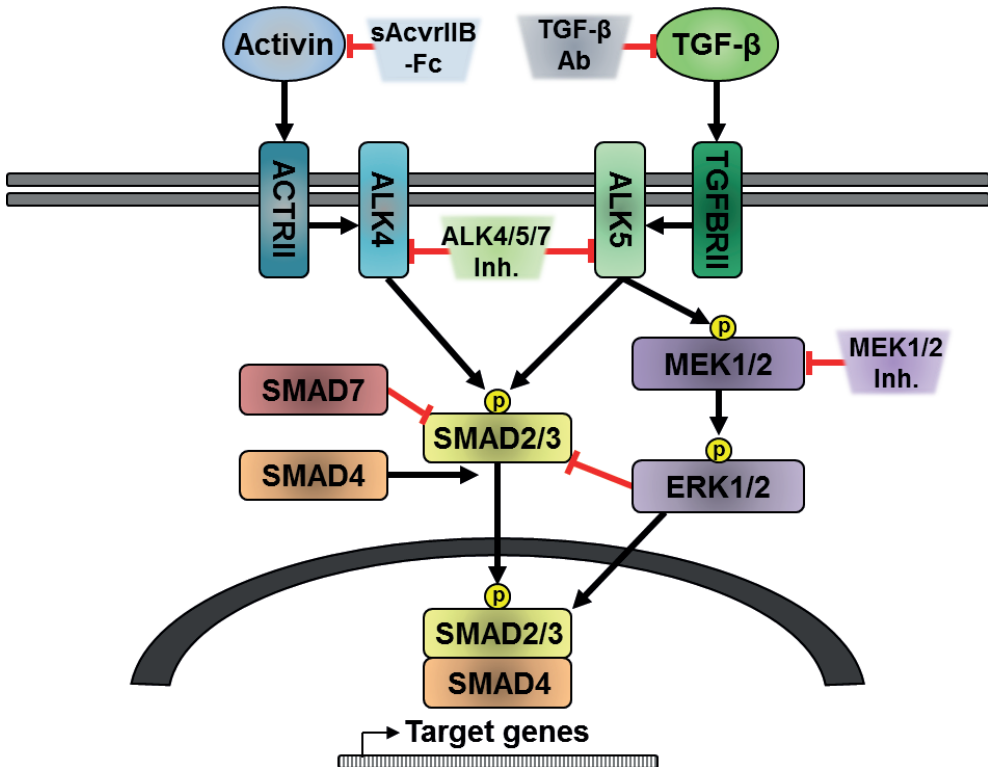


Figure 4. Representation of the TGF- β signaling pathway.

Activin or TGF- β ligands bind to their respective receptors, thereby recruiting and activating co-receptors, ALK4 (ACVRI) and ALK5 (TGFBR1), which can phosphorylate SMAD2/3 transcription factors. Activated SMAD2/3 proteins form a complex with SMAD4, which can enter the nucleus and thereby inducing target gene expression. The ALK5 receptor can also induce MEK1/2 and ERK1/2 phosphorylation via ShcA. Activated ERK1/2 can modulate transcriptional activity of the SMAD complex by cytoplasmic or nuclear SMAD retention. Several other proteins or compounds can modulate or inhibit TGF- β signaling (red lines).

Other shear regulated responses

Several studies report increased expression and reorganization of cytoskeletal components, cell adhesion and tight junction molecules under physiological shear stress, which is needed for differentiation and polarization of renal epithelial cells^{18,54,99,100}. In contrast, another study showed loss of renal epithelial cell morphology during high levels of pathological shear stress (5 dyn/cm²)¹⁰¹. Endocytosis was increased by fluid shear in proximal tubular epithelial cells as well^{34,64,102}. Flow-induced endocytosis is mediated via cilium dependent Ca²⁺ increase, and subsequent calmodulin mediated activation of Cdc42⁶⁵. Endocytosis is important for protein uptake and receptor internalization of several signaling pathways, indicating the importance of shear regulated endocytosis. Another cilia-dependent signaling cascade

affected by fluid flow is the canonical Wnt-signaling pathway, which is restrained by fluid-flow induced ciliary signaling in favor of non-canonical Wnt signaling⁵⁸. This suggests that fluid flow act as central switch of canonical to non-canonical Wnt signaling, which may be important for normal kidney development and homeostasis. Finally, STAT6/p100-regulated transcription is negatively regulated upon flow-induced bending of the cilium, independent from flow-induced Ca^{2+} influx⁶¹. The numerous cellular processes and signaling pathways that are modulated by shear stress in renal epithelial cells demonstrate the importance of shear stress sensing for cellular homeostasis.

RENAL DISEASES ASSOCIATED TO SHEAR STRESS

Defects in shear stress sensing and mechanotransduction have been associated with various diseases, including diseases affecting cilia formation and function, called ciliopathies^{5,38,39}. In kidneys, several physiological stimuli will expose renal epithelial cells to fluctuations in hydrodynamic forces, including fluid shear stress²⁰. Depending on the cell type and the magnitude of the hydrodynamic forces, different responses will be activated and mutations in critical components may modulate, accelerate or cause (kidney) diseases²⁸. In addition, strong variations in shear and other hydrodynamic forces are common in various kidney diseases due to tubular dilation, obstruction and hyperfiltration, which occur in functional nephrons to compensate for lost glomeruli and tubules, with diabetic nephropathy and Polycystic Kidney Disease as the most common examples²⁷. Renal shear stress is increased after unilateral nephrectomy as well^{103,104}, which accelerates cyst formation in *Ift88*^{-/-} and *Pkd1*^{-/-} mouse models^{105,106}, indicating the role of shear in a ciliopathy and autosomal dominant polycystic kidney disease (ADPKD) model. Additionally, long-term high shear exposure may contribute to fibrotic deposition and tubulointerstitial lesions, which is commonly seen in renal epithelial cells upon pathological shear exposure, after renal mass reduction or during progression of renal diseases^{19,47,107,108}.

Ciliopathies

The ciliopathies are a wide range of genetic disorders caused by mutations in genes encoding ciliary proteins, which impair cilia formation or function^{5,38,39}. Currently, there are 187 human genes associated to 35 ciliopathies, although the numbers are still rising because of the large quantity of genes involved in ciliary assembly and function¹⁰⁹. Renal cyst formation is common clinical feature occurring in many ciliopathies. Autosomal dominant and autosomal recessive PKD are ciliopathies as well, since the affected proteins, polycystins (*PKD1* and *PKD2*) and fibrocystin (*PKHD1*), localize in primary cilia¹¹⁰. Other ciliopathy phenotypes include polydactyly, hepatobiliary disease, mental retardation, retinal degeneration, skeletal abnormalities and *situs inversus*.

Nephronophthisis (NPHP) patients develop corticomedullary cysts and tubulointerstitial fibrosis, which resembles the ADPKD phenotype, but in NPHP patients the kidneys are not enlarged⁵. In many NPHP patients, renal cyst formation and loss of functional nephrons leads to end stage renal disease within the first three decades. NPHP is an autosomal recessive disorder caused by mutations in more than 20 genes, *NPHP1-20* and *NPHPL1*¹¹¹. Many of these gene mutations are classified as juvenile or adolescent NPHP, based on the age of onset, while *NPHP2* (inversin), *NPHP3*, *NPHP9* (*NEK8*) and *NPHP18* (*CEP83*), can cause infantile NPHP. The NPHP proteins interact with several cell adhesion, cytoskeletal and ciliary proteins to regulate various cellular signaling. One of the interaction partners of nephrocystin-1 (*NPHP1*) is *AHI1*, which is mutated in Joubert syndrome patients. Mutations in nineteen other cilia related genes (*BBS1-19*) have been associated with Bardet-Biedl syndrome (BBS)¹¹². The BBS proteins are located at the primary cilia, basal body and the BBSome, which is a complex of several BBS proteins. BBS proteins are involved in ciliary membrane assembly and intraflagellar transport (IFT), which is crucial for cilia formation¹¹³. Several other proteins involved in ciliary trafficking have been implicated in other ciliopathies as well, including IFT, kinesin and dynein proteins. For example, genetic mutations of *IFT80* and *DYNC2H1* are the cause of Jeune syndrome (asphyxiating thoracic dysplasia)¹¹⁴.

Oral-Facial-Digital Syndrome (OFD) is caused by mutations of the *OFD1* gene, but several other causal genes are described as well¹¹⁵. The main clinical features of OFD are oral, facial and digital abnormalities, as its name already implies. In addition, polycystic kidneys are a common phenotype, as well as malformations of the central nervous system. Meckel syndrome (MKS) is a lethal autosomal recessive disorder leading to renal or respiratory failure. *MKS1*, 3-5 are identified as causative genes and are essential for centriole movement and ciliogenesis. Mutations in *CC2D2A* can also cause Meckel syndrome (MKS6 subtype) or Joubert syndrome, depending on type and location of the mutation or genetic modifiers¹⁰⁹. This non-Mendelian type of inheritance is seen for various ciliopathy associated genes, likely caused by the multiple functions a gene/protein can have and the interactions with other proteins. The broad range of ciliopathy associated genes, as well as the disorder specific phenotypes and the overlapping clinical features between the ciliopathies, show the complexity and importance of the primary cilium function and its proposed role in mechanotransduction.

Autosomal Dominant Polycystic Kidney Disease

Autosomal dominant polycystic kidney disease (ADPKD) is a genetic disorder with a prevalence of 1:2,500 in European Union¹¹⁶. ADPKD is characterized by formation of many fluid-filled cysts and renal fibrosis, leading to deterioration or loss of renal function in adulthood^{117,118}. Around 50% of the patients will develop end stage renal disease (ESRD) at the age around 55 years, requiring hemodialysis or renal replacement therapy¹¹⁹. In addition,

extra-renal manifestations are occurring as well, including cysts in the liver and pancreas, intracranial aneurisms, hypertension and cardiovascular abnormalities¹²⁰.

Germline mutations in the Polycystic Kidney Disease-1 (*PKD1*) gene are the cause of ADPKD in around 85% of the patients, while 15% of the patients carry a mutation in the *PKD2* gene^{121,122}. The *PKD1* gene is located on chromosome 16 and has 46 exons, while there are several alternative splice variants described, including pathogenic splice variants¹²³. *PKD2* is found on chromosome 4 and spans 15 exons. *PKD1* and *PKD2* genes encode polycystin-1 (PC-1) and polycystin-2 (PC-2). Somatic mutations in the unaffected allele of *PKD1* or *PKD2* can initiate cyst formation, called “second hit”, but haploinsufficiency or stochastic fluctuations in gene expression can also lower PC-1 or PC-2 below critical levels¹²⁴⁻¹²⁸. Overall the probability of cyst formation is determined by functional polycystin protein levels and the biologic context¹²⁹. For example, a number of studies indicate that renal injury can accelerate cyst progression and fibrosis¹³⁰⁻¹³³. In addition, the presence of existing cysts can trigger the formation of new cysts in the surrounding tissue^{106,129}.

Polycystin-1 is a large 450 kDa receptor-like trans-membrane protein consisting of 4303 amino acids, while polycystin-2 is much smaller with only 968 amino acids weighing 110 kDa^{128,134}. PC-1 consists of a small intracellular C-terminal tail, eleven trans-membrane domains and a large extracellular N-terminal domain. PC-2 has six trans-membrane domains and a C-terminal calcium binding motif¹³⁵. The PC-1 and PC-2 proteins interact via the C-terminal tails and co-localize throughout the cell membrane of renal epithelial cells, at cell-cell contacts, extracellular matrix (ECM) and primary cilia. PC-2 functions as a non-selective cation channel transporting Ca^{2+} in a complex with PC-1^{67,136,137}. At the plasma membrane and in cilia, polycystins interact with diverse (mechanosensory) ion channels, signal transducers as well as cell-cell and cell-extracellular matrix junctional proteins^{21,56,71,107,138,139}. Therefore, the polycystins are thought to play a role in differentiation and maintenance of the cell structure, mechanical force transmission and mechanotransduction^{28,67,140}. Lack of the polycystin complex in primary cilia impairs epithelial differentiation and may play a role in cyst formation^{141,142}. Moreover, mutations or deletions of other ciliary proteins can cause renal cyst formation in mouse models and patients, indicating the role of cilia during cystogenesis^{39,143-146}. However, the cellular mechanism of cyst formations, caused by loss of functional PC-1 or 2 protein levels and the involvement of cilia and shear stress is still not completely understood.

What is known is that numerous signaling pathways are implicated in polycystic kidney disease, including mTOR, TGF- β , Wnt, Hippo, STAT, MAPK, PI3K-AKT, Hedgehog and cAMP signaling^{131,147-174}. Remarkable is that several of these signaling pathways are being modulated by fluid shear as well, suggesting that implicated shear regulated signaling

may contribute to PKD. Increased mTOR signaling is suggested to be involved cell growth and proliferation, thereby accelerating cyst growth^{147,148}. Activation of TGF- β signaling has been shown in several animal models for polycystic kidney disease and patient-derived tissues and is known to be involved in fibrosis, which is commonly seen in ADPKD^{82,146,175}. A recent study reports that Wnt/Ca²⁺ signaling is mediated by the polycystin complex, while canonical Wnt seems to be inhibited by polycystin-1^{176,177}. Altered Wnt signaling is described in ADPKD models as well and is suggested to be involved in disoriented cell division, leading to cyst expansion^{131,160,178,179}. Increased cAMP levels in ADPKD can activate MAPK/ERK signaling leading to induced proliferation. Tolvaptan and Sorafenib inhibit cAMP and ERK dependent cyst progression in ADPKD models^{172,180}. Although several treatments have been tested successfully in PKD mouse models, the efficacy in human patients is sometimes minimal or absent, which was published for several mTOR inhibitors^{152,181,182}. Therefore, it has been suggested to combine therapies and target multiple signaling pathways affected in ADPKD^{174,183}. For example, the natural herb curcumin can modulate multiple signaling cascades, including mTOR, Wnt and Stat3, and was shown to inhibit cyst formation in ADPKD mice¹⁶². Initial experiments using a combination of mTOR and/or cAMP inhibitors showed promising results to inhibit proliferation in ADPKD cells and mice, but additional research is needed to evaluate the efficacy in ADPKD patients^{184,185}.

AIM AND OUTLINE OF THIS THESIS

The aim of this thesis is to study fluid shear stress regulated signaling in renal epithelial cells and the relevance for ADPKD. Since several signaling pathways are regulated by fluid shear and are implicated in ADPKD as well, we expect that impaired shear stress signaling is contributing to the ADPKD phenotype. We will compare altered cellular signaling upon physiological and pathological relevant levels of shear stress. Furthermore, we will evaluate the role of cilia in the shear response, since the polycystins localize in this organelle and renal cyst formation is a common feature in several ciliopathies. In **chapter 2-4** we analyze the cellular response of proximal tubular epithelial cells (PTECs) to fluid shear stress and the involvement of cilia and *Pkd1* expression. In **chapter 2** we focus on shear stress induced canonical TGF- β (SMAD2/3) signaling and the participation of MAPK/ERK signaling. We show that fluid shear induced activation of SMAD2/3 and epithelial-to-mesenchymal transition (EMT) processes are TGF- β /ALK5 dependent. The shear response in PTECs is modulated by *Pkd1* gene disruption and MAPK/ERK signaling. However, cilia ablation does not reduce SMAD2/3 target gene expression, suggesting that other mechano-sensing structures are involved.

In **chapter 3** we investigate shear induced alterations of the transcriptome in proximal tubular epithelial cells, using RNA-sequencing. We describe several pathways that are altered by shear stress and we validate these changes by qPCR. Many of these pathways are modulated by TGF- β /ALK5 and MAPK/ERK signaling. The role of cilia during the shear stress response is evaluated as well. We show that cilia only have a minor contribution to shear stress regulated signaling in PTECs. Finally, pathological levels of shear stress are compared to physiological controls, showing elevated shear induced expression of several genes under pathological conditions.

Shear stress dependent signaling in an *in vitro* ADPKD model was evaluated in **chapter 4** using RNA sequencing. The effect of fluid shear stress in PTECs without *Pkd1* expression was compared to *Pkd1*^{wt} controls. We show that *Pkd1* is not directly involved in shear dependent activation of many signaling pathways. In addition, differential gene expression in *Pkd1*^{-/-} PTECs during shear is compared with *in vivo* transcriptome analysis of pre-cystic kidneys in a *Pkd1*^{del} mouse model, in which fluid flow is still present. Several signaling pathways that are known to be implicated in the renal cyst formation are altered in both the *in vitro* and *in vivo* models for *Pkd1* gene disruption. So, the data suggests that these processes are already altered at pre-cystic stage and may contribute to *in vivo* cyst formation.

In **chapter 5** we investigate the role of canonical TGF- β (SMAD2/3) signaling in cyst formation. Genetic disruption of TGF- β receptor type I (*Alk5*) in kidney epithelium doesn't reduce cyst progression in a *Pkd1*^{del} mouse model. Activin is another cytokine that can phosphorylate SMAD2/3 via the Activin receptors. Activin signaling was antagonized using a soluble Activin type IIB receptor (sActRIIB-Fc). Treatment with sActRIIB-Fc markedly reduced cyst progression in three different mouse models for ADPKD, suggesting that Activins drive the progression of PKD. Finally, the results of this thesis and future plans are summarized and discussed in **chapter 6**.

REFERENCES

1. Paluch E.K. *et al.* Mechanotransduction: use the force(s). *BMC. Biol.* **13**, 47 (2015).
2. Freund J.B., Goetz J.G., Hill K.L., & Vermot J. Fluid flows and forces in development: functions, features and biophysical principles. *Development* **139**, 1229-1245 (2012).
3. Wozniak M.A. & Chen C.S. Mechanotransduction in development: a growing role for contractility. *Nat. Rev. Mol. Cell Biol.* **10**, 34-43 (2009).
4. Kolahi K.S. & Mofrad M.R. Mechanotransduction: a major regulator of homeostasis and development. *Wiley. Interdiscip. Rev. Syst. Biol. Med.* **2**, 625-639 (2010).
5. Quinlan R.J., Tobin J.L., & Beales P.L. Modeling ciliopathies: Primary cilia in development and disease. *Curr. Top. Dev. Biol.* **84**, 249-310 (2008).
6. Goetz S.C. & Anderson K.V. The primary cilium: a signalling centre during vertebrate development. *Nat. Rev. Genet.* **11**, 331-344 (2010).
7. Tarbell J.M., Weinbaum S., & Kamm R.D. Cellular fluid mechanics and mechanotransduction. *Ann. Biomed. Eng* **33**, 1719-1723 (2005).
8. Chien S. Mechanotransduction and endothelial cell homeostasis: the wisdom of the cell. *Am. J. Physiol Heart Circ. Physiol* **292**, H1209-H1224 (2007).
9. Dewey C.F., Jr., Bussolari S.R., Gimbrone M.A., Jr., & Davies P.F. The dynamic response of vascular endothelial cells to fluid shear stress. *J. Biomech. Eng* **103**, 177-185 (1981).
10. Reich K.M., Gay C.V., & Frangos J.A. Fluid shear stress as a mediator of osteoblast cyclic adenosine monophosphate production. *J. Cell Physiol* **143**, 100-104 (1990).
11. Frick A., Rumrich G., Ullrich K.J., & Lassiter W.E. Microperfusion study of calcium transport in the proximal tubule of the rat kidney. *Pflugers Arch. Gesamte Physiol Menschen. Tiere.* **286**, 109-117 (1965).
12. Bank N. & Aynedjian H.S. A microperfusion study of bicarbonate accumulation in the proximal tubule of the rat kidney. *J. Clin. Invest* **46**, 95-102 (1967).
13. Bank N., Yarger W.E., & Aynedjian H.S. A microperfusion study of sucrose movement across the rat proximal tubule during renal vein constriction. *J. Clin. Invest* **50**, 294-302 (1971).
14. Bank N., Aynedjian H.S., & Weinstein S.W. A microperfusion study of phosphate reabsorption by the rat proximal renal tubule. Effect of parathyroid hormone. *J. Clin. Invest* **54**, 1040-1048 (1974).
15. Lingard J.M., Gyory A.Z., & Young J.A. Microperfusion study of the kinetics of reabsorption of cycloleucine in early and late segments of the proximal convolution of the rat nephron. *Pflugers Arch.* **357**, 51-61 (1975).
16. Burg M.B. & Knepper M.A. Single tubule perfusion techniques. *Kidney Int.* **30**, 166-170 (1986).
17. Praetorius H.A. & Spring K.R. Bending the MDCK cell primary cilium increases intracellular calcium. *J. Membr. Biol.* **184**, 71-79 (2001).
18. Essig M., Terzi F., Burtin M., & Friedlander G. Mechanical strains induced by tubular flow affect the phenotype of proximal tubular cells. *Am. J. Physiol Renal Physiol* **281**, F751-F762 (2001).
19. Essig M. & Friedlander G. Tubular shear stress and phenotype of renal proximal tubular cells. *J. Am. Soc. Nephrol.* **14**, S33-S35 (2003).
20. Carrisoza-Gaytan R., Carattino M.D., Kleyman T.R., & Satlin L.M. An unexpected journey: conceptual evolution of mechanoregulated potassium transport in the distal nephron. *Am. J. Physiol Cell Physiol* **310**, C243-C259 (2016).
21. Weinbaum S., Duan Y., Satlin L.M., Wang T., & Weinstein A.M. Mechanotransduction in the renal tubule. *Am. J. Physiol Renal Physiol* **299**, F1220-F1236 (2010).
22. Weinbaum S., Duan Y., Thi M.M., & You L. An Integrative Review of Mechanotransduction in Endothelial, Epithelial (Renal) and Dendritic Cells (Osteocytes). *Cell Mol. Bioeng.* **4**, 510-537 (2011).
23. Grabias B.M. & Konstantopoulos K. Epithelial-mesenchymal transition and fibrosis are mutually exclusive responses in shear-activated proximal tubular epithelial cells. *FASEB J.* **26**, 4131-4141 (2012).

24. Grabias B.M. & Konstantopoulos K. Notch4-dependent antagonism of canonical TGF-beta1 signaling defines unique temporal fluctuations of SMAD3 activity in sheared proximal tubular epithelial cells. *Am. J. Physiol Renal Physiol* **305**, F123-F133 (2013).
25. Carlstrom M., Wilcox C.S., & Arendshorst W.J. Renal autoregulation in health and disease. *Physiol Rev.* **95**, 405-511 (2015).
26. Holstein-Rathlou N.H. *et al.* Nephron blood flow dynamics measured by laser speckle contrast imaging. *Am. J. Physiol Renal Physiol* **300**, F319-F329 (2011).
27. Sharma A., Mucino M.J., & Ronco C. Renal functional reserve and renal recovery after acute kidney injury. *Nephron Clin. Pract.* **127**, 94-100 (2014).
28. Piperi C. & Basdra E.K. Polycystins and mechanotransduction: From physiology to disease. *World J. Exp. Med.* **5**, 200-205 (2015).
29. Campbell N.A. *et al.* Osmoregulation and Excretion. *Biology, 8th edition* (Pearson Benjamin Cummings, 2008).
30. Ingber D.E. Cellular mechanotransduction: putting all the pieces together again. *FASEB J.* **20**, 811-827 (2006).
31. Curry F.E. & Adamson R.H. Endothelial glycocalyx: permeability barrier and mechanosensor. *Ann. Biomed. Eng* **40**, 828-839 (2012).
32. Petersen E.N., Chung H.W., Nayebosadri A., & Hansen S.B. Kinetic disruption of lipid rafts is a mechanosensor for phospholipase D. *Nat. Commun.* **7**, 13873 (2016).
33. Praetorius H.A. The primary cilium as sensor of fluid flow: new building blocks to the model. A review in the theme: cell signaling: proteins, pathways and mechanisms. *Am. J. Physiol Cell Physiol* **308**, C198-C208 (2015).
34. Raghavan V. & Weisz O.A. Discerning the role of mechanosensors in regulating proximal tubule function. *Am. J. Physiol Renal Physiol* **310**, F1-F5 (2016).
35. Holthofer H. Cell type-specific glycoconjugates of collecting duct cells during maturation of the rat kidney. *Cell Tissue Res.* **253**, 305-309 (1988).
36. Basu B. & Brueckner M. Cilia multifunctional organelles at the center of vertebrate left-right asymmetry. *Curr. Top. Dev. Biol.* **85**, 151-174 (2008).
37. Pedersen L.B., Mogensen J.B., & Christensen S.T. Endocytic Control of Cellular Signaling at the Primary Cilium. *Trends Biochem. Sci.* **41**, 784-797 (2016).
38. Bisgrove B.W. & Yost H.J. The roles of cilia in developmental disorders and disease. *Development* **133**, 4131-4143 (2006).
39. Arts H.H. & Knoers N.V. Current insights into renal ciliopathies: what can genetics teach us? *Pediatr. Nephrol.* **28**, 863-874 (2013).
40. Gill P.S. & Rosenblum N.D. Control of murine kidney development by sonic hedgehog and its GLI effectors. *Cell Cycle* **5**, 1426-1430 (2006).
41. Ma R. *et al.* PKD2 functions as an epidermal growth factor-activated plasma membrane channel. *Mol. Cell Biol.* **25**, 8285-8298 (2005).
42. Clement C.A. *et al.* TGF-beta signaling is associated with endocytosis at the pocket region of the primary cilium. *Cell Rep.* **3**, 1806-1814 (2013).
43. Benmerah A. The ciliary pocket. *Curr. Opin. Cell Biol.* **25**, 78-84 (2013).
44. Sauvanet C., Wayt J., Pelaseyed T., & Bretscher A. Structure, regulation, and functional diversity of microvilli on the apical domain of epithelial cells. *Annu. Rev. Cell Dev. Biol.* **31**, 593-621 (2015).
45. Guo P., Weinstein A.M., & Weinbaum S. A hydrodynamic mechanosensory hypothesis for brush border microvilli. *Am. J. Physiol Renal Physiol* **279**, F698-F712 (2000).
46. Du Z. *et al.* Axial flow modulates proximal tubule NHE3 and H-ATPase activities by changing microvillus bending moments. *Am. J. Physiol Renal Physiol* **290**, F289-F296 (2006).
47. Grabias B.M. & Konstantopoulos K. The physical basis of renal fibrosis: effects of altered hydrodynamic

- forces on kidney homeostasis. *Am. J. Physiol Renal Physiol* **306**, F473-F485 (2014).
48. Muller T. *et al.* MYO5B mutations cause microvillus inclusion disease and disrupt epithelial cell polarity. *Nat. Genet.* **40**, 1163-1165 (2008).
 49. Dane M.J. *et al.* A microscopic view on the renal endothelial glycocalyx. *Am. J. Physiol Renal Physiol* **308**, F956-F966 (2015).
 50. Tarbell J.M. & Cancel L.M. The glycocalyx and its significance in human medicine. *J. Intern. Med.* **280**, 97-113 (2016).
 51. Tarbell J.M. & Ebong E.E. The endothelial glycocalyx: a mechano-sensor and -transducer. *Sci. Signal.* **1**, t8 (2008).
 52. Tarbell J.M., Simon S.I., & Curry F.R. Mechanosensing at the vascular interface. *Annu. Rev. Biomed. Eng* **16**, 505-532 (2014).
 53. Mochizuki S. *et al.* Role of hyaluronic acid glycosaminoglycans in shear-induced endothelium-derived nitric oxide release. *Am. J. Physiol Heart Circ. Physiol* **285**, H722-H726 (2003).
 54. Duan Y. *et al.* Shear-induced reorganization of renal proximal tubule cell actin cytoskeleton and apical junctional complexes. *Proc. Natl. Acad. Sci. U. S. A* **105**, 11418-11423 (2008).
 55. Zhuo J.L. & Li X.C. Proximal nephron. *Compr. Physiol* **3**, 1079-1123 (2013).
 56. Kotsis F., Boehlke C., & Kuehn E.W. The ciliary flow sensor and polycystic kidney disease. *Nephrol. Dial. Transplant.* **28**, 518-526 (2013).
 57. Weimbs T. Polycystic kidney disease and renal injury repair: common pathways, fluid flow, and the function of polycystin-1. *Am J Physiol Renal Physiol* **293**, F1423-F1432 (2007).
 58. Simons M. *et al.* Inversin, the gene product mutated in nephronophthisis type II, functions as a molecular switch between Wnt signaling pathways. *Nat. Genet.* **37**, 537-543 (2005).
 59. Boehlke C. *et al.* Primary cilia regulate mTORC1 activity and cell size through Lkb1. *Nat. Cell Biol.* **12**, 1115-1122 (2010).
 60. Zhong M. *et al.* Tumor Suppressor Folliculin Regulates mTORC1 through Primary Cilia. *J. Biol. Chem.* **291**, 11689-11697 (2016).
 61. Low S.H. *et al.* Polycystin-1, STAT6, and P100 function in a pathway that transduces ciliary mechanosensation and is activated in polycystic kidney disease. *Dev. Cell* **10**, 57-69 (2006).
 62. Flores D., Battini L., Gusella G.L., & Rohatgi R. Fluid shear stress induces renal epithelial gene expression through polycystin-2-dependent trafficking of extracellular regulated kinase. *Nephron Physiol* **117**, 27-36 (2011).
 63. Flores D., Liu Y., Liu W., Satlin L.M., & Rohatgi R. Flow-induced prostaglandin E2 release regulates Na and K transport in the collecting duct. *Am. J. Physiol Renal Physiol* **303**, F632-F638 (2012).
 64. Raghavan V., Rbaibi Y., Pastor-Soler N.M., Carattino M.D., & Weisz O.A. Shear stress-dependent regulation of apical endocytosis in renal proximal tubule cells mediated by primary cilia. *Proc. Natl. Acad. Sci. U. S. A* **111**, 8506-8511 (2014).
 65. Bhattacharyya S. *et al.* Cdc42 activation couples fluid shear stress to apical endocytosis in proximal tubule cells. *Physiol Rep.* **5**, (2017).
 66. Praetorius H.A., Frokiaer J., Nielsen S., & Spring K.R. Bending the Primary Cilium Opens Ca(2+)-sensitive Intermediate-Conductance K+ Channels in MDCK Cells. *J. Membr. Biol.* **191**, 193-200 (2003).
 67. Nauli S.M. *et al.* Polycystins 1 and 2 mediate mechanosensation in the primary cilium of kidney cells. *Nat. Genet.* **33**, 129-137 (2003).
 68. DeCaen P.G., Delling M., Vien T.N., & Clapham D.E. Direct recording and molecular identification of the calcium channel of primary cilia. *Nature* **504**, 315-318 (2013).
 69. Delling M., DeCaen P.G., Doerner J.F., Febvay S., & Clapham D.E. Primary cilia are specialized calcium signalling organelles. *Nature* **504**, 311-314 (2013).
 70. Delling M. *et al.* Primary cilia are not calcium-responsive mechanosensors. *Nature* **531**, 656-660 (2016).

71. Tran P.V., Sharma M., Li X., & Calvet J.P. Developmental signaling: does it bridge the gap between cilia dysfunction and renal cystogenesis? *Birth Defects Res. C. Embryo. Today* **102**, 159-173 (2014).
72. Yamaguchi T. *et al.* Calcium restriction allows cAMP activation of the B-Raf/ERK pathway, switching cells to a cAMP-dependent growth-stimulated phenotype. *J Biol. Chem.* **279**, 40419-40430 (2004).
73. Torres V.E. & Harris P.C. Mechanisms of Disease: autosomal dominant and recessive polycystic kidney diseases. *Nat. Clin. Pract. Nephrol.* **2**, 40-55 (2006).
74. Mohammed S.G. *et al.* Fluid shear stress increases transepithelial transport of Ca(2+) in ciliated distal convoluted and connecting tubule cells. *FASEB J.* **31**, 1796-1806 (2017).
75. Norris D.P. & Jackson P.K. Cell biology: Calcium contradictions in cilia. *Nature* **531**, 582-583 (2016).
76. Ma M., Gallagher A.R., & Somlo S. Ciliary Mechanisms of Cyst Formation in Polycystic Kidney Disease. *Cold Spring Harb. Perspect. Biol.* **9**, a028209 (2017).
77. Orhon I. *et al.* Primary-cilium-dependent autophagy controls epithelial cell volume in response to fluid flow. *Nat. Cell Biol.* **18**, 657-667 (2016).
78. Takacs Z. & Proikas-Cezanne T. Primary cilia mechanosensing triggers autophagy-regulated cell volume control. *Nat. Cell Biol.* **18**, 591-592 (2016).
79. Corradetti M.N. & Guan K.L. Upstream of the mammalian target of rapamycin: do all roads pass through mTOR? *Oncogene* **25**, 6347-6360 (2006).
80. Orhon I., Dupont N., & Codogno P. Primary cilium and autophagy: The avengers of cell-size regulation. *Autophagy*. **12**, 2258-2259 (2016).
81. Shi Y. & Massague J. Mechanisms of TGF-beta signaling from cell membrane to the nucleus. *Cell* **113**, 685-700 (2003).
82. Hassane S. *et al.* Elevated TGFbeta-Smad signalling in experimental Pkd1 models and human patients with polycystic kidney disease. *J. Pathol.* **222**, 21-31 (2010).
83. Schmierer B. & Hill C.S. TGFbeta-SMAD signal transduction: molecular specificity and functional flexibility. *Nat. Rev. Mol. Cell Biol.* **8**, 970-982 (2007).
84. Massague J. TGFbeta signalling in context. *Nat. Rev. Mol. Cell Biol.* **13**, 616-630 (2012).
85. Chapnick D.A., Warner L., Bernet J., Rao T., & Liu X. Partners in crime: the TGFbeta and MAPK pathways in cancer progression. *Cell Biosci.* **1**, 42 (2011).
86. Lee M.K. *et al.* TGF-beta activates Erk MAP kinase signalling through direct phosphorylation of ShcA. *EMBO J.* **26**, 3957-3967 (2007).
87. Muthusamy B.P. *et al.* ShcA Protects against Epithelial-Mesenchymal Transition through Compartmentalized Inhibition of TGF-beta-Induced Smad Activation. *PLoS. Biol.* **13**, e1002325 (2015).
88. Kretzschmar M., Doody J., Timokhina I., & Massague J. A mechanism of repression of TGFbeta/ Smad signaling by oncogenic Ras. *Genes Dev.* **13**, 804-816 (1999).
89. Hough C., Radu M., & Dore J.J. Tgf-beta induced Erk phosphorylation of smad linker region regulates smad signaling. *PLoS. One.* **7**, e42513 (2012).
90. Lamouille S., Xu J., & Derynck R. Molecular mechanisms of epithelial-mesenchymal transition. *Nat. Rev. Mol. Cell Biol.* **15**, 178-196 (2014).
91. Egorova A.D. *et al.* Lack of primary cilia primes shear-induced endothelial-to-mesenchymal transition. *Circ. Res.* **108**, 1093-1101 (2011).
92. Egorova A.D. *et al.* Tgfbeta/Alk5 signaling is required for shear stress induced klf2 expression in embryonic endothelial cells. *Dev. Dyn.* **240**, 1670-1680 (2011).
93. Warner G.M. *et al.* Genetic deficiency of Smad3 protects the kidneys from atrophy and interstitial fibrosis in 2K1C hypertension. *Am. J. Physiol Renal Physiol* **302**, F1455-F1464 (2012).
94. Therrien F.J., Agharazii M., Lebel M., & Lariviere R. Neutralization of tumor necrosis factor-alpha reduces renal fibrosis and hypertension in rats with renal failure. *Am. J. Nephrol.* **36**, 151-161 (2012).
95. Azibani F., Fazal L., Chatziantoniou C., Samuel J.L., & Delcayre C. Aldosterone mediates cardiac fibrosis in

- the setting of hypertension. *Curr. Hypertens. Rep.* **15**, 395-400 (2013).
96. Wang Y. & Wang D.H. Protective effect of TRPV1 against renal fibrosis via inhibition of TGF-beta/Smad signaling in DOCA-salt hypertension. *Mol. Med.* **17**, 1204-1212 (2011).
 97. Rai R. *et al.* A novel acetyltransferase p300 inhibitor ameliorates hypertension-associated cardio-renal fibrosis. *Epigenetics.* **12**, 1004-1013 (2017).
 98. Wei X. *et al.* Activation of TRPV4 by dietary apigenin antagonizes renal fibrosis in deoxycorticosterone acetate (DOCA)-salt-induced hypertension. *Clin. Sci.* **131**, 567-581 (2017).
 99. Jang K.J. *et al.* Human kidney proximal tubule-on-a-chip for drug transport and nephrotoxicity assessment. *Integr. Biol.* **5**, 1119-1129 (2013).
 100. Kotsis F., Nitschke R., Doerken M., Walz G., & Kuehn E.W. Flow modulates centriole movements in tubular epithelial cells. *Pflugers Arch.* **456**, 1025-1035 (2008).
 101. Maggiorani D. *et al.* Shear Stress-Induced Alteration of Epithelial Organization in Human Renal Tubular Cells. *PLoS. One.* **10**, e0131416 (2015).
 102. Raghavan V. & Weisz O.A. Flow stimulated endocytosis in the proximal tubule. *Curr. Opin. Nephrol. Hypertens.* **24**, 359-365 (2015).
 103. Srivastava T. *et al.* Fluid flow shear stress over podocytes is increased in the solitary kidney. *Nephrol. Dial. Transplant.* **29**, 65-72 (2014).
 104. Lenihan C.R. *et al.* Longitudinal study of living kidney donor glomerular dynamics after nephrectomy. *J. Clin. Invest* **125**, 1311-1318 (2015).
 105. Bell P.D. *et al.* Loss of primary cilia upregulates renal hypertrophic signaling and promotes cystogenesis. *J. Am. Soc. Nephrol.* **22**, 839-848 (2011).
 106. Leonhard W.N. *et al.* Scattered Deletion of PKD1 in Kidneys Causes a Cystic Snowball Effect and Recapitulates Polycystic Kidney Disease. *J. Am. Soc. Nephrol.* **26**, 1322-1333 (2015).
 107. Rohatgi R. & Flores D. Intratubular hydrodynamic forces influence tubulointerstitial fibrosis in the kidney. *Curr. Opin. Nephrol. Hypertens.* **19**, 65-71 (2010).
 108. Venkatachalam M.A. *et al.* Acute kidney injury: a springboard for progression in chronic kidney disease. *Am. J. Physiol Renal Physiol* **298**, F1078-F1094 (2010).
 109. Reiter J.F. & Leroux M.R. Genes and molecular pathways underpinning ciliopathies. *Nat. Rev. Mol. Cell Biol.* **18**, 533-547 (2017).
 110. Bergmann C. ARPKD and early manifestations of ADPKD: the original polycystic kidney disease and phenocopies. *Pediatr. Nephrol.* **30**, 15-30 (2015).
 111. Srivastava S., Molinari E., Raman S., & Sayer J.A. Many Genes-One Disease? Genetics of Nephronophthisis (NPHP) and NPHP-Associated Disorders. *Front Pediatr.* **5**, 287 (2018).
 112. Khan S.A. *et al.* Genetics of human Bardet-Biedl syndrome, an updates. *Clin. Genet.* **90**, 3-15 (2016).
 113. Blacque O.E. *et al.* Loss of *C. elegans* BBS-7 and BBS-8 protein function results in cilia defects and compromised intraflagellar transport. *Genes Dev.* **18**, 1630-1642 (2004).
 114. Beales P.L. *et al.* IFT80, which encodes a conserved intraflagellar transport protein, is mutated in Jeune asphyxiating thoracic dystrophy. *Nat. Genet.* **39**, 727-729 (2007).
 115. Bruel A.L. *et al.* Fifteen years of research on oral-facial-digital syndromes: from 1 to 16 causal genes. *J. Med. Genet.* **54**, 371-380 (2017).
 116. Willey C.J. *et al.* Prevalence of autosomal dominant polycystic kidney disease in the European Union. *Nephrol. Dial. Transplant.* **32**, 1356-1363 (2017).
 117. Igarashi P. & Somlo S. Genetics and pathogenesis of polycystic kidney disease. *J. Am. Soc. Nephrol.* **13**, 2384-2398 (2002).
 118. Wilson P.D. Polycystic kidney disease. *N. Engl. J. Med.* **350**, 151-164 (2004).
 119. Torres V.E., Harris P.C., & Pirson Y. Autosomal dominant polycystic kidney disease. *Lancet* **369**, 1287-1301 (2007).

120. Gabow P.A. Autosomal dominant polycystic kidney disease: More than a renal disease. *Am J Kidney Dis* **16**, 403-413 (1990).
121. The European Polycystic Kidney Disease Consortium *et al.* The polycystic kidney disease 1 gene encodes a 14 kb transcript and lies within a duplicated region on chromosome 16. *Cell* **77**, 881-894 (1994).
122. Mochizuki T. *et al.* PKD2, a gene for polycystic kidney disease that encodes an integral membrane protein. *Science* **272**, 1339-1342 (1996).
123. Claverie-Martin F., Gonzalez-Paredes F.J., & Ramos-Trujillo E. Splicing defects caused by exonic mutations in PKD1 as a new mechanism of pathogenesis in autosomal dominant polycystic kidney disease. *RNA. Biol.* **12**, 369-374 (2015).
124. Qian F.J., Watnick T.J., Onuchic L.F., & Germino G.G. The molecular basis of focal cyst formation in human autosomal dominant polycystic kidney disease. *Cell* **87**, 979-987 (1996).
125. Germino G.G. Autosomal dominant polycystic kidney disease: a two-hit model. *Hosp. Pract.* **32**, 81-102 (1997).
126. Martin G.M. *et al.* Somatic mutations are frequent and increase with age in human kidney epithelial cells. *Hum Mol Genet* **5**, 215-221 (1996).
127. Cook D.L., Gerber A.N., & Tapscott S.J. Modeling stochastic gene expression: implications for haploinsufficiency. *Proc Natl Acad Sci U. S. A* **95**, 15641-15646 (1998).
128. Cornec-Le G.E., Audrezet M.P., Le M.Y., Chen J.M., & Ferec C. Genetics and pathogenesis of autosomal dominant polycystic kidney disease: 20 years on. *Hum. Mutat.* **35**, 1393-1406 (2014).
129. Leonhard W.N., Happe H., & Peters D.J. Variable Cyst Development in Autosomal Dominant Polycystic Kidney Disease: The Biologic Context. *J. Am. Soc. Nephrol.* **27**, 3530-3538 (2016).
130. Patel V. *et al.* Acute kidney injury and aberrant planar cell polarity induce cyst formation in mice lacking renal cilia. *Hum. Mol. Genet.* **17**, 1578-1590 (2008).
131. Happe H. *et al.* Toxic tubular injury in kidneys from Pkd1-deletion mice accelerates cystogenesis accompanied by dysregulated planar cell polarity and canonical Wnt signaling pathways. *Hum. Mol. Genet.* **18**, 2532-2542 (2009).
132. Takakura A. *et al.* Renal injury is a third hit promoting rapid development of adult polycystic kidney disease. *Hum. Mol. Genet.* **18**, 2523-2531 (2009).
133. Sas K.M. *et al.* Hyperglycemia in the absence of cilia accelerates cystogenesis and induces renal damage. *Am. J. Physiol Renal Physiol* **309**, F79-F87 (2015).
134. Sutters M. & Germino G.G. Autosomal dominant polycystic kidney disease: molecular genetics and pathophysiology. *J. Lab Clin. Med.* **141**, 91-101 (2003).
135. Qian F. *et al.* PKD1 interacts with PKD2 through a probable coiled-coil domain. *Nature Genet* **16**, 179-183 (1997).
136. Yoder B.K., Hou X., & Guay-Woodford L.M. The polycystic kidney disease proteins, polycystin-1, polycystin-2, polaris, and cystin, are co-localized in renal cilia. *J. Am. Soc. Nephrol.* **13**, 2508-2516 (2002).
137. Seeger-Nukpezah T. & Golemis E.A. The extracellular matrix and ciliary signaling. *Curr. Opin. Cell Biol.* **24**, 652-661 (2012).
138. Patel A. & Honore E. Polycystins and renovascular mechanosensory transduction. *Nat. Rev. Nephrol.* **6**, 530-538 (2010).
139. Lee S.H. & Somlo S. Cyst growth, polycystins, and primary cilia in autosomal dominant polycystic kidney disease. *Kidney Res. Clin. Pract.* **33**, 73-78 (2014).
140. Peyronnet R. *et al.* Mechanoprotection by Polycystins against Apoptosis Is Mediated through the Opening of Stretch-Activated K2P Channels. *Cell Reports* **1**, 241-250 (2012).
141. Nauli S.M. *et al.* Loss of polycystin-1 in human cyst-lining epithelia leads to ciliary dysfunction. *J. Am. Soc. Nephrol.* **17**, 1015-1025 (2006).
142. Ma M., Tian X., Igarashi P., Pazour G.J., & Somlo S. Loss of cilia suppresses cyst growth in genetic models of autosomal dominant polycystic kidney disease. *Nat. Genet.* **45**, 1004-1012 (2013).

143. Lehman J.M. *et al.* The Oak Ridge Polycystic Kidney mouse: modeling ciliopathies of mice and men. *Dev. Dyn.* **237**, 1960-1971 (2008).
144. Jonassen J.A., San A.J., Follit J.A., & Pazour G.J. Deletion of IFT20 in the mouse kidney causes misorientation of the mitotic spindle and cystic kidney disease. *J. Cell Biol.* **183**, 377-384 (2008).
145. Jonassen J.A., SanAgustin J., Baker S.P., & Pazour G.J. Disruption of IFT complex A causes cystic kidneys without mitotic spindle misorientation. *J. Am. Soc. Nephrol.* **23**, 641-651 (2012).
146. Happe H. & Peters D.J. Translational research in ADPKD: lessons from animal models. *Nat. Rev. Nephrol.* **10**, 587-601 (2014).
147. Ibraghimov-Beskrovnaia O. & Natoli T.A. mTOR signaling in polycystic kidney disease. *Trends Mol. Med.* **17**, 625-633 (2011).
148. Fantus D., Rogers N.M., Grahmmer F., Huber T.B., & Thomson A.W. Roles of mTOR complexes in the kidney: implications for renal disease and transplantation. *Nat. Rev. Nephrol.* **12**, 587-609 (2016).
149. Novalic Z. *et al.* Dose-Dependent Effects of Sirolimus on mTOR Signaling and Polycystic Kidney Disease. *J. Am. Soc. Nephrol.* **23**, 842-853 (2012).
150. Ravichandran K., Zafar I., Ozkok A., & Edelstein C.L. An mTOR kinase inhibitor slows disease progression in a rat model of polycystic kidney disease. *Nephrol. Dial. Transplant.* **30**, 45-53 (2015).
151. Stallone G. *et al.* Rapamycin for treatment of type I autosomal dominant polycystic kidney disease (RAPYD-study): a randomized, controlled study. *Nephrol. Dial. Transplant.* **27**, 3560-3567 (2012).
152. He Q., Lin C., Ji S., & Chen J. Efficacy and safety of mTOR inhibitor therapy in patients with early-stage autosomal dominant polycystic kidney disease: a meta-analysis of randomized controlled trials. *Am. J. Med. Sci.* **344**, 491-497 (2012).
153. Jardine M.J., Liyanage T., Buxton E., & Perkovic V. mTOR inhibition in autosomal-dominant polycystic kidney disease (ADPKD): the question remains open. *Nephrol. Dial. Transplant.* **28**, 242-244 (2013).
154. de S.L. *et al.* Double inhibition of cAMP and mTOR signalling may potentiate the reduction of cell growth in ADPKD cells. *Clin. Exp. Nephrol.* **21**, 203-211 (2017).
155. Hassane S. *et al.* Elevated TGFbeta-Smad signalling in experimental Pkd1 models and human patients with polycystic kidney disease. *J. Pathol.* **222**, 21-31 (2010).
156. Liu D. *et al.* A Pkd1-Fbn1 genetic interaction implicates TGF-beta signaling in the pathogenesis of vascular complications in autosomal dominant polycystic kidney disease. *J. Am. Soc. Nephrol.* **25**, 81-91 (2014).
157. Carney E.F. Polycystic kidney disease: TGF-beta signalling and vascular complications in ADPKD. *Nat. Rev. Nephrol.* **9**, 694 (2013).
158. Goggolidou P. & Wilson P.D. Novel biomarkers in kidney disease: roles for cilia, Wnt signalling and ATMIN in polycystic kidney disease. *Biochem. Soc. Trans.* **44**, 1745-1751 (2016).
159. Wuebben A. & Schmidt-Ott K.M. WNT/beta-catenin signaling in polycystic kidney disease. *Kidney Int.* **80**, 135-138 (2011).
160. Kawakami T., Ren S., & Duffield J.S. Wnt signalling in kidney diseases: dual roles in renal injury and repair. *J. Pathol.* **229**, 221-231 (2013).
161. Happe H. *et al.* Altered Hippo signalling in polycystic kidney disease. *J. Pathol.* **224**, 133-142 (2011).
162. Leonhard W.N. *et al.* Curcumin inhibits cystogenesis by simultaneous interference of multiple signaling pathways: In vivo evidence from a Pkd1-deletion model. *Am. J. Physiol. Renal Physiol.* **300**, F1193-F1202 (2011).
163. Fragiadaki M. *et al.* STAT5 drives abnormal proliferation in autosomal dominant polycystic kidney disease. *Kidney Int.* **91**, 575-586 (2017).
164. Chen C.H. & Weiss R.H. Getting to know ADPKD proliferative signaling, STAT. *Kidney Int.* **91**, 524-526 (2017).
165. Xu T. *et al.* Celecoxib inhibits growth of human autosomal dominant polycystic kidney cyst-lining epithelial cells through the VEGF/Raf/MAPK/ERK signaling pathway. *Mol. Biol. Rep.* **39**, 7743-7753 (2012).
166. Ren X.S. *et al.* Activation of the PI3K/mTOR pathway is involved in cystic proliferation of cholangiocytes of

- the PCK rat. *PLoS. One.* **9**, e87660 (2014).
167. Hakim S. *et al.* Inpp5e suppresses polycystic kidney disease via inhibition of PI3K/Akt-dependent mTORC1 signaling. *Hum. Mol. Genet.* **25**, 2295-2313 (2016).
 168. De Santis M.C., Sala V., Martini M., Ferrero G.B., & Hirsch E. PI3K Signaling in Tissue Hyper-Proliferation: From Overgrowth Syndromes to Kidney Cysts. *Cancers* **9**, 30 (2017).
 169. Tran P.V. *et al.* Downregulating hedgehog signaling reduces renal cystogenic potential of mouse models. *J. Am. Soc. Nephrol.* **25**, 2201-2212 (2014).
 170. Yamaguchi T. *et al.* cAMP stimulates the in vitro proliferation of renal cyst epithelial cells by activating the extracellular signal-regulated kinase pathway. *Kidney Int.* **57**, 1460-1471 (2000).
 171. Yamaguchi T. *et al.* Cyclic AMP activates B-Raf and ERK in cyst epithelial cells from autosomal-dominant polycystic kidneys. *Kidney Int.* **63**, 1983-1994 (2003).
 172. Yamaguchi T., Reif G.A., Calvet J.P., & Wallace D.P. Sorafenib inhibits cAMP-dependent ERK activation, cell proliferation, and in vitro cyst growth of human ADPKD cyst epithelial cells. *Am. J. Physiol Renal Physiol* **299**, F944-F951 (2010).
 173. Torres V.E. & Harris P.C. Strategies targeting cAMP signaling in the treatment of polycystic kidney disease. *J. Am. Soc. Nephrol.* **25**, 18-32 (2014).
 174. Saigusa T. & Bell P.D. Molecular pathways and therapies in autosomal-dominant polycystic kidney disease. *Physiology* **30**, 195-207 (2015).
 175. Liu Y. *et al.* Rosiglitazone inhibits transforming growth factor-beta1 mediated fibrogenesis in ADPKD cyst-lining epithelial cells. *PLoS. One.* **6**, e28915 (2011).
 176. Lal M. *et al.* Polycystin-1 C-terminal tail associates with beta-catenin and inhibits canonical Wnt signaling. *Hum. Mol. Genet.* **17**, 3105-3117 (2008).
 177. Kim S. *et al.* The polycystin complex mediates Wnt/Ca(2+) signalling. *Nat. Cell Biol.* **18**, 752-764 (2016).
 178. Happe H., De Heer E., & Peters D.J. Polycystic kidney disease: The complexity of planar cell polarity and signaling during tissue regeneration and cyst formation. *Biochim. Biophys. Acta* **1812**, 1249-1255 (2011).
 179. Lancaster M.A. & Gleeson J.G. Cystic kidney disease: the role of Wnt signaling. *Trends Mol. Med.* **16**, 349-360 (2010).
 180. Reif G.A. *et al.* Tolvaptan inhibits ERK-dependent cell proliferation, Cl(-) secretion, and in vitro cyst growth of human ADPKD cells stimulated by vasopressin. *Am. J. Physiol Renal Physiol* **301**, F1005-F1013 (2011).
 181. Serra A.L. *et al.* Sirolimus and Kidney Growth in Autosomal Dominant Polycystic Kidney Disease. *N. Engl. J. Med.* **363**, 820-829 (2010).
 182. Walz G. *et al.* Everolimus in Patients with Autosomal Dominant Polycystic Kidney Disease. *N. Engl. J. Med.* **363**, 830-840 (2010).
 183. Rysz J., Gluba-Brzozka A., Franczyk B., Banach M., & Bartnicki P. Combination drug versus monotherapy for the treatment of autosomal dominant polycystic kidney disease. *Expert. Opin. Pharmacother.* **17**, 2049-2056 (2016).
 184. de Stephanis L. *et al.* Double inhibition of cAMP and mTOR signalling may potentiate the reduction of cell growth in ADPKD cells. *Clin. Exp. Nephrol.* **21**, 203-211 (2017).
 185. Liu C. *et al.* Concomitant use of rapamycin and rosiglitazone delays the progression of polycystic kidney disease in Han:SPRD rats: A study of the mechanism of action. *Am. J. Physiol Renal Physiol.* **314** (5), F844-F854 (2018).

CHAPTER 2

Fluid shear stress-induced TGF- β /ALK5 signaling in renal epithelial cells is modulated by MEK1/2

Steven J. Kunnen¹, Wouter N. Leonhard¹, Cornelis M. Semeins², Lukas J.A.C. Hawinkels^{3,4}, Christian Poelma⁵, Peter ten Dijke³, Astrid D. Bakker², Beerend P. Hierck⁶ and Dorien J.M. Peters¹

¹Department of Human Genetics, Leiden University Medical Center, 2300 RC Leiden, The Netherlands

²Department of Oral Cell Biology, Academic Centre for Dentistry Amsterdam (ACTA), University of Amsterdam and VU University Amsterdam, 1081 LA Amsterdam, The Netherlands

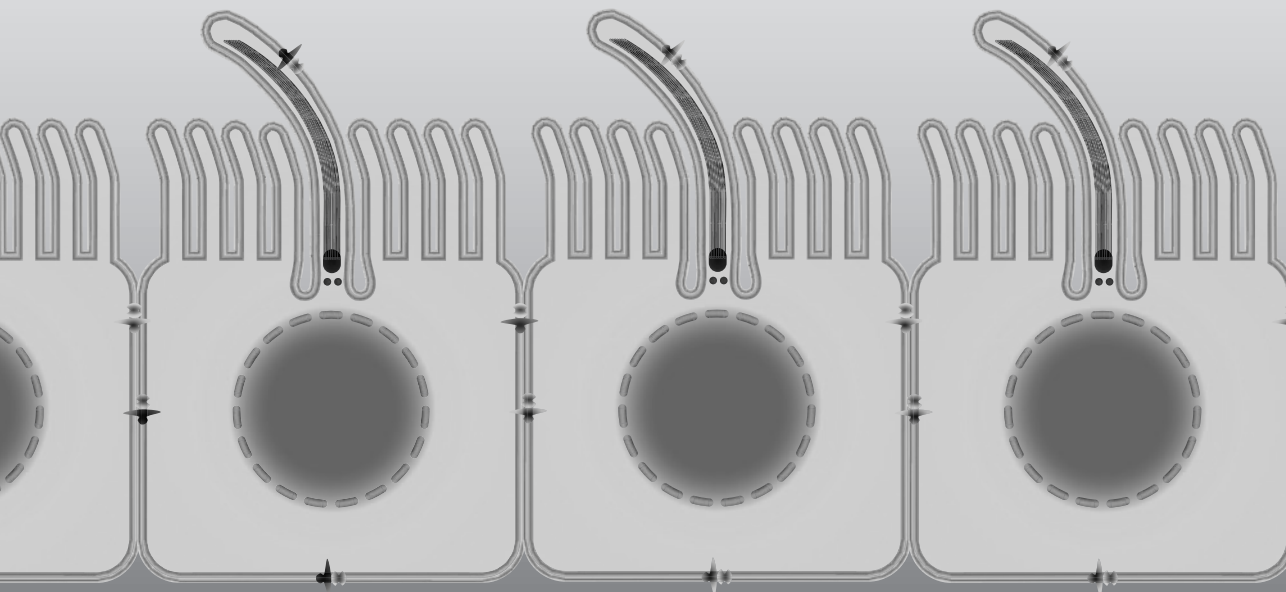
³Department of Molecular Cell Biology, Cancer Genomics Centre Netherlands, Leiden University Medical Center, 2300 RC Leiden, The Netherlands

⁴Department of Gastroenterology-Hepatology, Leiden University Medical Center, 2300 RC Leiden, The Netherlands

⁵Laboratory for Aero and Hydrodynamics, Delft University of Technology, 2628 CA Delft, The Netherlands

⁶Department of Anatomy and Embryology, Leiden University Medical Center, 2300 RC Leiden, The Netherlands

Cell Mol Life Sci. 2017; 74(12): 2283-2298



ABSTRACT

Renal tubular epithelial cells are exposed to mechanical forces due to fluid flow shear stress within the lumen of the nephron. These cells respond by activation of mechano-sensors located at the plasma membrane or the primary cilium, having crucial roles in maintenance of cellular homeostasis and signaling. In this paper we applied fluid-shear stress to study TGF- β signaling in renal epithelial cells with and without expression of the *Pkd1*-gene, encoding a mechano-sensor mutated in polycystic kidney disease. TGF- β signaling modulates cell proliferation, differentiation, apoptosis and fibrotic deposition, cellular programs that are altered in renal cystic epithelia. SMAD2/3-mediated signaling was activated by fluid flow, both in wild-type and *Pkd1*^{-/-} cells. This was characterized by phosphorylation and nuclear accumulation of p-SMAD2/3, as well as altered expression of downstream target genes and epithelial-to-mesenchymal transition markers. This response was still present after cilia ablation. An inhibitor of upstream type-I-receptors, ALK4/ALK5/ALK7, as well as TGF- β -neutralizing antibodies effectively blocked SMAD2/3 activity. In contrast, an activin-ligand trap was ineffective, indicating that increased autocrine TGF- β signaling is involved. To study potential involvement of MAPK/ERK signaling, cells were treated with a MEK1/2 inhibitor. Surprisingly, fluid-flow induced expression of most SMAD2/3 targets was further enhanced upon MEK inhibition. We conclude that fluid-shear stress induces autocrine TGF- β /ALK5-induced target gene expression in renal epithelial cells, which is partially restrained by MEK1/2-mediated signaling.

Keywords: Fluid-flow, mechanotransduction, cilia, SMAD2/3 signaling, ERK1/2, *Pkd1*^{-/-}

ABBREVIATIONS

ADPKD	Autosomal dominant polycystic kidney disease
ALK	Activin like kinase
AS	Ammonium sulfate
Cdh1	Cadherin-1
Col1a1	Collagen, type I, alpha 1
COX2	Cyclo-oxygenase-2
DPBS	Dulbecco's phosphate-buffered saline
ELISA	Enzyme-linked immunosorbent assay
EMT	Epithelial-to-mesenchymal transition
ERK	Extracellular signal-regulated kinase
Fn1	Fibronectin 1
Hprt	Hypoxanthine-guanine phosphoribosyltransferase
MAPK	Mitogen-activated protein kinase
MEK	MAPK/ERK kinase
qPCR	Quantitative polymerase chain reaction
PAGE	Polyacrylamide gel electrophoresis
Pai1	Plasminogen activator inhibitor 1
PC	Polycystin
Pkd1	Polycystic kidney disease 1
PTEC	Proximal tubular epithelial cell
Ptgs2	Prostaglandin G/H synthase 2
RIPA	Radioimmunoprecipitation assay
sActRIIB-Fc	Soluble Activin receptor-IIB fusion protein
SDS	Sodium dodecyl sulfate
SMAD	Mothers against decapentaplegic homolog
TBS	Tris-buffered saline
TGF- β	Transforming growth factor β
TGF- β Ab	TGF- β neutralizing antibody
Vim	Vimentin

INTRODUCTION

Cellular mechano-sensitivity plays fundamental roles in cell viability and function, tissue development and maintenance of organs¹. For example, the kidney has the capacity to increase glomerular filtration rate in response to physiological stimuli. In addition, in renal diseases hyperfiltration usually occurs in the remaining functional nephrons to compensate for the lost glomeruli and nephrons². Fundamental in the regulation of altered fluid shear stress are primary cilia and other mechano-sensors, and defects in cilia formation and function have profound effects on the development of body pattern and the physiology of multiple organ systems³. The signaling modules responsible for the flow-sensing response involve a number of proteins located in the cell membrane, cilium and/or at the ciliary base, including polycystin-1 (PC-1) and the ion channel polycystin-2 (PC-2), encoded by the genes mutated in patients with autosomal dominant polycystic kidney disease (ADPKD)^{4,5}. At the plasma membrane and in cilia, polycystins interact with diverse (mechanosensory) ion channels, signal transducers as well as cell-cell and cell-extracellular matrix junctional proteins⁶⁻¹¹. Therefore the polycystins are thought to play a role in differentiation and maintenance of the cell structure, mechanical force transmission and mechanotransduction^{1,12,13}. Lack of the polycystin complex in cilia is one of the proposed mechanisms of renal cyst formation^{14,15}. Moreover, mutations or deletions of other ciliary proteins can also cause renal cystic disease in mouse models and patients, indicating the role of cilia during cystogenesis^{16,17}. In the absence of polycystins, renal epithelial cells lack the capability to respond to signals needed to maintain the epithelium differentiated, finally resulting in cyst formation¹⁵.

Primary cilia also play essential roles as signal transducers in growth factor signaling. Ligands in the tubular fluid-flow bind to their receptors, inducing cellular responses through downstream signaling pathways, for instance affecting the hedgehog (Hh), epidermal growth factor receptor (EGFR), Wnt and transforming growth factor β (TGF- β) pathways^{3,18}. Although not exclusively, receptors involved in these pathways have been identified in the cilium of several cell types, including renal epithelial cells, suggesting that different signaling cascades are being regulated by this organelle^{3,18-20}. The above mentioned data indicate that primary cilia are essential in organizing different signaling systems that sense environmental cues and transmit signals to the cell interior. Gene expression and the overall cellular behavior will be the effect of an integration of the different signaling pathways, triggered by flow and by growth factor or cytokine stimulation.

A cytokine previously reported to be involved in fluid-flow and shear stress regulated signaling is TGF- β ^{21,22}. The TGF- β superfamily members are multifunctional cytokines and include among others TGF- β 's, activins and bone morphogenetic proteins (BMPs). TGF- β signaling modulates cell proliferation, differentiation, apoptosis, adhesion, cell migration

and is believed to play a crucial role in fibrotic deposition²³, which is seen in cyst formation²⁴. TGF- β , as well as Activin and Nodal, binds to a pair of serine/threonine kinase transmembrane receptors that mediate the phosphorylation of receptor-regulated SMAD2 and 3. These phosphorylated SMAD proteins, p-SMAD2 and -3, form a complex with SMAD4 and can enter the nucleus where they act as transcription factors to regulate the transcription of various genes.

In embryonic endothelial cells, shear stress mediated TGF- β /Activin receptor like kinase 5 (ALK5) signaling induced endothelial-to-mesenchymal transition, depending on the strength of shear and presence or absence of cilia^{21,25}. A similar type of observation was made for renal epithelial cells, where fluid shear stress dynamically regulated TGF- β gene expression and SMAD3 activation, depending on the magnitude of fluid shear, *i.e.* physiological versus pathological, and depending on NOTCH4 expression^{22,26}. Increased SMAD2/3 activation and increased TGF- β signaling has been shown in several animal models for renal cystic disease and patient-derived tissues^{24,27}.

Given the role for SMAD2/3 signaling in shear stress but also in cyst formation, we aim to characterize in this study the cellular response of renal epithelial cells to fluid shear stress by unraveling the signaling cascades, particularly focusing on SMAD2/3 signaling and the effect of MAPK/ERK signaling. Our data indicate that both SMAD2/3 and epithelial-to-mesenchymal transition (EMT) processes are altered upon fluid-flow stimulation in proximal tubular epithelial cells (PTEC) with and without *Pkd1*-gene expression, as shown by phosphorylation of SMAD2/3 and nuclear translocation of p-SMAD2/3 and Snail. This leads to altered expression of target genes and EMT markers, shown in ciliated and non-ciliated cells. These processes are regulated by an interplay between SMAD2/3 and ERK1/2 signaling, and can be partially modulated by upstream ALK4/5/7 and MEK1/2 inhibitors and TGF- β neutralizing antibodies, while the soluble Activin receptor-IIB fusion protein (sActRIIB-Fc) was ineffective. We conclude that the fluid shear stress response in PTECs is TGF- β /ALK5 dependent and can be modulated by MAPK/ERK signaling.

MATERIALS AND METHODS

Antibodies

SMAD2 (L16D3; #3103), and Snail (C15D3; #3879) antibodies were from Cell Signaling Technology. Acetylated α -tubulin (clone 6-11B-1; #T6793) antibody and Phalloidin-Atto 594 (#51927) were from Sigma-Aldrich. Antibody against α -tubulin (DM1A; #CP06) was from Calbiochem, Merck Millipore. Antibodies against p-SMAD2 and p-SMAD3 have been described previously^{28,29}. Goat anti-Rabbit IgG (H+L) Alexa Fluor 488 conjugate (#A-11008), Goat anti-Mouse IgG (H+L) Alexa Fluor 488 conjugate (#A-11029) and Goat anti-Mouse IgG (H+L) Alexa Fluor 594 conjugate (A-11032) were from Life Technologies. Goat-anti-Rabbit IRDye 800CW (#926-32211) and Goat-anti-Mouse IRDye 680 (#926-32220) were from LI-COR Biosciences.

Chemicals

ALK4/5/7 inhibitor LY-364947 (10 μ M; Calbiochem; #616451) was from Merck Millipore and SB431542 (10 μ M; #1614) was from Tocris Bioscience. TGF- β neutralizing antibody (clone 2G7) was a gift from Dr. E. de Heer (Pathology, LUMC, Leiden); sActRIIB-Fc was a gift from Prof. Olli Ritvos (Haartman Institute, Helsinki, Finland). MEK1/2 inhibitor Trametinib (GSK1120212; #S2673) was from Selleckchem. Recombinant human TGF- β 1 (#100-21) and recombinant human TGF- β 2 (#100-35B) were purchased from PeproTech. Recombinant human/mouse/rat activin A (#338-AC) and recombinant human activin B (#659-AB) were from R&D systems.

Cell culture

SV40 large T-antigen immortalized murine proximal tubular epithelial cells (PTEC) (*Pkd1*^{wt} and *Pkd1*^{-/-}) derived from a *Pkd1*^{lox,lox} mouse, were generated and cultured as described previously³⁰. Cells were maintained at 37°C and 5% CO₂ in DMEM/F-12 with GlutaMAX (Gibco, Life Technologies; #31331-093) supplemented with 100 U/mL Penicillin-Streptomycin (Gibco, Life Technologies; #15140-122), 2% Ultrosor G (Pall Corporation, Pall BioSeptra, Cergy St Christophe, France; #15950-017), 1x Insulin-Transferrin-Selenium-Ethanolamine (Gibco, Life Technologies; #51500-056), 25 ng/L Prostaglandin E1 (Sigma-Aldrich; #P7527) and 30 ng/L Hydrocortisone (Sigma-Aldrich; #H0135). Cell culture was monthly tested without mycoplasma contamination using MycoAlert Mycoplasma Detection Kit (Lonza; LT07-318). New ampules were started after 15 passages.

For growth factor stimulation or fluid-flow experiments, cells were cultured on collagen-I (Advanced BioMatrix; #5005) coated culture dishes or glass slides. Prior to treatment, cells were serum starved to exclude effects of serum-derived growth-factors and to synchronize cells and cilia formation. For growth factor stimulation, 100% confluent cells were serum starved overnight and incubated with the specified ligands in the absence of medium

supplements. Stimulation was done with 5 ng/ml TGF- β 1 or TGF- β 2 or 100 ng/ml activin A or activin B, unless differently specified. For fluid-flow stimulation, cells grown until high confluency underwent 24 hr serum starvation before the start of the treatment. Cilia formation was checked on a parallel slide by immunofluorescence using anti-acetylated α -tubulin antibodies (Sigma Aldrich; #T6793). ALK4/5/7 inhibitor (10 μ M), MEK1/2 inhibitor (10 μ M) or DMSO control (0.1%) were added 1 hr before start of ligand or flow stimulation in the absence of medium supplements. To sequester TGF- β or activin ligands, TGF- β neutralizing antibodies (10 μ g/ml) or sActRIIB-Fc (5 μ g/ml) was added at the start of treatment, by replacing serum-free medium.

Fluid flow stimulation

Cells were exposed to laminar fluid-flow (0.25-2.0 dyn/cm²) in a cone-plate device or parallel-plate flow chamber. The cone-plate device, adapted from Malek *et al.*^{31,32}, was designed for 3.5 cm cell culture dishes (Greiner Bio-One). Cells were grown on collagen-I coated dishes until confluence, followed by 24 hr serum starvation, before dishes were placed in the cone-plate flow system and incubated at 37°C and 5% CO₂. The confluent cell monolayer of 9.6 cm² was subjected to fluid shear stress using 2 ml serum-free DMEM/F-12 medium with viscosity (μ) of 0.0078 dyn s/cm²³³. Constant laminar ($Re = 0.3$) fluid-flow was induced using a cone angle (α) of 2° and a velocity (ω) of 80 rpm, generating a fluid shear stress ($\tau = \mu\omega/\alpha$) of 1.9 dyn/cm².

The parallel plate flow-chamber was previously described^{34,35}. Briefly, cells were grown on collagen-I coated glass slides of 36 x 76 mm (Fisher Scientific #15178219) until confluence, followed by 24 hr serum starvation, before glass slides were placed in a flow-chamber. A confluent cell monolayer of 14.2 cm² (24 x 59 mm) was subjected to fluid shear stress using 7.5 ml serum-free DMEM/F-12 medium. Fluid was pumped at a constant flow rate (Q) of 5.5 ml/min through the chamber with 300 μ m height (h), generating a constant laminar ($Re = 5.0$) fluid shear stress ($\tau = 6\mu Q/h^2b$) of 2.0 dyn/cm², unless differently specified. The parallel plate flow-chamber was placed in an incubator at 37°C and 5% CO₂.

Static control cells were incubated for the same time in equal amounts of serum-free DMEM/F12 medium at 37°C and 5% CO₂. After 4 until 20 hr fluid-flow or control (static) stimulation, medium was collected and cells have been harvested for mRNA isolation and/or protein isolation for gene expression analysis or western blot. Ammonium sulfate (AS) was used to remove primary cilia as previously described³⁶. Cells were pre-treated with 50 mM ammonium sulfate, followed by 6 hour fluid flow in serum-free medium or 16 hour fluid flow in medium containing 25 mM AS, to prevent cilia restoration. Control cells were treated similarly, but without AS.

Reporter assay

PTECs were cultured in 3.5 cm culture dishes and transfected after 24 hr with 4 μ g SMAD3-SMAD4 transcriptional reporter (CAGA₁₂-Luc)³⁷ and 200 ng renilla luciferase reporter as a transfection control (pGL4.75[hRlucCMV]; Promega; #E6931) using 10 μ l Lipofectamine 2000 according to the manufacturer's protocol (Life Technologies; #11668019). Cells were maintained under serum-free conditions from the moment of transfection and fluid-flow was started 24 hr after transfection. Cells were lysed after 20 hr of fluid-flow stimulation using a cone-plate device. Firefly and renilla luciferase activities were measured on a luminometer (Victor 3; PerkinElmer) using the Dual-Luciferase Reporter Assay System (#E1960) from Promega according to the manufacturer's instructions. Firefly luminescence was corrected for renilla to get the relative activity of the reporter.

Gene expression analysis

Total RNA was isolated from cultured cells using TRI Reagent (Sigma-Aldrich; #T9424) according to manufacturer's protocol. Gene expression analysis was performed by quantitative PCR (qPCR) as described previously³⁸. Briefly, cDNA synthesis was done using Transcriptor First Strand cDNA Synthesis Kit (Roche Applied Science; #04897030001) according to the manufacturer's protocol. Quantitative PCR was done in triplicate on the LightCycler 480 II (Roche) using 2x FastStart SYBR-Green Master (Roche; #04913914001) according to the manufacturer's protocol. Data was analyzed with LightCycler 480 Software, Version 1.5 (Roche). Gene expression was calculated using the $2^{-\Delta\Delta C_t}$ method as described previously³⁹ and normalized to the housekeeping gene *Hprt*, giving the relative gene expression. Mean gene expression and standard deviation of the different treatment groups were calculated. For primer sequences see Supplementary Material 1, Table S1.

ELISA

Total and endogenously active levels of TGF- β 1, TGF- β 2, and TGF- β 3 in medium collected after fluid flow experiments were determined by ELISA as previously described^{40,41} using ELISA Duosets of TGF- β 1 (DY1679), TGF- β 2 (DY302), and TGF- β 3 (DY243) from R&D systems.

Western blot analysis

Cells were either scraped in DPBS and 1:1 diluted in 2x RIPA buffer or directly lysed in 1x RIPA buffer (50 mM Tris-HCl, pH 7.4, 150 mM NaCl, 1 mM EDTA, 1% Na-DOC, 1% NP-40) Throughout the lysis procedure, 50 mM NaF, 1 mM Na₂VO₄ and 1x complete protease inhibitor cocktail (Roche; #05892970001) were used to inhibit phosphatase and protease activity. Cell lysate was homogenized by three 5 sec pulses of sonification followed by 30 min gentle shaking at 4°C. Insoluble cell debris was removed by 15 min centrifugation at 14,000 x g. Protein concentration was determined using Pierce BCA protein assay kit (ThermoFisher Scientific; #23227).

Western blot was performed on total protein cell extracts using p-SMAD2, SMAD2, p-SMAD3 or tubulin antibodies. Cell lysates (10-20 μ L) were separated on a 10% SDS-PAGE gel. Proteins were transferred to 0.2 μ m nitrocellulose membranes (Bio-Rad; #1704158) using Trans-Blot Turbo Transfer System (Bio-Rad; #1704155) at 1.3 A and 25 V for 10 min. Membranes were blocked for 1 h at room temperature in 25% SEA block blocking buffer (ThermoFisher Scientific; #37527) in TBS and incubated overnight at 4°C with antibodies against p-SMAD2 (1:1,000), SMAD2 (1:1,000) or p-SMAD3 (1:1,000) in 5% bovine serum albumin (BSA) in Tris-buffered saline containing 0.1 % Tween-20 (TBST). Tubulin or GAPDH were used as loading controls, with 1 hr antibody incubation at room temperature. Goat-anti-Rabbit IRDye 800CW (1:10,000) was used as secondary antibody for the detection of p-SMAD2. Goat-anti-Mouse IRDye 680 (1:12,000) was used as secondary antibody for the detection of total SMAD2 and Tubulin. Horseradish peroxidase conjugated secondary antibody (GE Healthcare, Waukesha, WI, USA) was used for the detection of p-SMAD3 or GAPDH using chemoluminescence according to the manufacturer's protocol (Pierce, Rockford, IL, USA) as described previously²⁹. Detection and densitometric analysis were carried out using the Odyssey Infrared Imaging System (LI-COR-Biosciences). Protein levels were quantified using p-SMAD2 / SMAD2 integrated intensity ratios. Tubulin or GAPDH were used as a loading control.

Immunofluorescence

Cells were fixed in 4% paraformaldehyde and permeabilized in 0.2% Triton-X100 in PBS for 15 min at room temperature. Cells were blocked in 5% non-fat dried milk in PBS for 1 hour. Immunostaining for p-SMAD2 (1:1,000) and Snail (1:1,000) was performed overnight at 4°C in 2% BSA in PBS followed by 1 hour incubation with Goat anti-Rabbit IgG (H+L), Alexa Fluor 488 conjugate (1:2,000) as secondary antibody. The cilium was stained with the antibody specific for acetylated- α -tubulin (1:2,000) and Goat anti-Mouse IgG (H+L) Alexa Fluor 594 conjugate (1:3,000) or Alexa Fluor 488 conjugate (1:3,000) as secondary antibody. F-actin was visualized using Phalloidin-Atto 594 (1:1,500). Immunofluorescence slides were mounted with Vectashield containing DAPI after secondary antibody incubation and pictures were taken on the Leica DM5500 B microscope.

Statistical analysis

Results are expressed as mean \pm SD. Differences between one treatment group and their controls were tested using two-tailed Student's *t*-tests. One- or two-way analysis of variance (ANOVA) was used, when 3 or more groups were compared, followed by post-hoc Fisher's LSD multiple comparison, if the overall ANOVA *F*-test was significant. *P* < 0.05 was considered to be significant.

RESULTS

Fluid shear stress increases SMAD2/3 activity and alters expression of epithelial-to-mesenchymal transition (EMT) markers

To study fluid-flow induced cellular alterations, ciliated proximal tubular epithelial cells (PTEC; Fig. 1a) were exposed to a fluid shear stress of ~ 1.9 dyn/cm², using a cone-plate device. After 6 or 16 hr fluid-flow exposure, gene expression was analyzed using quantitative PCR (qPCR). We first confirmed increased mRNA levels of *Ptgs2*, the gene encoding cyclooxygenase 2 (COX2), a known flow responsive gene (Fig. 1b)⁴².

A crucial step in TGF- β signaling is the activation and translocation of phosphorylated SMAD2 and 3 (p-SMAD2/3) to the nucleus to induce the expression of SMAD3 target genes, *i.e.*, *Pai1*, *Fn1* and *Col1a1*. Indeed, expression of these genes was significantly increased upon fluid-flow at both time points indicating activation of this pathway (Fig. 1b). Increased TGF- β signaling was confirmed using the SMAD3-SMAD4 transcriptional reporter CAGA₁₂-Luc (Fig. 1c)³⁷. In addition, elevated levels of p-SMAD2 and p-SMAD3 were detected by western blot analysis (Fig. 1d). Furthermore, nuclear translocation of p-SMAD2 was observed by immunofluorescence microscopy (Fig. 1e). Similar responses were seen in *Pkd1*^{-/-} PTECs, in which expression of the *Pkd1*-gene, encoding a potential flow sensor¹², is disrupted (Supplementary Material 1, Fig. S1). While expression of the SMAD2/3 targets was clearly elevated upon fluid-flow, expression of the canonical and non-canonical Wnt targets (*Ccnd1*, *Axin2*, *Birc5* (*Survivin*), *Lin7a*, *Ppard*, *Glis2*, *Insc*) and hedgehog targets (*Gli1*, *Gli2*, *Gli3*) was virtually not altered (Supplementary Material 1, Fig. S2).

Increased SMAD2/3 activity often is associated with dedifferentiation and EMT-like processes, regulated via the transcription factors Snail and/or Slug⁴³. Indeed, we also observed differential expression of EMT marker genes *Snai1*, *Snai2*, *Cdh1* and *Vim*, encoding the proteins Snail, Slug, E-cadherin and vimentin, respectively (Fig. 1f). mRNA levels of *Snai1* and *Vim* were increased while expression of the epithelial marker *Cdh1* was decreased. Even more, nuclear accumulation of Snail was detected upon fluid-flow (Fig. 1g). Similar flow responses were seen in *Pkd1*^{-/-} PTECs (Supplementary Material 1, Fig. S1). Interestingly, while Snail and Slug frequently show co-expression⁴⁴, our data clearly show fluid-flow induced down-regulation of *Snai2*, the gene encoding the protein Slug. These data suggest that in this context Snail is responsible for the expression of mesenchymal markers and for repression of the epithelial E-cadherin gene.

TGF- β / activin-induced dose- and time-dependent activation of SMAD2/3 signaling

Next, we wondered whether TGF- β or activin, the cytokines that can induce SMAD2/3 phosphorylation, could generate the same gene expression pattern as fluid-flow. Indeed, the same expression profile was observed upon TGF- β 1 stimulation, including upregulation of *Snai1* and downregulation of *Snai2* (Fig. 2a). A dose response curve and comparison of

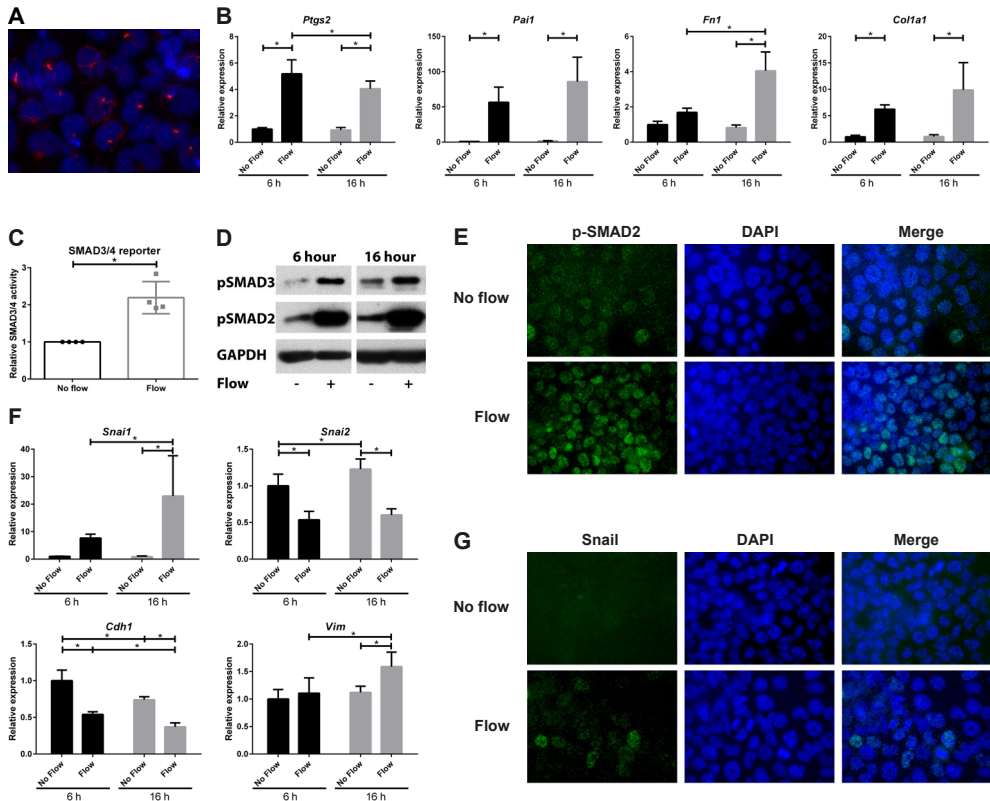


Figure 1. Activation of SMAD2/3 signaling by fluid-flow in ciliated PTECs.

(A) Serum starvation induces cilia formation in proximal tubular epithelial cells (PTECs). Cilia are visualized using anti-acetylated α -tubulin antibodies (red) and nuclei are stained with DAPI (blue). (B) Relative expression of *Ptgs2* (COX2) and *Pai1* (plasminogen activator inhibitor 1; Serpine1), *Fn1* (EDA region; fibronectin) and *Col1a1* (collagen, type I, alpha 1) is increased upon fluid-flow, as measured by quantitative PCR. Cone-plate induced fluid-flow at $t = 6$ or 16 hr; *Hprt* served as housekeeping gene to correct for cDNA input; data normalized to unstimulated PTECs at 6 hr; $n = 5$ per condition; * indicates $P < 0.05$ using two-way ANOVA. (C) SMAD3-SMAD4 (GACA₁₂-Luciferase) transcriptional reporter activity was elevated, as measured upon 20 hr of fluid-flow stimulation. Data normalized to unstimulated PTECs (fold change); $n = 4$ per condition; * indicates $P < 0.05$ using a two-tailed Student's t -test. (D) Western blot analysis of p-SMAD2 and p-SMAD3 shows increased phosphorylation upon 6 hr and 16 hr fluid-flow stimulation. GAPDH served as loading control. (E) Nuclear accumulation of p-SMAD2 (green; $t = 6$ hr, IF). Nuclei are visualized with DAPI (blue). (F) Relative expression of *Snai1* (Snail) and *Vim* (vimentin) is increased, while relative expression of *Snai2* (Slug) and *Cdh1* (E-cadherin) is reduced in PTECs stimulated with fluid-flow, as measured by quantitative PCR. Cone-plate induced fluid-flow at $t = 6$ or 16 hr; *Hprt* served as housekeeping gene to correct for cDNA input; data normalized to unstimulated PTECs at 6 hr; $n = 5$ per condition; * indicates $P < 0.05$ using two-way ANOVA. (G) Nuclear accumulation of Snail (green; $t = 6$ hr, IF). Nuclei are visualized with DAPI (blue).

the cytokines indicated that the cells were more sensitive to TGF- β 1 or - β 2 as to activin A or B (Fig. 2b, c).

A time course experiment showed that expression of the canonical SMAD2/3 target, *Pai1*, was already significantly induced after 30 min of TGF- β 1 stimulation (Fig. 2d), while *Col1a1*

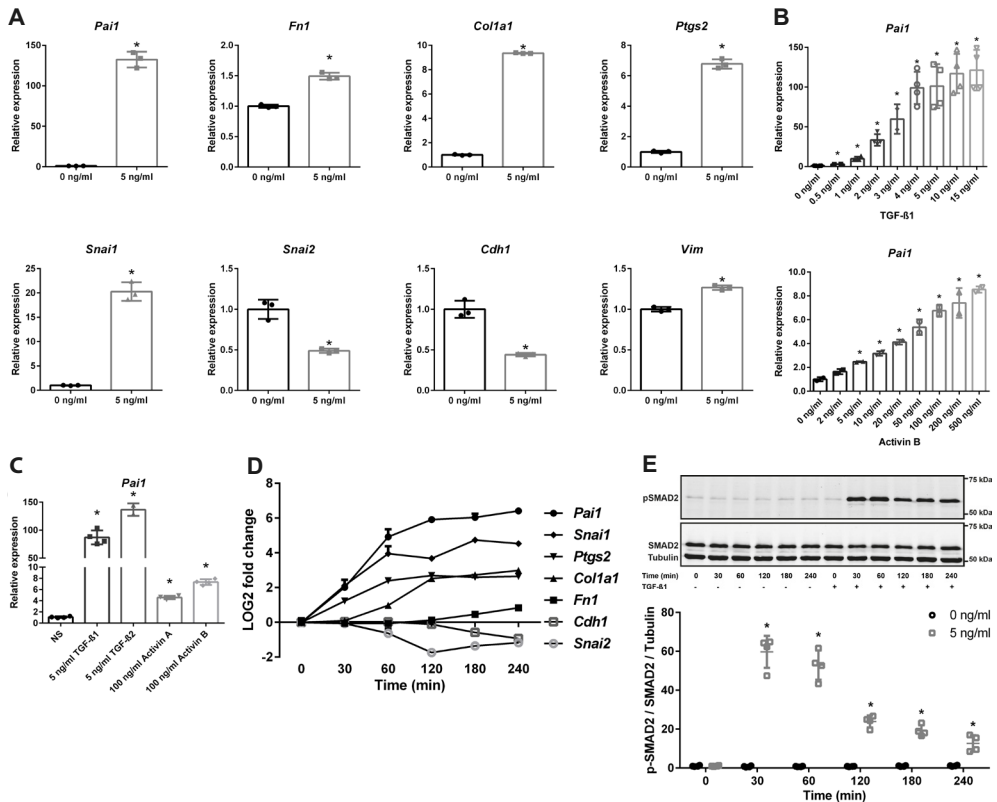


Figure 2. Dose- and time-dependent activation of SMAD2/3 signaling by TGF- β and activin.

(A) Increased expression of *Pai1*, *Fn1*, *Col1a1*, *Ptgs2*, *Snai1* and *Vim*, and reduced expression of *Snai2* and *Cdh1*, upon stimulation with 5 ng/ml TGF- β 1 ($n = 3$, $t = 4$ hr). (B) A dose response experiment shows increased sensitivity of *Pai1* mRNA expression for TGF- β 1 ($n = 4$) compared to activin B ($n = 2$) stimulation ($t = 4$ hr). (C) *Pai1* expression shows stronger induction upon TGF- β 1 or TGF- β 2, compared to activin A or activin B ($n = 4$ per condition, $t = 4$ hr). (D) Time response (0 - 240 min) of target genes upon 5 ng/ml TGF- β 1 stimulation ($n = 2$). Expression was significantly different ($P < 0.05$; one-way ANOVA) with 5 ng/ml TGF- β 1 stimulation compared to non-treated controls for *Pai1*, *Ptgs2* and *Snai1* at 30 min; for *Col1a1* and *Snai2* at 60 min; for *Fn1* and *Cdh1* at 180 min. (E) Representative western blot of p-SMAD2 and SMAD2 upon 5 ng/ml TGF- β 1 stimulation (time response of 0 - 240 min). Tubulin served as loading control. For quantification, p-SMAD2 levels were corrected for total SMAD2 and tubulin levels ($n = 4$). Relative mRNA expression was measured by quantitative PCR, where *Hprt* served as housekeeping gene to correct for cDNA input (A-D). * indicates $P < 0.05$ compared to non-treated control using a two-tailed Student's t -test. NS = not stimulated control.

followed at 60 min and *Fn1* at 180 min. Surprisingly, *Ptgs2* and *Snai1* expression were also induced after 30 min (Fig. 2d) suggesting that these genes could be SMAD2/3 targets as well, because SMAD2 is phosphorylated within 30 min after TGF- β stimulation (Fig. 2e). The downregulated genes, *Snai2* and *Cdh1*, showed a significant decrease in expression starting at 60 and 180 min, respectively. Our data indicate that, *Pai1*, *Ptgs2*, *Snai1* and *Col1a1* are early responsive genes upon TGF- β stimulation, while *Fn1* is a late responsive gene.

Altered expression of TGF- β / Activin ligands and receptors upon fluid-flow

Activation of SMAD2/3 is largely regulated via TGF- β or activin receptor complexes, upon binding of their respective ligands²³. Therefore, expression of the genes coding for ligands TGF- β 1, -2 and -3 or coding for activin A and B (*i.e.* *Inhba* and *Inhbb*) was measured by qPCR. Our data show a significant flow-induced increase in expression of *Tgfb1* and *Tgfb3* as well as *Inhba* and *Inhbb* upon 16 hour fluid-flow stimulation, while this trend was already visible upon 6 hour fluid-flow (Fig. 3a). At both time-points *Tgfb2* transcript levels were significantly decreased. Next we measured protein levels of TGF- β ligands in the medium collected after 16 hr fluid shear (Fig. 3c). Total TGF- β 1 and TGF- β 2 levels were significantly decreased upon fluid-flow in the medium, while active TGF- β 1 was lower, but not significantly changed by flow. TGF- β levels at 16 hr fluid shear stress were significantly higher compared to 6 hr (Fig. 3c), suggesting there is production of latent TGF- β protein in time. Active and total TGF- β 3 as well as active TGF- β 2 were below detection levels (data not shown). In cell lysates, total TGF- β levels were mainly below detection level, except TGF- β 1 levels of a few of the measured fluid flow samples at 16 hour (data not shown).

We also analyzed expression of the different receptors. The type-I receptor ALK4 or ALK5 is recruited and trans-phosphorylated by their specific type-II receptor upon binding of activin or TGF- β ligands, respectively. Expression of *Alk5* (*Tgfb1*) transcript was significantly increased upon fluid-flow, while *Alk4* (*Acvr1b*) was decreased (Fig. 3b). Expression of the type-II receptors did not change and *Alk7* (*Acvr1c*) was not expressed in PTECs (data not shown). Similar shear stress responses were seen in *Pkd1*^{-/-} PTEC cells (Supplementary Material 1, Fig. S3). Overall, our data are inconclusive about the role of the ligands and receptors during fluid-flow induced SMAD2/3 activation. Nevertheless, increased SMAD2/3 activation could be the result of receptor activation.

Shear stress induced SMAD2/3 target gene expression is flow-rate dependent, but partially cilia independent

We subsequently performed experiments using a parallel plate flow-chamber^{34,35} and confirmed the fluid-shear induced expression of SMAD2/3 target genes and EMT markers. With this device, fluid-shear stress induced SMAD2/3 target gene expression is lower compared to the cone-plate flow system and for several genes only the 16 hr responses are significant (Fig. 4a). Likely, this can be attributed to the larger volume of culture medium that

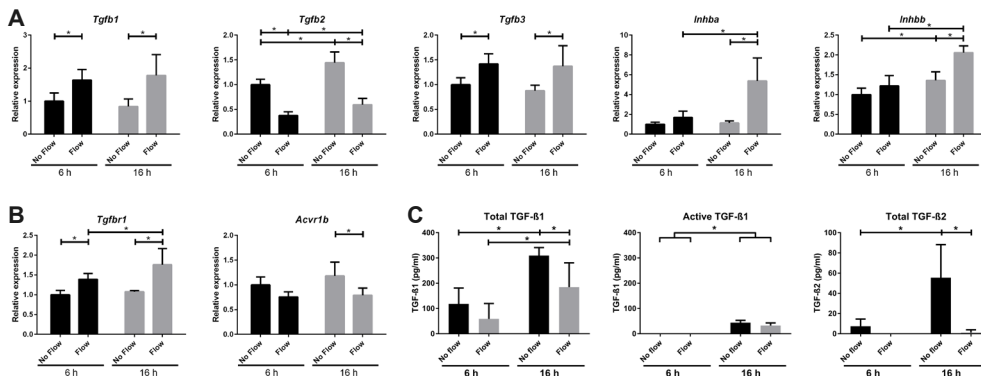


Figure 3. Fluid-flow altered expression of the TGF- β and activin ligands as well as their receptors *Alk5* and *Alk4*.

(A) Relative expression of *Tgfb1*, *Tgfb2*, *Tgfb3*, *Inhba*, *Inhbb* and (B) *Tgfr1* (*Alk5*) and *Acvr1b* (*Alk4*) mRNA in PTECs upon fluid-flow. Cone-plate induced fluid-flow at $t = 6$ or 16 hr; qPCR, *Hprt* served as housekeeping gene to correct for cDNA input; data normalized to unstimulated PTECs at 6 hr; $n = 5$ per condition; * indicates $P < 0.05$ using two-way ANOVA, followed by post-hoc Fisher's LSD multiple comparison. (C) Levels of TGF- β 1 (total and active) and TGF- β 2 (total) in the medium of PTECs collected after 6 or 16 hr fluid-flow. TGF- β 3 and active TGF- β 2 levels in medium and TGF- β 1, 2 and 3 levels in cell lysates were below the detection limit. Cone-plate induced fluid shear stress; TGF- β levels measured by ELISA; $n = 5$ per condition; * indicates $P < 0.05$ using two-way ANOVA, followed by post-hoc Fisher's LSD multiple comparison.

is circulated in the parallel plate flow system, thereby diluting the concentration of ligands produced by the cells. A flow-rate response curve showed a gradual increase of SMAD2/3 target gene expression (Fig. 4b). Surprisingly, removal of cilia by ammonium sulfate (AS) further enhanced the fluid-flow induced expression of *Pai1* and *Ptgs2* (Fig. 4c-e), though *Fn1* induction was lower. Our data suggest that cilia don't fully control the SMAD2/3 response in PTECs, indicating a complex fluid shear stress response, where yet unidentified mechanosensors might be involved.

Shear stress induced SMAD2/3 activation can be largely blocked by ALK4/5/7 inhibitors

To interfere with receptor activation, an ALK5 inhibitor (LY-364947) that abrogates ALK4, ALK5 and ALK7 kinase activity⁴⁵⁻⁴⁸, was added to the medium. Cells were pre-incubated with the inhibitor and stimulated by fluid-flow for 16 hours using the parallel plate flow-chamber. Expression of the SMAD2/3 target genes (*Pai1*, *Fn1* and *Col1a1*), but also *Ptgs2* was strongly reduced by the inhibitor in samples with and without flow, as shown for LY-364947 (Fig. 5a). However, expression was not entirely blocked and a very mild flow response can still be appreciated, which is only significant for *Ptgs2*. These effects were confirmed using another ALK4/5/7 inhibitor, SB431542, which resulted in a similar pattern (data not shown). TGF- β 1 induced expression of SMAD2/3 targets (*Pai1*, *Fn1* and *Ptgs2*) was similarly blocked by the ALK4/5/7 inhibitor (Supplementary Material 1, Fig. S4a).

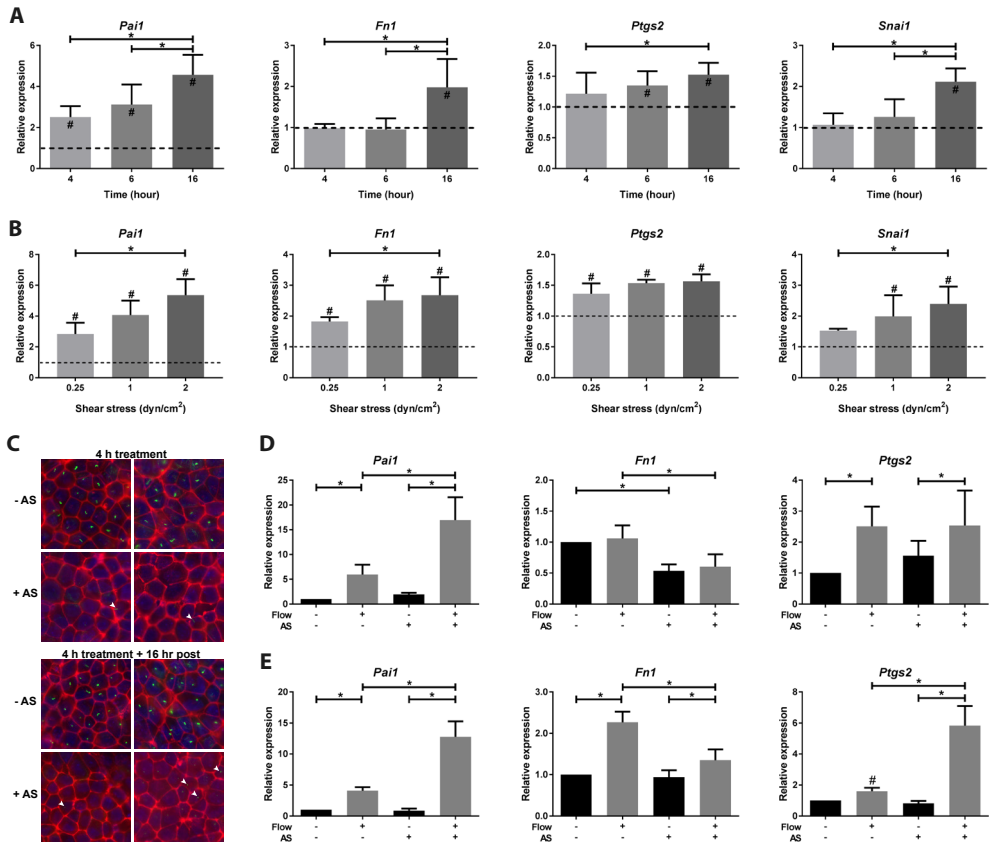


Figure 4. Shear stress induced SMAD2/3 target gene expression in PTECs is flow-rate dependent, but partially cilia independent. (A-B) Relative expression (fold change) of *Pai1*, *Fn1*, *Ptgs2* and *Snai1* is gradually increased in time (A; $t = 4, 6$ or 16 hr; $n = 5$ per condition) and upon increasing flow-rates in PTECs (B; $0.25, 1.0$ or 2.0 dyn/cm²; $n = 3$ per condition), as measured by quantitative PCR. Parallel plate flow-chamber induced fluid shear stress; *Hprt* served as housekeeping gene to correct for cDNA input; data were normalized to static controls (fold change). # significant difference compared to unstimulated control (dashed line) or * significant difference between treatment groups ($P < 0.05$ by two-way ANOVA, followed by post-hoc Fisher's LSD multiple comparison). (C) To remove cilia, cells were treated with 50 mM ammonium sulfate (AS) for 4 hr, followed by 16 hr post incubation. Cilia were visualized by IF using anti-acetylated α -tubulin antibodies (green), F-actin using phalloidin antibodies (red) and nuclei were stained with DAPI (blue). Control cells clearly showed cilia staining, while AS-treated cells only showed weak or stunted cilia staining (arrow head). (D-E) Relative expression of *Pai1*, *Fn1* and *Ptgs2* is increased upon 6 (D) or 16 (E) hour fluid shear stress in controls and cells treated with 50 mM ammonium sulfate (AS), as measured by quantitative PCR. Parallel plate flow-chamber induced fluid shear stress at 2.0 dyn/cm² in PTECs; $n = 5$ per condition; *Hprt* served as housekeeping gene to correct for cDNA input; data were normalized to static controls (fold change). * indicates $P < 0.05$ by two-way ANOVA, followed by post-hoc Fisher's LSD multiple comparison. # indicates significantly altered expression by flow versus no flow ($P < 0.05$) using a two-tailed Student's t -test.

Interestingly, the increased expression of *Snai1* (encoding Snail) was also strongly reduced with the ALK4/5/7 inhibitor, while the expression of *Snai2* (encoding Slug) was less reduced (Fig. 5a). Expression of the Snail target *Cdh1* is increased with the ALK4/5/7 inhibitor, but not altered by fluid-flow, probably caused by the low induction of *Snai1*. These data suggest that, besides *Pai1*, *Fn1*, *Col1a1* and *Ptgs2*, also expression of *Snai1* is largely mediated via SMAD2/3 signaling.

Shear stress induced SMAD2/3 activation is abrogated by TGF- β neutralizing antibodies, but not by an activin ligand trap

To discriminate between ALK5 and ALK4 activation and to prevent ligand binding, TGF- β neutralizing antibodies (TGF- β Ab) or soluble activin receptor-IIB fusion proteins (sActRIIB-Fc), that functions as ligand trap for activin, have been added to the medium of fluid-flow stimulated cells and controls⁴⁹⁻⁵¹. Fluid shear stress induced expression of SMAD3 target genes, *Pai1* and *Fn1*, was significantly decreased with TGF- β Ab, but not with sActRIIB-Fc (Fig. 5b, c). In control samples, *i.e.*, static cells stimulated with exogenous TGF- β or activin, the responses were blocked, proving the efficacy of the inhibitors (Fig. 5e, Supplementary Material 1, Fig. S4c, d). Also, the combination of TGF- β Ab and sActRIIB-Fc showed a similar decrease in fluid-shear induced expression of SMAD3 target genes as TGF- β neutralizing Ab alone (Fig. 5d). From this we conclude that shear-stress induced SMAD2/3 activity was strongly reduced by the ALK4/5/7 receptor kinase inhibitor and by TGF- β neutralizing Ab, but was not affected by the ligand trap sActRIIB-Fc, indicating a major role for TGF- β in the fluid shear stress response.

SMAD2/3 regulated gene expression is modulated by MEK1/2

In addition to activation of SMAD2/3 signaling, TGF- β receptors can also activate MAPK/ERK signaling, which is able to modulate SMAD2/3 transcriptional activity^{52,53}. To interfere with MAPK/ERK signaling, an inhibitor was used that abolished MEK1/2 kinase activity, thereby preventing ERK1/2 phosphorylation⁵⁴. Indeed, a MEK1/2 inhibitor (2 or 10 μ M Trametinib, GSK1120212) reduced TGF- β 1 induced expression of the canonical SMAD3 targets genes (*Pai1*, *Fn1* and *Col1a1*) as well as *Ptgs2* (Fig. 6a, Supplementary Material 1, Fig. S4b). Furthermore, expression of *Snai1* and *Vim* was reduced and, correspondingly, expression of the epithelial marker *Cdh1* was less decreased (Fig. 6a). Surprisingly, fluid-flow induction of *Pai1*, *Col1a1*, *Ptgs2*, *Snai1* and *Vim* was further enhanced with the MEK1/2 inhibitor, while the baseline and fluid-flow induced *Fn1* expression was lower during MEK inhibition (Fig. 6b, Supplementary Material 1, Fig. S5a). This cannot be explained by a low TGF- β dose that is produced by PTECs during fluid flow, because SMAD2/3 target gene expression was also reduced by the MEK1/2 inhibitor during low dose (0.25-2 ng/ml) TGF- β 1 stimulation

(Supplementary Material 1, Fig. S5b). This suggests a complex regulation of SMAD2/3 target genes during shear stress, which is differently modulated by MEK1/2 than in static cells upon exogenous TGF- β stimulation.

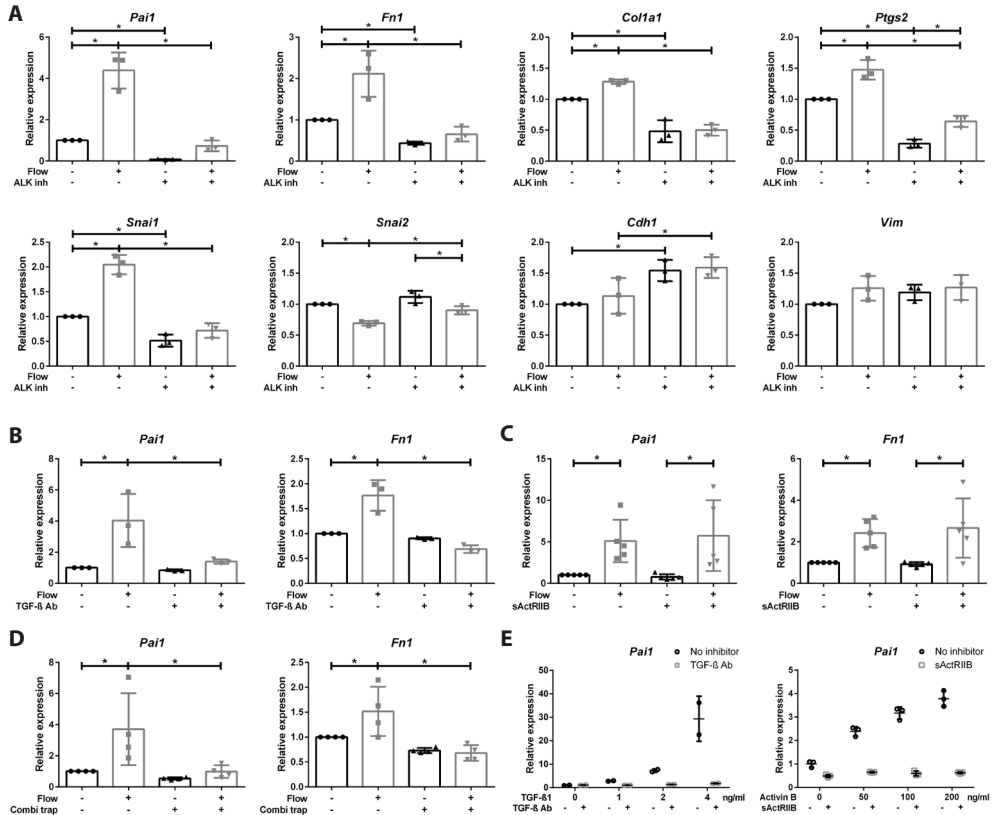


Figure 5. ALK4/5/7 inhibitor and TGF- β neutralizing antibodies, but not sActRIIB-Fc, effectively block SMAD2/3 signaling upon fluid-flow stimulation.

(A) ALK4/5/7 inhibitor (LY-364947; $n = 3$) significantly reduces baseline and fluid flow increased expression of *Pai1*, *Fn1*, *Col1a1*, *Ptgs2*, and *Snai1* while the expression of *Snai2* is less decreased. (B) TGF- β neutralizing antibodies (TGF- β Ab; $n = 3$) inhibited fluid-flow induced expression of SMAD2/3 target genes (*Pai1* and *Fn1*), while (C) soluble activin type-II-B-receptor fusion protein (sActRIIB-Fc; $n = 5$) did not. (D) Combining TGF- β Ab with sActRIIB-Fc ($n = 4$) did not further increase the inhibitory effect. (E) TGF- β 1 ($n = 2$) or activin B ($n = 3$) ligand induced *Pai1* expression was effectively inhibited by TGF- β Ab or sActRIIB-Fc, respectively ($t = 4$ hr). Parallel plate flow-chamber induced fluid shear stress in PTECs at $t = 16$ hr (A-D); qPCR, *Hprt* served as housekeeping gene to correct for cDNA input; data normalized to unstimulated controls (fold change); $n = 2-5$ per condition as indicated. * indicates $P < 0.05$ by two-way ANOVA, followed by post-hoc Fisher's LSD multiple comparison. ALK inh = ALK4/5/7 inhibitor (LY-364947); Combi trap = combined ligand traps (TGF- β Ab and sActRIIB-Fc).



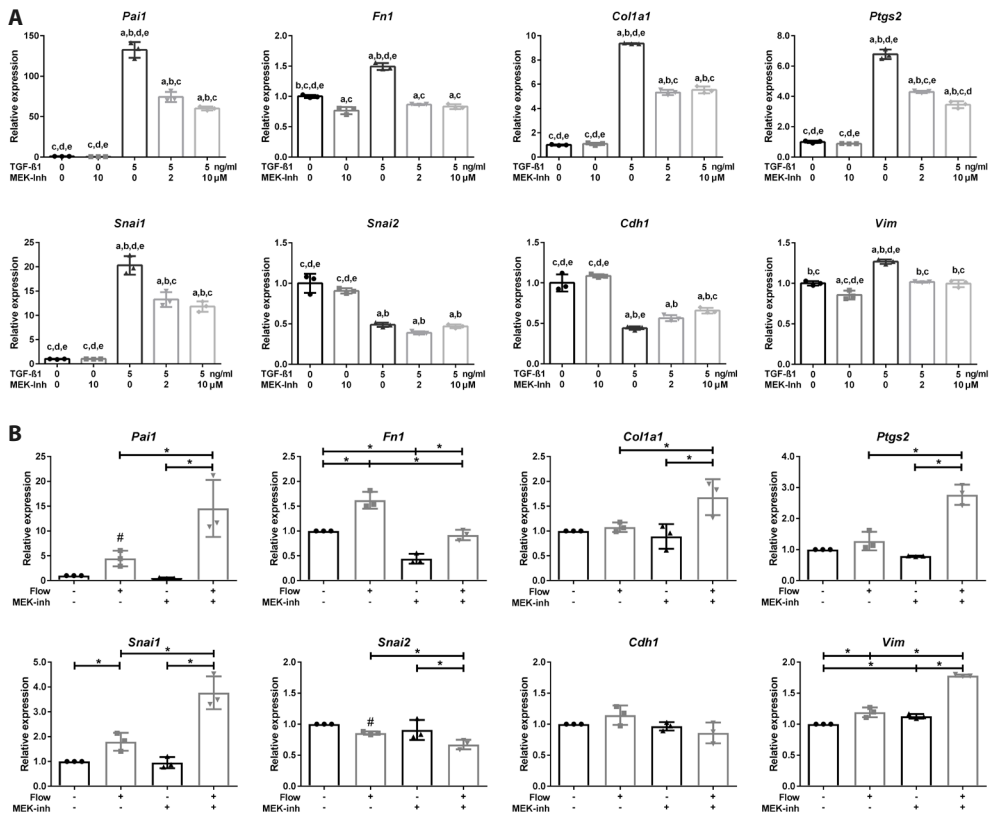


Figure 6. MEK inhibition modulates fluid-shear induced and TGF- β -stimulated expression of SMAD2/3 target genes.

(A) MEK inhibition (Trametinib, GSK1120212) reduces TGF- β 1 increased expression of *Pai1*, *Fn1*, *Col1a1*, *Ptgs2*, *Snai1* and *Vim*, while expression of *Cdh1* is less decreased. *Snai2* expression was not significantly changed upon MEK inhibition. Relative mRNA expression measured at $t = 4$ hr; $n = 3$; *Hprt* served as housekeeping gene to correct for cDNA input; data normalized to unstimulated controls. Significant difference ($P < 0.05$) by one-way ANOVA: ^a compared to 0 ng/ml TGF- β 1, ^b compared to 0 ng/ml TGF- β 1 + 10 μ M MEK-inh, ^c compared to 5 ng/ml TGF- β 1, ^d compared to 5 ng/ml TGF- β 1 + 2 μ M MEK-inh or ^e compared to 5 ng/ml TGF- β 1 + 10 μ M MEK-inh.

(B) MEK inhibition (10 μ M Trametinib) reduces fluid-flow increased expression of *Fn1*, while fluid-flow increased expression of *Pai1*, *Col1a1*, *Ptgs2*, *Snai1* and *Vim* is further elevated. Parallel plate flow-chamber induced fluid shear stress in PTECs at $t = 16$ hr; qPCR, *Hprt* served as housekeeping gene to correct for cDNA input; data normalized to unstimulated controls (fold change); $n = 3$ per condition. * indicates $P < 0.05$ by two-way ANOVA, followed by post-hoc Fisher's LSD multiple comparison. # indicates significantly altered expression by flow vs no flow ($P < 0.05$) using a two-tailed Student's t -test. MEK-inh = MEK1/2 inhibitor (2 or 10 μ M Trametinib, GSK1120212).

DISCUSSION

Fluid-flow stimulation has been used to study mechanical shear stress in endothelial cells and osteoblasts for many years^{55,56}. In the last decade, this was extended to epithelial cells⁵⁷. Even more, several inherited renal diseases are a consequence of dysfunctional primary cilia, with Polycystic Kidney Disease (PKD) as most prominent example¹⁵. In PKD, a gradual decline of functional nephrons results in compensatory hyperfiltration and increased shear-stress in the remaining nephrons. In contrast, in a nephron that becomes cystic, tubular dilation will result in reduced fluid flow.

Our results show fluid-flow induced TGF- β /ALK5 mediated signaling, SMAD2/3 phosphorylation and target gene expression in PTECs. This can be inhibited by an ALK4/5/7 inhibitor, which indicates that, like in endothelial cells²¹, autocrine signaling is involved. Even more, TGF- β neutralizing antibodies block the flow response, similar to the inhibition of exogenously added active TGF- β 1 under static conditions. In contrast, sActRIIB-Fc, a ligand trap that sequesters activin did not block the flow response, while the effect of exogenously added activin under static conditions was completely blocked. A previous study reported that fluid shear stress dynamically regulated TGF- β gene expression and SMAD3 activation, depending on the magnitude of fluid shear^{22,26}. In the current study we confirmed in ciliated cells that the flow-induced response was depending on the magnitude of shear (0.25-2 dyn/cm²). In addition, cells were grown on a collagen type-I extracellular matrix, which is known to influence the mechanical forces that are sensed by cells⁵⁸. Upon deciliation of renal epithelial cells by ammonium sulfate³⁶, however, the fluid-flow response remained (Fig. 4c-e). Moreover, expression of early responsive genes was enhanced upon deciliation, suggesting that to a certain extent primary cilia restrain TGF- β /ALK5 signaling. However, expression of the late-responsive gene *Fn1* was less increased, indicating a complex regulation of the shear-induced SMAD2/3 response in PTECs. These data also suggest involvement of yet unidentified mechano-sensors located at other parts of the plasma membrane.

The flow response could be inhibited by the ALK4/5/7 inhibitor and TGF- β neutralizing antibodies, and TGF- β 1 and -3 mRNA levels were increased by fluid-flow. However, latent TGF- β protein levels were lower in culture medium of shear stress treated PTECs. It is conceivable that under flow conditions TGF- β processing and binding of the active ligand is enhanced, and therefore local effects are stronger. For example, growth factor shedding and autocrine signaling via the intercellular space upon mechanical stimulation of epithelial cells, had previously been shown for HB-EGF⁵⁹. However, this explanation is less likely, since latent TGF- β is excreted fast after production⁶⁰ and we showed accumulation in the medium (Fig. 3c, Supplementary Material 1, Fig. S3c). An alternative explanation could be associated to enhanced sensitivity for TGF- β , since we observed increased mRNA expression of the ALK5 receptor upon fluid-flow. In addition, increased flow-induced apical endocytosis might play a role, as recently published for PTECs⁶¹.

Also *Pkd1*^{-/-} PTECs showed increased SMAD2/3 activation upon fluid-flow treatment, suggesting that polycystin-1, the protein encoded by *Pkd1*, is not directly involved in this response. Nevertheless, the response is slightly but significantly stronger in *Pkd1*^{-/-} PTECs (Supplementary Material 1, Fig. S1k). Higher responsiveness in *Pkd1* deficient vascular smooth muscle cells and murine embryonic fibroblast cells by TGF- β acting stimuli have been reported previously⁶². Alternatively, higher levels of TGF- β 2, measured in the medium of *Pkd1*^{-/-} PTECs during fluid-flow (Supplementary Material 1, Fig. S3), might be responsible for the enhanced response, which seems more likely given the fact that exogenous TGF- β 1 or activin B stimulation of static cells did not induce an enhanced response in *Pkd1*^{-/-} PTECs (data not shown). In ADPKD kidneys, somatic inactivation of *PKD1* or *PKD2* is a critical step in cyst formation^{63,64}. ADPKD is a progressive disease in which the number and size of cysts increase in time accompanied by increased fibrosis. Consequently, the landscape of cells with and without polycystin expression, and nephrons with increased, reduced or no-flow conditions alters in time as well. This is related to hyperfiltration, tubular dilation or tubular obstruction. Increased fluid shear stress and TGF- β signaling will occur in the nephrons compensating the functional loss. So, the elevated response of *Pkd1*^{-/-} cells upon fluid-flow is most relevant in the early phase upon disruption of the gene and during hyperfiltration in the remaining nephrons. Of course, when nephrons are dilated and the fluid-flow itself is altered, the flow response will change again and probably diminish.

In ADPKD nuclear accumulation of SMAD2/3 in cystic epithelial cells and in interstitial fibroblasts, as well as elevated expression of target genes, points to a role of SMAD2/3 regulated signaling in epithelial dedifferentiation and fibrosis^{24,27,65}. In cystic epithelial cells of end-stage PKD, TGF- β 1 and SMAD2/3 signaling was upregulated and associated with renal EMT and renal fibrosis⁶⁶. Paradoxically, genetic disruption of the ALK5 receptor in renal epithelial cells did not affect cyst formation/growth and only slightly reduced expression of SMAD2/3 target genes, while the activin ligand trap, sActRIIB-Fc, significantly slowed down PKD progression in mice⁶⁵. This indicates that for cyst formation and PKD-progression, the tissue context and the different cell-types involved are critical.

Increased SMAD2/3 activity is often associated with dedifferentiation and EMT-like processes, which is needed for epithelial cell plasticity and homeostasis during tissue development, maintenance and repair⁶⁷. TGF- β can induce Snail expression, which is known to directly repress epithelial markers like E-cadherin⁶⁸, and TGF- β can induce expression of markers of the mesenchymal phenotype, including vimentin⁶⁹. Indeed, we observed fluid-flow induced expression and nuclear accumulation of Snail, as well as increased vimentin and reduced E-cadherin expression. Interestingly, while Snail and the highly homologous protein Slug are frequently co-expressed⁴⁴, *Snai2*, the gene encoding Slug, is clearly down-regulated upon fluid-flow. Therefore, we conclude that in this context Snail, but not Slug, is responsible for the expression of mesenchymal markers and for repression of the epithelial E-cadherin gene.

In renal epithelial cells, TGF- β induced expression of canonical SMAD2/3 targets and EMT markers is the consequence of both SMAD2/3 and ERK1/2 activation, since upstream ALK4/5/7 and MEK1/2 inhibitors both reduce but not completely block the ligand-induced response (Fig. 6, Supplementary Material 1, Fig. S4). While the fluid-flow induced response was largely blocked by the ALK4/5/7 inhibitor, the MEK-inhibitor, however, further enhanced expression of *Pai1*, *Col1a1*, *Ptgs2*, *Snai1* and *Vim*, though *Fn1* expression was less increased (Fig. 5, 6). It is well known that a cross-talk between the canonical (SMAD2/3) and the non-canonical (MAPK/ERK) TGF- β pathways take place at different levels and via direct or indirect pathways⁷⁰. These data support a previous study describing antagonistic interactions between TGF- β 1-mediated expression of fibrogenesis genes and the cAMP/PKA pathway. On the one hand cAMP/PKA promoted TGF- β 1 production and expression of target genes (including collagen-I and fibronectin) in MDCK cells and an embryonic kidney cyst model, being inhibited by an ALK5-inhibitor. On the other hand, upon addition of TGF- β 1 to the culture medium of MDCK cells, fibronectin expression is negatively regulated upon cAMP treatment, via ERK1/2⁷¹. A direct link between TGF- β and MAPK/ERK signaling, is the phosphorylation of ShcA by the activated TGF- β receptor complex⁵². ShcA competes with SMAD2/3 for binding to the TGF- β receptor, and stabilizes the TGF- β receptor complexes in caveolae, where it activates MAPK/ERK signaling⁷². Consequently, reduced ShcA expression results in increased levels of TGF- β receptor complexes in clathrin-coated pits, leading to enhanced SMAD2/3 activation. Alternatively, activated ERK1/2, by TGF- β /ALK5 or by other growth factors, can mediate phosphorylation of the regulatory SMADs (R-SMAD) as well as phosphorylation of the SMAD2/3 linker region, which modulate transcriptional activity of the SMAD complex^{53,73}. Because the multiple interactions between the MAPK/ERK and the TGF- β signaling cascades, the integration of these pathways is biological context dependent and complex, and therefore difficult to predict .

Since *Fn1* expression was significantly increased by TGF- β 1 at a later time point than the other target genes (Fig. 2D), it is likely that besides SMAD2/3 other transcription factors are involved in its mRNA expression. The literature indeed shows that *Fn1* expression was dependent on Snail or Slug expression and other transcription factors^{74,75}. Furthermore, to induce *Fn1* expression, it likely needs stabilized SMAD2/3 phosphorylation, which is achieved by ERK-mediated nuclear SMAD linker phosphorylation. This could be the explanation that TGF- β and fluid-flow induced *Fn1* expression is largely blocked upon MEK inhibition as proposed in the model depicted in Fig. 7.

The *Ptgs2* gene, encoding the COX2 protein, is widely used as a control for fluid-flow. COX2 derived prostaglandins have been shown to stimulate cell proliferation, fluid secretion, and cyst formation *in vitro*, probably via increasing the cAMP levels. Furthermore, COX2 derived products show increased expression in animal models for PKD, and COX2 inhibitors showed minimal beneficial effect on PKD progression in rodent models^{76,77}. Our data show that *Ptgs2* expression is also TGF- β dependent and is regulated via shear stress in PTECs.

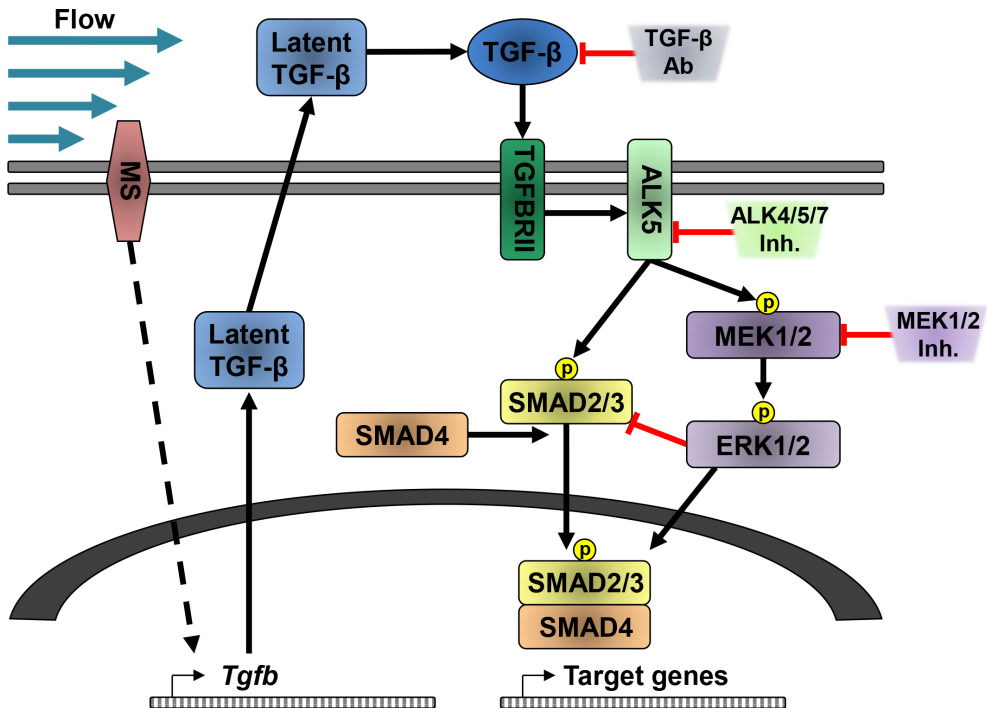


Figure 7. Schematic representation of the fluid shear stress response in PTECs.

Fluid shear stress activates a yet unidentified mechano-sensor (MS) at the cell membrane. This leads to increased *Tgfb* mRNA expression. Upon activation, TGF- β will bind to TGFBR11, which recruits and activates ALK5. This is followed by SMAD2/3 phosphorylation, which recruits SMAD4 for nuclear entry, to enable target gene expression. Both the TGF- β blocking antibodies (TGF- β Ab) and ALK4/5/7 inhibitors can block the shear stress response, inhibiting SMAD2/3 target gene expression.

Alternatively, ALK5 can activate MEK1/2, a kinase known to phosphorylate ERK1/2⁷², which can be prevented by MEK inhibition. ERK1/2 can either enhance or repress SMAD2/3-mediated target gene expression, depending on the biological context and the cellular location where SMAD linker regions are phosphorylated by ERK1/2^{53,73}. Cytoplasmic phosphorylation of SMAD2/3 by ERK1/2 can inhibit nuclear translocation, thereby restraining SMAD2/3 target gene expression. Upon MEK inhibition, more SMAD2/3 can translocate to the nucleus, thereby enhancing expression of early expressed SMAD2/3 target genes (*Pai1*, *Col1a1*, *Ptgs2* and *Snai1*; see Fig. 2D). However, nuclear phosphorylation of SMAD2/3 linker regions increases the duration of their target gene expression, which is likely needed for fluid shear stress induced expression of late genes (*Fn1*), since its induction is inhibited by the MEK inhibitor.

In conclusion, we found fluid-shear stress induced SMAD2/3 activation and target gene expression in ciliated and non-ciliated PTECs, suggesting that cilia are not critically inducing the shear stress-induced SMAD2/3 response of renal epithelial cells. Overall, our data indicate a complex response, in which yet unidentified mechano-sensors are involved. The response is dependent on autocrine TGF- β /ALK5 mediated signaling, but not on activin/ALK4. Under fluid-shear stress conditions, the expression of most SMAD2/3 target genes is partially repressed by MAPK/ERK possibly via TGF- β /ALK5 mediated activation of MEK1/2 (Fig. 7) or via activation of this pathway by other yet unidentified autocrine (growth) factors. In renal (cystic) disease, compensatory hyperfiltration and increased shear stress might contribute to induced SMAD2/3 activation, a well-known factor in the control of epithelial cell plasticity and fibrosis.

Acknowledgements

We thank Ron Wolterbeek (Medical Statistics, LUMC) for support with statistical analysis and Prof. Jenneke Klein-Nulend for facilitating the research with the parallel-plate fluid flow system. We are thankful to dr. Robin Maser, who provided samples for preliminary testing. sActRIIB-Fc was kindly provided by Prof. Olli Ritvos (Haartman Institute, University of Helsinki, Helsinki, Finland) and TGF- β neutralizing antibodies by dr. Emile de Heer (Pathology, LUMC). We would like to thank undergraduate students, Maaïke Rijkers and Aliesha de Bray, for experimental support.

This work was supported by funding from the Netherlands Organization for Scientific Research (NWO) [grant number 820.02.016 to S.J.K.]; the Dutch Technology Foundation STW [grant number 11823 to W.N.L.], which is part of the Netherlands Organization for Scientific Research (NWO) and which is partially funded by the Ministry of Economic Affairs; by the Dutch Kidney Foundation [grant numbers NSN IP11.34 and 14OIP12 to W.N.L.]; as well as the Alpe d'HuZes/Bas Mulder award 2011 [grant number UL2011-5051 to L.J.A.C.H.], which is part of the Dutch KWF cancer foundation.

Compliance with ethical standards

Competing interests

The authors declare no competing or financial interests.

REFERENCES

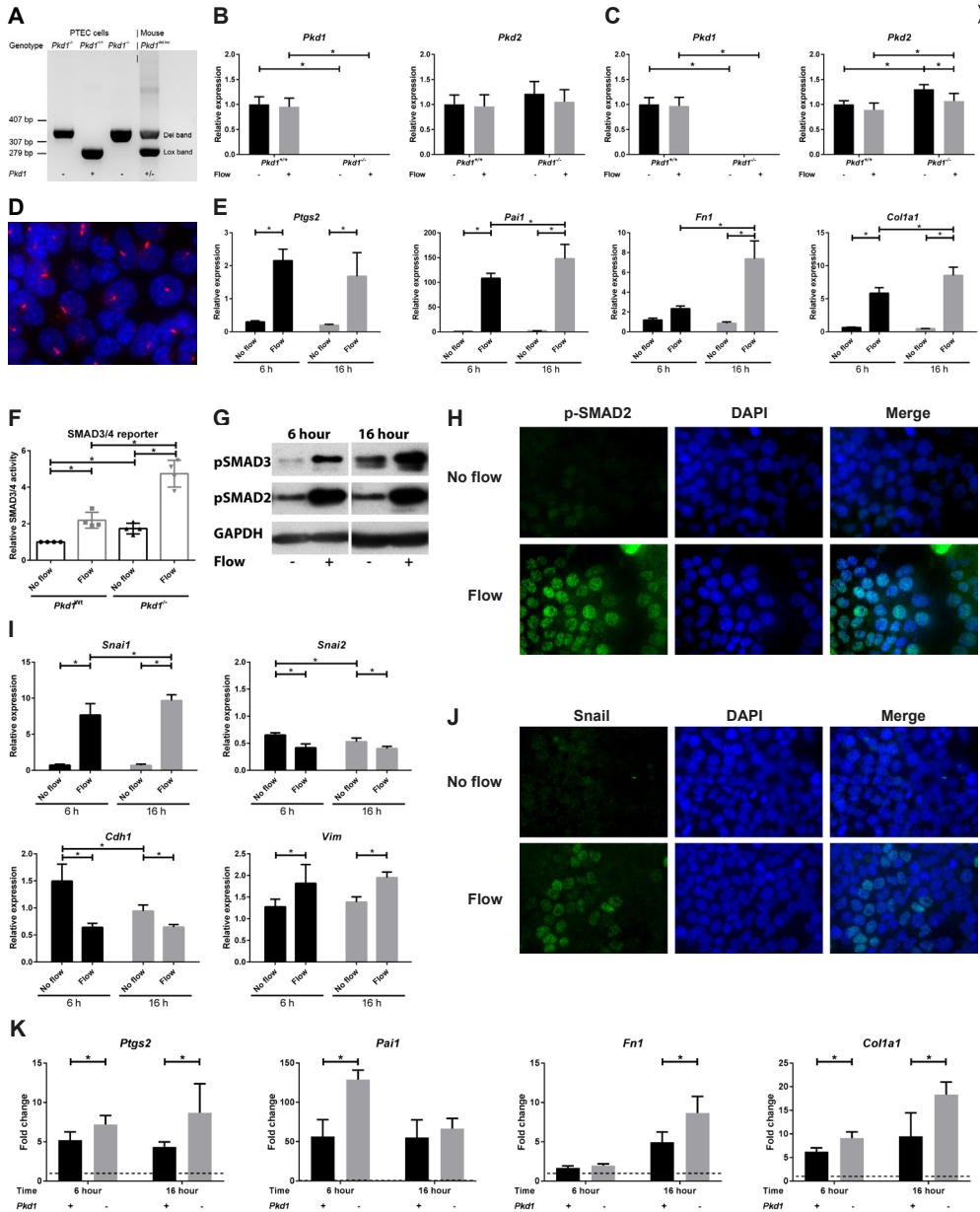
1. Piperi C. & Basdra E.K. Polycystins and mechanotransduction: From physiology to disease. *World J. Exp. Med.* **5**, 200-205 (2015).
2. Sharma A., Mucino M.J., & Ronco C. Renal functional reserve and renal recovery after acute kidney injury. *Nephron Clin. Pract.* **127**, 94-100 (2014).
3. Bisgrove B.W. & Yost H.J. The roles of cilia in developmental disorders and disease. *Development* **133**, 4131-4143 (2006).
4. Yoder B.K., Hou X., & Guay-Woodford L.M. The polycystic kidney disease proteins, polycystin-1, polycystin-2, polaris, and cystin, are co-localized in renal cilia. *J. Am. Soc. Nephrol.* **13**, 2508-2516 (2002).
5. Seeger-Nukpezah T. & Golemis E.A. The extracellular matrix and ciliary signaling. *Curr. Opin. Cell Biol.* **24**, 652-661 (2012).
6. Patel A. & Honore E. Polycystins and renovascular mechanosensory transduction. *Nat. Rev. Nephrol.* **6**, 530-538 (2010).
7. Weinbaum S., Duan Y., Satlin L.M., Wang T., & Weinstein A.M. Mechanotransduction in the renal tubule. *Am. J. Physiol Renal Physiol* **299**, F1220-F1236 (2010).
8. Tran P.V., Sharma M., Li X., & Calvet J.P. Developmental signaling: does it bridge the gap between cilia dysfunction and renal cystogenesis? *Birth Defects Res. C. Embryo. Today* **102**, 159-173 (2014).
9. Kotsis F., Boehlke C., & Kuehn E.W. The ciliary flow sensor and polycystic kidney disease. *Nephrol. Dial. Transplant.* **28**, 518-526 (2013).
10. Rohatgi R. & Flores D. Intratubular hydrodynamic forces influence tubulointerstitial fibrosis in the kidney. *Curr. Opin. Nephrol. Hypertens.* **19**, 65-71 (2010).
11. Lee S.H. & Somlo S. Cyst growth, polycystins, and primary cilia in autosomal dominant polycystic kidney disease. *Kidney Res. Clin. Pract.* **33**, 73-78 (2014).
12. Nauli S.M. *et al.* Polycystins 1 and 2 mediate mechanosensation in the primary cilium of kidney cells. *Nat. Genet.* **33**, 129-137 (2003).
13. Peyronnet R. *et al.* Mechanoprotection by Polycystins against Apoptosis Is Mediated through the Opening of Stretch-Activated K2P Channels. *Cell Reports* **1**, 241-250 (2012).
14. Nauli S.M. *et al.* Loss of polycystin-1 in human cyst-lining epithelia leads to ciliary dysfunction. *J. Am. Soc. Nephrol.* **17**, 1015-1025 (2006).
15. Ma M., Tian X., Igarashi P., Pazour G.J., & Somlo S. Loss of cilia suppresses cyst growth in genetic models of autosomal dominant polycystic kidney disease. *Nat. Genet.* **45**, 1004-1012 (2013).
16. Arts H.H. & Knoers N.V. Current insights into renal ciliopathies: what can genetics teach us? *Pediatr. Nephrol.* **28**, 863-874 (2013).
17. Happe H. & Peters D.J. Translational research in ADPKD: lessons from animal models. *Nat. Rev. Nephrol.* **10**, 587-601 (2014).
18. Clement C.A. *et al.* TGF-beta signaling is associated with endocytosis at the pocket region of the primary cilium. *Cell Rep.* **3**, 1806-1814 (2013).
19. Gill P.S. & Rosenblum N.D. Control of murine kidney development by sonic hedgehog and its GLI effectors. *Cell Cycle* **5**, 1426-1430 (2006).
20. Ma R. *et al.* PKD2 functions as an epidermal growth factor-activated plasma membrane channel. *Mol. Cell Biol.* **25**, 8285-8298 (2005).
21. Egorova A.D. *et al.* Tgfbeta/Alk5 signaling is required for shear stress induced klf2 expression in embryonic endothelial cells. *Dev. Dyn.* **240**, 1670-1680 (2011).
22. Grabias B.M. & Konstantopoulos K. Notch4-dependent antagonism of canonical TGF-beta1 signaling defines unique temporal fluctuations of SMAD3 activity in sheared proximal tubular epithelial cells. *Am. J. Physiol Renal Physiol* **305**, F123-F133 (2013).

23. Shi Y. & Massague J. Mechanisms of TGF-beta signaling from cell membrane to the nucleus. *Cell* **113**, 685-700 (2003).
24. Hassane S. *et al.* Elevated TGFbeta-Smad signalling in experimental Pkd1 models and human patients with polycystic kidney disease. *J. Pathol.* **222**, 21-31 (2010).
25. Egorova A.D. *et al.* Lack of primary cilia primes shear-induced endothelial-to-mesenchymal transition. *Circ. Res.* **108**, 1093-1101 (2011).
26. Grabias B.M. & Konstantopoulos K. Epithelial-mesenchymal transition and fibrosis are mutually exclusive responses in shear-activated proximal tubular epithelial cells. *FASEB J.* **26**, 4131-4141 (2012).
27. Liu Y. *et al.* Rosiglitazone inhibits transforming growth factor-beta1 mediated fibrogenesis in ADPKD cyst-lining epithelial cells. *PLoS. One.* **6**, e28915 (2011).
28. Persson U. *et al.* The L45 loop in type I receptors for TGF-beta family members is a critical determinant in specifying Smad isoform activation. *FEBS Lett.* **434**, 83-87 (1998).
29. Hawinkels L.J. *et al.* Interaction with colon cancer cells hyperactivates TGF-beta signaling in cancer-associated fibroblasts. *Oncogene* **33**, 97-107 (2014).
30. Leonhard W.N. *et al.* Curcumin inhibits cystogenesis by simultaneous interference of multiple signaling pathways: In vivo evidence from a Pkd1-deletion model. *Am. J. Physiol Renal Physiol* **300**, F1193-F1202 (2011).
31. Malek A.M., Gibbons G.H., Dzau V.J., & Izumo S. Fluid shear stress differentially modulates expression of genes encoding basic fibroblast growth factor and platelet-derived growth factor B chain in vascular endothelium. *J Clin. Invest* **92**, 2013-2021 (1993).
32. Malek A.M., Ahlquist R., Gibbons G.H., Dzau V.J., & Izumo S. A cone-plate apparatus for the in vitro biochemical and molecular analysis of the effect of shear stress on adherent cells. *Methods in Cell Science* **17**, 165-176 (1995).
33. Bacabac R.G. *et al.* Dynamic shear stress in parallel-plate flow chambers. *J. Biomech.* **38**, 159-167 (2005).
34. Klein-Nulend J., Semeins C.M., Ajubi N.E., Nijweide P.J., & Burger E.H. Pulsating fluid flow increases nitric oxide (NO) synthesis by osteocytes but not periosteal fibroblasts--correlation with prostaglandin upregulation. *Biochem. Biophys. Res. Commun.* **217**, 640-648 (1995).
35. Juffer P., Bakker A.D., Klein-Nulend J., & Jaspers R.T. Mechanical loading by fluid shear stress of myotube glyocalyx stimulates growth factor expression and nitric oxide production. *Cell Biochem. Biophys.* **69**, 411-419 (2014).
36. Overgaard C.E. *et al.* Deciliation is associated with dramatic remodeling of epithelial cell junctions and surface domains. *Mol. Biol. Cell* **20**, 102-113 (2009).
37. Dennler S. *et al.* Direct binding of Smad3 and Smad4 to critical TGF beta-inducible elements in the promoter of human plasminogen activator inhibitor-type 1 gene. *EMBO J.* **17**, 3091-3100 (1998).
38. Happe H. *et al.* Altered Hippo signalling in polycystic kidney disease. *J. Pathol.* **224**, 133-142 (2011).
39. Livak K.J. & Schmittgen T.D. Analysis of relative gene expression data using real-time quantitative PCR and the 2(-Delta Delta C(T)) Method. *Methods* **25**, 402-408 (2001).
40. Hawinkels L.J. *et al.* Tissue level, activation and cellular localisation of TGF-beta1 and association with survival in gastric cancer patients. *Br. J. Cancer* **97**, 398-404 (2007).
41. Ramnath N.W. *et al.* Fibulin-4 deficiency increases TGF-beta signalling in aortic smooth muscle cells due to elevated TGF-beta2 levels. *Sci. Rep.* **5**, 16872 (2015).
42. Flores D., Liu Y., Liu W., Satlin L.M., & Rohatgi R. Flow-induced prostaglandin E2 release regulates Na and K transport in the collecting duct. *Am. J. Physiol Renal Physiol* **303**, F632-F638 (2012).
43. Zavadil J. & Bottinger E.P. TGF-beta and epithelial-to-mesenchymal transitions. *Oncogene* **24**, 5764-5774 (2005).
44. Medici D., Hay E.D., & Olsen B.R. Snail and Slug promote epithelial-mesenchymal transition through beta-catenin-T-cell factor-4-dependent expression of transforming growth factor-beta3. *Mol. Biol. Cell* **19**, 4875-4887 (2008).

45. Sawyer J.S. *et al.* Synthesis and activity of new aryl- and heteroaryl-substituted pyrazole inhibitors of the transforming growth factor-beta type I receptor kinase domain. *J. Med. Chem.* **46**, 3953-3956 (2003).
46. Peng S.B. *et al.* Kinetic characterization of novel pyrazole TGF-beta receptor I kinase inhibitors and their blockade of the epithelial-mesenchymal transition. *Biochemistry* **44**, 2293-2304 (2005).
47. Inman G.J. *et al.* SB-431542 is a potent and specific inhibitor of transforming growth factor-beta superfamily type I activin receptor-like kinase (ALK) receptors ALK4, ALK5, and ALK7. *Mol. Pharmacol.* **62**, 65-74 (2002).
48. Vogt J., Traynor R., & Sapkota G.P. The specificities of small molecule inhibitors of the TGFβs and BMP pathways. *Cell Signal.* **23**, 1831-1842 (2011).
49. Lucas C. *et al.* The autocrine production of transforming growth factor-beta 1 during lymphocyte activation. A study with a monoclonal antibody-based ELISA. *J. Immunol.* **145**, 1415-1422 (1990).
50. Arteaga C.L. *et al.* Anti-transforming growth factor (TGF)-beta antibodies inhibit breast cancer cell tumorigenicity and increase mouse spleen natural killer cell activity. Implications for a possible role of tumor cell/host TGF-beta interactions in human breast cancer progression. *J. Clin. Invest* **92**, 2569-2576 (1993).
51. Hulmi J.J. *et al.* Muscle protein synthesis, mTORC1/MAPK/Hippo signaling, and capillary density are altered by blocking of myostatin and activins. *Am. J. Physiol Endocrinol. Metab* **304**, E41-E50 (2013).
52. Lee M.K. *et al.* TGF-beta activates Erk MAP kinase signalling through direct phosphorylation of ShcA. *EMBO J.* **26**, 3957-3967 (2007).
53. Hough C., Radu M., & Dore J.J. Tgf-beta induced Erk phosphorylation of smad linker region regulates smad signaling. *PLoS. One.* **7**, e42513 (2012).
54. Yamaguchi T., Kakefuda R., Tajima N., Sowa Y., & Sakai T. Antitumor activities of JTP-74057 (GSK1120212), a novel MEK1/2 inhibitor, on colorectal cancer cell lines in vitro and in vivo. *Int. J. Oncol.* **39**, 23-31 (2011).
55. Dewey C.F., Jr., Bussolari S.R., Gimbrone M.A., Jr., & Davies P.F. The dynamic response of vascular endothelial cells to fluid shear stress. *J. Biomech. Eng* **103**, 177-185 (1981).
56. Reich K.M., Gay C.V., & Frangos J.A. Fluid shear stress as a mediator of osteoblast cyclic adenosine monophosphate production. *J. Cell Physiol* **143**, 100-104 (1990).
57. Essig M. & Friedlander G. Tubular shear stress and phenotype of renal proximal tubular cells. *J. Am. Soc. Nephrol.* **14**, S33-S35 (2003).
58. Ross T.D. *et al.* Integrins in mechanotransduction. *Curr. Opin. Cell Biol.* **25**, 613-618 (2013).
59. Tschumperlin D.J. *et al.* Mechanotransduction through growth-factor shedding into the extracellular space. *Nature* **429**, 83-86 (2004).
60. Miyazono K., Olofsson A., Colosetti P., & Heldin C.H. A role of the latent TGF-beta 1-binding protein in the assembly and secretion of TGF-beta 1. *EMBO J.* **10**, 1091-1101 (1991).
61. Raghavan V., Rbaibi Y., Pastor-Soler N.M., Carattino M.D., & Weisz O.A. Shear stress-dependent regulation of apical endocytosis in renal proximal tubule cells mediated by primary cilia. *Proc. Natl. Acad. Sci. U. S. A* **111**, 8506-8511 (2014).
62. Liu D. *et al.* A Pkd1-Fbn1 genetic interaction implicates TGF-beta signaling in the pathogenesis of vascular complications in autosomal dominant polycystic kidney disease. *J. Am. Soc. Nephrol.* **25**, 81-91 (2014).
63. Lantinga-van Leeuwen I.S. *et al.* Kidney-specific inactivation of the Pkd1 gene induces rapid cyst formation in developing kidneys and a slow onset of disease in adult mice. *Hum. Mol. Genet.* **16**, 3188-3196 (2007).
64. Wu G. *et al.* Somatic inactivation of Pkd2 results in polycystic kidney disease. *Cell* **93**, 177-188 (1998).
65. Leonhard W.N. *et al.* Inhibition of Activin Signaling Slows Progression of Polycystic Kidney Disease. *J. Am. Soc. Nephrol.* **27**, 3589-3599 (2016).
66. Chea S.W. & Lee K.B. TGF-beta mediated epithelial-mesenchymal transition in autosomal dominant polycystic kidney disease. *Yonsei Med. J.* **50**, 105-111 (2009).
67. Sundqvist A., Ten Dijke P., & van Dam H. Key signaling nodes in mammary gland development and cancer:

- Smad signal integration in epithelial cell plasticity. *Breast Cancer Res.* **14**, 204 (2012).
68. Sato M., Muragaki Y., Saika S., Roberts A.B., & Ooshima A. Targeted disruption of TGF-beta1/Smad3 signaling protects against renal tubulointerstitial fibrosis induced by unilateral ureteral obstruction. *J. Clin. Invest* **112**, 1486-1494 (2003).
69. Rogel M.R. *et al.* Vimentin is sufficient and required for wound repair and remodeling in alveolar epithelial cells. *FASEB J.* **25**, 3873-3883 (2011).
70. Chapnick D.A., Warner L., Bernet J., Rao T., & Liu X. Partners in crime: the TGFbeta and MAPK pathways in cancer progression. *Cell Biosci.* **1**, 42 (2011).
71. Weng L. *et al.* The Effect of cAMP-PKA Activation on TGF-beta1-Induced Profibrotic Signaling. *Cell Physiol Biochem.* **36**, 1911-1927 (2015).
72. Muthusamy B.P. *et al.* ShcA Protects against Epithelial-Mesenchymal Transition through Compartmentalized Inhibition of TGF-beta-Induced Smad Activation. *PLoS. Biol.* **13**, e1002325 (2015).
73. Kretzschmar M., Doody J., Timokhina I., & Massague J. A mechanism of repression of TGFbeta/ Smad signaling by oncogenic Ras. *Genes Dev.* **13**, 804-816 (1999).
74. Lamouille S., Xu J., & Derynck R. Molecular mechanisms of epithelial-mesenchymal transition. *Nat. Rev. Mol. Cell Biol.* **15**, 178-196 (2014).
75. Kim Y.S., Yi B.R., Kim N.H., & Choi K.C. Role of the epithelial-mesenchymal transition and its effects on embryonic stem cells. *Exp. Mol. Med.* **46**, e108 (2014).
76. Sankaran D., Bankovic-Calic N., Ogborn M.R., Crow G., & Aukema H.M. Selective COX-2 inhibition markedly slows disease progression and attenuates altered prostanoid production in Han:SPRD-cy rats with inherited kidney disease. *Am. J. Physiol Renal Physiol* **293**, F821-F830 (2007).
77. Ibrahim N.H. *et al.* Cyclooxygenase product inhibition with acetylsalicylic acid slows disease progression in the Han:SPRD-Cy rat model of polycystic kidney disease. *Prostaglandins Other Lipid Mediat.* **116-117**, 19-25 (2015).

SUPPLEMENTARY FIGURES



◀ **Supplementary Figure S1. Activation of SMAD2/3 signaling by fluid-flow in ciliated *Pkd1*^{-/-} PTECs.**

(A) *Pkd1* gene knockout was confirmed by PCR on DNA of *Pkd1*^{-/-} PTECs, which only showed the deletion band, indicating deletion of exon 2-11 of the *Pkd1* gene. *Pkd1*^{+/+} cells only showed the lox band, indicating that the floxed region was still present. As control the *Pkd1*^{del/lox} mouse showed both bands. Primers used LoxF: ACCCTTCCTGAGCCTCCAC; LoxR: CCACAGGGGAAGCCATCATA; Delf: CACTGTGGTGCGGGGTATC.

(B-C) *Pkd1* mRNA expression (exon 1-3) is absent in *Pkd1*^{-/-} PTECs, while *Pkd2* expression is not reduced in *Pkd1*^{-/-} PTECs. Expression of *Pkd1* or *Pkd2* was virtually not altered by fluid shear stress, as measured by quantitative PCR. Cone-plate induced fluid-flow in *Pkd1*^{+/+} and *Pkd1*^{-/-} PTECs at t = 6 (b) or 16 (c) hr; *Hprt* served as housekeeping gene to correct for cDNA input; data normalized to unstimulated PTECs; n=5 per condition; * indicates P < 0.05 using two-way ANOVA.

(D) Serum starvation induces cilia formation in *Pkd1*^{-/-} PTECs. Cilia are visualized using anti-acetylated α -tubulin antibodies (red) and nuclei are stained with DAPI (blue).

(E) Relative expression of *Ptgs2* (COX2) and *Pai1* (plasminogen activator inhibitor 1; *Serpine1*), *Fn1*(EDA region; fibronectin) and *Col1a1* (collagen, type I, alpha 1) is increased upon fluid-flow, as measured by quantitative PCR. Cone-plate induced fluid-flow in *Pkd1*^{-/-} PTECs at t = 6 or 16 hr; *Hprt* served as housekeeping gene to correct for cDNA input; data normalized to unstimulated PTECs at 6 hr presented in Fig. 1; n=5 per condition; * indicates P < 0.05 using two-way ANOVA.

(F) SMAD3-SMAD4 (GACA₁₂-Luciferase) transcriptional reporter activity was elevated, as measured upon 20 hr of fluid-flow stimulation. Data normalized to unstimulated PTECs; n=4 per condition; * indicates P < 0.05 using two-way ANOVA.

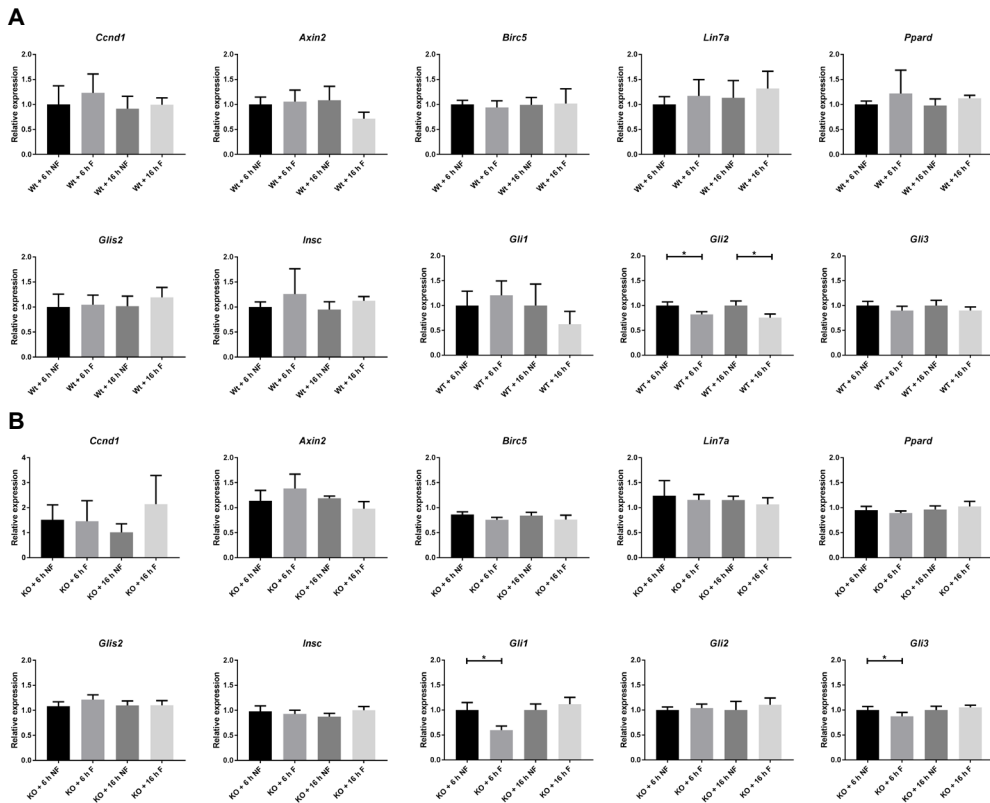
(G) Western blot analysis of p-SMAD2 and p-SMAD3 shows increased phosphorylation upon 6 hr and 16 hr fluid-flow stimulation. GAPDH served as loading control.

(H) Nuclear accumulation of p-SMAD2 (green; t = 6 hr, IF). Nuclei are visualized with DAPI (blue).

(I) Relative expression of *Snai1* (Snail) and *Vim* (vimentin) is increased, while relative expression of *Snai2* (Slug) and *Cdh1* (E-cadherin) is reduced in *Pkd1*^{-/-} PTECs stimulated with fluid-flow, as measured by quantitative PCR. Cone-plate induced fluid-flow in *Pkd1*^{-/-} PTECs at t = 6 or 16 hr; *Hprt* served as housekeeping gene to correct for cDNA input; data normalized to unstimulated PTECs at 6 hr presented in Fig. 1; n=5 per condition; * indicates P < 0.05 using two-way ANOVA.

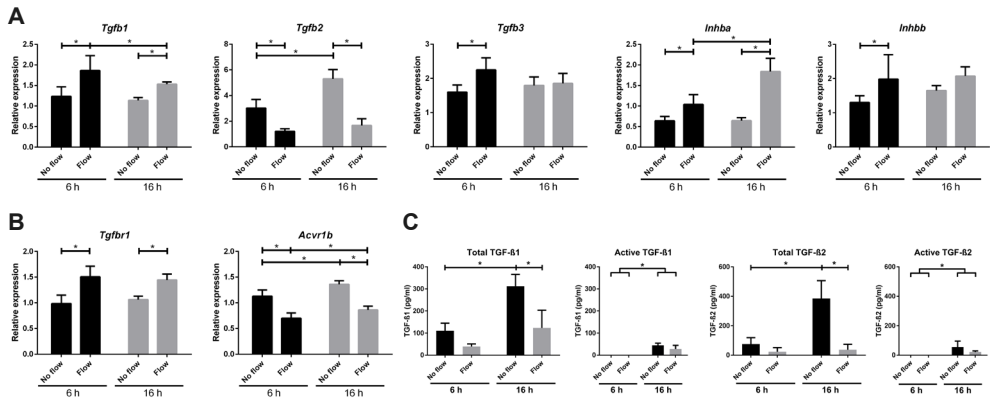
(J) Nuclear accumulation of Snail (green; t = 6 hr, IF). Nuclei are visualized with DAPI (blue).

(K) Relative expression of *Ptgs2*, *Pai1*, *Fn1* and *Col1a1* shown as fold change induction by fluid shear stress (cone-plate) compared to the no flow control (dashed line), as measured by quantitative PCR. Comparison between *Pkd1*^{+/+} and *Pkd1*^{-/-} PTECs at t = 6 or 16 hr showed stronger induction of target genes by fluid shear stress in *Pkd1*^{-/-} PTECs; *Hprt* served as housekeeping gene to correct for cDNA input; data normalized to unstimulated PTECs (dashed line); n=5 per condition; * indicates P < 0.05 using two-tailed Student's t-test.



Supplementary Figure S2. Expression of Wnt and Hedgehog targets in PTECs upon fluid-flow stimulation.

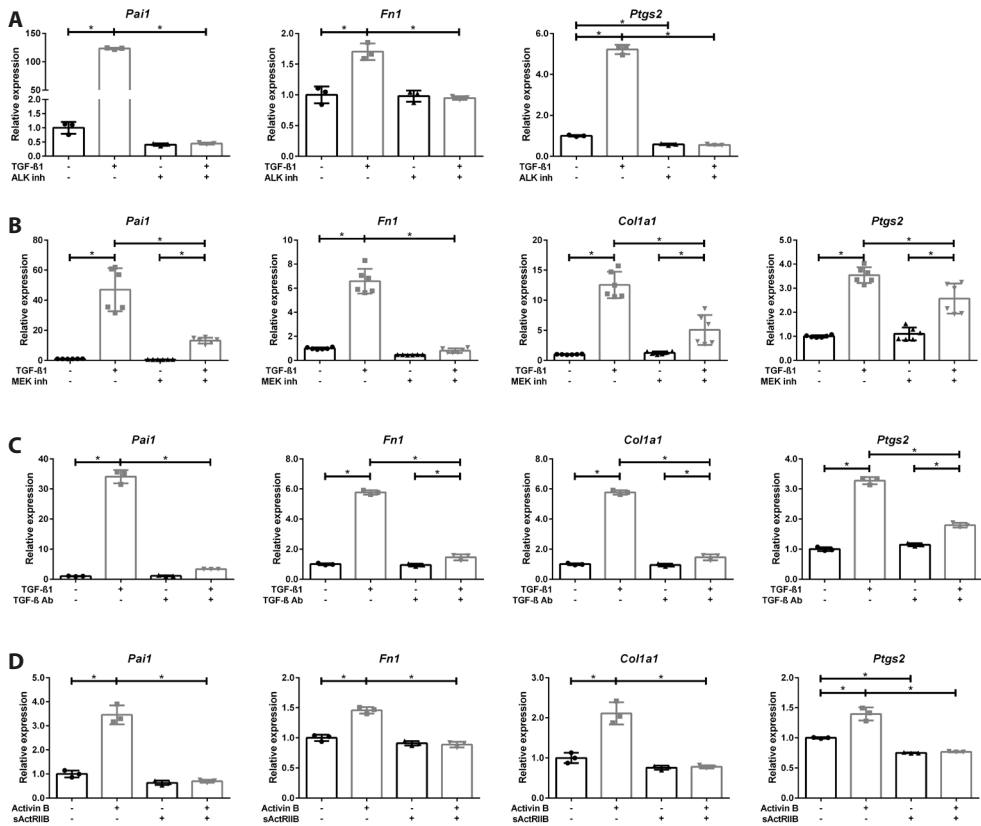
Relative expression of Wnt target genes (*Ccnd1*, *Axin2*, *Birc5*, *Lin7a*, *Ppard*, *Glis2*, *Insc*) and hedgehog targets (*Gli1*, *Gli2*, *Gli3*) is virtually not altered by fluid shear stress. Cone-plate induced fluid-flow in *Pkd1*^{+/+} (A) and *Pkd1*^{-/-} (B) PTECs at t = 6 or 16 h. Wnt target gene expression was measured by reverse transcriptase multiplex ligation-dependent probe amplification (RT-MLPA) as described previously (Leonhard *et al.* (2008) BMC Biotechnol., 8: 18). Briefly, cDNA was synthesized from total RNA and hybridized to probes (sequences available upon request) in a reaction containing MLPA probe mix and SALSA MLPA buffer (MRC-Holland) by incubation at 95°C for 1 min followed by 60°C for 4 h. Ligation of annealed oligonucleotides was performed at 54°C for 15 min followed by ligase inactivation at 98°C for 5 min. Products were amplified by PCR using SalsaTaq (MRC-Holland) and FAM or HEX-labeled primers. Amplified samples were mixed with Hi-Di formamide containing GeneScan-500 ROX size standard (Applied Biosystems), heated for 5 min at 95°C, and run on a 3730 DNA analyzer (Applied Biosystems). Data was analyzed using GeneScan 3.5 analysis software. Expression of housekeeping genes *Ywhaz* and *Hprt* served as reference for cDNA input. Peak ratios of target genes and housekeeping genes were calculated and results were normalized to unstimulated PTECs. n=3 per condition. Hedgehog targets were measured by quantitative PCR. *Hprt* served as housekeeping gene to correct for cDNA input; data normalized to unstimulated PTECs; n=5 per condition; * indicates P < 0.05 using one-way ANOVA.



Supplementary Figure S3. Expression of ligands and receptors in *Pkd1*^{-/-} PTECs upon fluid-flow stimulation.

(A) Relative expression of *Tgfb1*, *Tgfb2*, *Tgfb3*, *Inhba*, *Inhbb* and (B) *Tgfb1* (*Alk5*) and *Acvr1b* (*Alk4*) mRNA in *Pkd1*^{-/-} PTECs upon fluid-flow. Cone-plate induced fluid-flow at t = 6 or 16 hr; qPCR, *Hprt* served as housekeeping gene to correct for cDNA input; data normalized to unstimulated PTECs at 6 hr presented in Fig. 3; n=5 per condition; * indicates P < 0.05 using two-way ANOVA, followed by post-hoc Fisher's LSD multiple comparison.

(C) Levels of total and active TGF- β 1 and TGF- β 2 in the medium of *Pkd1*^{-/-} PTECs collected after 6 or 16 hr fluid-flow. TGF- β 3 levels in medium and TGF- β 1, 2 and 3 levels in cell lysates were below the detection limit. Cone-plate induced fluid shear stress; TGF- β levels measured by ELISA; n=5 per condition; * indicates P < 0.05 using two-way ANOVA, followed by post-hoc Fisher's LSD multiple comparison.

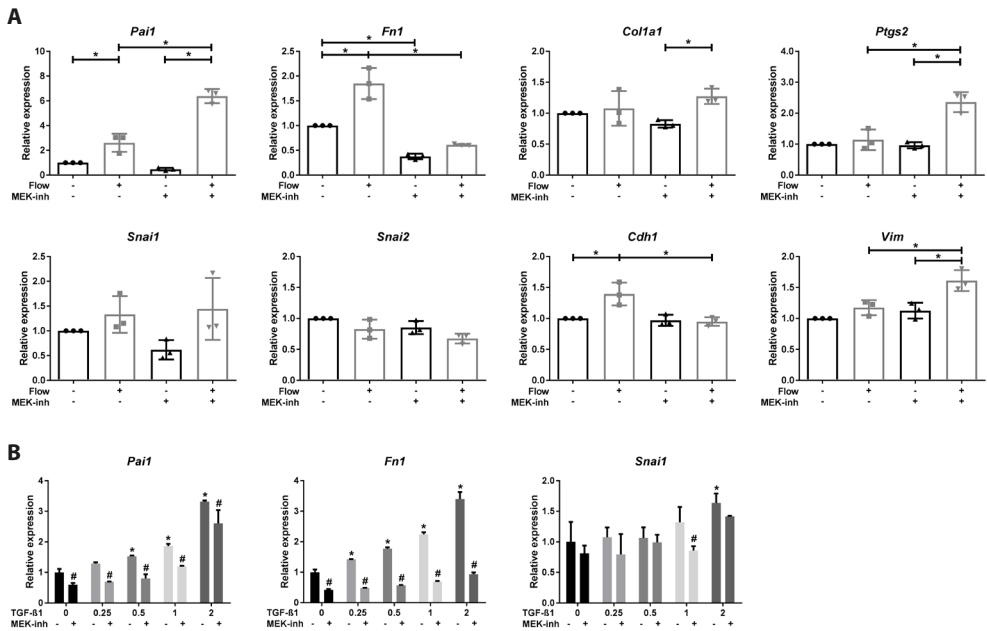


Supplementary Figure S4. Expression of SMAD2/3 targets upon TGF-β1 or activin B stimulation when using inhibitors.

(A-C) TGF-β1 induced expression of SMAD2/3 targets *Pai1*, *Fn1*, *Col1a1* and *Ptgs2*, was decreased with 10 μM ALK4/5/7 inhibitor (A; n=3), 10 μM MEK inhibitor (B; n=6) or 10 μg/ml TGF-β neutralizing Ab (C; n=3).

(D) Activin B induced expression of SMAD2/3 targets *Pai1*, *Fn1*, *Col1a1* and *Ptgs2*, was decreased with 5 μg/ml sActRIIB-Fc (n=3).

Relative mRNA expression measured by qPCR at t = 4 hr (A) or 16 hr (B-D). *Hprt* served as housekeeping gene to correct for cDNA input; data was normalized to unstimulated controls. * indicates $P < 0.05$ using two-way ANOVA, followed by post-hoc Fisher's LSD multiple comparison. ALK inh = 10 μM ALK4/5/7 inhibitor (LY-364947); MEK inh = 10 μM MEK1/2 inhibitor (Trametinib, GSK1120212). TGF-β Ab = 10 μg/ml TGF-β neutralizing Ab (clone 2G7). sActRIIB = 5 μg/ml soluble activin receptor-IIB fusion protein.



Supplementary Figure S5. MEK inhibition modulates fluid-flow or TGF- β 1 induced expression of SMAD2/3 target genes.

(A) MEK inhibition (5 μ M Trametinib; GSK1120212) reduces fluid-flow increased expression of *Fn1*, while fluid-flow increased expression of *Pai1*, *Col1a1*, *Ptgs2* and *Snai1* is further elevated. Parallel plate flow-chamber induced fluid-flow in PTECs at t = 16 hr; *qPCR*, *Hprt* served as housekeeping gene to correct for cDNA input; data normalized to unstimulated controls (fold change); n=3 per condition. * indicates $P < 0.05$ by two-way ANOVA, followed by post-hoc Fisher's LSD multiple comparison.

(B) *Pai1* and *Fn1* expression was reduced by MEK inhibition (10 μ M Trametinib; GSK1120212) upon low dose TGF- β 1 (0.25-2 ng/ml) stimulation, as measured by quantitative PCR; *Hprt* served as housekeeping gene to correct for cDNA input; data normalized to unstimulated controls; n=2 per condition. * indicates significant difference compared to unstimulated control (0 ng/ml TGF- β 1) or # significant difference upon MEK inhibition ($P < 0.05$ by two-way ANOVA, followed by post-hoc Fisher's LSD multiple comparison).

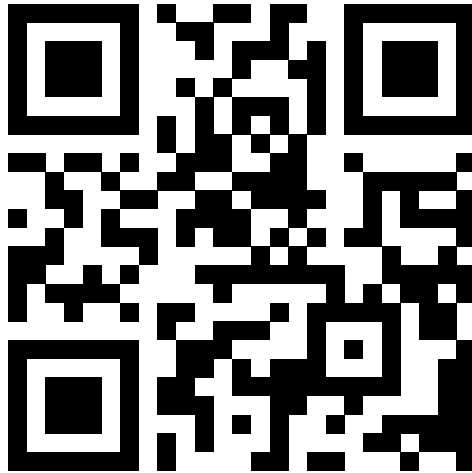


SUPPLEMENTARY TABLES
Supplementary Table S1. Primer sequences used for qPCR.

Gene	Accession #	Forward primer	Reverse primer
<i>Pai1</i>	NM_008871.2	GCCAACAAGAGCCAATCAC	ACCCTTTCCCAGAGACCAG
<i>Fn1</i> (EDA)	NM_010233.2	AATCCAGTCCACAGCCATTCC	CCTGTCTTCTTTTCGGTTCA
<i>Col1a1</i>	NM_007742.4	TGACTGGAAGAGCGGAGAGT	AGACGGCTGAGTAGGGAACA
<i>Ptgs2</i>	NM_011198.4	ACTGGGCCATGGAGTGGA	ACCTGAGTGTCTTTGACTGTGG
<i>Snai1</i>	NM_011427.3	CTTGTGTCTGCACGACCTG	CAGTGGGAGCAGGAGAATG
<i>Snai2</i>	NM_011415.2	GAAGTGGACACACACAGTTATT	TGCCGACAGTGCCATACAG
<i>Cdh1</i>	NM_009864.3	ATCCTCGCCCTGCTGATT	ACCACCGTTCTCTCCGTA
<i>Vim</i>	NM_011701.4	CCAACCTTTTCTCCCTGAA	TGAGTGGGTGCAACCAGAG
<i>Tgfb1</i>	NM_011577.2	ACTATTGCTTCAGCTCCACAGA	AAGTTGGCATGGTAGCCCTT
<i>Tgfb2</i>	NM_009367.3	CAGGAGTGGCTTACCACAA	TCAATACCTGCAATCTCGCTT
<i>Tgfb3</i>	NM_009368.3	AGGATCACACAACCCACAC	CCAGGTTGCGGAAGCAGTAA
<i>Inhba</i>	NM_008380.1	GACCTCGGAGATCATCACCTT	TGCCTTCTTGAAATCTCA
<i>Inhbb</i>	NM_008381.3	CGAGATCATCAGCTTTGAG	CATAGGGGAGCAGTTTCAGG
<i>Tgfb1</i>	NM_009370.3	ACATCAGGGTCTGGATCAGGTT	CGACCTTGCCAATGCTTTCTT
<i>Avcr1b</i>	NM_007395.3	CGAAGATGCAATTCTGGAGGAG	CCGTAGCTTCTGGTCACATACA
<i>Gli1</i>	NM_010296.2	CGACCTGCAAACCGTAATC	AGAGATGGCCGTAGGAACC
<i>Gli2</i>	NM_001081125.1	TGTGCAGTGAATGAGGTG	TTGCTGTGAGGAAAGGAG
<i>Gli3</i>	NM_008130.2	GCCATTCACAGTCCAGGTC	TTCCCGCTTTGAGGTAGTG
<i>Pkd1</i>	NM_013630.2	GCCACCGCGCTAGACCTG	TAGCAAACACGCCTTCTTAATG
<i>Pkd2</i>	NM_008861.3	GGGAAGCATCTCCAGTGGG	GATGCTGCCAATGGAGTGC

SUPPLEMENTARY MATERIALS CAN BE DOWNLOADED FROM

<https://goo.gl/rjKWj5>



CHAPTER 3

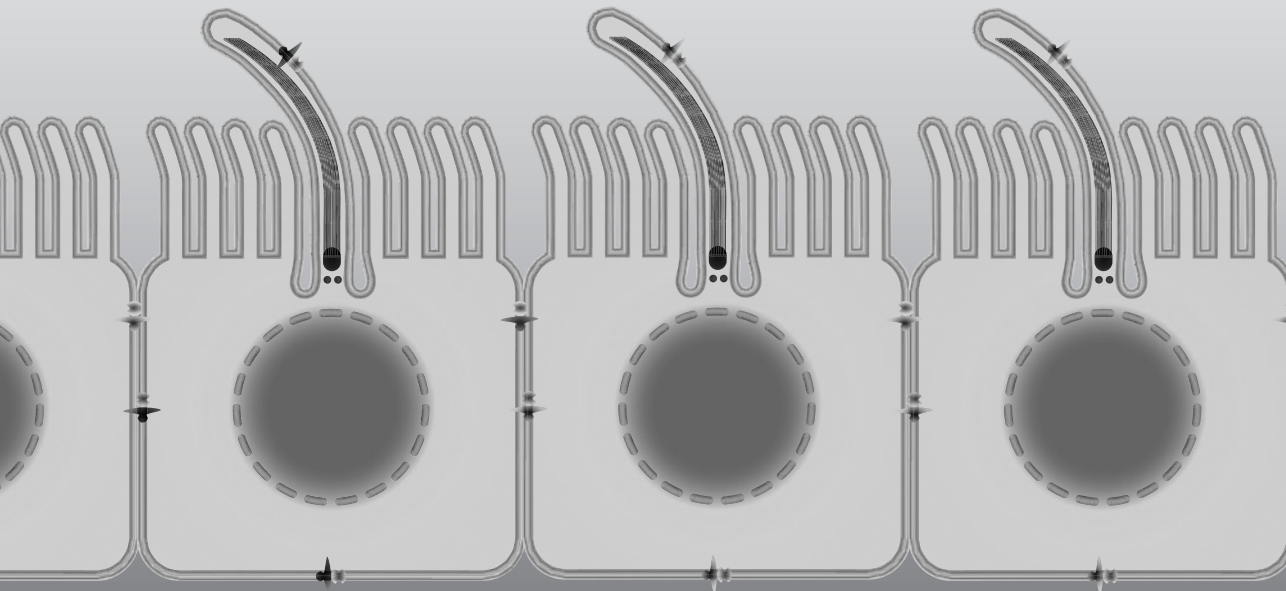
Comprehensive transcriptome analysis of fluid shear stress altered gene expression in renal epithelial cells

Steven J. Kunnen¹, Tareq B. Malas¹, Cornelis M. Semeins², Astrid D. Bakker², and Dorien J.M. Peters¹

¹ Department of Human Genetics, Leiden University Medical Center, 2300 RC Leiden, The Netherlands

² Department of Oral Cell Biology, Academic Centre for Dentistry Amsterdam (ACTA), University of Amsterdam and VU University Amsterdam, 1081 LA Amsterdam, The Netherlands

J Cell Physiol. 2018; 233(4): 3615-3628



ABSTRACT

Renal epithelial cells are exposed to mechanical forces due to flow-induced shear stress within the nephrons. Shear stress is altered in renal diseases caused by tubular dilation, obstruction and hyperfiltration, which occur to compensate for lost nephrons. Fundamental in regulation of shear stress are primary cilia and other mechano-sensors, and defects in cilia formation and function have profound effects on development and physiology of kidneys and other organs. We applied RNA sequencing to get a comprehensive overview of fluid-shear regulated genes and pathways in renal epithelial cells. Functional enrichment-analysis revealed TGF- β , MAPK and Wnt signaling as core signaling pathways up-regulated by shear. Inhibitors of TGF- β and MAPK/ERK signaling modulate a wide range of mechanosensitive genes, identifying these pathways as master regulators of shear-induced gene expression. However, the main down-regulated pathway, *i.e.* JAK/STAT, is independent of TGF- β and MAPK/ERK. Other up-regulated cytokine pathways include FGF, HB-EGF, PDGF and CXCL. Cellular responses to shear are modified at several levels, indicated by altered expression of genes involved in cell-matrix, cytoskeleton and glycocalyx remodeling, as well as glycolysis and cholesterol metabolism. Cilia ablation abolished shear induced expression of a subset of genes, but genes involved in TGF- β , MAPK and Wnt signaling were hardly affected, suggesting that other mechano-sensors play a prominent role in the shear stress response of renal epithelial cells. Modulations in signaling due to variations in fluid shear stress are relevant for renal physiology and pathology, as suggested by elevated gene expression at pathological levels of shear stress compared to physiological shear.

Keywords: next generation sequencing, mechanotransduction, fluid flow, cilium, glycocalyx

INTRODUCTION

Several organs are subject to variations in fluid flow rate in response to physiological stimuli, which could be detected by different cell types via mechano-sensing proteins or complexes. Cellular mechano-sensitivity and mechanotransduction are essential for normal cell function, tissue development and maintenance of organs¹⁻⁴. In the kidneys, where urinary volume, diuretics, and diet will expose the renal epithelial cells to variations in hydrodynamic forces including fluid shear stress, circumferential stretch, and drag/torque on apical cilia and probably also on microvilli⁵. Depending on the cell type and the magnitude of the hydrodynamic forces, different responses will be activated and mutations in critical components may modulate or cause (kidney) diseases⁶. In addition, strong variations in hydrodynamic forces and shear stress are common in kidney diseases due to hyperfiltration, tubular dilation and obstruction, which occur in functional nephrons, to compensate for lost glomeruli and tubules, with diabetic nephropathy and Polycystic Kidney Disease as the most common examples⁷.

Fundamental in flow-sensing are a number of proteins located throughout the cell membrane, cilium/ciliary base, as well as the cytoskeleton. These include ion channels, G-protein coupled receptors (GPCRs), adherens junction proteins, focal adhesion proteins, components of the actin cytoskeleton, but also glycocalyx and lipid rafts can act as mechano-sensors to shear stress⁸⁻¹⁰. Activation of aforementioned sensors upon shear stress leads to alteration of cellular signaling. Bending of the primary cilium causes ciliary influx of Ca^{2+} , followed by an increase in cytosolic Ca^{2+} ¹¹⁻¹⁴. It is likely that the increase in intraciliary Ca^{2+} does not spread to the cytosol suggesting the requirement of additional steps for amplification of the Ca^{2+} signal, although details are not entirely clear and under debate¹⁴⁻¹⁶. Other cilia-dependent signaling cascades affected by fluid flow include the canonical Wnt-signaling pathway, which is restrained by fluid-flow induced ciliary signaling in favor of non-canonical Wnt signaling¹⁷. Furthermore, mTOR signaling and cell-size control, as well as STAT6/p100-regulated transcription are thought to be negatively regulated upon flow-induced bending of the cilium, independent from flow-induced Ca^{2+} influx¹⁸⁻²¹. Cilia-independent shear-induced alterations in renal signaling include increased Na^+ and HCO_3^- reabsorption and autocrine TGF- β /ALK5 signaling^{22,23}.

It is currently not known in detail how fluid shear stress affects cellular behavior and which signaling pathways are altered. Furthermore, gene expression and the overall cellular behavior will be the effect of an integration of the different signaling pathways, triggered by shear stress and by cytokine stimulation. In this study we set out to obtain a comprehensive overview of the transcriptome under static and shear stress conditions in renal epithelial cells to get more insight in the pathways and processes involved in the shear

response. Therefore, we applied RNA-sequencing as an unbiased means to interrogate renal epithelial cell type-specific transcriptome alterations upon fluid shear stress. Our data indicate that genes involved in TGF- β , MAPK and Wnt signaling are up-regulated by shear stress, while the JAK-STAT related genes seems to be down-regulated. Using ALK4/5/7 and MEK1/2 inhibitors, we showed that the shear stress-induced signaling cascades are largely modulated by TGF- β /ALK5 and MAPK/ERK signaling. Cilia removal abrogated shear induced gene expression of a subset of genes, but genes involved in TGF- β , MAPK and Wnt signaling were hardly affected, suggesting that other mechano-sensors also play an evident role in the shear stress response of renal epithelial cells. Furthermore, altered expression of genes involved in cell-matrix, cytoskeleton and glycocalyx remodeling, as well as amino acid, carbohydrate and cholesterol metabolism, indicate that shear stress is regulating gene expression at several levels for cellular homeostasis. Finally, we showed that expression of several genes is elevated at pathological levels of shear stress compared to physiological controls, suggesting that variations in fluid shear stress might be relevant for the pathology in kidney diseases due to an imbalance in cellular signaling.

MATERIALS AND METHODS

Chemicals

ALK4/5/7 inhibitor LY-364947 (Calbiochem; #616451) from Merck Millipore (Darmstadt, Germany), MEK1/2 inhibitor Trametinib (GSK1120212; #S2673) from Selleckchem (Bio-Connect, Huissen, The Netherlands) and ammonium sulfate (#A-2939) from Sigma-Aldrich (Zwijndrecht, The Netherlands) were used as previously described²³.

Cell culture

SV40 large T-antigen immortalized murine proximal tubular epithelial cells (PTEC), derived from a *Pkd1*^{lox,lox} mouse, were generated and cultured as described previously^{23,24}. Briefly, cells were maintained at 37°C and 5% CO₂ in DMEM/F-12 with GlutaMAX (Gibco, Fisher Scientific, Landsmeer, The Netherlands; #31331-093) supplemented with 100 U/mL Penicillin-Streptomycin (Gibco, Fisher Scientific, Landsmeer, The Netherlands; #15140-122), 2% Ultrosor G (Pall Corporation, Pall BioSeptra, Cergy St Christophe, France; #15950-017), 1x Insulin-Transferrin-Selenium-Ethanolamine (Gibco, Fisher Scientific, Landsmeer, The Netherlands; #51500-056), 25 ng/L Prostaglandin E1 (Sigma-Aldrich, Zwijndrecht, The Netherlands; #P7527) and 30 ng/L Hydrocortisone (Sigma-Aldrich, Zwijndrecht, The Netherlands; #H0135). Cell culture was monthly tested without mycoplasma contamination using MycoAlert Mycoplasma Detection Kit (Lonza, Basel, Switzerland; LT07-318). New ampules were started after 15 passages.

For fluid-flow experiments, cells were cultured on collagen-I (Advanced BioMatrix, San Diego, CA, USA; #5005) coated culture dishes or glass slides. Cells grown until high confluency underwent 24 hr serum starvation before the start of the treatment to exclude effects of serum-derived growth-factors and to synchronize cells and cilia formation.

Fluid shear stress stimulation

Cells were exposed to laminar fluid shear stress (0.25 - 2.0 dyn/cm²) in a cone-plate device or parallel-plate flow chamber as described previously²³. The cone-plate device, adapted from Malek *et al.*^{25,26}, was designed for 3.5 cm cell culture dishes (Greiner Bio-One, Alphen aan de Rijn, The Netherlands). Cells were grown on collagen-I coated dishes until confluence, followed by 24 hr serum starvation, before dishes were placed in the cone-plate flow system and incubated at 37°C and 5% CO₂. The confluent cell monolayer of 9.6 cm² was subjected to fluid shear stress using 2 ml serum-free DMEM/F-12 medium containing penicillin-streptomycin, with viscosity (μ) of 0.0078 dyn s/cm²²⁷. Constant laminar ($Re = 0.3$) fluid-flow was induced using a cone angle (α) of 2° and a velocity (ω) of 80 rpm, generating a fluid shear stress ($\tau = \mu\omega/\alpha$) of 1.9 dyn/cm².

Alternatively, cells were exposed to shear stress using a parallel plate flow chamber, as previously described^{28,29}. Briefly, cells were grown on collagen-I coated glass slides of 36 x 76

mm (Fisher Scientific, Landsmeer, The Netherlands; #15178219) until confluence, followed by 24 hr serum starvation, before glass slides were placed in a flow-chamber. A confluent cell monolayer of 14.2 cm² (24 x 59 mm) was subjected to fluid shear stress using 7.5 ml serum-free DMEM/F-12 medium containing penicillin-streptomycin. Fluid was pumped at a constant flow rate (Q) of 5.5 ml/min through the chamber with 300 μm height (h), generating a constant laminar ($Re = 5.0$) fluid shear stress ($\tau = 6\mu Q/h^2b$) of 2.0 dyn/cm². The parallel plate flow-chamber was placed in an incubator at 37°C and 5% CO₂.

Static control cells were incubated for the same time in equal amounts of serum-free DMEM/F12 medium containing penicillin-streptomycin at 37°C and 5% CO₂. After 4, 6 or 16 hr fluid-flow or static (control) stimulation, cells have been harvested for mRNA isolation and gene expression analysis. In select experiments, cells were pre-exposed to low levels of shear stress (0.25 dyn/cm²), followed by 16 hr shear stress at the same levels (physiological control) or at pathological levels of shear (2.0 dyn/cm²). ALK4/5/7 inhibitor (10 μM), MEK1/2 inhibitor (10 μM) or DMSO control (0.1%) were added 1 hr before start of fluid-flow stimulation in the absence of medium supplements. Ammonium sulfate (AS) was used to remove primary cilia. Cells were pre-treated with 50 mM ammonium sulfate, followed by 16 hr fluid flow in medium containing 25 mM AS, to prevent cilia restoration. Control cells were treated similarly, but without AS. Cilia formation was checked on a parallel slide by immunofluorescence using anti-acetylated α-tubulin antibodies (Sigma-Aldrich, Zwijndrecht, The Netherlands; #T6793) as previously described²³.

RNA sequencing

Total RNA was isolated from fluid shear stress treated PTECs or static controls ($n = 4$) using TRI Reagent (Sigma-Aldrich, Zwijndrecht, The Netherlands; #T9424) and purified using Nucleospin RNA Clean-up (Macherey-Nagel, Düren, Germany; #740948) according to manufacturer's protocols. Next generation sequencing of mRNA was done by ServiceXS (GenomeScan, Leiden, The Netherlands) using the Illumina[®] HiSeq 2500 platform (San Diego, CA, USA). Illumina mRNA-Seq Sample Prep Kit was used to process the samples according to the manufacturer's protocol. Briefly, mRNA was isolated from total RNA using the oligo-dT magnetic beads. After fragmentation of the mRNA, a cDNA synthesis was performed. This was used for ligation with the sequencing adapters and PCR amplification of the resulting product. The quality and yield after sample preparation was measured with a DNA 1000 Lab-on-a-Chip. The size of the resulting products was consistent with expected size distribution (a broad peak between 300-500 bp). Clustering and cDNA sequencing using the Illumina cBot and HiSeq 2500 was performed according manufacturer's protocols. A concentration of 5.8 pM of cDNA was used. All samples were run on Pair Ends mode and 125 bp long reads. HiSeq control software HCS v2.2.38 was used. Image analysis, base calling, and quality check was performed with the Illumina data analysis pipeline RTA v1.18.61 and/or OLB v1.9 and Bcl2fastq v1.8.4. At least 87.3% of bases had a Q-score ≥ 30 .

Reads were aligned to mouse genome build GRCm38 - Ensembl³⁰ using TopHat2 version 2.0.10³¹. Gene expression was quantified using HTSeq-Count version 0.6.1³², using default options (stranded = no, mode = union). Differential gene expression analysis was performed in R version 3.0.2 using DESeq (Version1.16.0). Differentially expressed genes were selected with an adjusted p-value (corrected for multiple hypotheses testing) of < 0.05. Count per million (CPM) values were calculated by dividing the read counts by total read counts of the sample, which is a measure for the abundance of the transcript. CPM > 2 was used to exclude low expressed genes.

Quantitative PCR

Gene expression analysis by quantitative PCR (qPCR) was performed as described previously³³. Briefly, cDNA synthesis of total RNA was done using Transcriptor First Strand cDNA Synthesis Kit (Roche, Almere, The Netherlands; #04897030001) according to the manufacturer's protocol. Quantitative PCR was done in triplicate on the LightCycler 480 II (Roche, Almere, The Netherlands) using 2x FastStart SYBR-Green Master (Roche; #04913914001) according to the manufacturer's protocol. Data was analyzed with LightCycler 480 Software, Version 1.5 (Roche). Gene expression was calculated using the $2^{-\Delta\Delta Ct}$ method³⁴ and normalized to the housekeeping gene *Hprt*, giving the relative gene expression. For primer sequences see Supplementary Table S1. Mean gene expression and standard deviation (SD) of the different treatment groups were calculated. Differences between fluid shear stress treated cells and static controls were tested using one sample *t*-tests. One-way analysis of variance (ANOVA) was used when cells were exposed for a different time or to a different flow rate. Two-way analysis of variance (ANOVA) was used, when the shear stress response was compared to a second treatment. The ANOVA was followed by post-hoc Fisher's LSD multiple comparison, if the overall ANOVA F-test was significant. $P < 0.05$ was considered to be statistically significant.

Pathway analysis

Functional enrichment analysis was performed against the Molecular Signature Database (MSigDB: <http://software.broadinstitute.org/gsea/msigdb/annotate.jsp>) v5.2³⁵ using standard hypergeometric distribution with correction for multiple hypotheses testing according to Benjamini and Hochberg. From this source we included pathway databases (KEGG, BIOCARTA and REACTOME). Up- and down-regulated genes by fluid shear stress were used as separate gene sets to discriminate between generally up- and down-regulated pathways. Terms with false discovery rate (FDR) < 0.01 were considered significantly enriched, giving 209 up-regulated and 55 down-regulated terms. Interaction networks of up- and down-regulated DEG and their connecting pathways/processes were plotted using Cytoscape, version 3.4.0.

RESULTS

Fluid shear stress induced transcriptional changes in PTECs

To study genome wide fluid-flow induced cellular alterations, proximal tubular epithelial cells (PTEC) were exposed to fluid shear stress of 1.9 dyn/cm² using a cone-plate device. Controls were similarly treated under static conditions. After 6 hr fluid shear stress or static exposure, total RNA was isolated and gene expression was analyzed using next generation sequencing (NGS) on the Illumina HiSeq 2500 platform. After quality checks the reads were aligned to mouse genome (GRCm38) and gene expression was quantified using HTSeq-Count. Count per million (CPM) values were calculated as a measure for the abundance of the transcript (Supplementary Table S2).

A scatter plot was constructed comparing the log₂ CPM values of flow vs static treated cultures, showing a substantial number of genes that are significantly ($p < 0.05$) up- or down-regulated (Fig. 1A, blue dots). Overall, RNA sequencing identified 2015 differentially expressed genes (DEG) upon shear stress exposure in PTECs (Table 1). Low expressed genes with an average counts per million (CMP) < 2 were excluded, resulting in a list of 1551 DEG (Supplementary Table S3). A heat map of all 8 PTEC samples shows a clear distinction between fluid shear stress treated samples and static controls (Fig. 1B). Furthermore, our genome wide RNA sequencing analysis confirmed genes known to be altered by fluid shear stress in renal epithelial cells, including *Ptgs2* (*Cox2*), *Ccl2* (*Mcp1*), *Edn1*, *Egr1*, *Snai1*, *Cdh1* and *Tgfb1*³⁶⁻⁴².

Table 1. Differentially expressed genes by fluid shear stress in PTECs using next generation sequencing.

Number of differentially expressed genes ($p < 0.05$) of flow versus static treated PTECs. Low expressed genes were excluded with an enrichment filter of CPM > 2 . DEG = differentially expressed gene; CPM = counts per million.

	All DEG	DEG with CPM > 2
Up	1023	813
Down	992	738
Total	2015	1551

Pathway analysis of RNA sequencing data

We used functional enrichment analysis of the MSigDB³⁵ as the tool to identify biological pathways or processes associated with fluid-shear stress in PTECs. The list of 1551 DEG (Supplementary Table S3) was split into up-regulated (813) and down-regulated (738) genes in order to get pathways that are generally up- or down-regulated. The 209 up-regulated and 55 down-regulated biological annotations in flow-stimulated cells are presented in Supplementary Tables S4 and S5, respectively. We subdivided the biological pathways in core signal transduction, as well as cell-cell/matrix interaction, metabolism, cytokine signaling,

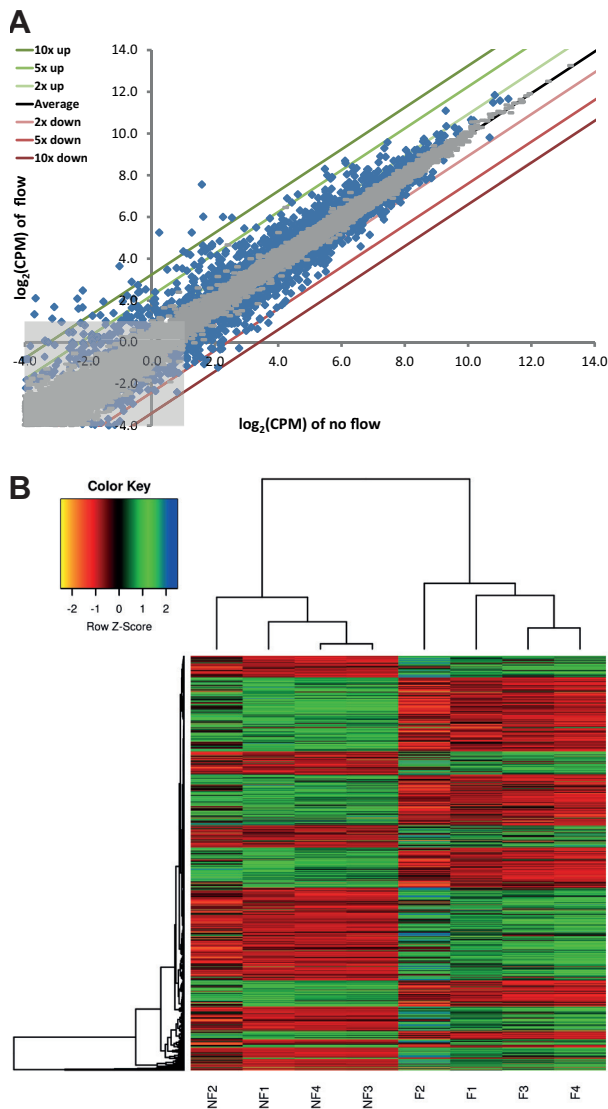


Figure 1. Gene expression profiling shows a strong difference between fluid shear stress treated PTECs and static controls.

(A) \log_2 comparison of the counts per million (CPM) values of flow versus no flow treated PTEC cultures. Differentially expressed genes (DEG) are indicated by blue dots ($p < 0.05$). Not significant genes are indicated by grey dots. Labeled lines indicate a 2, 5 or 10 fold up- or down-regulation. Black line (Average) represents equal expression for both conditions. Light-grey box indicates the area of low expressed genes ($CPM < 2$). (B) Heat map showing the expression values of 1551 DEG ($p < 0.05$; $CPM > 2$) in 4 fluid shear stress treated samples (F = Flow) and 4 static controls (NF = No flow). Expression values were normalized using the Voom function in *limma* R package. Hierarchical clustering was applied on the samples and values were scaled by row.

3

other cellular processes and diseases. These processes show many connections as indicated by interaction networks of genes with the annotated pathways (Supplementary Fig. S1). Cell-cell/matrix interactions are clearly affected by fluid-flow (Supplementary Table S4). This is revealed by increased gene expression of cytoskeletal components (*Actb*, *Actg1*, *Actn1*, *Flna*), cadherins (*Cdh10*, *Cdh11*), tight junction molecule (*Cldn4*), cell adhesion molecules (*Cadm1*, *Cadm3*, *Epcam*, *Ncam1*, *Vcam1*), extracellular matrix components (*Col1a1*, *Col5a1*, *Fn1*, *Lamc1*, *Lamc2*), and integrins (*Itgav*, *Itga2*, *Itga5*, *Itgb1*, *Itgb3*, *Itgb4*, *Itgb5*). Furthermore, we see a shear stress enhanced expression of genes involved in glycosaminoglycan and

carbohydrate metabolism, including proteoglycans (*Gpc1*, *Sdc1*, *Sdc2*, *Sdc3*, *Cd44*), heparan sulfate, carbohydrate or uronyl sulfotransferases (*Hs2st1*, *Hs3st3b1*, *Hs6st1*, *Chst7*, *Chst11*, *Ust*). Genes involved in apoptosis and cell cycle activity are increased by shear stress, including pro-apoptotic (*Trp53*, *Bid*, *Fas*, *Pmaip1*) as well as pro-survival (*Bcl2*, *E2f3*, *Cttnb1*, *Myc*) and cell cycle arrest (*Gadd45*, *Sfn*, *Cdkn2b*) genes, while key players in apoptosis (*Bad*, *Bak*, *Bax*, and caspases) and cell cycle (cyclins and CDKs) were not altered in gene expression (Supplementary Tables S2-S5). Pathways involved in cytokine signaling and other cellular processes and diseases are up-regulated as well and have broad overlap with the core signal transduction pathways. Of those, the most prominently up-regulated pathways by fluid flow include MAPK, TGF- β , Wnt, PDGF and p53 signaling (Table 2).

We previously reported changes in TGF- β signaling, involving genes encoding proteins relaying the signal from cell membrane towards the nucleus, *i.e.* the ligands *Tgfb1-3* and the receptor *Alk5* (*Tgfbr1*), as well as down-stream targets, *i.e.* *Pai1* (*Serpine1*), *Fn1*, *Col1a1* and *Snai1*²³. Our gene expression profile now also shows increased expression of genes encoding proteins involved in TGF- β ligand activation (*Furin*, *Thbs1*) or ligand inhibition (*Ltbp2*), the transcription factor *Smad3*, but also the inhibitors *Smad7*, *Smurf1*, *Skil*, and *Tgif1*, all critical components of the pathway (Table 2). However, the most prominently activated signaling pathway is the mitogen-activated protein kinase (MAPK) pathway (Tables 2, S4). The MAPK pathway is a set of intracellular signal transduction cascades that regulate a wide variety of stimulated cellular processes, including proliferation, differentiation, apoptosis and stress responses. The canonical cascades identified in mammals are extracellular signal-regulated kinase 1 and 2 (ERK1/2), c-Jun N-terminal kinase (JNK), p38, and ERK5, responding to different mitogens or forms of stress. Consequently, the MAPK pathway comprises a large number of molecules. Increased expression by fluid shear was observed for several MAP kinases (*i.e.* *Map2k1*, *Map2k3*, *Map4k4*, *Mapk6*, *Map3k20* = *Zak*) as well as dual-specific phosphatases (*Dusp1*, 4, 6, 7 and 9), which negatively regulate members of the MAP kinase superfamily. The classical MAP kinase (ERK1/2) pathway, activating proliferation and differentiation, shows increased expression of Ras (*Rras*), MEK1 (*Map2k1*) and c-Fos (*Fos*). Upstream mitogens, PDGF (*Pdgfa*, *b* and *c*), HB-EGF (*Hbegf*) and FGF (*Fgf1,9*) are increased by fluid shear as well. Also the stress-mitogen pathway is modified, including increased mRNA levels of TNF α and TNF α -receptors (*Tnfaip2*, *Tnfaip3*, *C1qtnf3*, *Fas*, *Tnfrsf1b*, *Tnfrsf12a*, *Tnfrsf23*, *Relt*). Furthermore, CXC, CX3C and CC chemokines and receptors are increased by shear (*Cxcl10*, *Cxcl14*, *Cxcl16*, *Cx3cl1*, *Ccl2*, *Cxcr4*). Cooperation between MAPK pathway and NFAT proteins integrates two important signaling pathways that are altered by shear stress, the MAPK-pathway and calcium signaling. This involves elevated expression of *Nfatc2* and *Nfatc4*, as well as expression of several calcium channels (*Cacnb3*, *Cacna1g*) and calcium/calmodulin dependent proteins (*Camk2n1*, *Ccbe1*, *Ncs1*, *Carhsp1*). Other transcription factors that are reported to be regulated by MAPK/ERK are *Ets1* and *Ets2*⁴³, which are both increased by fluid shear stress as well (Table 2).

Table 2. Core signaling pathways affected by fluid shear stress - up-regulated genes.

Pathway analysis (KEGG, Reactome and Biocarta) done on 813 significantly up-regulated genes upon fluid shear stress in PTECs using MSigDB. The most significantly altered core signaling pathways are shown and ordered together, followed by the lowest false discovery rate (FDR). K = number of genes in pathway database; k = number of genes in overlap. For the complete list of the pathway analysis of up-regulated genes upon fluid shear stress see Supplementary Table S4.

Pathway	Pathways description	Database	k/K	FDR	Genes
MAPK	MAPK signaling pathway	KEGG	39 / 267	3.1E-23	MAP2K1; TGFB1; PAK1; RRAS; CACNB3; CACNA1G; PDGFA; PDGFB; PRKCA; FGF1; FGF9; TGFB3; TP53; TGFB1; MYC; FAS; RAS; RAP1B; FLNA; PLA2G4A; PPP3CA; NFATC2; NFATC4; RASA1; ZAK; NR4A1; GADD45A; GADD45B; GADD45G; MAP2K3; DUSP4; DUSP6; DUSP7; SRF; DUSP1; HSPB1; MAP4K4; DUSP9; RELB
			8 / 50	2.9E-05	MAP2K1; FOS; MAP2K3; DUSP4; DUSP6; DUSP7; PPP2R1B; IRAK2
			10 / 87	4.5E-05	MAP2K1; TGFB1; PAK1; TGFB3; TGFB1; MYC; FOS; MAP2K3; MAP4K4; MAPK6
TGF-β	Signaling by TGF-beta Receptor Complex	REACTOME	15 / 63	7.6E-12	TGFB1; TGFB1; MYC; SMAD3; FURIN; NCOR2; CDKN2B; SERPINE1; SMURF1; SMAD7; UBE2D1; JUNB; SKI; TGIF1; PMEPA1
			15 / 86	1.3E-10	TGFB1; TGFB3; TGFB1; MYC; SMAD3; CDKN2B; THBS1; PPP2R1B; SMURF1; SMAD7; BMPR2; ACVR1; INHBA; NOG; ID1
			7 / 19	2.6E-06	MAP2K1; TGFB1; TGFB3; TGFB1; SMAD3; SMAD7; SKI
Wnt	Signaling by BMP	REACTOME	6 / 23	2.9E-05	SMURF1; SMAD7; UBE2D1; BMPR2; NOG; FSTL1
			17 / 151	6.6E-09	PRKCA; TP53; MYC; PPP3CA; NFATC2; NFATC4; CTNNB1; SMAD3; TCF7; FZD7; FZD8; WNT7A; WNT7B; PPP2R1B; CSNK1E; FOSL1; PORCN
			16 / 122	1.0E-08	MAP2K1; PDGFA; PDGFB; PRKCA; RASA1; NR4A1; FOXO1; COL1A1; COL5A1; COL4A3; FURIN; PDGFC; THBS1; ITPR3; ADCY7; PHLPP1
PDGF	Signaling by PDGF	REACTOME	6 / 32	1.8E-04	MAP2K1; PDGFA; PRKCA; FOS; RASA1; SRF
			12 / 69	1.3E-08	TP53; FAS; GADD45A; GADD45B; GADD45G; BID; THBS1; SERPINE1; IGFBP3; PMAIP1; SFN; CCGG2
			4 / 16	7.6E-04	TP53; GADD45A; BCL2; TIMP3
p53	p53 signaling pathway	KEGG	10 / 76	3.6E-06	MAP2K1; PRKCA; PLA2G4A; PPP3CA; NFATC2; NFATC4; HSPB1; PTK2; PTGS2; SPHK1
			8 / 37	6.1E-06	MAP2K1; PAK1; FOS; RAP1B; RASA1; ITGB1; PTK2; PTK2B
			5 / 18	1.4E-04	FOS; NCOR2; ETS1; CSF1; ETS2
VEGF	VEGF signaling pathway	KEGG	10 / 112	2.2E-04	MAP2K1; PRKCA; FGF1; FGF9; NR4A1; FOXO1; CBL; ITPR3; ADCY7; PHLPP1
			10 / 112	2.2E-04	MAP2K1; PRKCA; FGF1; FGF9; NR4A1; FOXO1; CBL; ITPR3; ADCY7; PHLPP1
HGF	Signaling of Hepatocyte Growth Factor Receptor	BIOCARTA	8 / 37	6.1E-06	MAP2K1; PAK1; FOS; RAP1B; RASA1; ITGB1; PTK2; PTK2B
ETS	ETS pathway	BIOCARTA	5 / 18	1.4E-04	FOS; NCOR2; ETS1; CSF1; ETS2
FGF	Signaling by FGFR	REACTOME	10 / 112	2.2E-04	MAP2K1; PRKCA; FGF1; FGF9; NR4A1; FOXO1; CBL; ITPR3; ADCY7; PHLPP1



Wnt signaling is activated when secreted Wnt ligands bind to specific Frizzled (FzD) receptors on the surface of target cells to trigger the canonical (Wnt/ β -catenin) or non-canonical (β -catenin-independent) pathways. Particularly, canonical Wnt signaling seems activated by fluid shear. Expression of both *Wnt7a* and *Wnt7b* is increased, as well as Porcupine (*Porcn*), required for Wnt secretion. Also expression of FzD receptors (*Fzd7* and *8*) is up-regulated (although the co-receptor *Lrp6* is down-regulated) as well as the key players β -catenin (*Cttnb1*) and *Tcf7*, which are regulating the expression of down-stream target genes (*Wisp1*, *Fosl1*, *Myc*). Overall, less core signaling pathways were identified that were down-regulated by fluid shear stress. The most prominently down-regulated pathway is JAK/STAT or Interferon signaling (Table 3), with reduced expression of receptors (*Ifngr1*, *Il6st*, *Il5ra* and *Lifr*), signal transducers (*Jak2*, *Stat1*, *Stat5a* and *Irf7,8,9*) as well as target genes (*Socs2* and *Gbp6,7*). Other down-regulated pathways include Rho, PDGF, Hedgehog and Insulin signaling, as well as different metabolic pathways (Tables 3, S5). This also includes PI3K/AKT related signaling, which is not included as core signaling pathway from KEGG in the MSigDB. Expression of a selected set of genes was validated by quantitative PCR using a parallel plate flow-chamber²³ and confirmed fluid-shear induced expression of *Ccbe1*, *Prune2*, *Wisp1*, *Fbln5*, *Plk2*, *Junb*, *Gsto1*, *Hbefg*, *Map3k20* (*Zak*), *Wnt7b*, *Tes*, *Runx1*, *Ets1*, *Map4k4*, *Itgb1* and *Itgav*, while *Jak2* and *Stat1* expression was decreased by fluid shear stress (Fig. 2). After 16 hr gene expression was significantly increased for all tested genes (Supplementary Fig. S2). While several genes reached significance already at 6 hr, others did not. Furthermore, we investigated if the changes in gene expression by shear stress were reversible, by doing a static post incubation of 8 hr, after removal of shear. For several genes, shear stress induced gene expression returned to levels close to the static controls, while other genes showed similar or higher expression levels after post incubation without shear (Supplementary Fig. S3), indicating that in time genes can respond differently to variations in fluid shear stress.

Fluid shear stress response in PTECs is dominated by TGF- β /ALK5 and MAPK/ERK pathways

We previously showed shear stress induced TGF- β /ALK5 dependent SMAD2/3 signaling and target gene expression²³. In addition to increased expression of canonical SMAD2/3 targets, we see shear stress induced expression of other genes known to be induced by TGF- β signaling, including *Junb* and *Fbln5* (Fig. 2)⁴⁴⁻⁴⁶. Our results indicate that shear stress induced *Junb* and *Fbln5* expression was ALK4/5/7 dependent (Fig. 3A). In addition, genes involved in other (core) signaling pathways, like MAPK (*Map3k20* and *Map4k4*), Wnt (*Wisp1*), ETS (*Ets1*) and other pathways (*Plk2*, *Prune2*), were strongly repressed by the ALK4/5/7 inhibitor (Fig. 3A), suggesting that TGF- β /ALK5 signaling is interacting with more pathways than the canonical TGF- β pathway alone. In contrast, fluid shear stress induced down-regulation of *Stat1* and *Jak2* was not altered upon ALK4/5/7 inhibition, although *Jak2* basal levels were already higher with the ALK4/5/7 inhibitor (Fig. 3A).

Since SMAD2/3 mediated gene transcription can be either restrained or induced by ERK1/2

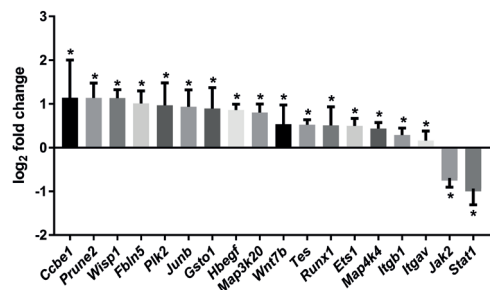
Table 3. Core signaling pathways affected by fluid shear stress - down-regulated genes.

Pathway analysis (KEGG, Reactome and Biocarta) done on 738 significantly down-regulated genes upon fluid shear stress in PTECs using MSigDB. The most significantly altered core signaling pathways are shown and ordered together, followed by the lowest false discovery rate (FDR). K = number of genes in pathway database; k = number of genes in overlap. For the complete list of the pathway analysis of down-regulated genes upon fluid shear stress see Supplementary Table S5.

Pathway	Pathways description	Database	k/K	FDR	Genes
JAK-STAT	Cytokine Signaling in Immune system	REACTOME	25 / 270	2.3E-10	STAT1; IRF7; IRF9; H2-M3; IRF8; ISG15; USP18; IFIT1; MX2; IFI27; IFI35; IFIT3; XAF1; JAK2; IFNGR1; GBP7; DDX58; TRIM25; UBA7; PIK3R1; STAT5A; MAP2K6; IL6ST; SOCS2; BLNK; PTEN; CDH1; RASGRP2; PPP2R5A; IFIH1; DHX58; RAP1GAP2; RAP1GAP; DUSP3; ICOSL; KLHL13; FBXO44
	Interferon Signaling	REACTOME	19 / 159	9.9E-10	
	Interferon alpha/beta signaling	REACTOME	13 / 64	2.2E-09	
	Immune System	REACTOME	37 / 933	4.5E-06	
	Interferon gamma signaling	REACTOME	8 / 63	2.9E-04	
	Jak-STAT signaling pathway	KEGG	10 / 155	2.7E-03	STAT1; IRF9; JAK2; IFNGR1; PIK3R1; STAT5A; IL6ST; SOCS2; PIK3R5; LIFR
Rho	Signaling by Rho GTPases	REACTOME	9 / 113	1.6E-03	NGEF; ARHGEF9; FAM13A; CHN2; RHO; ARHGAP24; ARHGAP19; ARHGAP18; ARHGAP29
PDGF	Signaling by PDGF	REACTOME	9 / 122	2.5E-03	STAT1; PIK3R1; STAT5A; PTEN; GRB7; PRKAR2B; PRKCE; COL4A5; ADCY9
Hedgehog	Hedgehog signaling pathway	KEGG	6 / 56	3.9E-03	LRP2; WNT16; WNT6; PTCH1; BMP7; GAS1
Insulin	Insulin signaling pathway	KEGG	9 / 137	4.2E-03	PIK3R1; SOCS2; PIK3R5; PPARGC1A; LIPE; PRKAR2B; MKNK2; SORBS1; PPP1R3C

Figure 2. qPCR validation of RNA sequencing results

Gene expression (\log_2 fold change) of selected target genes is altered upon 16 hr fluid shear stress, as measured by quantitative PCR. Parallel plate flow-chamber induced fluid shear stress at 2.0 dyn/cm^2 in PTECs; $n = 13$ per condition; *Hprt* served as housekeeping gene to correct for cDNA input; data were normalized to static controls (\log_2 fold change = 0). * indicates significantly altered expression by flow versus no flow ($P < 0.05$) using a one sample *t*-test.



signaling, as shown before^{23,47,48}, we also investigated the involvement of MAPK/ERK signaling in the shear stress response. Our data indicate that only *Plk2* and *Flnb5* induction by fluid-shear is lowered using MEK1/2 inhibitors (Fig. 3B), although the flow response is still present. In contrast, *Junb*, *Map3k20* (*Zak*), *Ets1* and *Prune2* expression was further elevated using

3

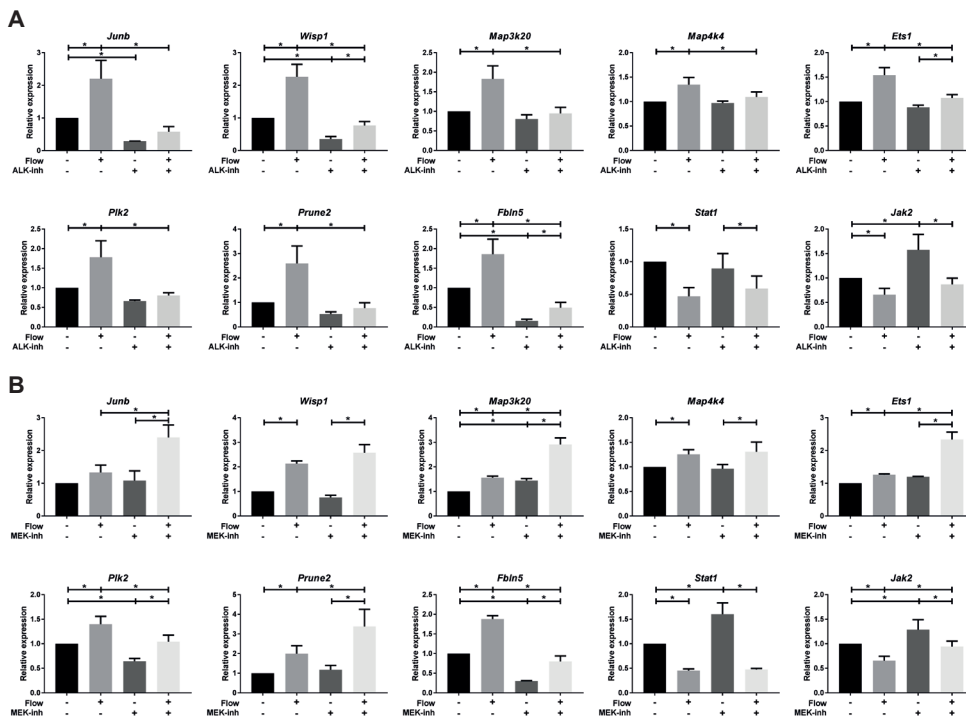


Figure 3. Shear stress response in PTECs is modulated by ALK4/5/7 and MEK1/2 inhibitors.

Relative expression of selected genes upon 16 hr fluid shear stress exposure, as measured by quantitative PCR. (A) ALK4/5/7 inhibitor (10 μ M LY-364947) significantly reduces shear stress increased expression of *Junb*, *Wisp1*, *Map3k20*, *Map4k4*, *Ets1*, *Plk2*, *Prune2* and *Fbn5*, while shear stress induced down-regulation of *Jak2* and *Stat1* was not altered. (B) MEK1/2 inhibition (10 μ M Trametinib) significantly reduces shear stress increased expression of *Plk2* and *Fbn5*, while fluid-flow increased expression of *Junb*, *Map3k20*, *Ets1* and *Prune2* is further elevated. *Wisp1* and *Map4k4* expression was not altered upon MEK inhibition. *Jak2* and *Stat1* expression was still down-regulated by shear stress upon MEK inhibition, although basal levels were slightly higher. (A, B) Parallel plate flow-chamber induced fluid shear stress at 2.0 dyn/cm² in PTECs; $t = 16$ hr; qPCR, *Hprt* served as housekeeping gene to correct for cDNA input; data normalized to unstimulated controls (fold change); $n = 3-5$ per condition. * indicates $P < 0.05$ by two-way ANOVA, followed by post-hoc Fisher's LSD multiple comparison. ALK-inh = ALK4/5/7 inhibitor (LY-364947). MEK-inh = MEK1/2 inhibitor (Trametinib, GSK1120212).

MEK inhibitors, which was also seen for many canonical SMAD2/3 targets²³, while the shear stress response of *Wisp1* and *Map4k4* was not significantly changed upon MEK inhibition (Fig. 3B). Fluid shear stress induced down-regulation of *Jak2* and *Stat1* is still present upon MEK inhibition (Fig. 3B), although basal levels were slightly higher with MEK1/2 inhibitors. In conclusion, our data suggest complex regulation of the fluid shear stress response in PTECs, which is largely modulated by TGF- β /ALK5 and MAPK/ERK pathways.

Primary cilia only play a role in a part of the shear stress response in PTECs

Since defects in cilia formation and function have profound effects on the development and physiology of kidneys and other organs^{1,2}, we investigated the shear stress response in PTECs after cilia removal by ammonium sulfate. Expression of *Plk2*, *Prune2* and *Ets1* were clearly cilia dependent, since the shear stress induced response was completely lost after cilia ablation (Fig. 4). In contrast, genes involved in TGF- β , Wnt, MAPK and JAK/STAT signaling, i.e. *Junb*, *Fbln5*, *Wisp1*, *Map3k20*, *Map4k4* as well as *Stat1*, were only slightly or not affected in the shear stress response upon cilia removal (Fig. 4). Although shear induced down-regulation of *Jak2* was abrogated, *Jak2* expression in static cells was already reduced upon ammonium sulfate treatment (Fig. 4). Our data suggests that shear stress regulated gene expression in PTECs is only partially cilia dependent and other mechano-sensors are involved as well.

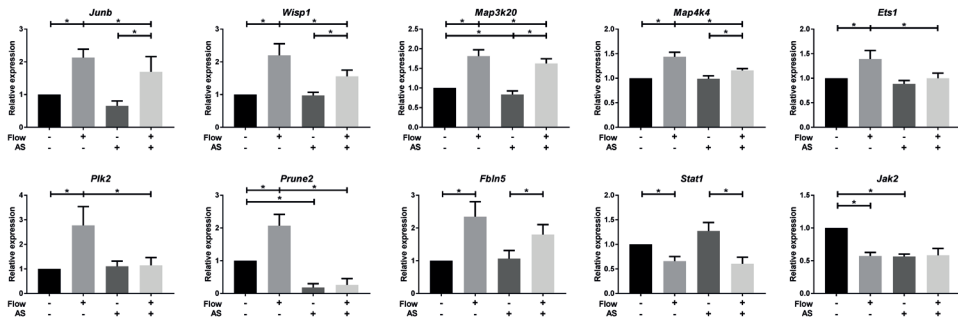


Figure 4. Shear stress altered gene expression in PTECs is partially cilia dependent.

Relative expression of selected genes upon 16 hr fluid shear stress exposure in controls and cells treated with 50 mM ammonium sulfate (AS), as measured by quantitative PCR. Shear stress induced expression of *Ets1*, *Plk2* and *Prune2* was abrogated after cilia ablation. *Junb*, *Wisp1*, *Map3k20*, *Map4k4*, *Fbln5* and *Stat1* expression was only slightly or not affected in the shear stress response upon cilia removal. Shear induced down-regulation of *Jak2* was abrogated, since *Jak2* expression in static cells was already reduced upon ammonium sulfate treatment. Parallel plate flow-chamber induced fluid shear stress at 2.0 dyn/cm² in PTECs; *Hprt* served as housekeeping gene to correct for cDNA input; data were normalized to static controls (fold change); $n = 5$ per condition. * indicates $P < 0.05$ by two-way ANOVA, followed by post-hoc Fisher's LSD multiple comparison.

Shear stress induced gene expression in PTECs is flow rate dependent

Thus far we applied fluid shear stress of 2.0 dyn/cm², which is known to be an increased physio-pathological shear stress^{4,41,42,49}. To compare the gene expression to physiological levels of shear, we exposed the cells to a shear stress range of 0.25 - 2.0 dyn/cm². Expression of *Wisp1*, *Map3k20*, *Map4k4* and *Ets1* was clearly flow rate dependent and this trend was also visible for *Junb*, *Plk2*, *Prune2* and *Fbln5* (Fig. 5A). To mimic the induction of hyperfiltration, PTECs were pre-exposed to physiological levels of shear (0.25 dyn/cm²) for 4 hr, followed

by 16 hr shear stress at the same physiological level or at pathological levels of shear (2.0 dyn/cm²). Expression of *Wisp1*, *Map3k20*, *Map4k4*, *Ets1* and *Fbln5* was significantly higher at pathological levels of shear compared to physiological levels, while this trend was also visible for *Junb* and *Plk2* (Fig. 5B). For the downregulated genes, *Stat1* and *Jak2*, there was no difference in expression between physiological and pathological shear. So, our data indicate that higher levels of shear and a switch from physiological to pathological shear, result in increased gene expression, at least for most the genes analyzed in this experiment.

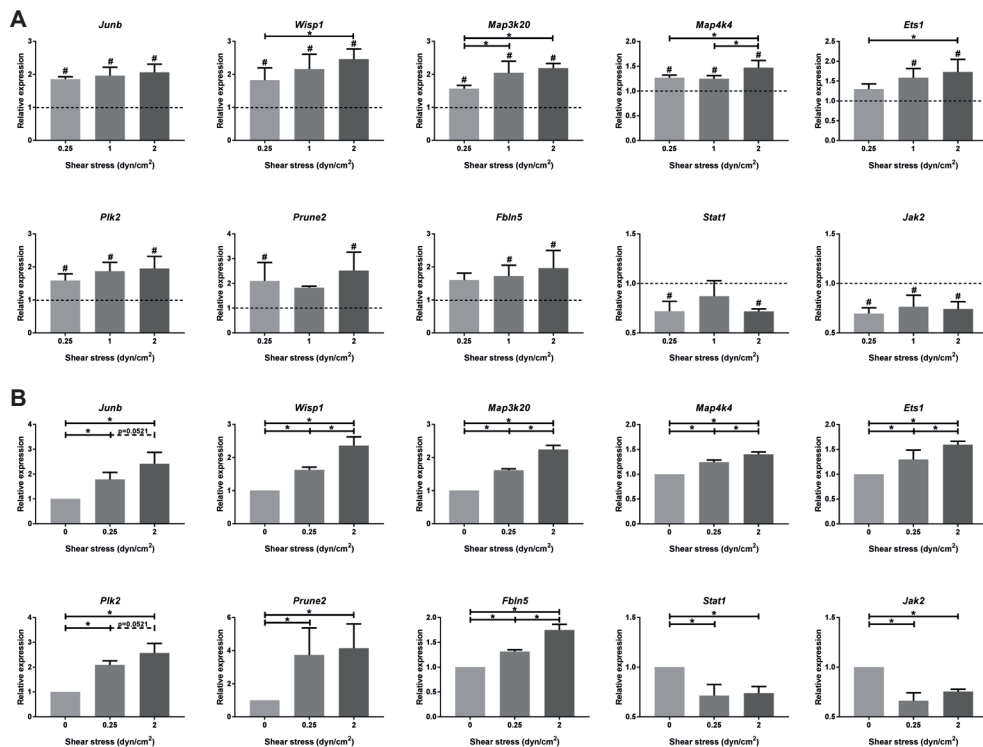


Figure 5. Shear stress altered gene expression in PTECs is flow rate dependent.

Relative expression of selected genes upon different levels of fluid shear stress exposure (0.25 - 2.0 dyn/cm²) for 16 hr, as measured by quantitative PCR. (A) After starvation under static conditions, cells were directly exposed to the indicated level of fluid shear stress. (B) Cells were first pre-exposed for 4 hr to low levels of shear stress (0.25 dyn/cm²), followed by 16 hr shear stress exposure at indicated levels. Expression of all genes was significantly increased by shear stress compared to static controls (dashed line in A) and was flow rate dependent for most genes. (A, B) Parallel plate flow-chamber induced fluid shear stress of 0.25 - 2.0 dyn/cm² in PTECs; t = 16 hr (A) or t = 4 + 16 hr (B); qPCR, *Hprt* served as housekeeping gene to correct for cDNA input; data normalized to unstimulated controls (fold change); n = 3 per condition. # significant difference compared to unstimulated control (dashed line in A) or * significant difference between treatment groups (P < 0.05 by one-way ANOVA, followed by post-hoc Fisher's LSD multiple comparison).

DISCUSSION

In this study we used RNA sequencing to get a comprehensive overview of the transcriptome alterations upon fluid shear stress in proximal tubular epithelial cells. Physiological shear stress in renal epithelial cells is ranging from 0.05 - 1.0 dyn/cm², where proximal tubular cells experience the highest range of shear stress^{4,41,42,49}. We applied a fluid shear stress of 2.0 dyn/cm², which is known to be an increased physio-pathological shear stress, mimicking hyperfiltration after renal mass reduction or during progression of renal disease. Our genome wide RNA sequencing data confirmed previously reported fluid flow-induced changes in gene expression of *Cox2* (*Ptgs2*), *Ccl2* (*Mcp1*), *Edn1*, *Egr1*, *Snai1* and *Cdh1* in renal epithelial cells³⁶⁻⁴⁰. Furthermore, our data reveal >1500 other genes to be altered by fluid shear stress in PTECs. We validated a subset of genes by qPCR and showed that the shear stress response was time dependent within the first 16 hr. In addition, after removal of the shear, the shear-induced gene expression was reversible for some of the genes, while other genes showed similar or higher differential gene expression upon static post incubation. Differences in signaling and cytokine production upon shear may explain the different responses as well as differences in transcriptional activation and stability of transcripts. For example, *Fn1* is a very long transcript, which requires more time for transcription and degradation, while *Pai1* (*Serpine1*) has an faster turn-over^{23,50}.

Pathway analysis indicated increased expression of cell-cell/cell-matrix interaction genes, including cytoskeletal components, cell adhesion and tight junction molecules, extracellular matrix components and integrins. This suggests strengthening of epithelial cells and their surroundings to resist (increased) physiological shear stress^{49,51,52}. Another study showed loss of epithelial cell morphology during high pathological shear stress of 5 dyn/cm²⁴⁰. Long-term high shear exposure therefore might also lead to fibrotic deposition and tubulointerstitial lesions, which is commonly seen after renal mass reduction or during progression of renal diseases^{49,53-56}. Pro-apoptotic as well as pro-survival and cell cycle arrest genes were induced by shear stress, while key players in apoptosis (*Bad*, *Bak*, *Bax*, and caspases) and cell cycle (cyclins and CDKs) were not altered in gene expression. This suggests that apoptosis and cell cycle related gene expression are not dramatically altered during shear exposure.

Core signaling pathways altered by shear stress comprise MAPK and TGF- β signaling. Even more, TGF- β /ALK5-induced target gene expression in renal epithelial cells is partially restrained by MEK1/2-mediated signaling²³. Using ALK4/5/7 inhibitors, we showed that many genes, but not all genes, are dependent on shear induced TGF- β /ALK5 signaling, including genes involved in other core signaling pathways like MAPK and Wnt signaling. The role of TGF- β as a master regulator of the shear response is related to the TGF- β /ALK5 interaction since we previously showed that also TGF- β neutralizing antibodies inhibit the

response²³. It is conceivable that under flow conditions TGF- β processing and binding of the active ligand is enhanced. Interestingly, a recent publication showed that TGF- β can be released from its latency-associated peptide (LAP) by shear stress, probably by forces exerted on $\alpha_v\beta_6$ -integrins via the actin cytoskeleton^{57,58}. We also noticed an increase in gene expression of several integrins during shear stress, including integrin α_v (*Itgav*). In addition, there are several connections between TGF- β and MAPK signaling^{47,48,59,60}, thereby modulating the response to shear. Our data show that the shear stress response of a subset of genes is attenuated upon MEK1/2 inhibition, while other genes showed an enhanced response. Since there are multiple interactions between TGF- β and MAPK/ERK signaling pathways, the integration of these pathways is complex and biological context dependent, and therefore difficult to predict²³.

In addition to TGF- β signaling, increased expression of other cytokines observed in our study suggests attraction and activation of macrophages and inflammatory cells upon shear *in vivo*. This is a common phenomenon during development of kidney diseases, where shear stress is fluctuating due to changes in glomerular filtration rate, tubular hyperfiltration and obstruction⁶¹. Altered expression of other growth factors or cytokine signaling pathways include FGF, HB-EGF, PDGF, CXC and other cytokines. FGF, HB-EGF and PDGF can bind to tyrosine kinase receptors that upon activation stimulate the Ras/Raf/ERK (MAPK) pathway and/or the PI3K/AKT pathway (up-regulated upon shear stress) and/or STAT-signaling (down-regulated upon shear stress)^{62,63}. At several levels these pathways can be amplified or negatively modulated, and they can interact with each other as well. Multiple ligand isoforms can bind to the receptors with different affinities. Upon fluid flow, transcript levels of several ligands is increased (*Fgf1*, *Fgf9*, *Hbegf*, *Pdgfa*, *Pdgfb*, *Pdgfc*), but not the receptors. Whether increased signaling is related to endocrine/paracrine loops, as seen for TGF- β , needs more extensive investigation.

Interestingly, we also observed altered expression of proteoglycans, like syndecans and glypican, as well as modifying enzymes involved in glycosaminoglycan, heparan-sulphate or chondroitin-sulphate metabolism, which are all involved in glycocalyx remodeling⁶⁴. Cell-surface-associated heparan sulfate proteoglycans have been shown to be essential for FGF signal transduction and, more general, the glycocalyx is able to significantly modify the cellular response to growth factors including PDGF and FGF. It has been shown that the glycocalyx plays an important role in mechanotransduction of shear stress in endothelial cells. It is required for the cytoskeleton to respond to shear stress and acts as a signaling platform integrating shear stress, growth factor, chemokine and cytokine signaling⁶⁵⁻⁶⁸. So, our data indicate that fluid shear stress induce genes involved in glycocalyx remodeling in PTECs, although it has to be further investigated whether the glycocalyx is equally involved in mechano-sensing upon shear stress in renal epithelial cells.

The shear stress response in PTECs can be regulated by a variety of mechano-sensors at different sub-cellular locations⁸⁻¹⁰. We investigated the role of primary cilia, since defects in cilia formation and function are associated with developmental disorders and (kidney) diseases^{1,2}. Our results indicate that fluid shear stress induced *Plk2*, *Prune2* and *Ets1* expression is cilia dependent, since 'removal' of the cilium by ammonium sulphate completely abolished the shear stress response. Genes involved in TGF- β , MAPK and Wnt signaling were not or only slightly reduced upon ammonium sulphate treatment, suggesting that mechano-sensors at other cellular locations are also contributing to the shear stress response in PTECs.

The main shear stress down-regulated pathway is JAK/STAT signaling. However, this is largely related to reduced expression of components of the interferon signaling pathway since only a few STAT1 target genes are differentially expressed (*Irf7*, *Irf9*, *Irf35*, *Irf27*, *Trim25*)⁶⁹. Interferon itself is not expressed in our *in vitro* system (Supplementary Table S2), but reduced expression of components of the signaling pathway support a study in endothelial cells, describing attenuation of IFN γ -induced responses by laminar flow, via the suppression of STAT1 activation⁷⁰. We show that reduced *Stat1* expression by shear stress was ALK4/5/7, MEK1/2 as well as cilium independent, although there was slightly higher expression when using the MEK1/2 inhibitors in static cells. A similar pattern was observed for *Jak2* expression, with the notification that ammonium sulphate treatment already reduced expression of *Jak2* as much as shear stress. For another Stat-family member, STAT6, reduced expression of target genes has been reported. During fluid flow both STAT6 and the transcriptional co-activator p100 locate in the primary cilia, while at static conditions these proteins translocate to the nucleus¹⁸.

Other down-regulated genes by shear stress include genes involved in amino acid, carbohydrate, fatty acid, ketone body and cholesterol metabolism (Supplementary Fig. S1B, Table S5). Also in endothelial cells shear stress exposure decreased expression of genes involved in glycolysis^{71,72}, lipid metabolism⁷³⁻⁷⁵ and cholesterol biosynthesis^{76,77}. This was dependent on AMPK, which is an important kinase in energy metabolism^{73,78} and plays a central role in fluid flow induced primary cilium bending and down-regulation of mTORC1 activity in renal epithelial cells^{20,21}. Overall, the data show that increased shear stress reduces metabolic activity in renal epithelial cells.

This *in vitro* study gives a comprehensive overview of fluid shear stress altered gene expression in renal epithelial cells, but is not fully representative for the *in vivo* situation, since several other cells types and cytokines in the nephrons are involved. Nevertheless, our results give an overview of genes and pathways that are modulated by shear stress in renal epithelial cells, which could help us to understand relevant biological processes involved in

mechano-sensing. Several of the shear regulated processes are altered in kidney diseases as well, including TGF- β , Wnt and JAK-STAT signaling⁷⁹. We hypothesize that large variations in shear stress, occurring in kidney diseases, might contribute to the disease phenotype. This hypothesis is supported by our data showing that the expression of several genes involved in TGF- β , MAPK and Wnt signaling is further elevated upon switching from physiological to pathological levels of shear.

In conclusion, this study provides a comprehensive profile of genes altered upon shear stress in PTECs. Both cell cycle activity and apoptosis are not dramatically altered and molecular alterations are more related to cell remodeling, involving cell-cell and cell-matrix interactions, cytoskeleton and glycocalyx remodeling, as well as glycolysis and cholesterol metabolism. MAPK/ERK and TGF- β signaling are master regulators of shear-induced gene expression, since inhibitors modulate other signaling pathways as well. Nevertheless, altered JAK/STAT signaling, the main core signaling pathways down-regulated upon shear stress, is independent of MAPK/ERK and TGF- β . Our results indicate that different mechanosensors are involved in shear stress sensing in PTECs, because cilia ablation did only affect expression of a subset of shear modulated genes. Imbalance in cellular signaling due to variations in fluid shear stress are probably relevant for renal physiology and pathology as suggested by elevated expression of genes at pathological levels of shear stress compared to physiological controls. At this moment only a limited number of genes have been annotated to pathways and transcriptional target genes are hardly included, thereby limiting the interpretation of data to what is currently known. In the future the use of gene-specific targeting, high-throughput RNA-sequencing and connectivity maps will probably reveal additional information on shear induced signaling and how shear stress regulated processes influence epithelial cell integrity and cellular plasticity in renal disease.

Acknowledgements

We thank Ron Wolterbeek (Medical Statistics, LUMC) for support with statistical analysis and Prof. Jenneke Klein-Nuland for facilitating the research with the parallel-plate fluid flow system. This work was supported by funding from the Netherlands Organization for Scientific Research (NWO) [grant number 820.02.016] and from the People Program (Marie Curie Actions) of the European Union's Seventh Framework Program FP7/2007-2013 [REA grant agreement no. 317246].

Compliance with ethical standards

Competing interests

The authors declare no competing or financial interests.

REFERENCES

1. Goetz S.C. & Anderson K.V. The primary cilium: a signalling centre during vertebrate development. *Nat. Rev. Genet.* **11**, 331-344 (2010).
2. Quinlan R.J., Tobin J.L., & Beales P.L. Modeling ciliopathies: Primary cilia in development and disease. *Curr. Top. Dev. Biol.* **84**, 249-310 (2008).
3. Freund J.B., Goetz J.G., Hill K.L., & Vermot J. Fluid flows and forces in development: functions, features and biophysical principles. *Development* **139**, 1229-1245 (2012).
4. Weinbaum S., Duan Y., Satlin L.M., Wang T., & Weinstein A.M. Mechanotransduction in the renal tubule. *Am. J. Physiol Renal Physiol* **299**, F1220-F1236 (2010).
5. Carrisoza-Gaytan R., Carattino M.D., Kleyman T.R., & Satlin L.M. An unexpected journey: conceptual evolution of mechanoregulated potassium transport in the distal nephron. *Am. J. Physiol Cell Physiol* **310**, C243-C259 (2016).
6. Piperi C. & Basdra E.K. Polycystins and mechanotransduction: From physiology to disease. *World J. Exp. Med.* **5**, 200-205 (2015).
7. Sharma A., Mucino M.J., & Ronco C. Renal functional reserve and renal recovery after acute kidney injury. *Nephron Clin. Pract.* **127**, 94-100 (2014).
8. Ingber D.E. Cellular mechanotransduction: putting all the pieces together again. *FASEB J.* **20**, 811-827 (2006).
9. Curry F.E. & Adamson R.H. Endothelial glycocalyx: permeability barrier and mechanosensor. *Ann. Biomed. Eng* **40**, 828-839 (2012).
10. Petersen E.N., Chung H.W., Nayebosadri A., & Hansen S.B. Kinetic disruption of lipid rafts is a mechanosensor for phospholipase D. *Nat. Commun.* **7**, 13873 (2016).
11. Praetorius H.A. & Spring K.R. Bending the MDCK cell primary cilium increases intracellular calcium. *J. Membr. Biol.* **184**, 71-79 (2001).
12. Praetorius H.A., Frokiaer J., Nielsen S., & Spring K.R. Bending the Primary Cilium Opens Ca(2+)-sensitive Intermediate-Conductance K⁺ Channels in MDCK Cells. *J. Membr. Biol.* **191**, 193-200 (2003).
13. DeCaen P.G., Delling M., Vien T.N., & Clapham D.E. Direct recording and molecular identification of the calcium channel of primary cilia. *Nature* **504**, 315-318 (2013).
14. Delling M., DeCaen P.G., Doerner J.F., Febvay S., & Clapham D.E. Primary cilia are specialized calcium signalling organelles. *Nature* **504**, 311-314 (2013).
15. Praetorius H.A. The primary cilium as sensor of fluid flow: new building blocks to the model. A review in the theme: cell signaling: proteins, pathways and mechanisms. *Am. J. Physiol Cell Physiol* **308**, C198-C208 (2015).
16. Delling M. *et al.* Primary cilia are not calcium-responsive mechanosensors. *Nature* **531**, 656-660 (2016).
17. Simons M. *et al.* Inversin, the gene product mutated in nephronophthisis type II, functions as a molecular switch between Wnt signaling pathways. *Nat. Genet.* **37**, 537-543 (2005).
18. Low S.H. *et al.* Polycystin-1, STAT6, and P100 function in a pathway that transduces ciliary mechanosensation and is activated in polycystic kidney disease. *Dev. Cell* **10**, 57-69 (2006).
19. Weimbs T. Polycystic kidney disease and renal injury repair: common pathways, fluid flow, and the function of polycystin-1. *Am J Physiol Renal Physiol* **293**, F1423-F1432 (2007).
20. Boehlke C. *et al.* Primary cilia regulate mTORC1 activity and cell size through Lkb1. *Nat. Cell Biol.* **12**, 1115-1122 (2010).
21. Zhong M. *et al.* Tumor Suppressor Folliculin Regulates mTORC1 through Primary Cilia. *J. Biol. Chem.* **291**, 11689-11697 (2016).
22. Kotsis F., Boehlke C., & Kuehn E.W. The ciliary flow sensor and polycystic kidney disease. *Nephrol. Dial. Transplant.* **28**, 518-526 (2013).

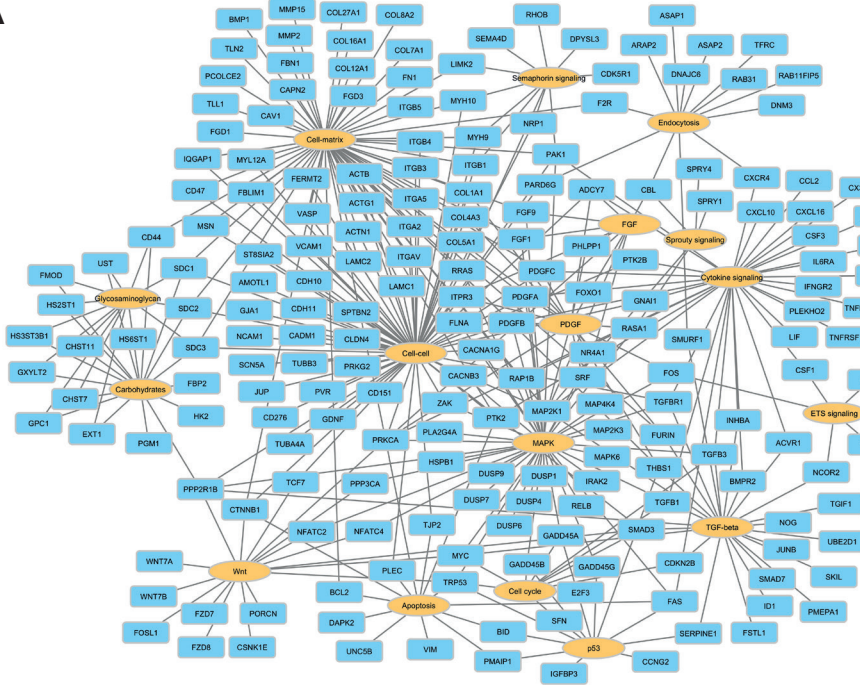
23. Kunnen S.J. *et al.* Fluid shear stress-induced TGF-beta/ALK5 signaling in renal epithelial cells is modulated by MEK1/2. *Cell Mol. Life Sci.* **74**, 2283-2298 (2017).
24. Leonhard W.N. *et al.* Curcumin inhibits cystogenesis by simultaneous interference of multiple signaling pathways: In vivo evidence from a Pkd1-deletion model. *Am. J. Physiol Renal Physiol* **300**, F1193-F1202 (2011).
25. Malek A.M., Gibbons G.H., Dzau V.J., & Izumo S. Fluid shear stress differentially modulates expression of genes encoding basic fibroblast growth factor and platelet-derived growth factor B chain in vascular endothelium. *J Clin. Invest* **92**, 2013-2021 (1993).
26. Malek A.M., Ahlquist R., Gibbons G.H., Dzau V.J., & Izumo S. A cone-plate apparatus for the in vitro biochemical and molecular analysis of the effect of shear stress on adherent cells. *Methods in Cell Science* **17**, 165-176 (1995).
27. Bacabac R.G. *et al.* Dynamic shear stress in parallel-plate flow chambers. *J. Biomech.* **38**, 159-167 (2005).
28. Klein-Nulend J., Semeins C.M., Ajubi N.E., Nijweide P.J., & Burger E.H. Pulsating fluid flow increases nitric oxide (NO) synthesis by osteocytes but not periosteal fibroblasts--correlation with prostaglandin upregulation. *Biochem. Biophys. Res. Commun.* **217**, 640-648 (1995).
29. Juffer P., Bakker A.D., Klein-Nulend J., & Jaspers R.T. Mechanical loading by fluid shear stress of myotube glycocalyx stimulates growth factor expression and nitric oxide production. *Cell Biochem. Biophys.* **69**, 411-419 (2014).
30. Waterston R.H. *et al.* Initial sequencing and comparative analysis of the mouse genome. *Nature* **420**, 520-562 (2002).
31. Kim D. *et al.* TopHat2: accurate alignment of transcriptomes in the presence of insertions, deletions and gene fusions. *Genome Biol.* **14**, R36 (2013).
32. Anders S., Pyl P.T., & Huber W. HTSeq--a Python framework to work with high-throughput sequencing data. *Bioinformatics.* **31**, 166-169 (2015).
33. Happe H. *et al.* Altered Hippo signalling in polycystic kidney disease. *J. Pathol.* **224**, 133-142 (2011).
34. Livak K.J. & Schmittgen T.D. Analysis of relative gene expression data using real-time quantitative PCR and the 2(-Delta Delta C(T)) Method. *Methods* **25**, 402-408 (2001).
35. Subramanian A. *et al.* Gene set enrichment analysis: a knowledge-based approach for interpreting genome-wide expression profiles. *Proc. Natl. Acad. Sci. U. S. A* **102**, 15545-15550 (2005).
36. Flores D., Liu Y., Liu W., Satlin L.M., & Rohatgi R. Flow-induced prostaglandin E2 release regulates Na and K transport in the collecting duct. *Am. J. Physiol Renal Physiol* **303**, F632-F638 (2012).
37. Flores D., Battini L., Gusella G.L., & Rohatgi R. Fluid shear stress induces renal epithelial gene expression through polycystin-2-dependent trafficking of extracellular regulated kinase. *Nephron Physiol* **117**, 27-36 (2011).
38. Pandit M.M. *et al.* Flow regulation of endothelin-1 production in the inner medullary collecting duct. *Am. J. Physiol Renal Physiol* **308**, F541-F552 (2015).
39. Schwachtgen J.L., Houston P., Campbell C., Sukhatme V., & Braddock M. Fluid shear stress activation of egr-1 transcription in cultured human endothelial and epithelial cells is mediated via the extracellular signal-related kinase 1/2 mitogen-activated protein kinase pathway. *J. Clin. Invest* **101**, 2540-2549 (1998).
40. Maggiorani D. *et al.* Shear Stress-Induced Alteration of Epithelial Organization in Human Renal Tubular Cells. *PLoS. One.* **10**, e0131416 (2015).
41. Grabias B.M. & Konstantopoulos K. Epithelial-mesenchymal transition and fibrosis are mutually exclusive responses in shear-activated proximal tubular epithelial cells. *FASEB J.* **26**, 4131-4141 (2012).
42. Grabias B.M. & Konstantopoulos K. Notch4-dependent antagonism of canonical TGF-beta1 signaling defines unique temporal fluctuations of SMAD3 activity in sheared proximal tubular epithelial cells. *Am. J. Physiol Renal Physiol* **305**, F123-F133 (2013).
43. Foulds C.E., Nelson M.L., Blaszcak A.G., & Graves B.J. Ras/mitogen-activated protein kinase signaling activates Ets-1 and Ets-2 by CBP/p300 recruitment. *Mol. Cell Biol.* **24**, 10954-10964 (2004).
44. Lee K.S., Hong S.H., & Bae S.C. Both the Smad and p38 MAPK pathways play a crucial role in Runx2

- expression following induction by transforming growth factor-beta and bone morphogenetic protein. *Oncogene* **21**, 7156-7163 (2002).
45. Schiemann W.P., Globe G.C., Kalume D.E., Pandey A., & Lodish H.F. Context-specific effects of fibulin-5 (DANCE/EVEC) on cell proliferation, motility, and invasion. Fibulin-5 is induced by transforming growth factor-beta and affects protein kinase cascades. *J. Biol. Chem.* **277**, 27367-27377 (2002).
 46. Topalovski M., Hagopian M., Wang M., & Brekken R.A. Hypoxia and Transforming Growth Factor beta Cooperate to Induce Fibulin-5 Expression in Pancreatic Cancer. *J. Biol. Chem.* **291**, 22244-22252 (2016).
 47. Kretzschmar M., Doody J., Timokhina I., & Massague J. A mechanism of repression of TGFbeta/ Smad signaling by oncogenic Ras. *Genes Dev.* **13**, 804-816 (1999).
 48. Hough C., Radu M., & Dore J.J. Tgf-beta induced Erk phosphorylation of smad linker region regulates smad signaling. *PLoS. One.* **7**, e42513 (2012).
 49. Essig M., Terzi F., Burtin M., & Friedlander G. Mechanical strains induced by tubular flow affect the phenotype of proximal tubular cells. *Am. J. Physiol Renal Physiol* **281**, F751-F762 (2001).
 50. 't Hoen P.A. *et al.* mRNA degradation controls differentiation state-dependent differences in transcript and splice variant abundance. *Nucleic Acids Res.* **39**, 556-566 (2011).
 51. Duan Y. *et al.* Shear-induced reorganization of renal proximal tubule cell actin cytoskeleton and apical junctional complexes. *Proc. Natl. Acad. Sci. U.S.A.* **105**, 11418-11423 (2008).
 52. Jang K.J. *et al.* Human kidney proximal tubule-on-a-chip for drug transport and nephrotoxicity assessment. *Integr. Biol.* **5**, 1119-1129 (2013).
 53. Essig M. & Friedlander G. Tubular shear stress and phenotype of renal proximal tubular cells. *J. Am. Soc. Nephrol.* **14**, S33-S35 (2003).
 54. Rohatgi R. & Flores D. Intratubular hydrodynamic forces influence tubulointerstitial fibrosis in the kidney. *Curr. Opin. Nephrol. Hypertens.* **19**, 65-71 (2010).
 55. Grabias B.M. & Konstantopoulos K. The physical basis of renal fibrosis: effects of altered hydrodynamic forces on kidney homeostasis. *Am. J. Physiol Renal Physiol* **306**, F473-F485 (2014).
 56. Venkatachalam M.A. *et al.* Acute kidney injury: a springboard for progression in chronic kidney disease. *Am. J. Physiol Renal Physiol* **298**, F1078-F1094 (2010).
 57. Dong X. *et al.* Force interacts with macromolecular structure in activation of TGF-beta. *Nature* **542**, 55-59 (2017).
 58. Ha T. Structural biology: Growth factor rattled out of its cage. *Nature* **542**, 40-41 (2017).
 59. Lee M.K. *et al.* TGF-beta activates Erk MAP kinase signalling through direct phosphorylation of ShcA. *EMBO J.* **26**, 3957-3967 (2007).
 60. Muthusamy B.P. *et al.* ShcA Protects against Epithelial-Mesenchymal Transition through Compartmentalized Inhibition of TGF-beta-Induced Smad Activation. *PLoS. Biol.* **13**, e1002325 (2015).
 61. Akchurin O.M. & Kaskel F. Update on inflammation in chronic kidney disease. *Blood Purif.* **39**, 84-92 (2015).
 62. Turner N. & Grose R. Fibroblast growth factor signalling: from development to cancer. *Nat. Rev. Cancer* **10**, 116-129 (2010).
 63. Pileri S.A. & Piccaluga P.P. New molecular insights into peripheral T cell lymphomas. *J. Clin. Invest* **122**, 3448-3455 (2012).
 64. Reitsma S., Slaaf D.W., Vink H., van Zandvoort M.A., & oude Egbrink M.G. The endothelial glycocalyx: composition, functions, and visualization. *Pflugers Arch.* **454**, 345-359 (2007).
 65. Thi M.M., Tarbell J.M., Weinbaum S., & Spray D.C. The role of the glycocalyx in reorganization of the actin cytoskeleton under fluid shear stress: a "bumper-car" model. *Proc. Natl. Acad. Sci. U. S. A* **101**, 16483-16488 (2004).
 66. Zeng Y. & Liu J. Role of glypican-1 in endothelial NOS activation under various steady shear stress magnitudes. *Exp. Cell Res.* **348**, 184-189 (2016).
 67. Zeng Y. Endothelial glycocalyx as a critical signalling platform integrating the extracellular haemodynamic forces and chemical signalling. *J. Cell Mol. Med.* **21**, 1457-1462 (2017).

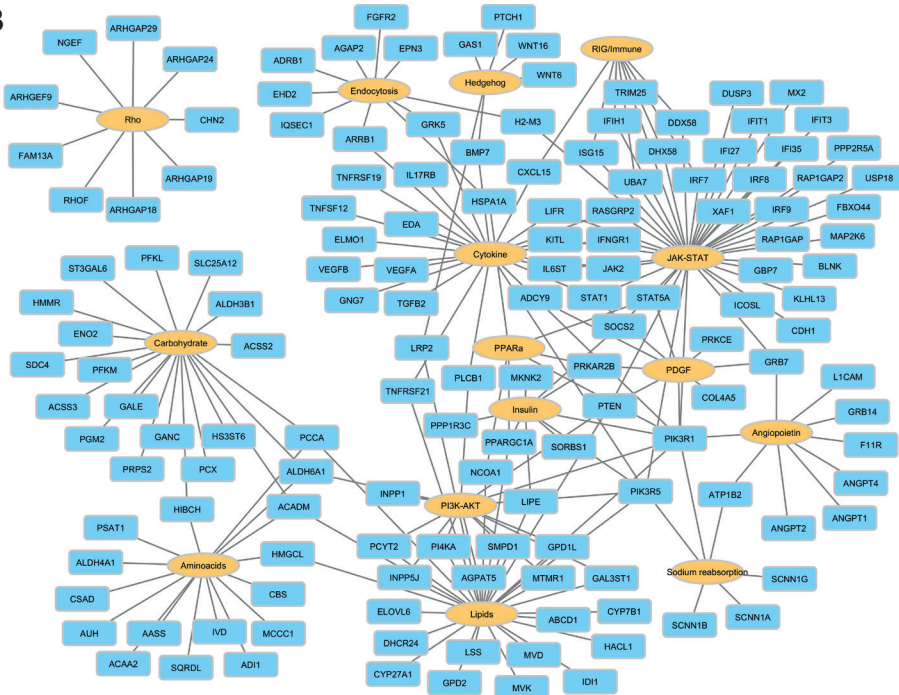
68. Ebong E.E., Lopez-Quintero S.V., Rizzo V., Spray D.C., & Tarbell J.M. Shear-induced endothelial NOS activation and remodeling via heparan sulfate, glypican-1, and syndecan-1. *Integr. Biol.* **6**, 338-347 (2014).
69. Satoh J. & Tabunoki H. A Comprehensive Profile of ChIP-Seq-Based STAT1 Target Genes Suggests the Complexity of STAT1-Mediated Gene Regulatory Mechanisms. *Gene Regul. Syst. Bio* **7**, 41-56 (2013).
70. Tsai Y.C. *et al.* Laminar flow attenuates interferon-induced inflammatory responses in endothelial cells. *Cardiovasc. Res.* **74**, 497-505 (2007).
71. Kim B., Lee H., Kawata K., & Park J.Y. Exercise-mediated wall shear stress increases mitochondrial biogenesis in vascular endothelium. *PLoS. One.* **9**, e111409 (2014).
72. Doddaballapur A. *et al.* Laminar shear stress inhibits endothelial cell metabolism via KLF2-mediated repression of PFKFB3. *Arterioscler. Thromb. Vasc. Biol.* **35**, 137-145 (2015).
73. Fisslthaler B. & Fleming I. Activation and signaling by the AMP-activated protein kinase in endothelial cells. *Circ. Res.* **105**, 114-127 (2009).
74. Mun G.I., An S.M., Park H., Jo H., & Boo Y.C. Laminar shear stress inhibits lipid peroxidation induced by high glucose plus arachidonic acid in endothelial cells. *Am. J. Physiol Heart Circ. Physiol* **295**, H1966-H1973 (2008).
75. Yamamoto K. & Ando J. Endothelial cell and model membranes respond to shear stress by rapidly decreasing the order of their lipid phases. *J. Cell Sci.* **126**, 1227-1234 (2013).
76. Fisslthaler B., Fleming I., Keseru B., Walsh K., & Busse R. Fluid shear stress and NO decrease the activity of the hydroxy-methylglutaryl coenzyme A reductase in endothelial cells via the AMP-activated protein kinase and FoxO1. *Circ. Res.* **100**, e12-e21 (2007).
77. Yamamoto K. & Ando J. Vascular endothelial cell membranes differentiate between stretch and shear stress through transitions in their lipid phases. *Am. J. Physiol Heart Circ. Physiol* **309**, H1178-H1185 (2015).
78. Carling D. The AMP-activated protein kinase cascade--a unifying system for energy control. *Trends Biochem. Sci.* **29**, 18-24 (2004).
79. Gewin L., Zent R., & Pozzi A. Progression of chronic kidney disease: too much cellular talk causes damage. *Kidney Int.* **91**, 552-560 (2017).

SUPPLEMENTARY FIGURES

A



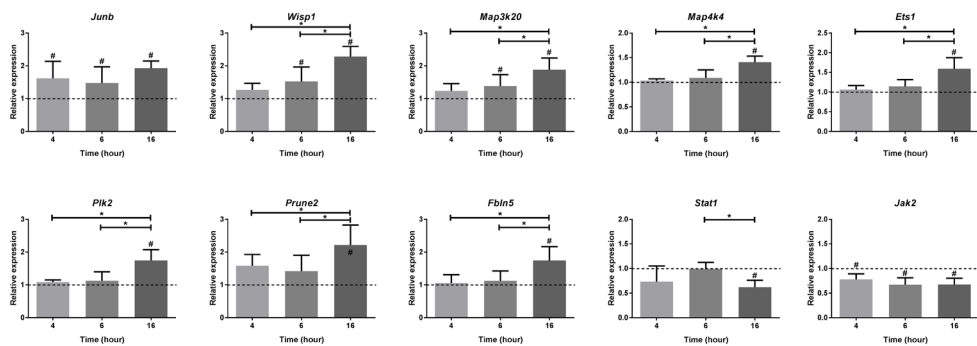
B



3

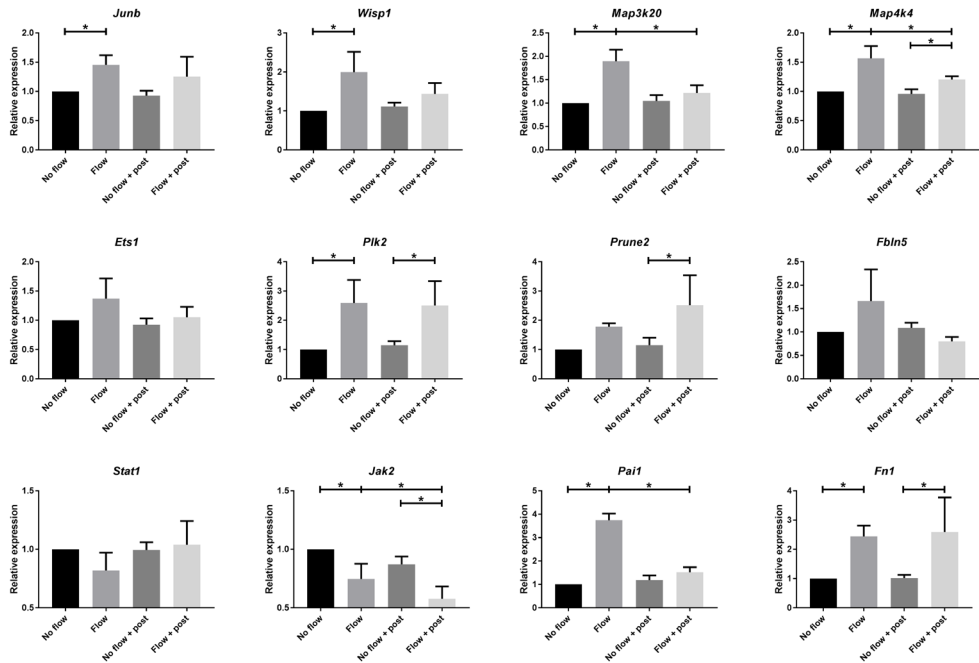
Supplementary Figure S1. Interaction network of genes regulated by fluid shear stress.

Interaction networks of up-regulated (A) and down-regulated (B) genes by shear stress were made using Cytoscape version 3.4.0. Interactions between genes (blue nodes) and their annotated pathways or processes (orange nodes) are shown. For annotated terms the common subgroup names were used, as given in Supplementary Tables S4 (top 100 up-regulated terms) and S5 (top 50 down-regulated terms), thereby including terms involved in core signaling pathways, cell-cell or cell matrix interactions, metabolism, cytokine signaling or other general cellular processes that are not disease or specific cell type related. Most pathway databases didn't include the transcriptional target genes of the pathways, but only the signal transducers, thereby limiting the interpretation of the pathway analysis.



Supplementary Figure S2. Shear stress induced expression in PTECs in time.

Relative expression of selected genes upon fluid shear stress exposure for 4, 6 or 16 hr, as measured by quantitative PCR. Expression of all genes was significantly altered by 16 hr shear stress compared to static controls (dashed line). Parallel plate flow-chamber induced fluid shear stress of 2.0 dyn/cm² in PTECs; t = 4, 6 or 16 hr; qPCR, *Hprt* served as housekeeping gene to correct for cDNA input; data normalized to unstimulated controls (fold change); n = 4-6 per condition. # significant difference compared to unstimulated control (dashed line) or * significant difference between treatment groups (P < 0.05 by one-way ANOVA, followed by post-hoc Fisher's LSD multiple comparison).

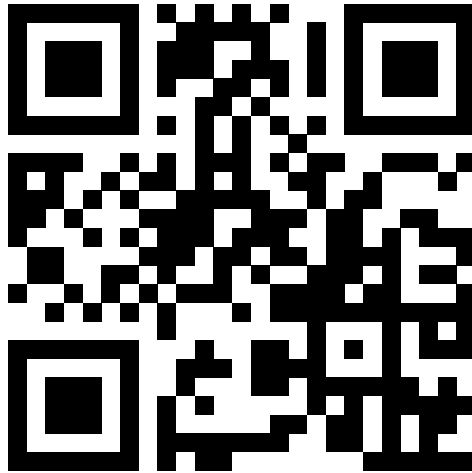


Supplementary Figure S3. Shear stress induced expression in PTECs is partially reversible after removal of shear.

Relative expression of selected genes upon fluid shear stress exposure for 16 hr followed by static recovery (post incubation) for 8 hr, as measured by quantitative PCR. Expression of some genes (*Map3k20*, *Map4k4*, *Pai1*) was reversible after recovery, while other genes (*Plk2*, *Prune2*, *Jak2*, *Fn1*) show similar or stronger differential expression after recovery. Parallel plate flow-chamber induced fluid shear stress of 2.0 dyn/cm² in PTECs; t = 16 + 8 hr; qPCR, *Hprt* served as housekeeping gene to correct for cDNA input; data normalized to unstimulated controls (fold change); n = 3 per condition. * significant difference between treatment groups (P < 0.05 by two-way ANOVA, followed by post-hoc Fisher's LSD multiple comparison).

SUPPLEMENTARY TABLES

<https://goo.gl/CY6aga>



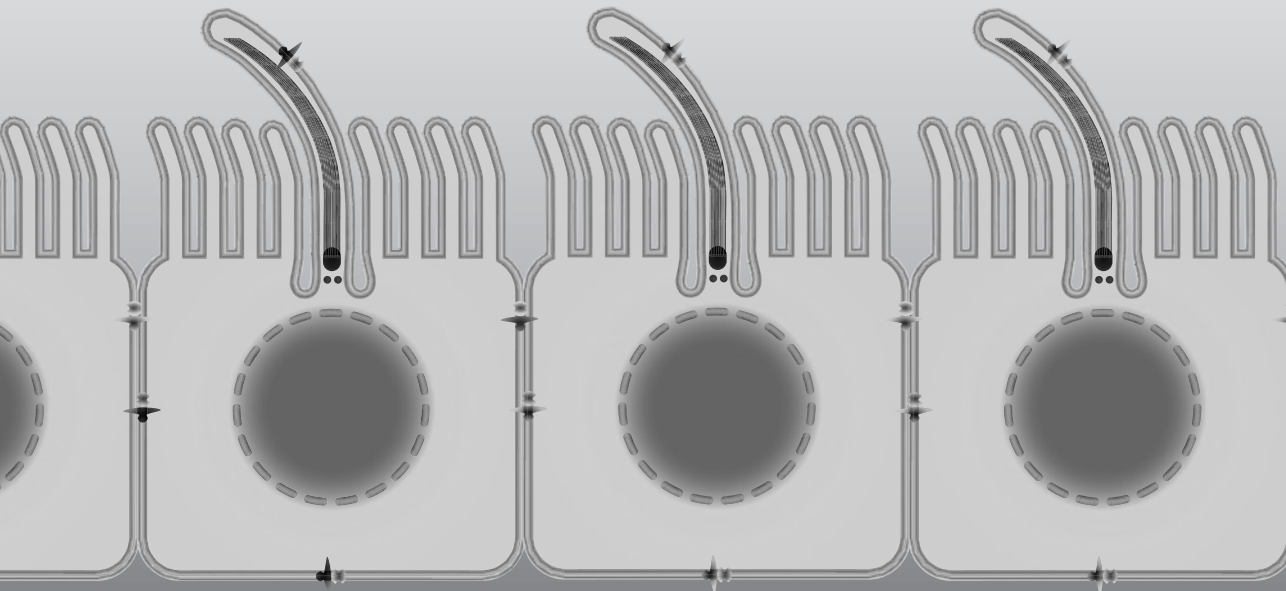
CHAPTER 4

Comparative transcriptomics of shear stress treated *Pkd1*^{-/-} cells and pre-cystic kidneys reveals pathways involved in early Polycystic Kidney Disease

Steven J. Kunnen, Tareq B. Malas, Chiara Formica, Wouter N. Leonhard, Peter A.C. 't Hoen and Dorien J.M. Peters

Department of Human Genetics, Leiden University Medical Center, 2300 RC Leiden, The Netherlands

Biomedicine & Pharmacotherapy. 2018; in press

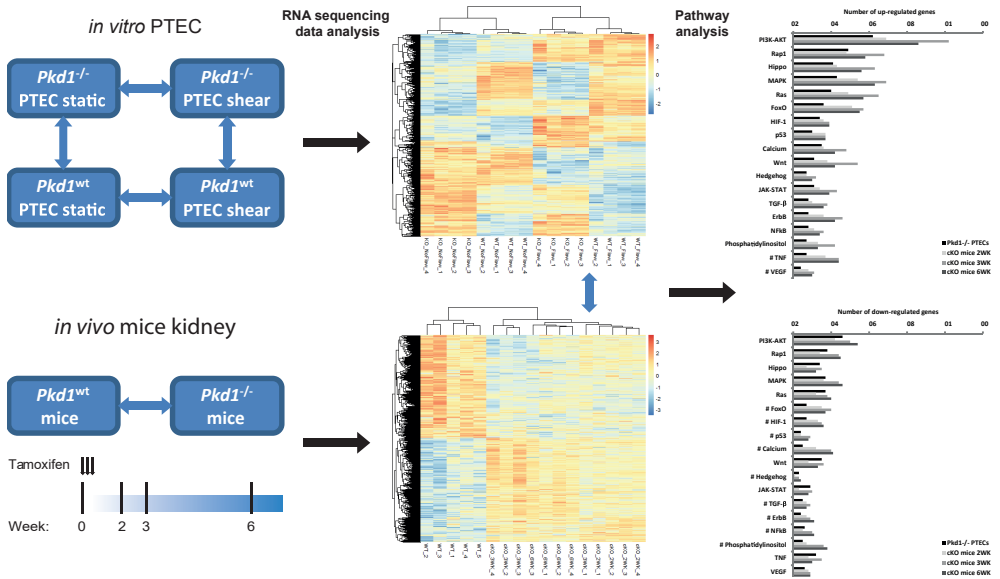


ABSTRACT

Mutations in the *PKD1* or *PKD2* genes are the cause of autosomal dominant polycystic kidney disease (ADPKD). The encoded proteins localize within the cell membrane and primary cilia and are proposed to be involved in mechanotransduction. Therefore, we evaluate shear stress dependent signaling in renal epithelial cells and the relevance for ADPKD. Using RNA sequencing and pathway analysis, we compared gene expression of *in vitro* shear stress treated *Pkd1*^{-/-} renal epithelial cells and *in vivo* pre-cystic *Pkd1*^{del} models. We show that shear stress alters the same signaling pathways in *Pkd1*^{-/-} renal epithelial cells and *Pkd1*^{wt} controls. However, expression of a number of genes was slightly more induced by shear stress in *Pkd1*^{-/-} cells, suggesting that *Pkd1* has the function to restrain shear regulated signaling instead of being a mechano-sensing activator. We also compared altered gene expression in *Pkd1*^{-/-} cells during shear with *in vivo* transcriptome data of kidneys from *Pkd1*^{del} mice at three early pre-cystic time-points. This revealed overlap of a limited number of differentially expressed genes. However, the overlap between cells and mice is much higher when looking at pathways and molecular processes, largely due to altered expression of paralogous genes. Several of the altered pathways in the *in vitro* and *in vivo* *Pkd1*^{del} models are known to be implicated in ADPKD pathways, including PI3K-AKT, MAPK, Hippo, calcium, Wnt, and TGF- β signaling. We hypothesize that increased activation of selected genes in renal epithelial cells early upon *Pkd1* gene disruption may disturb the balance in signaling and may contribute to cyst formation.

Key words: Next generation sequencing, mechanotransduction, shear stress, polycystic kidney disease, renal epithelial cell

GRAPHICAL ABSTRACT



ABBREVIATIONS

ADPKD	Autosomal dominant polycystic kidney disease
cKO	Conditional knock-out
CPM	Counts per million
DEG	Differentially expressed genes
ECM	Extracellular matrix
EGFR	Epidermal growth factor receptor
FDR	False discovery rate
MAPK	Mitogen-activated protein kinase
mTOR	Mechanistic Target Of Rapamycin
NGS	Next generation sequencing
PC	Polycystin
PI3K	Phosphoinositide 3-kinase
PKD1	Polycystic kidney disease 1 gene
PKD2	Polycystic kidney disease 2 gene
PTEC	Proximal tubular epithelial cell
TGF-β	Transforming growth factor β

INTRODUCTION

Autosomal dominant polycystic kidney disease (ADPKD) is characterized by formation of many fluid-filled cysts and renal fibrosis, leading to deterioration or loss of renal function in adulthood^{1,2}. ADPKD is caused by germline mutations in the *PKD1* or *PKD2* genes, encoding polycystin-1 (PC-1) and polycystin-2 (PC-2), respectively³⁻⁵. Somatic mutations in the unaffected allele of *PKD1* or *PKD2* can initiate cyst formation, the so called “second hit”, but stochastic fluctuations in gene expression can also lower PC-1 or PC-2 below critical levels^{6,7}.

The PC-1 and PC-2 proteins co-localize throughout the cell membrane of renal epithelial cells, at the cell-cell contacts, extracellular matrix (ECM) and primary cilia, where PC-2 functions as a non-selective cation channel⁸⁻¹⁰. Primary cilia are central in organizing signaling systems that sense environmental cues, triggered by fluid flow and growth factor stimulation. Lack of the PC1-PC2 complex in cilia is proposed to play a role in cyst formation^{11,12}. Moreover, mutations or deletions of other ciliary proteins can cause renal cysts in mouse models and patients, indicating the role of cilia during cystogenesis^{13,14}. Several signaling pathways are modulated by cilium dependent and independent shear stress responses of renal epithelial cells, including Wnt, mTOR, STAT6/p100, TGF- β /ALK5 and MAPK signaling, as well as Ca²⁺ influx and Na⁺ and HCO₃⁻ reabsorption^{9,15-25}. In addition, receptors of various signaling pathways have been identified in the primary cilium, including TGF- β , epidermal growth factor receptor (EGFR), Wnt and hedgehog signaling, suggesting that different signaling cascades are being regulated by this organelle^{19,26-28}. Cellular physiology and gene expression are determined by integration and interaction of the different signaling pathways, triggered by fluid shear stress and by growth factor or cytokine stimulation.

Luminal fluid shear and growth factors related signaling are essential for normal cell function, cell viability, tissue development and maintenance of organs²⁹⁻³². In the kidneys, urinary volume, diuretics, and diet will expose the renal epithelial cells to variations in hydrodynamic forces including fluid shear stress, circumferential stretch, and drag/torque on apical cilia and probably also on microvilli³³. For example, the kidney has the capacity to increase glomerular filtration rate in response to physiological stimuli. In addition, strong variations in hydrodynamic forces and shear stress are common in kidney diseases due to tubular dilation, obstruction and hyperfiltration, which occur in functional nephrons to compensate for lost glomeruli and tubules³⁴. Renal shear stress is increased after unilateral nephrectomy^{35,36}, which accelerates cyst formation in *Ift88*^{-/-} and *Pkd1*^{-/-} mouse models^{37,38}. Therefore, we hypothesize that shear stress induced alterations in cellular signaling may contribute to (early) cystogenesis.

To study shear stress dependent signaling in ADPKD, we examined the effect of fluid flow in proximal tubular epithelial cells (PTECs) without *Pkd1* expression and compared this with *Pkd1*^{wt} controls using RNA sequencing. In addition, we compared differential gene expression in *Pkd1*^{-/-} PTECs during shear with *in vivo* transcriptome analysis of pre-cystic kidneys in *Pkd1*^{del} mice, in which fluid flow is still present. Functional enrichment analysis revealed that several *in vitro* disturbed signaling pathways in *Pkd1*^{-/-} PTECs were also altered in pre-cystic kidneys of *Pkd1*^{del} mice.

MATERIAL AND METHODS

Cell culture

SV40 large T-antigen immortalized murine proximal tubular epithelial cells (PTEC; *Pkd1*^{-/-} and *Pkd1*^{wt}), derived from a *Pkd1*^{lox,lox} mouse, were generated and cultured as described previously^{19,39}. Briefly, cells were maintained at 37°C and 5% CO₂ in DMEM/F-12 with GlutaMAX (Thermo Fisher Scientific; #31331-093) supplemented with 100 U/mL Penicillin-Streptomycin (Thermo Fisher Scientific; #15140-122), 2% Ultrosor G (Pall Corporation; #15950-017), 1x Insulin-Transferrin-Selenium-Ethanolamine (Thermo Fisher Scientific; #51500-056), 25 ng/L Prostaglandin E1 (Sigma-Aldrich; #P7527) and 30 ng/L Hydrocortisone (Sigma-Aldrich; #H0135). Cell culture was monthly tested without mycoplasma contamination using MycoAlert Mycoplasma Detection Kit (Lonza; LT07-318). New ampules were started after 15 passages.

Fluid shear stress stimulation and RNA sequencing

PTECs were exposed to laminar fluid shear stress (1.9 dyn/cm²) in a cone-plate device as described previously¹⁹. Briefly, the cone-plate device, adapted from Malek *et al.*⁴⁰, was designed for 3.5 cm cell culture dishes (Greiner Bio-One). Cells were grown on collagen-I (Advanced BioMatrix; #5005) coated dishes until confluence, followed by 24 hr serum starvation, before the start of the treatment to exclude effects of serum-derived growth-factors and to synchronize cells and cilia formation. Culture dishes were placed in the cone-plate flow system and incubated at 37°C and 5% CO₂. The confluent cell monolayer of 9.6 cm² was subjected to constant laminar ($Re = 0.3$) fluid shear stress, using 2 ml serum-free DMEM/F-12 medium containing penicillin-streptomycin, with viscosity (μ) of 0.0078 dyn s/cm²⁴¹, a cone with an angle (α) of 2° and a velocity (ω) of 80 rpm, generating a fluid shear stress ($\tau = \mu\omega/\alpha$) of 1.9 dyn/cm². Static control cells were incubated for the same time in equal amounts of serum-free DMEM/F12 medium containing penicillin-streptomycin at 37°C and 5% CO₂. Cilia formation was checked on a parallel slide by immunofluorescence using anti-acetylated α -tubulin antibodies (Sigma Aldrich; #T6793) as previously described¹⁹. RNA sequencing was performed on isolated mRNA from fluid shear stress treated PTECs or static controls ($n = 4$ per condition) as previously described²⁰. Briefly, next generation sequencing (NGS) was performed by ServiceXS (GenomeScan) using the Illumina® HiSeq 2500 platform. Illumina mRNA-Seq Sample Prep Kit was used to process the samples according to the manufacturer's protocol. Clustering and cDNA sequencing using the Illumina cBot and HiSeq 2500 was performed according manufacturer's protocols. A concentration of 5.8 pM of cDNA was used. All samples were run on Paired End mode and 125 bp long reads. HiSeq control software HCS v2.2.38 was used. Image analysis, base calling, and quality check was performed with the Illumina data analysis pipeline RTA v1.18.61 and/or OLB v1.9 and Bcl2fastq v1.8.4. At least 87.3% of bases had a Q-score ≥ 30 . Reads were aligned to mouse

genome build GRCm38 - Ensembl using TopHat2 version 2.0.10⁴². Gene expression was quantified using HTSeq-Count version 0.6.1⁴³, using default options (stranded = no, mode = union). Differential gene expression analysis was performed in R version 3.0.2 using DESeq (Version1.16.0). Differentially expressed genes were selected with an adjusted p-value (corrected for multiple hypotheses testing using Benjamini and Hochberg's False Discovery Rate method) of < 0.05. Counts per million (CPM) values were calculated by dividing the read counts of a gene by total read counts of all genes in a sample, which is a measure for the abundance of the transcript. Only genes with average CPM > 2 were considered. Raw RNA sequencing data was deposited online at <http://www.ebi.ac.uk/arrayexpress/> (authors: S.J. Kunnen, D.J.M. Peters; year: 2018; ArrayExpress: E-MTAB-6640; ArrayExpress: E-MTAB-6641).

Experimental animals and RNA sequencing

Tamoxifen inducible kidney-specific *Pkd1*-deletion mouse model (tam-KspCad-CreER^{T2}; *Pkd1*^{lox2-11;lox2-11}, referred to as iKsp-*Pkd1*^{del}) and tamoxifen treatments were previously described⁴⁴⁻⁴⁶. Briefly, iKsp-*Pkd1*^{del} male mice were fed with tamoxifen (5 mg/day, 3 consecutive days) at adult age, *i.e.* between 13 to 14 weeks of age. Mice euthanized at determined time points (2, 3, and 6 weeks after tamoxifen treatment) had no visible signs of cystic disease (4 mice per time point). Adult male mice that did not receive tamoxifen treatment were used as *Pkd1*^{wt} controls (5 mice). RNA sequencing was performed on isolated mRNA from kidneys of iKsp-*Pkd1*^{del} and *Pkd1*^{wt} mice as previously described⁴⁶. The local animal experimental committee of the Leiden University Medical Center and the Commission Biotechnology in Animals of the Dutch Ministry of Agriculture approved the experiments performed. Animal experiments have been carried out in accordance with the EU Directive 2010/63/EU for animal experiments.

Pathway analysis

Functional enrichment analysis was performed with the online tool GeneTrail2 v1.5 (<https://genetrail2.bioinf.uni-sb.de/>) using standard settings of the over-representation analysis enrichment algorithm with correction for multiple hypotheses testing (FDR adjustment) according to Benjamini and Yekutieli⁴⁷. From this source we included pathway databases (KEGG, BIOCARTA, REACTOME and WIKI). Up- and down-regulated genes by fluid shear stress were used as separate gene sets to discriminate between generally up- and down-regulated pathways. Terms with false discovery rate (FDR) < 0.01 were considered significantly enriched. Venn diagrams were made using Venny 2.1 (Oliveros, J.C. (2007-2015) Venny. An interactive tool for comparing lists with Venn's diagrams. <http://bioinfogp.cnb.csic.es/tools/venny/index.html>).

RESULTS

Fluid shear stress induced transcriptional changes in *Pkd1*^{-/-} PTECs

To study shear stress altered gene expression, *Pkd1*^{-/-} proximal tubular epithelial cells (PTEC) were exposed to fluid shear of 1.9 dyn/cm². Static controls were incubated without fluid flow treatment in equal amounts of medium. After 6 hr fluid-flow or static exposure, total RNA was isolated and gene expression was analyzed using next generation sequencing (NGS) on the Illumina HiSeq 2500 platform. From the RNA sequencing data, the count per million (CPM) values were calculated by dividing the read counts of a gene by total read counts of all genes in a sample, which is a measure for the abundance of the transcript (Suppl. Table S1). Low expressed genes with an average CPM < 2 were excluded. In our previous study we presented the RNA sequencing results of shear stress treated *Pkd1*^{wt} PTECs²⁰, which we used as shear stress control in this study (Figure 1A).

After normalization, a total of 1749 genes were differentially expressed ($p < 0.05$; CPM > 2) upon shear stress stimulation in *Pkd1*^{-/-} PTECs (Table 1; Suppl. Table S2A). A heat map of *Pkd1*^{-/-} PTEC samples shows a clear distinction between fluid shear stress treated samples and static controls (Figure 1B). RNA sequencing results were compared to *Pkd1*^{wt} PTECs, again showing that shear stress samples clustered separately from the static controls, while the genotype has less influence on the hierarchical clustering (Figure 1C). The comparison of *Pkd1*^{-/-} and *Pkd1*^{wt} PTEC shows an overlap of 1220 differentially expressed genes (DEG) by shear stress (Table 1; Suppl. Table S2A-B). Furthermore, *Pkd1*^{-/-} have 529 unique DEG compared to *Pkd1*^{wt}, while 339 genes were exclusively altered in *Pkd1*^{wt} cells in response to fluid shear stress (Figure 1D-F; Table 1).

Table 1. Differentially expressed genes by shear stress in and *Pkd1*^{-/-} and *Pkd1*^{wt} PTECs.

Number of differentially expressed genes ($p < 0.05$; CPM > 2) of shear stress (flow) versus static (no flow) treated cultures in *Pkd1*^{-/-} and *Pkd1*^{wt} PTECs. Low expressed genes were excluded with an enrichment filter of CPM (counts per million) < 2. *Pkd1*^{-/-} only or *Pkd1*^{wt} only means genes differentially expressed upon shear, uniquely in *Pkd1*^{-/-} or *Pkd1*^{wt} PTECs, respectively.

Cell line	Up	Down	Total
<i>Pkd1</i> ^{-/-}	943	806	1749
<i>Pkd1</i> ^{wt}	811	748	1559
Overlap	673	547	1220
<i>Pkd1</i> ^{-/-} only	270	259	529
<i>Pkd1</i> ^{wt} only	138	201	339

Table 2. Differentially expressed genes in *Pkd1*^{-/-} vs *Pkd1*^{wt} PTECs.

Number of differentially expressed genes ($p < 0.05$; CPM > 2) of *Pkd1*^{-/-} vs *Pkd1*^{wt} PTECs during static (no flow) or fluid shear stress (flow) conditions. Low expressed genes were excluded with an enrichment filter of CPM < 2. No flow only or flow only means genes uniquely differentially expressed in *Pkd1*^{-/-} vs *Pkd1*^{wt} PTECs under static (no flow) or shear exposure (flow), respectively.

Treatment	Up	Down	Total
No flow	828	816	1644
Flow	943	832	1775
Overlap	656	624	1280
No flow only	172	192	364
Flow only	287	208	495

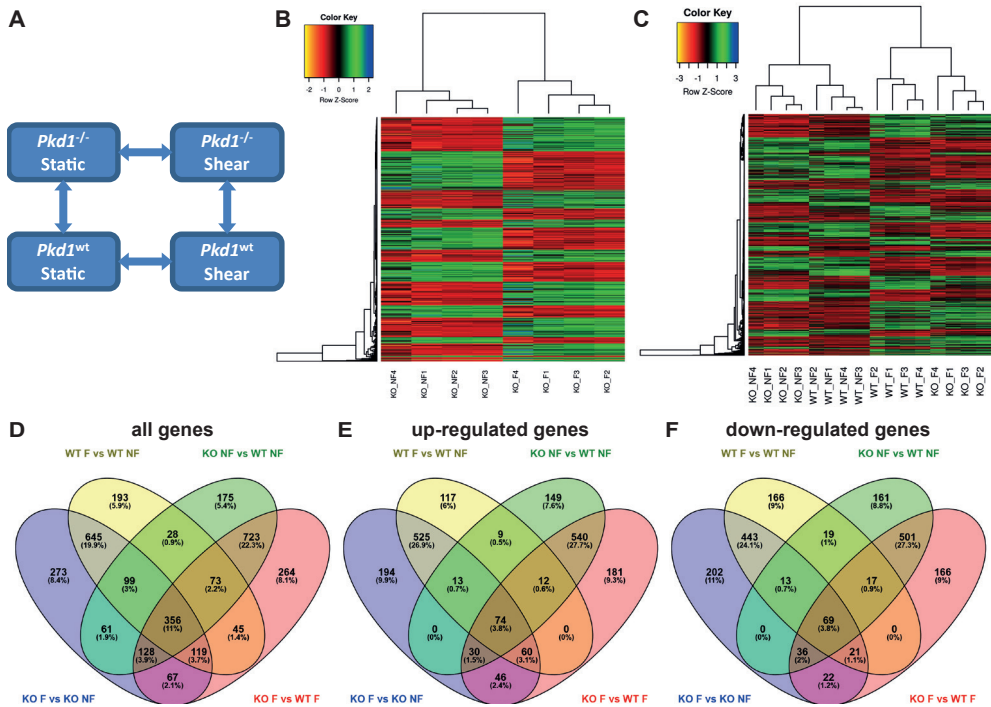


Figure 1. Gene expression profiling in *Pkd1*^{-/-} and *Pkd1*^{wt} PTECs shows a strong difference between fluid shear stress treated PTECs and static controls.

(A) Groups used for the *in vitro* RNA-sequencing study and the comparisons that were made between shear stress treated *Pkd1*^{-/-} or *Pkd1*^{wt} PTECs and static controls. (B) Heat map representing the differentially expressed genes ($p < 0.05$; CPM > 2) identified in 4 shear stress treated *Pkd1*^{-/-} (KO) samples (F = Flow) and 4 static controls (NF = No Flow). (C) Heat map of differentially expressed genes ($p < 0.05$; CPM > 2) identified in *Pkd1*^{-/-} (KO) and *Pkd1*^{wt} (WT) fluid shear stress treated samples and static controls. Unsupervised hierarchical clustering clearly distinguished fluid shear from static controls and grouped *Pkd1*^{wt} and *Pkd1*^{-/-} within these clusters. (B, C) Expression values were normalized using the Voom function in *limma* R package. Hierarchical clustering was applied and values were scaled by row. (D-F) Venn diagrams of differentially expressed genes upon shear stress treatment or *Pkd1* gene disruption in PTECs. The overlap between shear stress treatment or *Pkd1* gene disruption is shown for all (D) up- (E) or down-regulated (F) genes. (%) means the percentage of genes of all (D) up-regulated (E) or down-regulated (F) genes.

***Pkd1* induced transcriptional changes in PTECs**

To further investigate differences between the *Pkd1*^{-/-} and *Pkd1*^{wt} cells, we compared the gene expression profiles (Figure 1A). In static culture conditions there were 1644 genes differentially expressed between the *Pkd1*^{-/-} and *Pkd1*^{wt} cells, while there were 1775 DEG during fluid flow (Table 2, Suppl. Table S2C-D). In total, 1280 genes were differentially expressed due to the *Pkd1* phenotype in both static and flow conditions, while smaller subsets of genes were uniquely differentially expressed in either of the two conditions



(Figure 1D-F). The lists of differentially expressed genes in PTEC cells were further analyzed using functional enrichment analysis.

Pathway analysis of altered gene expression upon fluid shear in $Pkd1^{-/-}$ and $Pkd1^{wt}$ PTECs

We used GeneTrail2 v1.5⁴⁷ as tool for functional enrichment analysis to identify biological pathways or processes associated with fluid-shear stress or the *Pkd1* phenotype in PTECs (*in vitro*). The 4 lists of DEG (Suppl. Table S2A-D) were split into up- and down-regulated genes in order to get pathways that are generally up- or down-regulated. The up- or down-regulated biological annotations by fluid shear in *Pkd1^{-/-}* and *Pkd1^{wt}* PTECs are presented in Supplementary Tables S3 and S4, respectively. We subdivided the biological annotations in core signal transduction, as well as cytokine/endocrine signaling, metabolism, cell-cell/matrix interaction, other cellular processes and diseases. Additionally, we used subgroup terms for the biological annotations similar to the subgroups used in the KEGG database. Several pathways or biological processes contain both up- or down-regulated genes, although in most cases there were more up-regulated genes in the enriched biological annotations. Pathway analysis of unique shear regulated genes in *Pkd1^{-/-}* (270 up; 259 down) or *Pkd1^{wt}* (138 up; 201 down) PTECs are presented in Supplementary Table S5.

Core signaling pathways altered upon shear stress

The most prominently altered signaling pathways by fluid shear in *Pkd1^{-/-}* PTEC are the mitogen-activated protein kinase (MAPK) and PI3K-AKT pathway (Table 3, Suppl. Table S3), which is similar to the shear response in *Pkd1^{wt}* PTEC (Suppl. Table S4). Both pathways have clearly more up-regulated than down-regulated genes, while one of the main inhibitors of the PI3K-AKT signaling, *i.e.* *Pten*, is down-regulated. MAPK and PI3K-AKT signaling show various interactions with other pathways that are altered by shear stress as well, both in *Pkd1^{-/-}* and *Pkd1^{wt}* PTECs, including TGF- β , Wnt, p53 and JAK-STAT^{19,20}. Of those pathways, TGF- β , Wnt, and p53 had clearly more up-regulated genes, suggesting that these pathways are up-regulated. In contrast, only JAK-STAT signaling contains more genes that were down-regulated, including receptors (*Ifngr1*, *Il6st*, *Lifr*) and signal transducers (*Stat1*, *Stat5a*, *Irf9*). Furthermore, our results indicate that Hippo, Rap1, Ras, TNF, FoxO, calcium, HIF-1, VEGF, mTOR and ErbB signaling are altered as well by fluid shear, both in *Pkd1^{-/-}* and *Pkd1^{wt}* PTEC (Tables 3, S3-4). Furthermore, there are no pathways altered exclusively in *Pkd1^{-/-}* or *Pkd1^{wt}* cells, but pathways are more or less active (Suppl. Table S5). Altered Hippo signaling is probably attributed to interaction of YAP/TAZ with the TGF- β and Wnt signaling pathways, resulting in increased expression of Smad2/3 targets (*Serpine1*, *Ctgf*, *Smad7*) and TCF/LEF targets (*Myc*, *Cd44* and *Wisp1*), while transcriptional regulators Taz (*Wwtr1*), *Tead4*, *Tcf7l1* and *Axin2* are increased upon shear in *Pkd1^{-/-}* PTECs only (Suppl. Table S5). Rap1 and Ras are core signal transducers of MAPK and PI3K-AKT signaling and show up-regulation of signaling related genes (*Rap1b*, *Rapgef5*, *Rras*), while several inhibitors of Rap1 and Ras (*Rap1gap*,

Rasa1, *Rasa2*, *Rasa4*, *Syngap1*, *Sipa1l2*) and cytokines (*Angpt*, *Csf*, *Fgf*, *Igf*, *Pgf*, *Vegf*) were altered as well, contributing to the up-regulation of Rap1/Ras effectors (*Ets1*, *Ets2*, *Rassf1*, *Rassf5*, *Rin1*). In addition, activity of FoxO transcription factors can be modulated by MAPK, PI3K-AKT, JAK-STAT and insulin signaling, thereby modulating gene transcription upon interaction with Smad3/4 transcription factors. This FoxO-Smad interaction is revealed by shear induced up-regulation of genes involved in cell cycle (*Ccng2*, *Cdkn2b*, *Cdkn1a*, *Plk2*, *Plk3*) and DNA repair (*Gadd45a*, *Gadd45b*, *Gadd45g*), while other cell cycle genes were down-regulated (*Cdkn2d*, *Rbl2*), as well as autophagy genes (*Bnip3*, *Gabarapl1*). Altered TNF, FGF, PDGF, VEGF and ErbB signaling upon shear stress is attributed to altered gene expression of ligands (*Csf1*, *Csf3*, *Fgf1*, *Fgf9*, *Hbegf*, *Igf1*, *Pdgfa*, *Pdgfb*, *Pdgfc*, *Vegfa*, *Vegfb*) and receptors (*Egfr*, *Fgfr1*, *Fgfr2*, *Tnfrsf1b*, *Tnfrsf12a*, *Tnfrsf19*, *Tnfrsf21*, *Tnfrsf23*, *Relt*), while downstream components of MAPK and PI3K-AKT signaling are modulated as well.

Other biological processes altered upon shear stress

Expression of genes involved in various other cytokine and endocrine signaling pathways were also altered by shear in both *Pkd1*^{-/-} and *Pkd1*^{wt} PTEC, including interleukin, insulin, B cell receptor, thyroid, estrogen, T cell receptor and chemokine signaling pathways. Altered expression include genes from aforementioned core signaling, as well as additional genes, including chemokines with C-C or C-X-C motifs (*Ccl2*, *Cx3cl1*, *Cxcl10*, *Cxcr4*, *Ccl27a*, *Cxcl15*). Regulation of cell-cell and extracellular matrix (ECM) interactions were altered by fluid shear in *Pkd1*^{-/-} and *Pkd1*^{wt} PTEC, whereas much more genes involved in these interactions are up-regulated, including several actins, actinin, cadherins, β -catenin, cell adhesion molecules, collagens, fibronectin, integrins and laminins. The glycosaminoglycan biosynthesis pathway is induced by shear, which is involved in glycocalyx remodeling. Although several genes were differentially expressed in both *Pkd1*^{-/-} and *Pkd1*^{wt} PTEC, a number of genes (*Hs2st1*, *Hs3st3b1*, *Sdc1* and *Sdc2*) were only induced by shear in *Pkd1*^{wt}, suggesting that this pathway is more controlled in *Pkd1*^{wt} cells (Suppl. Table S5). Genes involved in endocytosis were also increased by fluid shear in PTECs, which was reported in previous studies as well⁴⁸⁻⁵⁰. Genes involved in purine metabolism were altered by shear stress as well, which showed an equal number of up- and down-regulated genes. These include genes involved in cAMP processing (*Adcy1*, *Adcy7*, *Adcy9*, *Pde4d*, *Pde7a*), adenine nucleotide homeostasis (*Ak1*, *Ak2*, *Ak4*, *Ak5*), and RNA transcription (*Polr1b*, *Polr3d*, *Polr3e*). Genes involved in energy, carbohydrate, amino acid and cholesterol metabolism were mainly down-regulated by shear stress in *Pkd1*^{-/-} and *Pkd1*^{wt} PTECs, while several other genes involved in energy metabolism and lysosomal degradation were exclusively down-regulated in *Pkd1*^{-/-} cells (Suppl. Table S5). Other cellular processes altered by shear stress include the protein-protein interactions, Rho GTPase cycle and collagen metabolism. Only a small number of genes involved in apoptosis and cell cycle were altered by shear, indicating that these processes are not dramatically altered during shear exposure.

Table 3. Core signaling pathways affected by fluid shear stress in *Pkd1*^{-/-} PTECs.

Pathway analysis done on differentially expressed genes upon fluid shear stress in *Pkd1*^{-/-} PTECs using GeneTrail2. The most significantly altered core signaling pathways of the KEGG database are shown and ordered by the lowest false discovery rate (FDR). Number of hits / total number of genes and the up- or down-regulated genes are presented. For the complete list of the pathway analysis of differentially expressed genes upon fluid shear stress, see Supplementary Table S3.

Pathway	Hits Up	FDR Up	Up-regulated genes	Hits Down	FDR Down	Down-regulated genes
MAPK	39/253	1.42E-24	CACNA1A; CACNA1G; CACNB3; DUSP1; DUSP4; DUSP6; DUSP7; EGFR; FGF1; FGF9; FGFR1; FLNA; FOS; GADD45A; GADD45B; GADD45G; HSPA2; HSPB1; MAP2K1; MAP2K3; MAP3K14; MAP4K4; MAPKAPK2; MYC; NFATC1; NFKB1; PAK1; PDGFA; PDGFB; PPP3CA; RAP1B; RASA1; RRAS; SRF; TGFB1; TGFB3; TGFBR1; TRP53; ZAK	13/253	7.78E-04	ARRB1; BDNF; CACNA1B; DUSP3; FGFR2; HSPA1A; MAP2K6; MAP3K1; MAP3K5; MAPT; MKNK2; RASGRP2; TGFB2
PI3K-AKT	44/347	2.35E-24	CDKN1A; COL1A1; COL27A1; COL4A3; COL4A4; COL5A1; CREB3L2; CSF1; CSF3; DDT14; EGFR; EPHA2; F2R; FGF1; FGF9; FGFR1; FN1; IGF1; IL6RA; ITGA2; ITGAS; ITGAV; ITGB1; ITGB3; ITGB4; ITGB5; ITGB6; LAMC2; LPAR6; MAP2K1; MCL1; MYC; NFKB1; PDGFA; PDGFB; PDGFC; PHLP1; PHLP2; RHEB; SGK1; THBS1; TLR2; TRP53; YWHAH	19/347	1.10E-05	ANGPT1; ANGPT2; ANGPT4; COL3A1; COL4A5; FGFR2; ITGA1; ITGA6; OSMR; PIK3R1; PIK3R5; PKN3; PPP2R2C; PRKAA2; PTEN; RBL2; SGK2; VEGFA; VEGFB
Hippo	31/154	1.30E-22	ACTB; ACTG1; AXIN2; BMPR2; CRB2; CSNK1E; CTGF; CTNNB1; FGF1; FRMD6; FZD2; FZD6; FZD8; ID1; MYC; PARD6G; RASSF1; SERPINE1; SMAD3; SMAD7; TCF7; TCF7L1; TEAD4; TGFB1; TGFB3; TGFB8; WNT7A; WNT7B; WNT9A; WNT9A; YWHAH	10/154	1.03E-03	APC2; BMP7; CDH1; ID2; PPP2R2C; RASSF6; TGFB2; WNT16; WNT6; WNT8B
Rap1	33/215	9.45E-21	ACTB; ACTG1; ADCY7; ARAP2; CSF1; CTNNB1; CTNND1; DOCK4; EGFR; EPHA2; F2R; FGF1; FGF9; FGFR1; ID1; IGF1; ITGB1; ITGB3; MAP2K1; MAP2K3; PARD6G; PDGFA; PDGFB; PDGFC; PLCE1; RAP1B; RAPGEF5; RASSF5; RRAS; SIPA1L2; THBS1; TLN2; VASP	16/215	3.36E-06	ADCY1; ADCY9; ANGPT1; ANGPT2; ANGPT4; CDH1; FGFR2; MAP2K6; PIK3R1; PIK3R5; PLCB1; RAP1GAP; RAPGEF3; RASGRP2; VEGFA; VEGFB
Wnt	21/143	8.71E-13	AXIN2; CSNK1E; CTNNB1; DAAM1; DAAM2; FZD2; FZD6; FZD8; MYC; NFATC1; NFATC2; NFATC4; PORCN; PPP3CA; SMAD3; TCF7; TCF7L1; TRP53; WNT7A; WNT7B; WNT9A	5/143	3.37E-01	APC2; PLCB1; WNT16; WNT6; WNT8B
Ras	25/227	1.12E-12	CSF1; EGFR; EPHA2; ETS1; ETS2; FGF1; FGF9; FGFR1; IGF1; MAP2K1; NFKB1; PAK1; PDGFA; PDGFB; PDGFC; PLA2G16; PLCE1; RAP1B; RAPGEF5; RASA1; RASAL2; RASSF1; RASSF5; RINI; RRAS	11/227	4.09E-03	ANGPT1; ANGPT2; ANGPT4; FGFR2; PIK3R1; PIK3R5; RASA4; RASGRP2; SYNGAP1; VEGFA; VEGFB
TNF	19/109	1.12E-12	CCL2; CEBPB; CREB3L2; CSF1; CX3CL1; CXCL10; EDN1; FOS; IFI47; JUNB; LIF; MAP2K1; MAP2K3; MAP3K14; NFKB1; PTGS2; TNFAIP3; TNFRSF1B; VCAM1	4/109	5.05E-01	MAP2K6; MAP3K5; PIK3R1; PIK3R5
p53	14/68	1.99E-10	BID; CCNG2; CDKN1A; GADD45A; GADD45B; GADD45G; IGF1; IGFBP3; PERP; PMAIP1; SERPINE1; SFN; THBS1; TRP53	3/68	5.05E-01	CD82; PTEN; SESN1
FoxO	18/135	2.08E-10	CCNG2; CDKN1A; CDKN2B; CSNK1E; EGFR; FOXO1; GADD45A; GADD45B; GADD45G; IGF1; MAP2K1; PIK2; PIK3; SGK1; SMAD3; TGFB1; TGFB3; TGFB8	12/135	1.86E-05	AGAP2; BNIP3; CDKN2D; FOXO6; GABARAPL1; PIK3R1; PIK3R5; PRKAA2; PTEN; RBL2; SGK2; TGFB2
TGF-β	13/82	2.69E-08	ACVR1; BMPR2; CDKN2B; ID1; INHBB; MYC; SMAD3; SMAD7; SMURF1; TGFB1; TGFB3; TGFB8; THBS1	3/82	7.70E-01	BMP7; ID2; TGFB2

Calcium	15/182	2.44E-06	ADCY7; ATP2B4; CACNA1A; CACNA1G; EGFR; F2R; ITPKB; ITPR2; ITPR3; MYLK; PLCD3; PLCE1; PPP3CA; PTK2B; SPHK1	7/182	9.35E-02	ADCY1; ADCY9; ADRB1; ATP2B1; CACNA1B; PDE1C; PLCB1
HIF-1	10/112	1.48E-04	CDKN1A; EDN1; EGFR; HK2; IGF1; IL6RA; MAP2K1; NFKB1; SERPINE1; TERC	12/112	4.10E-06	ANGPT1; ANGPT2; ANGPT4; ENO2; IFNGR1; MKNK2; PDK1; PFKL; PIK3R1; PIK3R5; SLCA2A1; VEGFA
JAK-STAT	7/153	7.97E-02	CSF3; IL6RA; LIF; MYC; PIM1; SPRV1; SPRY4	12/153	5.04E-05	CBLB; IFNGR1; IFNLR1; IL6ST; IRF9; LIFR; OSMR; PIK3R1; PIK3R5; SOCS2; STAT1; STAT5A
VEGF	7/60	7.79E-04	HSPB1; MAP2K1; MAPKAPK2; NFATC2; PPP3CA; PTGS2; SPHK1	3/60	4.32E-01	PIK3R1; PIK3R5; VEGFA
Phosphati-dylinositol	6/81	1.96E-02	DGKH; ITPKB; ITPR2; ITPR3; PLCD3; PLCE1	7/81	3.02E-03	INPP1; INPP5J; PI4KA; PIK3R1; PIK3R5; PLCB1; PTEN
mTOR	3/62	6.12E-01	DDIT4; IGF1; RHEB	6/62	4.77E-03	PIK3R1; PIK3R5; PRKAA2; PTEN; RRAGD; VEGFA
ErbB	7/87	4.91E-03	CDKN1A; EGFR; HBEGF; MAP2K1; MYC; NRG1; PAK1	4/87	2.74E-01	CBLB; PIK3R1; PIK3R5; STAT5A

Cilia related gene expression upon shear stress

To investigate whether shear is affecting structural components of the cilium, we compared differential gene expression upon fluid flow with the SysCilia Goldstandard database for cilia related genes (<http://www.syscilia.org/goldstandard.shtml>). Only a minority of cilia genes was differentially expressed by shear and these genes were not involved in a specific cilia-assembly mechanism (Suppl. Table S6). Therefore, we conclude that shear stress does not result in major structural alterations in the experimental time-frame of 6 hours.

From the pathway analysis we conclude that shear stress exposure in *Pkd1*^{-/-} and *Pkd1*^{wt} PTEC modified expression of genes involved in the same signaling pathways and biological processes, suggesting that *Pkd1* is not directly involved in shear dependent activation of these pathways. These altered processes include several core signaling pathways, cytokine/endocrine pathways, cell-cell and ECM interactions, endocytosis, and various metabolic pathways. However, there were several genes involved in Hippo, Wnt and calcium signaling exclusively altered by shear in *Pkd1*^{-/-} PTECs, while some important genes in the glycosaminoglycan biosynthesis were uniquely increased by shear in *Pkd1*^{wt} PTECs (Suppl. Table S5). Nevertheless, these pathways or molecular mechanisms are not uniquely altered in *Pkd1*^{-/-} or *Pkd1*^{wt} cells, but our data show that the pathways are more or less active.

Differential activation of signaling in $Pkd1^{-/-}$ compared to $Pkd1^{wt}$ PTECs

We compared the canonical signaling pathways that were altered by shear stress in $Pkd1^{-/-}$ vs $Pkd1^{wt}$ PTECs. Scatter plots were constructed comparing the \log_2 fold change (\log_2 FC) values of differentially expressed genes by fluid shear in $Pkd1^{-/-}$ vs $Pkd1^{wt}$ PTEC cultures normalized to their respective static controls (Suppl. Figure S1). These plots show a substantial number of genes that have a higher \log_2 FC for $Pkd1^{-/-}$ cells for up-regulated (KEGG) pathways (MAPK, PI3K-AKT, Hippo, Rap1, Wnt, TNF, Ras and TGF- β), while this phenomenon was less evident for down-regulated pathways. These genes are more elevated in $Pkd1^{-/-}$ PTECs upon shear stress exposure compared to $Pkd1^{wt}$ controls (Figure 2), which we previously showed for TGF- β target genes¹⁹. Nevertheless, some of the pathways contain genes that are not differentially expressed between $Pkd1^{-/-}$ cells and $Pkd1^{wt}$ controls. Differential gene expression between $Pkd1^{-/-}$ vs $Pkd1^{wt}$ PTECs, presented in Suppl. Table S2C-D, was further assessed using functional enrichment analysis (Suppl. Tables S7-8).

Core signaling pathways altered upon in vitro $Pkd1$ gene disruption

Evaluating the absolute expression levels in $Pkd1^{-/-}$ compared to $Pkd1^{wt}$ PTECs, revealed higher expression of genes involved in PI3K-AKT, Rap1, Hippo, MAPK, Ras, HIF-1, Wnt and TGF- β signaling pathways in shear-induced $Pkd1^{-/-}$ cells (Table 4, Suppl. Tables S7-8). Furthermore, FoxO, TNF, p53, calcium, hedgehog and JAK-STAT signaling were altered in $Pkd1^{-/-}$ PTECs as well. Most of the signaling pathways with altered expression in $Pkd1^{-/-}$ PTECs contain more up-regulated genes.

Other biological processes altered upon in vitro $Pkd1$ gene disruption

Other cytokine/endocrine signaling pathways are altered in $Pkd1^{-/-}$ PTEC as well, including GnRH, interleukin, insulin, thyroid and cytokine signaling. Biological processes that are increased in $Pkd1^{-/-}$ PTEC compared to $Pkd1^{wt}$ PTEC include cholesterol biosynthesis, prostaglandin synthesis, carbohydrate and purine metabolism, while glycosaminoglycan metabolism is down-regulated. Several genes involved in cell-cell, extracellular matrix and semaphorin interactions were altered in $Pkd1^{-/-}$ cells, although there were both up- and down-regulated genes involved in these interactions. Interestingly, genes involved in endocytosis and circadian regulation were induced in $Pkd1^{-/-}$ cells compared to $Pkd1^{wt}$. Several cell cycle and apoptosis regulating genes were altered as well.

From the *in vitro* functional enrichment analysis, we conclude that several core signaling pathways and cellular processes were altered by both shear stress and $Pkd1$ gene disruption, including PI3K-AKT, MAPK, Ras, Rap1, Hippo, Wnt and TGF- β signaling, as well as endocytosis and purine, cholesterol, carbohydrate and glycosaminoglycan metabolism. In addition, shear induced expression of several genes was stronger in $Pkd1^{-/-}$ PTECs.

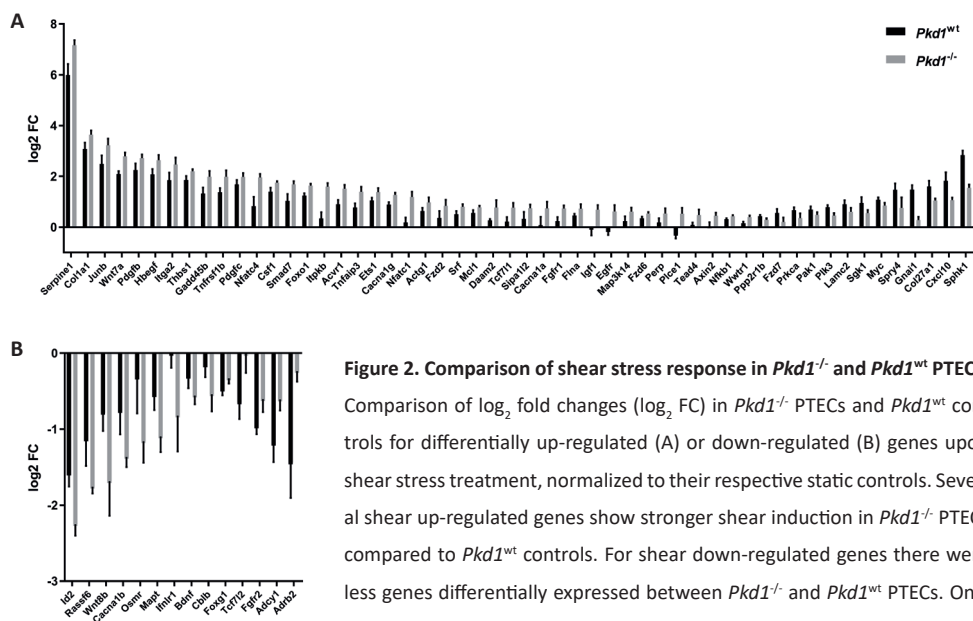


Figure 2. Comparison of shear stress response in *Pkd1*^{-/-} and *Pkd1*^{wt} PTECs.

Comparison of log₂ fold changes (log₂ FC) in *Pkd1*^{-/-} PTECs and *Pkd1*^{wt} controls for differentially up-regulated (A) or down-regulated (B) genes upon shear stress treatment, normalized to their respective static controls. Several shear up-regulated genes show stronger shear induction in *Pkd1*^{-/-} PTECs compared to *Pkd1*^{wt} controls. For shear down-regulated genes there were less genes differentially expressed between *Pkd1*^{-/-} and *Pkd1*^{wt} PTECs. Only the genes are shown that were annotated to canonical signaling pathways

(KEGG) using functional enrichment, as presented in Supplementary Tables S3-4 and Figure S1. All genes presented have a significantly different shear stress response between *Pkd1*^{-/-} vs *Pkd1*^{wt} PTECs ($p < 0.05$ by a two-sample *t*-test with Welch's correction).

Comparison of *Pkd1* gene disruption *in vitro* and *in vivo*

Expression profiles of *in vitro* *Pkd1*^{-/-} PTECs were compared with the RNA-sequencing data of the *in vivo* iKsp-*Pkd1*^{del} conditional knock-out (cKO) mice (Suppl. Table S9). In the iKsp-*Pkd1*^{del} (adult) mouse model *Pkd1* gene disruption is specifically induced in renal epithelial cells, with the largest proportion in proximal tubular epithelial cells. In the early phase upon *in vivo* *Pkd1* disruption, there is still fluid flow, but no *Pkd1* expression in 40-50% of cells^{36,38}. For this reason the *in vitro* *Pkd1* phenotype during fluid shear exposure will be compared to the gene expression profile of early phase adult iKsp-*Pkd1*^{del} mice at 2, 3 or 6 weeks after gene disruption. At these pre-cystic time-points the kidneys did not show any sign of cyst formation and had 2KW/BW ratios comparable to *Pkd1*^{wt} mice (Figure 3), while this iKsp-*Pkd1*^{del} model reaches end stage renal disease (ESRD) at 20 weeks after *Pkd1* gene disruption (Suppl. Figure S2). The number of differentially expressed genes in iKsp-*Pkd1*^{del} mice (2, 3 or 6 weeks) versus wild-type controls was higher compared to flow-stimulated *Pkd1*^{-/-} versus *Pkd1*^{wt} PTEC cells (Figure 4A, Suppl. Table S2D, S9A-C). There was an overlap of 131 genes up-regulated and 48 genes down-regulated upon *Pkd1* disruption in *Pkd1*^{-/-} PTEC cells and all three iKsp-*Pkd1*^{del} mice groups (Figure 4B-C, Suppl. Table S10). The comparison between *in vitro* and *in vivo* *Pkd1*^{del} models was further assessed using functional enrichment analysis.

Table 4. Core signaling pathways altered in *Pkd1^{-/-}* vs *Pkd1^{wt}* PTECs during shear stress.

Pathway analysis done on differentially expressed genes in *Pkd1^{-/-}* vs *Pkd1^{wt}* PTECs during fluid shear exposure using GeneTrail2. The most significantly altered core signaling pathways of the KEGG database are shown and ordered by the lowest false discovery rate (FDR). Number of hits / total number of genes and the up- or down-regulated genes are presented. For the complete list of the pathway analysis of differentially expressed genes upon *Pkd1* disruption in PTECs, see Supplementary Table S7.

Pathway	Hits Up	FDR Up	Up-regulated genes	Hits Down	FDR Down	Down-regulated genes
PI3K-AKT	42/347	7.74E-22	ANGPT4; BCL2L1; CDKN1A; COL11A1; COL4A2; COL4A3; COL4A4; CREB3; CREB3L2; CSF1R; CSF3; DDIT4; EGFR; EPHA2; FGF1; FGF9; FGF2; FN1; G6PC2; GHR; GNG12; GNG5; IGF1; ITGA5; ITGA9; ITGB6; JAK2; LAMB3; LPAR1; LPAR3; MAP2K1; MCL1; MDM2; NGF; PDGFB; PHLP2; PPP2R5A; PRKCA; PTEN; SGK1; TLR4; YWHAQ	26/347	6.82E-10	ANGPT1; COL27A1; COL3A1; COL5A1; COL6A1; COL6A2; COL6A3; EFNA1; EFNA5; FGF13; FGF1; GNG11; IFNAR1; IFNAR2; IRS1; ITGB3; ITGB8; JAK3; LAMA5; OSMR; PDGFC; PDGFRB; PIK3CD; PIK3R5; PPP2R2C; PRKCZ
Rap1	29/215	1.98E-16	ADCY1; ADCY9; ANGPT4; ARAP2; CALM1; CSF1R; EGFR; EPHA2; FARP2; FGF1; FGF9; FGF2; ID1; IGF1; LPAR1; LPAR3; MAP2K1; MAP2K6; NGF; PARD6B; PDGFB; PLCE1; PRKCA; RAP1GAP; RASGEF3; RASGRP3; RASSF5; SIPA1L2; SIPA1L3	18/215	1.12E-07	ADCY3; ANGPT1; EFNA1; EFNA5; FGF13; FGF1; GNAS; ITGB3; MAGI1; MAPK13; PDGFC; PDGFRB; PIK3CD; PIK3R5; PRKCZ; RALGDS; RAPGEF5; RASGRP2
Hippo	21/154	6.96E-12	AJUBA; BMP4; CRB2; CTGF; FGF1; ID1; LATS1; LEF1; LLGL2; PARD6B; SERPINE1; SMAD7; TCF7L2; TGFB2; TGFB3; WNT16; WNT17B; WNT8B; WNT9A; WWCI; YWHAQ	14/154	1.66E-06	FZD1; FZD5; FZD7; FZD8; GDF6; ID2; LLGL1; PPP2R2C; PRKCZ; SMAD1; TCF7; TCF7L1; TEAD3; WNT6
MAPK	23/253	7.11E-10	BDNF; CD14; DUSP3; DUSP6; DUSP8; ECSIT; EGFR; FGF1; FGF9; FGF2; GADD45B; GADD45G; GNG12; MAP2K1; MAP2K6; MKNK2; NGF; PDGFB; PPP3CA; PRKCA; RASGRP3; TGFB2; TGFB3	17/253	2.80E-06	ARRB1; CACNG7; CDC25B; DUSP9; FAS; FGF13; FGF1; HSPB1; IL1R1; MAP4K1; MAPK13; MECOM; NFATC1; PDGFRB; PLA2G4A; RASGRP2; RELB
Ras	20/227	2.82E-08	ANGPT4; BCL2L1; CALM1; CSF1R; EGFR; EPHA2; FGF1; FGF9; FGF2; GAB2; GNG12; GNG5; IGF1; MAP2K1; NGF; PDGFB; PLCE1; PRKCA; RASGRP3; RASSF5	17/227	1.06E-06	ANGPT1; EFNA1; EFNA5; FGF13; FGF1; GNG11; KSR1; PAK3; PDGFC; PDGFRB; PIK3CD; PIK3R5; PLA2G4A; RALGDS; RAPGEF5; RASGRP2; RGL2
FoxO	16/135	2.98E-08	AGAP2; CDKN1A; CDKN2B; EGFR; FOXO6; G6PC2; GADD45B; GADD45G; IGF1; IRS4; MAP2K1; MDM2; PTEN; SGK1; TGFB2; TGFB3	7/135	3.65E-02	CCNB1; IRS1; IRS2; MAPK13; PIK3CD; PIK3R5; SLC24A4
HIF-1	14/112	1.33E-07	ANGPT4; CAMK2D; CDKN1A; EDN1; EGFR; HK2; IGF1; MAP2K1; MKNK2; PFKFB3; PRKCA; SERPINE1; TERC; TLR4	7/112	1.45E-02	ANGPT1; EGN3; ENO2; LTBR; PFKFB1; PIK3CD; PIK3R5
Wnt	11/143	2.33E-04	CAMK2D; DAAMI1; LEF1; PPP3CA; PRKCA; SFRP2; TCF7L2; WNT16; WNT7B; WNT8B; WNT9A	15/143	1.35E-07	FRAT2; FZD1; FZD5; FZD7; FZD8; NFATC1; NFATC4; PORCN; PRICKLE1; SFRP1; TCF7; TCF7L1; VANGL1; VANGL2; WNT6
TNF	7/109	1.78E-02	CREB3; CREB3L2; EDN1; MAP2K1; MAP2K6; NFKBIA; TRAF5	12/109	2.80E-06	BCL3; BIRC3; CEBPB; CX3CL1; CXCL10; FAS; LIF; MAPK13; PIK3CD; PIK3R5; PTGS2; TNFRSF1B
p53	10/68	4.40E-06	CCNG1; CDKN1A; GADD45B; GADD45G; IGF1; MDM2; PERP; PTEN; SERPINE1; SESN2	4/68	1.37E-01	BID; CCNB1; FAS; IGFBP3

Calcium	15/182	4.58E-06	ADCY1; ADCY9; ADRA1B; ADRB2; ATP2A2; CALM1; CAMK2D; EGFR; ITPKB; PICE1; PPP3CA; PRKCA; PTK2B; SPHK1; TNNC1	5/182	7.38E-01	ADCY3; CD38; GNAL; GNAS; PDGFRB
Hedgehog	7/49	3.21E-04	BMP4; LRP2; PTCH1; WNT16; WNT17; WNT8B; WNT9A	3/49	3.21E-01	GAS1; SMO; WNT6
JAK-STAT	11/153	3.99E-04	BCL2L1; CSF3; GHR; IL5RA; IL6ST; JAK2; PIM1; SOCS2; SPRY1; STAT5A; STAT5B	9/153	5.29E-03	IFNAR1; IFNAR2; IFNL1; JAK3; LIF; LIFR; OSMR; PIK3CD; PIK3RS
TGF-β	8/82	7.97E-04	ACVR1; BMP4; CDKN2B; DCN; ID1; SMAD7; TGFβ2; TGFβ3	5/82	7.22E-02	CHRD; GDF6; ID2; PITX2; SMAD1
ErbB	8/87	9.67E-04	CAMK2D; CDKN1A; EGFR; HBEGF; MAP2K1; PRKCA; STAT5A; STAT5B	4/87	2.91E-01	PAK3; PIK3CD; PIK3RS; TGFA
NFKB	8/96	2.68E-03	BCL2L1; BLNK; CD14; GADD45B; NFKBIA; PLAU; TLR4; TRAF5	6/96	4.10E-02	BIRC3; CXCL12; IL1R1; LTBR; PTGS2; RELB
Phosphati-dylinositol	7/81	4.05E-03	CALM1; DGKA; ITPK1; ITPKB; PICE1; PRKCA; PTEN	5/81	7.04E-02	DGKH; PIK3C2B; PIK3CD; PIK3RS; SYNJ2
VEGF	4/60	1.30E-01	MAP2K1; PPP3CA; PRKCA; SPHK1	6/60	5.29E-03	HSPB1; MAPK13; PIK3CD; PIK3RS; PLA2G4A; PTGS2

Core signaling pathways altered upon *Pkd1* gene disruption

Altered gene expression caused by *Pkd1* gene disruption in both flow-stimulated *Pkd1*^{-/-} PTEC cells and *Pkd1*^{del} mice was attributed to changes in several core signaling pathways, including PI3K-AKT, Rap1, Hippo, MAPK, Ras, FoxO, HIF-1, p53, calcium, Wnt, Hedgehog, JAK-STAT, TGF-β and TNF signaling (Figure 5, Suppl. Figure S3-S5, Suppl. Table S11). Most of the pathways had more up-regulated than down-regulated genes (Figure 5), indicating that these signaling cascades are induced in *Pkd1*^{-/-} PTEC cells and *Pkd1*^{del} mice compared to *Pkd1*^{wt} controls. A subset of genes in these pathways is identical but also paralogous genes were changed upon *Pkd1* disruption in cells and mice (Suppl. Figure S3, Suppl. Table S11). For example, *Itgb6* in the PI3K/AKT pathway is up-regulated in *Pkd1*^{-/-} PTEC cells and *Pkd1*^{del} mice, while several other integrin's were also up-regulated upon *Pkd1* gene disruption in the different models. Altered expression of identical genes in cells and mice is also observed for various signal transducers (*Adcy1*, *Ccng1*, *Egfr*, *Il6st*, *Itpkb*), transcription factor (*Creb3l2*), inhibitors (*Bcl2l1*, *Cdkn1a*, *Lats1*, *Nfkbia*, *Pten*, *Sipa1l*) and other genes (*Atp2a2*, *Camk2d*, *Pard6b*, *Plau*), as well as several paralogous genes, like collagens (*Col*), laminins (*Lam*), phospholipases (*Pla*), protein kinases (*Mapk*, *Prk*, *Jak*, *Pik3*, *Rapgef*), phosphatases (*Dusp*, *Ppp*), growth factors (*Bmp*, *Ctgf*, *Pdgf*, *Tgfb*), receptors (*Fgfr*, *Pdgfr*) and transcriptions factors (*Creb*, *Foxo*, *Smad*, *Tead*). These genes are active in several of the aforementioned pathways, suggesting that these genes might contribute to the *Pkd1* phenotype, since they are altered in both *in vitro* and *in vivo* *Pkd1*^{del} models. In contrast, altered expression of genes involved in Wnt signaling did not show

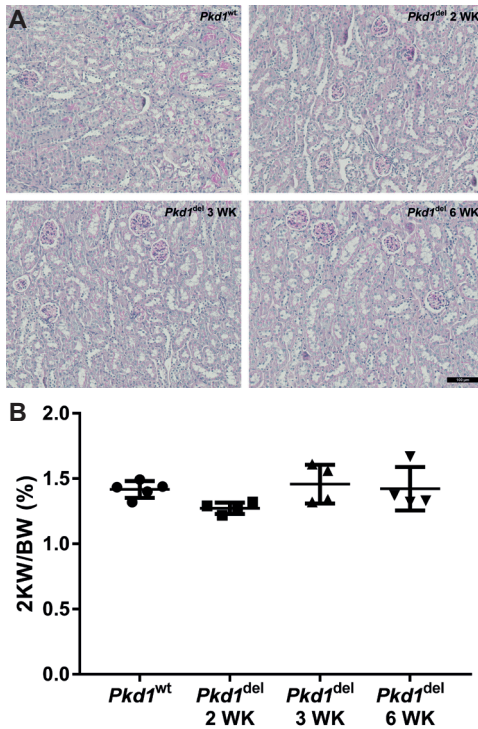


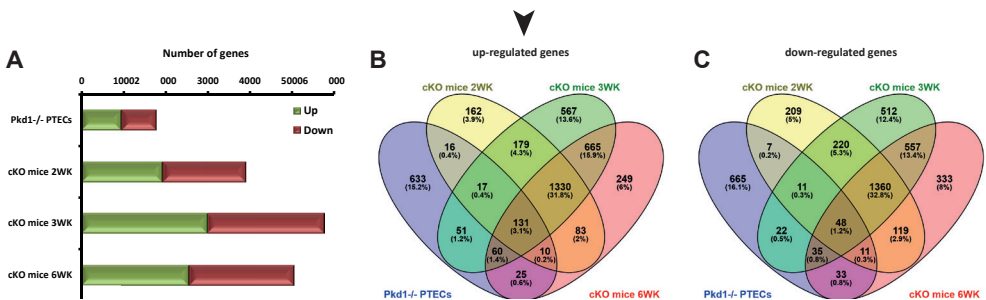
Figure 3. Kidney morphology and kidney weight (KW/BW) of *Pkd1*^{wt} and pre-cystic iKsp-*Pkd1*^{del} mice.

(A) Representative images of periodic-acid Schiff (PAS) staining on formalin fixed, paraffin embedded kidney sections of *Pkd1*^{wt} (top left) and iKsp-*Pkd1*^{del} mice at 2 (top right), 3 (bottom left) or 6 (bottom right) weeks after gene disruption. No visual difference in kidney morphology between *Pkd1*^{wt} and pre-cystic iKsp-*Pkd1*^{del} mice; scale bar = 100 μ m. (B) Similar kidney weight to body weight ratio's (2KW/BW %) in *Pkd1*^{wt} and iKsp-*Pkd1*^{del} mice at 2, 3 or 6 weeks after gene disruption.

a clear overlap between the *in vitro* and *in vivo* RNA sequencing data (Suppl. Table S11), but the overall effect in the two models indicates decreased non-canonical Wnt signaling. In *Pkd1*^{-/-} PTEC cells, there is altered expression of several canonical Wnt ligands (Wnt proteins), receptors (Fz's), transcription factors (up: *Lef1*, *Tcf7l2*; down: *Tcf7l1*, *Tcf7*) and modulators (up: *Sfrp2*; down: *Frat2*, *Porcn*, *Sfrp1*), while non-canonical Wnt proteins (*Vangl1*, *2*, *Prickle1*) and Ca²⁺ dependent NFAT (*Nfatc1,4*) transcription factors were decreased, which might suggest decreased non-canonical Wnt. In *Pkd1*^{del} mice there is decreased expression of several β -catenin inhibitors (*Chd8*, *Rb*, *Skp1a*, *Sox17*), while expression of β -catenin (*Cttnb1*) itself is increased, as well as receptors (Fz's and *Lrp5,6*) and target genes (*Axin1*, *Ccnd1*, *Ccnd2*, *Ppard*),

Figure 4. Comparison of DEG upon *Pkd1* gene disruption in *Pkd1*^{-/-} cells and iKsp-*Pkd1*^{del} mice.

(A) Number of differentially up- or down-regulated genes in *Pkd1*^{-/-} PTECs or iKsp-*Pkd1*^{del} (cKO) mice at 2, 3 or 6 weeks (WK) after gene disruption. (B, C) Venn diagram of up-regulated (B) and down-regulated (C) genes showing the number of genes in overlap between *Pkd1*^{-/-} PTEC cells and iKsp-*Pkd1*^{del} mice. (%) means the percentage of genes of all up-regulated or down-regulated genes.



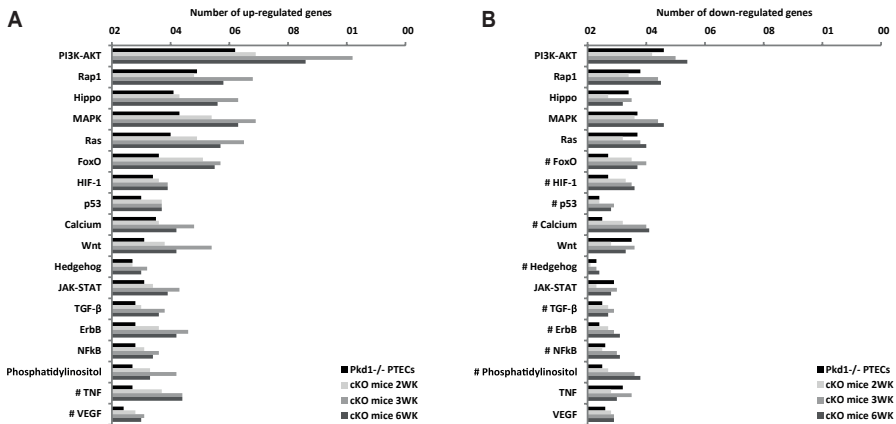


Figure 5. Core signaling pathways altered upon *Pkd1* gene disruption in *Pkd1*^{-/-} cells and iKsp-*Pkd1*^{del} mice.

Number of differentially expressed genes per condition, which were annotated to up-regulated (A) or down-regulated (B) core signaling pathways (KEGG) for *Pkd1*^{-/-} PTECs or iKsp-*Pkd1*^{del} (cKO) mice at 2, 3 or 6 weeks (WK) after gene disruption. Pathways are ordered by lowest false discovery rate (FDR) of up-regulated pathways in *Pkd1*^{-/-} PTECs. # = Not significantly enriched pathways in *Pkd1*^{-/-} PTECs from functional enrichment analysis (FDR >= 0.01).

suggesting increased canonical Wnt signaling. Down-regulation of *Dvl1* and Wnt proteins that activate non-canonical Wnt (*Wnt5b*, *Wnt7b*, *Wnt11*) may also suggest reduced non-canonical Wnt-signaling.

Other biological processes altered upon *Pkd1* gene disruption

Other altered signaling pathways with mainly up-regulated genes in *Pkd1*^{-/-} cells and mice include cytokine/endocrine signaling (GPCR, GnRH, interleukin, insulin, thyroid and estrogen signaling) as depicted in Suppl. Figure S4-5 and Table S11. Genes involved in protein and ECM interactions, endocytosis, focal adhesion, cell adhesion, actin cytoskeleton, endoplasmic reticulum protein processing, adipogenesis, purine metabolism and circadian regulation were altered as well in both *Pkd1*^{-/-} cells and *Pkd1*^{del} mice compared to *Pkd1*^{wt} controls. Cholesterol biosynthesis was up-regulated *in vitro*, but not *in vivo*, while lysosome related gene expression was only up-regulated *in vivo*. Genes involved in mRNA processing, protein translation, ribosomal proteins and electron transport were only down-regulated in iKsp-*Pkd1*^{del} mice (Suppl. Figure S5). This was attributed to down-regulation of various ATP synthases and transporters, NADH ubiquinone oxidoreductases, cytochrome C oxidases and reductases, eukaryotic translation initiation factor, RNA polymerases, general transcription factors, splicing factors and ribosomal proteins. From the comparison between the *in vitro* and *in vivo* RNA sequencing data and pathway analysis we conclude that various identical and paralogous genes were altered upon *Pkd1* gene disruption in both model systems. These genes are already altered in the pre-cystic phase and are involved in several core signaling pathways, which suggest that these processes may contribute to *in vivo* cyst formation.

DISCUSSION

In this study we present an overview of transcriptome alterations upon fluid shear stress exposure and *Pkd1* gene disruption in proximal tubular epithelial cells. We compared gene expression profiles of shear stress treated *Pkd1*^{-/-} PTECs with *Pkd1*^{wt} controls and showed that 1219 genes were altered by fluid shear in both cell lines. Functional enrichment analysis revealed that shear regulated genes in *Pkd1*^{-/-} and *Pkd1*^{wt} PTECs are involved in the same signaling pathways. Shear stress activated pathways include MAPK, PI3K-AKT, TGF- β , Wnt, p53, Hippo, FoxO, calcium and mTOR signaling, while only JAK-STAT signaling is down-regulated upon shear. Several of these pathways have been published previously^{9,15-21,32}. Increased intracellular Ca²⁺ is one of the first responses of epithelial cells to the onset of shear, thereby modulating several signaling cascades, but it is currently under debate if the Ca²⁺ influx is cilium dependent^{9,21,23-25,51}. In addition, the cilium is only involved in part of the shear stress response of PTECs, suggesting that other mechano-sensing complexes are involved as well^{19,20}.

Previously, we showed that inhibitors of TGF- β and MAPK/ERK signaling modulate a wide range of mechanosensitive genes, identifying these pathways as master regulators of shear-induced gene expression^{19,20}. This is attributed to the many interactions of TGF- β and MAPK signaling with other pathways. One of these pathways is Hippo signaling, which controls organ size in animals and is modulated upon fluid shear. Interaction of the core components YAP and TAZ (also called *Wwtr1*) with TGF- β and Wnt signaling pathways has been described previously, thereby regulating Smad2/3 and TCF/LEF target gene expression, respectively⁵²⁻⁵⁵. In addition, activity of FoxO transcription factors can be modulated by MAPK, PI3K-AKT, JAK-STAT and insulin signaling, thereby modulating gene transcription upon interaction with Smad3/4 transcription factors⁵⁶.

Other shear regulated pathways include TNF, FGF, PDGF, VEGF and ErbB signaling, for which functional enrichment is largely attributed to altered gene expression of ligands, receptors and downstream components of MAPK and PI3K-AKT signaling. Important signal transducers of MAPK and PI3K-AKT signaling are Ras and Rap1, which shows again the interaction between cellular signaling pathways. Shear induced activation of several other cytokine or endocrine signaling pathways and shear altered expression of genes involved in cell-cell contacts, ECM, glycocalyx remodeling and endocytosis has been discussed in Kunnen *et al.*²⁰. Remarkably, several genes involved in energy metabolism and autophagy (the process of lysosomal degradation) were exclusively down-regulated by shear stress in *Pkd1*^{-/-} PTECs. These processes are also implicated in ADPKD, but how it affects cyst progression is currently unclear^{57,58}. These findings suggest a complex interaction of processes and pathways to regulate the shear stress response in PTECs and to maintain cellular physiology.

Shear stress induced expression of a number of genes involved in MAPK, PI3K-AKT, Hippo, Rap1, Wnt, TNF, Ras and TGF- β was slightly more activated in *Pkd1*^{-/-} PTECs compared to *Pkd1*^{wt} controls (Figures 2 and S1), which we previously showed for TGF- β /ALK5 target genes¹⁹. Similarly, genes with differential expression in *Pkd1*^{-/-} PTECs compared to *Pkd1*^{wt} cells, were indeed involved in PI3K-AKT, Rap1, Hippo, MAPK, Ras, Wnt and TGF- β signaling, which indicates that shear induced gene expression is further elevated due to *Pkd1* gene disruption. In addition, functional enrichment analysis of shear regulated genes that were exclusively induced in *Pkd1*^{-/-} PTECs confirms that a subset of these genes is involved in Hippo, Wnt, MAPK and calcium signaling (Suppl. Table S5). These include several transcriptional regulators of the Hippo and Wnt signaling pathways. Overall, these data suggest that *Pkd1* has the function to restrain shear regulated signaling instead of being a mechano-sensing activator. Accordingly, *Ma et al.* previously proposed a role for *Pkd1* in restraining an unknown cilia-dependent signaling pathway involved in cyst formation⁵⁹. Further research is required to investigate if and how *Pkd1* is inhibiting shear induced signaling. In addition, pathological shear stress can also elevate gene expression of aforementioned pathways compared to physiological levels of shear²⁰. Moreover, strong variations in fluid shear stress are common in kidney diseases, including ADPKD, due to tubular dilation obstruction and hyperfiltration, which occur in functional nephrons, to compensate for lost glomeruli and tubules³⁴. Increased or pathological shear stress after unilateral nephrectomy^{35,36}, can accelerate cyst formation in a *Pkd1*^{-/-} mouse model³⁸. This leads to the hypothesis that pathological shear stress and *Pkd1* gene disruption can both cause imbalanced cellular signaling, which may contribute to renal cyst formation and fibrosis.

To study shear stress dependent signaling in ADPKD, we compared changes in gene expression in *Pkd1*^{-/-} PTECs during shear with *in vivo* transcriptome analysis of pre-cystic kidneys in mice. In the iKsp-*Pkd1*^{del} mouse model *Pkd1* gene disruption is specifically induced in around 40-50% of the renal epithelial cells, with the largest proportion in proximal tubular epithelial cells^{36,38}. In the early phase upon *in vivo* *Pkd1* disruption, there is still fluid flow without signs of cyst formation. In contrast, in the late/end phase of PKD, there are many cysts and fibrotic tissue, causing disturbance or loss of fluid flow in numerous nephrons. At this stage, the remaining nephrons experience increased fluid shear to compensate for the cystic or fibrotic tissue. Therefore, altered signaling of biological pathways or processes in late phase PKD can be caused by several factors, like loss of fluid shear, increased shear, increased pressure, changes in tissue composition, fibrosis or inflammation⁶⁰. For this reason, the *in vitro* *Pkd1* phenotype during fluid shear exposure in PTECs was compared with the gene expression profiles of pre-cystic adult iKsp-*Pkd1*^{del} mice at 2, 3 or 6 weeks after *Pkd1* gene disruption⁴⁶.

In the comparison between the *in vitro* and *in vivo* transcriptome analysis we identified 131 genes up-regulated and 48 genes down-regulated in *Pkd1*^{-/-} PTECs and iKsp-*Pkd1*^{del} mice at all three time points (Suppl. Table S10). Therefore, we can conclude that these genes are already altered in the earliest phase upon *Pkd1* gene disruption. Looking at the pathways and molecular processes, we noticed extensive overlap between cells and mice, although this can largely be attributed to the expression of paralogous genes, rather than to the identical genes. Examples include collagens, integrins, kinases, phosphatases, growth factors, receptors, signal transducers, inhibitors and transcription factors. These genes are involved in several core signaling pathways (Suppl. Table S11) of which several are known to be implicated in ADPKD (*i.e.* PI3K-AKT, MAPK, Hippo, JAK-STAT and TGF- β signaling)^{39,45,55,61-74}, suggesting that these pathways are already modified at pre-cystic stage.

Interpretation of the Wnt signaling is complex since canonical (Wnt/ β -catenin) or non-canonical (β -catenin-independent) Wnt signaling share components, but also may have reciprocal effects. In addition, non-canonical Wnt signaling can be subdivided into the Wnt/planar cell polarity (PCP) and Wnt/ Ca^{2+} pathways. Genes involved in Wnt signaling do not show much overlap between *in vitro* and *in vivo* transcriptome data, however, the overall picture suggests decreased non-canonical Wnt signaling in *Pkd1*^{-/-} cells and mice. Increased canonical Wnt might be involved in cyst formation, although aberrant PCP signaling at early stage has been suggested as well^{67,75}. Recent data suggest that the polycystin-complex itself mediates Wnt-induced Ca^{2+} signaling, although independent of Fz-receptors^{76,77}.

Interestingly, several genes involved in endocytosis showed altered expression in *Pkd1*^{del} mice and PTEC cells, while this process was also increased by *in vitro* fluid shear exposure⁴⁸⁻⁵⁰. The involvement of endocytosis in several growth factor signaling cascades like TGF- β and MAPK^{28,78}, makes this finding more interesting, suggesting that altered endocytosis, upon shear stress or *Pkd1* gene disruption, might contribute to imbalanced signaling.

Besides the clear overlap in altered cellular signaling between *Pkd1*^{-/-} cells and *Pkd1*^{del} mice, there were some differences. Genes involved in oxidative phosphorylation, mRNA processing, protein translation and ribosomal proteins were explicitly down-regulated in iKsp-*Pkd1*^{del} mice, while lysosome related gene expression was up-regulated. This might be caused by the different cell types that are present in the kidney, as well as variations in shear stress, and will depend on the overall biological context.

It has been hypothesized that critical Polycystin-1 levels are needed to restrain cellular and cilia related signaling^{59,79}. Increased activation of selected genes in renal epithelial cells upon *Pkd1* gene disruption, as shown in this paper, may disturb the balance in signaling and might contribute to cyst formation. Of course, the signaling cascades that trigger cyst

formation will depend on several factors, in addition to local and functional PKD protein levels, like renal injury, shear stress, inflammation, the metabolic status and more general, the biological context⁶⁰. For example, a number of studies indicate that renal injury can accelerate cyst progression and fibrosis^{67,80,81}. Numerous pre-clinical studies effectively inhibited implicated signaling pathways and reduced cyst formation and fibrosis. However, various clinical studies were unsuccessful to delay cyst growth in patients, while only Tolvaptan, a vasopressin receptor antagonist, has been approved as drug for ADPKD patients in a number of countries⁸²⁻⁸⁶. Therefore, effective therapies should target multiple signaling pathways, to re-establishing the balance in cellular signaling in renal epithelial cells and to maintain cellular homeostasis within physiological boundaries^{60,87,88}.

CONCLUSIONS

In conclusion, shear stress alters the same signaling pathways in *Pkd1*^{-/-} PTECs and in *Pkd1*^{wt} controls *in vitro*. However, the expression of a substantial number of genes was slightly more elevated by shear in *Pkd1*^{-/-} compared to *Pkd1*^{wt} cells, which are involved in Hippo, Wnt, MAPK, TGF- β and calcium signaling. Based on these results we hypothesize that *Pkd1* restrains shear stress induced signaling, rather than being directly involved in shear dependent activation of these pathways.

A comparison of shear-induced changes in *Pkd1*^{-/-} PTECs with *in vivo* transcriptome data of kidneys at three early pre-cystic time-points, revealed overlap in pathways and molecular processes, involving identical genes (approx. 180) as well as paralogous genes. These pathways include PI3K-AKT, MAPK, JAK-STAT, Hippo, p53, calcium, Wnt and TGF- β signaling, which are known to be implicated in the renal cyst formation as well. So, our results suggest that these processes are already altered at pre-cystic stage and may contribute to *in vivo* cyst formation caused by imbalanced signaling upon *Pkd1* gene disruption.

Acknowledgements

This work was supported by funding from the Netherlands Organization for Scientific Research (NWO) [grant number 820.02.016]; the Dutch Technology Foundation STW [grant number 11823], which is part of the Netherlands Organization for Scientific Research (NWO) and which is partially funded by the Ministry of Economic Affairs; the Dutch Kidney Foundation [grant numbers NSN IP11.34 and 14OIP12]; and the People Program (Marie Curie Actions) of the European Union's Seventh Framework Program FP7/2007-2013 [REA grant agreement no. 317246].

Compliance with ethical standards

Animal experiments have been carried out in accordance with the EU Directive 2010/63/EU for animal experiments.

Declarations of interest

None

Authorship

SJK carried out experiments, pathways analysis and wrote the manuscript

TBM carried out bioinformatics gene expression analysis

CF and WNL carried out animal experiments

PACH advised on the experimental setup and analysis

DJMP advised on the experimental setup, analysis and wrote the manuscript

All authors approved manuscript

REFERENCES

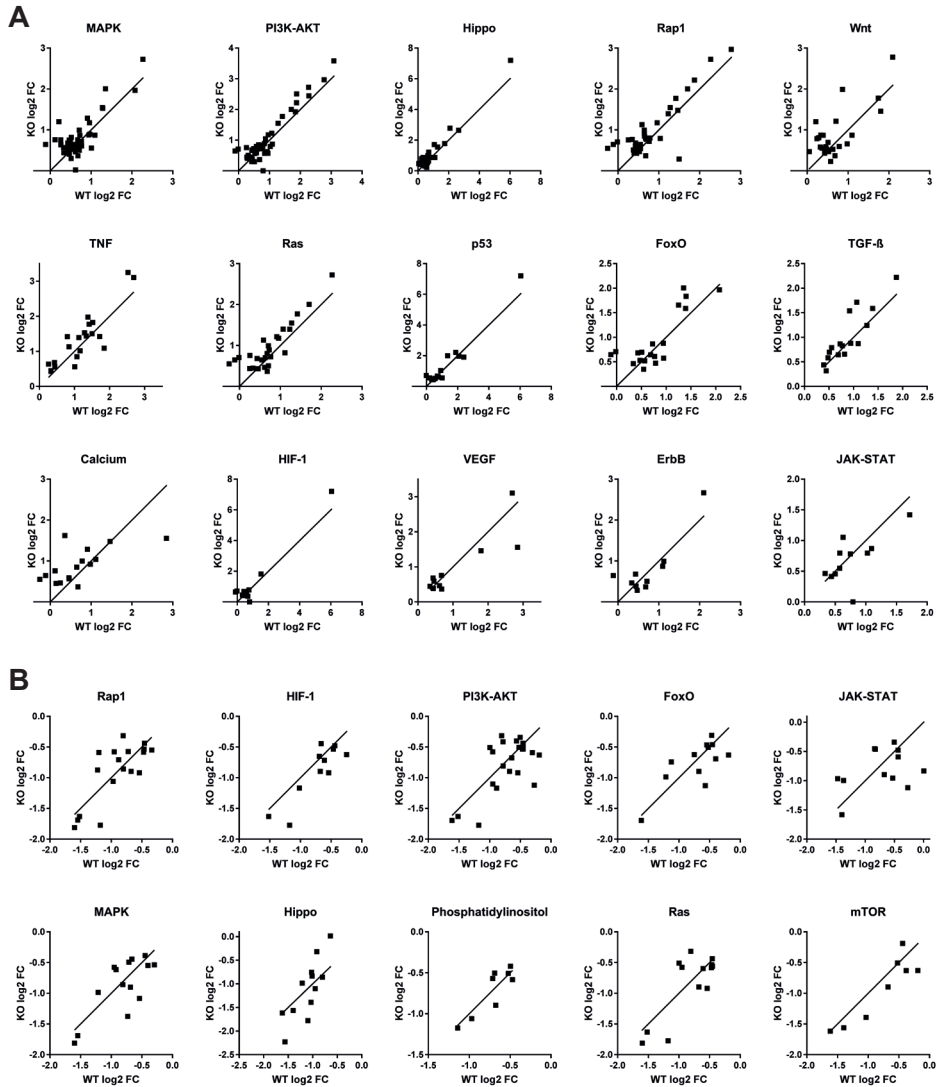
1. Igarashi P. & Somlo S. Genetics and pathogenesis of polycystic kidney disease. *J. Am. Soc. Nephrol.* **13**, 2384-2398 (2002).
2. Wilson P.D. Polycystic kidney disease. *N. Engl. J. Med.* **350**, 151-164 (2004).
3. Peters D.J.M. & Sandkuijl L.A. Genetic heterogeneity of polycystic kidney disease in Europe. *Contributions to Nephrology*. **97**, 128-139 (1992). *Polycystic Kidney Disease. 2nd International Workshop of the European Concerted Action Towards Prevention of Renal Failure Caused by Polycystic Kidney Disease, Parma, September 1991.* (eds: Breuning M.H., Devoto M., Romeo G.; Karger, Basel, 1992).
4. The European Polycystic Kidney Disease Consortium *et al.* The polycystic kidney disease 1 gene encodes a 14 kb transcript and lies within a duplicated region on chromosome 16. *Cell* **77**, 881-894 (1994).
5. Mochizuki T. *et al.* PKD2, a gene for polycystic kidney disease that encodes an integral membrane protein. *Science* **272**, 1339-1342 (1996).
6. Qian F.J., Watnick T.J., Onuchic L.F., & Germino G.G. The molecular basis of focal cyst formation in human autosomal dominant polycystic kidney disease. *Cell* **87**, 979-987 (1996).
7. Martin G.M. *et al.* Somatic mutations are frequent and increase with age in human kidney epithelial cells. *Hum Mol Genet* **5**, 215-221 (1996).
8. Yoder B.K., Hou X., & Guay-Woodford L.M. The polycystic kidney disease proteins, polycystin-1, polycystin-2, polaris, and cystin, are co-localized in renal cilia. *J. Am. Soc. Nephrol.* **13**, 2508-2516 (2002).
9. Nauli S.M. *et al.* Polycystins 1 and 2 mediate mechanosensation in the primary cilium of kidney cells. *Nat. Genet.* **33**, 129-137 (2003).
10. Liu X. *et al.* Polycystin-2 is an essential ion channel subunit in the primary cilium of the renal collecting duct epithelium. *Elife*. **7**, e33183 (2018).
11. Nauli S.M. *et al.* Loss of polycystin-1 in human cyst-lining epithelia leads to ciliary dysfunction. *J. Am. Soc. Nephrol.* **17**, 1015-1025 (2006).
12. Ma M., Tian X., Igarashi P., Pazour G.J., & Somlo S. Loss of cilia suppresses cyst growth in genetic models of autosomal dominant polycystic kidney disease. *Nat. Genet.* **45**, 1004-1012 (2013).
13. Jonassen J.A., San A.J., Follit J.A., & Pazour G.J. Deletion of IFT20 in the mouse kidney causes misorientation of the mitotic spindle and cystic kidney disease. *J. Cell Biol.* **183**, 377-384 (2008).
14. Arts H.H. & Knoers N.V. Current insights into renal ciliopathies: what can genetics teach us? *Pediatr. Nephrol.* **28**, 863-874 (2013).
15. Simons M. *et al.* Inversin, the gene product mutated in nephronophthisis type II, functions as a molecular switch between Wnt signaling pathways. *Nat. Genet.* **37**, 537-543 (2005).
16. Boehlke C. *et al.* Primary cilia regulate mTORC1 activity and cell size through Lkb1. *Nat. Cell Biol.* **12**, 1115-1122 (2010).
17. Zhong M. *et al.* Tumor Suppressor Folliculin Regulates mTORC1 through Primary Cilia. *J. Biol. Chem.* **291**, 11689-11697 (2016).
18. Low S.H. *et al.* Polycystin-1, STAT6, and P100 function in a pathway that transduces ciliary mechanosensation and is activated in polycystic kidney disease. *Dev. Cell* **10**, 57-69 (2006).
19. Kunnen S.J. *et al.* Fluid shear stress-induced TGF-beta/ALK5 signaling in renal epithelial cells is modulated by MEK1/2. *Cell Mol. Life Sci.* **74**, 2283-2298 (2017).
20. Kunnen S.J., Malas T.B., Semeins C.M., Bakker A.D., & Peters D.J.M. Comprehensive transcriptome analysis of fluid shear stress altered gene expression in renal epithelial cells. *J. Cell Physiol* **233**, 3615-3628 (2018).
21. Praetorius H.A. & Spring K.R. Bending the MDCK cell primary cilium increases intracellular calcium. *J. Membr. Biol.* **184**, 71-79 (2001).
22. Praetorius H.A., Frokiaer J., Nielsen S., & Spring K.R. Bending the Primary Cilium Opens Ca(2+)-sensitive Intermediate-Conductance K+ Channels in MDCK Cells. *J. Membr. Biol.* **191**, 193-200 (2003).

23. DeCaen P.G., Delling M., Vien T.N., & Clapham D.E. Direct recording and molecular identification of the calcium channel of primary cilia. *Nature* **504**, 315-318 (2013).
24. Delling M., DeCaen P.G., Doerner J.F., Febvay S., & Clapham D.E. Primary cilia are specialized calcium signalling organelles. *Nature* **504**, 311-314 (2013).
25. Delling M. *et al.* Primary cilia are not calcium-responsive mechanosensors. *Nature* **531**, 656-660 (2016).
26. Ma R. *et al.* PKD2 functions as an epidermal growth factor-activated plasma membrane channel. *Mol. Cell Biol.* **25**, 8285-8298 (2005).
27. Gill P.S. & Rosenblum N.D. Control of murine kidney development by sonic hedgehog and its GLI effectors. *Cell Cycle* **5**, 1426-1430 (2006).
28. Clement C.A. *et al.* TGF-beta signaling is associated with endocytosis at the pocket region of the primary cilium. *Cell Rep.* **3**, 1806-1814 (2013).
29. Bisgrove B.W. & Yost H.J. The roles of cilia in developmental disorders and disease. *Development* **133**, 4131-4143 (2006).
30. Goetz S.C. & Anderson K.V. The primary cilium: a signalling centre during vertebrate development. *Nat. Rev. Genet.* **11**, 331-344 (2010).
31. Freund J.B., Goetz J.G., Hill K.L., & Vermot J. Fluid flows and forces in development: functions, features and biophysical principles. *Development* **139**, 1229-1245 (2012).
32. Weinbaum S., Duan Y., Satlin L.M., Wang T., & Weinstein A.M. Mechanotransduction in the renal tubule. *Am. J. Physiol Renal Physiol* **299**, F1220-F1236 (2010).
33. Carrisoza-Gaytan R., Carattino M.D., Kleyman T.R., & Satlin L.M. An unexpected journey: conceptual evolution of mechanoregulated potassium transport in the distal nephron. *Am. J. Physiol Cell Physiol* **310**, C243-C259 (2016).
34. Sharma A., Mucino M.J., & Ronco C. Renal functional reserve and renal recovery after acute kidney injury. *Nephron Clin. Pract.* **127**, 94-100 (2014).
35. Srivastava T. *et al.* Fluid flow shear stress over podocytes is increased in the solitary kidney. *Nephrol. Dial. Transplant.* **29**, 65-72 (2014).
36. Lenihan C.R. *et al.* Longitudinal study of living kidney donor glomerular dynamics after nephrectomy. *J. Clin. Invest* **125**, 1311-1318 (2015).
37. Bell P.D. *et al.* Loss of primary cilia upregulates renal hypertrophic signaling and promotes cystogenesis. *J. Am. Soc. Nephrol.* **22**, 839-848 (2011).
38. Leonhard W.N. *et al.* Scattered Deletion of PKD1 in Kidneys Causes a Cystic Snowball Effect and Recapitulates Polycystic Kidney Disease. *J. Am. Soc. Nephrol.* **26**, 1322-1333 (2015).
39. Leonhard W.N. *et al.* Curcumin inhibits cystogenesis by simultaneous interference of multiple signaling pathways: In vivo evidence from a Pkd1-deletion model. *Am. J. Physiol Renal Physiol* **300**, F1193-F1202 (2011).
40. Malek A.M., Ahlquist R., Gibbons G.H., Dzau V.J., & Izumo S. A cone-plate apparatus for the in vitro biochemical and molecular analysis of the effect of shear stress on adherent cells. *Methods in Cell Science* **17**, 165-176 (1995).
41. Bacabac R.G. *et al.* Dynamic shear stress in parallel-plate flow chambers. *J. Biomech.* **38**, 159-167 (2005).
42. Kim D. *et al.* TopHat2: accurate alignment of transcriptomes in the presence of insertions, deletions and gene fusions. *Genome Biol.* **14**, R36 (2013).
43. Anders S., Pyl P.T., & Huber W. HTSeq—a Python framework to work with high-throughput sequencing data. *Bioinformatics.* **31**, 166-169 (2015).
44. Lantinga-van Leeuwen I.S. *et al.* Kidney-specific inactivation of the Pkd1 gene induces rapid cyst formation in developing kidneys and a slow onset of disease in adult mice. *Hum. Mol. Genet.* **16**, 3188-3196 (2007).
45. Novalic Z. *et al.* Dose-Dependent Effects of Sirolimus on mTOR Signaling and Polycystic Kidney Disease. *J. Am. Soc. Nephrol.* **23**, 842-853 (2012).

46. Malas T.B. *et al.* Meta-analysis of Polycystic Kidney Disease expression profiles defines strong involvement of injury repair processes. *Am. J. Physiol Renal Physiol* **312**, F806-F817 (2017).
47. Stockel D. *et al.* Multi-omics enrichment analysis using the GeneTrail2 web service. *Bioinformatics*. **32**, 1502-1508 (2016).
48. Raghavan V., Rbaibi Y., Pastor-Soler N.M., Carattino M.D., & Weisz O.A. Shear stress-dependent regulation of apical endocytosis in renal proximal tubule cells mediated by primary cilia. *Proc. Natl. Acad. Sci. U. S. A* **111**, 8506-8511 (2014).
49. Raghavan V. & Weisz O.A. Discerning the role of mechanosensors in regulating proximal tubule function. *Am. J. Physiol Renal Physiol* **310**, F1-F5 (2016).
50. Bhattacharyya S. *et al.* Cdc42 activation couples fluid shear stress to apical endocytosis in proximal tubule cells. *Physiol Rep*. **5**, e13460 (2017).
51. Praetorius H.A. & Leipziger J. Primary cilium-dependent sensing of urinary flow and paracrine purinergic signaling. *Semin. Cell Dev. Biol.* **24**, 3-10 (2013).
52. Fujii M. *et al.* TGF-beta synergizes with defects in the Hippo pathway to stimulate human malignant mesothelioma growth. *J. Exp. Med.* **209**, 479-494 (2012).
53. Xie M., Wu X., Zhang J., Zhang J., & Li X. Ski regulates Smads and TAZ signaling to suppress lung cancer progression. *Mol. Carcinog.* **56**, 2178-2189 (2017).
54. Alam M. *et al.* MUC1-C Represses the Crumbs Complex Polarity Factor CRB3 and Downregulates the Hippo Pathway. *Mol. Cancer Res.* **14**, 1266-1276 (2016).
55. Happe H. *et al.* Altered Hippo signalling in polycystic kidney disease. *J. Pathol.* **224**, 133-142 (2011).
56. Eijkelenboom A. & Burgering B.M. FOXOs: signalling integrators for homeostasis maintenance. *Nat. Rev. Mol. Cell Biol.* **14**, 83-97 (2013).
57. Rowe I. & Boletta A. Defective metabolism in polycystic kidney disease: potential for therapy and open questions. *Nephrol. Dial. Transplant.* **29**, 1480-1486 (2014).
58. De R.S. *et al.* Autophagy in renal diseases. *Pediatr. Nephrol.* **31**, 737-752 (2016).
59. Ma M., Gallagher A.R., & Somlo S. Ciliary Mechanisms of Cyst Formation in Polycystic Kidney Disease. *Cold Spring Harb. Perspect. Biol.* **9**, a028209 (2017).
60. Leonhard W.N., Happe H., & Peters D.J. Variable Cyst Development in Autosomal Dominant Polycystic Kidney Disease: The Biologic Context. *J. Am. Soc. Nephrol.* **27**, 3530-3538 (2016).
61. Fantus D., Rogers N.M., Grahammer F., Huber T.B., & Thomson A.W. Roles of mTOR complexes in the kidney: implications for renal disease and transplantation. *Nat. Rev. Nephrol.* **12**, 587-609 (2016).
62. Stallone G. *et al.* Rapamycin for treatment of type I autosomal dominant polycystic kidney disease (RAPYD-study): a randomized, controlled study. *Nephrol. Dial. Transplant.* **27**, 3560-3567 (2012).
63. He Q., Lin C., Ji S., & Chen J. Efficacy and safety of mTOR inhibitor therapy in patients with early-stage autosomal dominant polycystic kidney disease: a meta-analysis of randomized controlled trials. *Am. J. Med. Sci.* **344**, 491-497 (2012).
64. Hassane S. *et al.* Elevated TGFbeta-Smad signalling in experimental Pkd1 models and human patients with polycystic kidney disease. *J. Pathol.* **222**, 21-31 (2010).
65. Leonhard W.N. *et al.* Inhibition of Activin Signaling Slows Progression of Polycystic Kidney Disease. *J. Am. Soc. Nephrol.* **27**, 3589-3599 (2016).
66. Liu D. *et al.* A Pkd1-Fbn1 genetic interaction implicates TGF-beta signaling in the pathogenesis of vascular complications in autosomal dominant polycystic kidney disease. *J. Am. Soc. Nephrol.* **25**, 81-91 (2014).
67. Happe H. *et al.* Toxic tubular injury in kidneys from Pkd1-deletion mice accelerates cystogenesis accompanied by dysregulated planar cell polarity and canonical Wnt signaling pathways. *Hum. Mol. Genet.* **18**, 2532-2542 (2009).
68. Wuebkén A. & Schmidt-Ott K.M. WNT/beta-catenin signaling in polycystic kidney disease. *Kidney Int.* **80**, 135-138 (2011).
69. Fragiadaki M. *et al.* STAT5 drives abnormal proliferation in autosomal dominant polycystic kidney disease.

- Kidney Int.* **91**, 575-586 (2017).
70. Talbot J.J. *et al.* Polycystin-1 regulates STAT activity by a dual mechanism. *Proc. Natl. Acad. Sci. U. S. A* **108**, 7985-7990 (2011).
 71. Xu T. *et al.* Celecoxib inhibits growth of human autosomal dominant polycystic kidney cyst-lining epithelial cells through the VEGF/Raf/MAPK/ERK signaling pathway. *Mol. Biol. Rep.* **39**, 7743-7753 (2012).
 72. Hakim S. *et al.* Inpp5e suppresses polycystic kidney disease via inhibition of PI3K/Akt-dependent mTORC1 signaling. *Hum. Mol. Genet.* **25**, 2295-2313 (2016).
 73. Tran P.V. *et al.* Downregulating hedgehog signaling reduces renal cystogenic potential of mouse models. *J. Am. Soc. Nephrol.* **25**, 2201-2212 (2014).
 74. Yamaguchi T. *et al.* cAMP stimulates the in vitro proliferation of renal cyst epithelial cells by activating the extracellular signal-regulated kinase pathway. *Kidney Int.* **57**, 1460-1471 (2000).
 75. Happe H. & Peters D.J. Translational research in ADPKD: lessons from animal models. *Nat. Rev. Nephrol.* **10**, 587-601 (2014).
 76. Puri S. *et al.* Polycystin-1 activates the calcineurin/NFAT (nuclear factor of activated T-cells) signaling pathway. *J. Biol. Chem.* **279**, 55455-55464 (2004).
 77. Kim S. *et al.* The polycystin complex mediates Wnt/Ca(2+) signalling. *Nat. Cell Biol.* **18**, 752-764 (2016).
 78. Tomas A., Jones S., Vaughan S.O., Hochhauser D., & Futter C.E. Stress-specific p38 MAPK activation is sufficient to drive EGFR endocytosis but not its nuclear translocation. *J. Cell Sci.* **130**, 2481-2490 (2017).
 79. Lee S.H. & Somlo S. Cyst growth, polycystins, and primary cilia in autosomal dominant polycystic kidney disease. *Kidney Res. Clin. Pract.* **33**, 73-78 (2014).
 80. Patel V. *et al.* Acute kidney injury and aberrant planar cell polarity induce cyst formation in mice lacking renal cilia. *Hum. Mol. Genet.* **17**, 1578-1590 (2008).
 81. Sas K.M. *et al.* Hyperglycemia in the absence of cilia accelerates cystogenesis and induces renal damage. *Am. J. Physiol Renal Physiol* **309**, F79-F87 (2015).
 82. Torres V.E. *et al.* Tolvaptan in patients with autosomal dominant polycystic kidney disease. *N. Engl. J. Med.* **367**, 2407-2418 (2012).
 83. Torres V.E. & Harris P.C. Polycystic kidney disease in 2011: Connecting the dots toward a polycystic kidney disease therapy. *Nat. Rev. Nephrol.* **8**, 66-68 (2011).
 84. Riella C., Czarnecki P.G., & Steinman T.I. Therapeutic advances in the treatment of polycystic kidney disease. *Nephron Clin. Pract.* **128**, 297-302 (2014).
 85. Santoro D. *et al.* An overview of experimental and early investigational therapies for the treatment of polycystic kidney disease. *Expert. Opin. Investig. Drugs* **24**, 1199-1218 (2015).
 86. Chang M.Y. & Ong A.C.M. Targeting new cellular disease pathways in autosomal dominant polycystic kidney disease. *Nephrol. Dial. Transplant.* **33**, 1310-1316 (2018).
 87. Aguiari G., Catizone L., & del S.L. Multidrug therapy for polycystic kidney disease: a review and perspective. *Am. J. Nephrol.* **37**, 175-182 (2013).
 88. Rysz J., Gluba-Brzozka A., Franczyk B., Banach M., & Bartnicki P. Combination drug versus monotherapy for the treatment of autosomal dominant polycystic kidney disease. *Expert. Opin. Pharmacother.* **17**, 2049-2056 (2016).

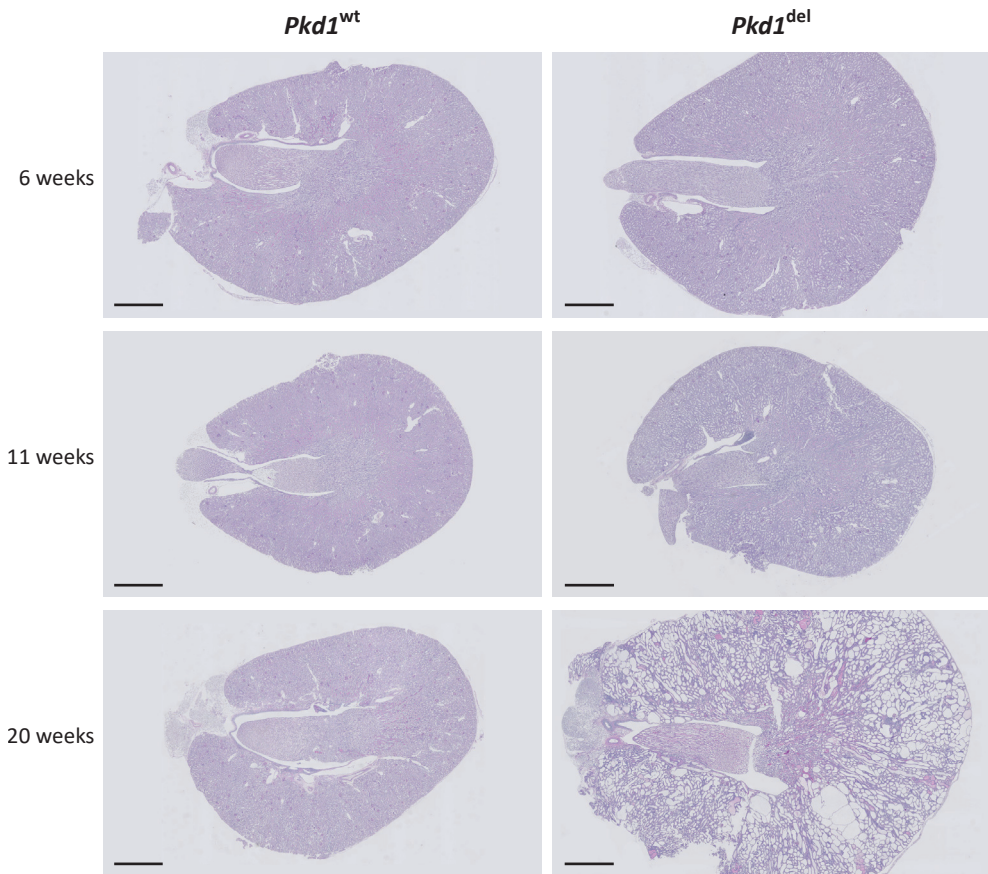
SUPPLEMENTARY FIGURES



Supplementary Figure S1. Comparison of shear stress response in *Pkd1*^{-/-} vs *Pkd1*^{wt} PTECs.

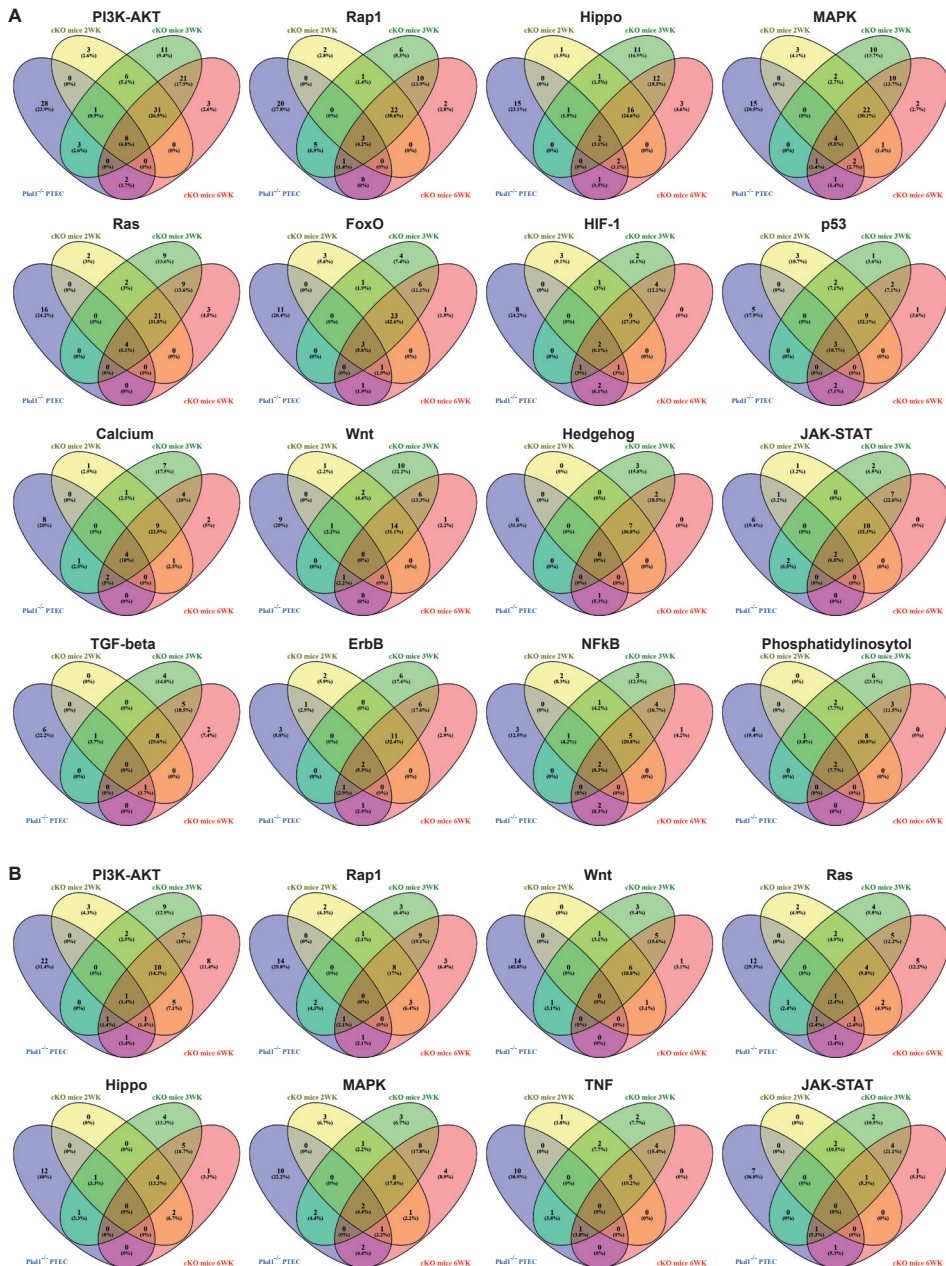
Comparison of log₂ fold changes (log₂ FC) in *Pkd1*^{-/-} PTECs (KO; y-axis) vs *Pkd1*^{wt} controls (WT; x-axis) for differentially up-regulated (A) or down-regulated (B) genes upon shear stress treatment. Several shear up-regulated genes, involved in MAPK, PI3K-AKT, Hippo, Rap1, Wnt, TNF, Ras, TGF-β and calcium signaling pathways, show stronger shear induction in *Pkd1*^{-/-} PTECs compared to *Pkd1*^{wt} controls. For shear down-regulated genes there was less difference between *Pkd1*^{-/-} and *Pkd1*^{wt} PTECs, although several genes involved in HIF-1 and mTOR signaling seems to be stronger down-regulated in *Pkd1*^{-/-} PTECs. Black lines represent equal differential expression upon shear stress in *Pkd1*^{-/-} and *Pkd1*^{wt} PTECs.





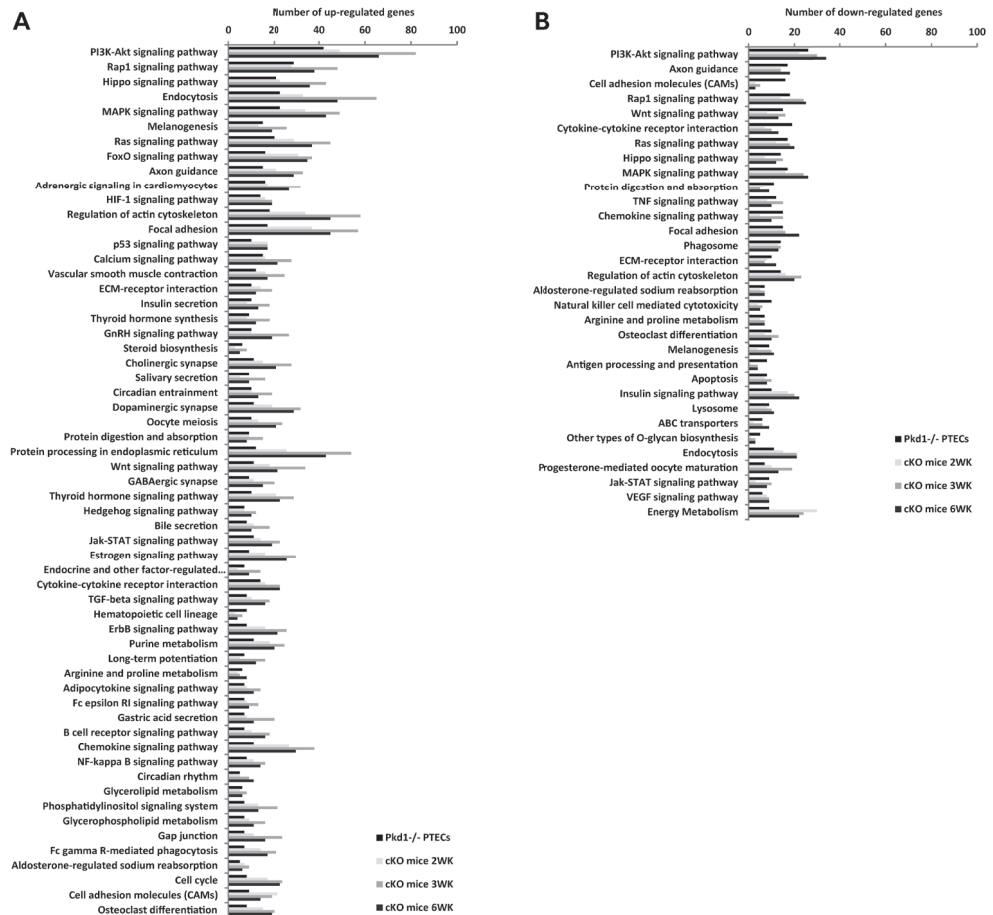
Supplementary Figure S2. Kidney morphology of *Pkd1*^{wt} and iKsp-*Pkd1*^{del} mice.

Representative images of periodic-acid Schiff (PAS) staining on formalin fixed, paraffin embedded kidney sections of *Pkd1*^{wt} (left) and iKsp-*Pkd1*^{del} (right) mice at 6 (top), 11 (middle) or 20 (bottom) weeks after *Pkd1* gene disruption at the age of 13 to 14 weeks. Cyst formation is clearly visible when iKsp-*Pkd1*^{del} mice reaches kidney failure at 20 weeks; scale bar = 1 mm.



Supplementary Figure S3. Comparison of differentially expressed genes in core signaling pathways upon *Pkd1* gene disruption in cells and mice.

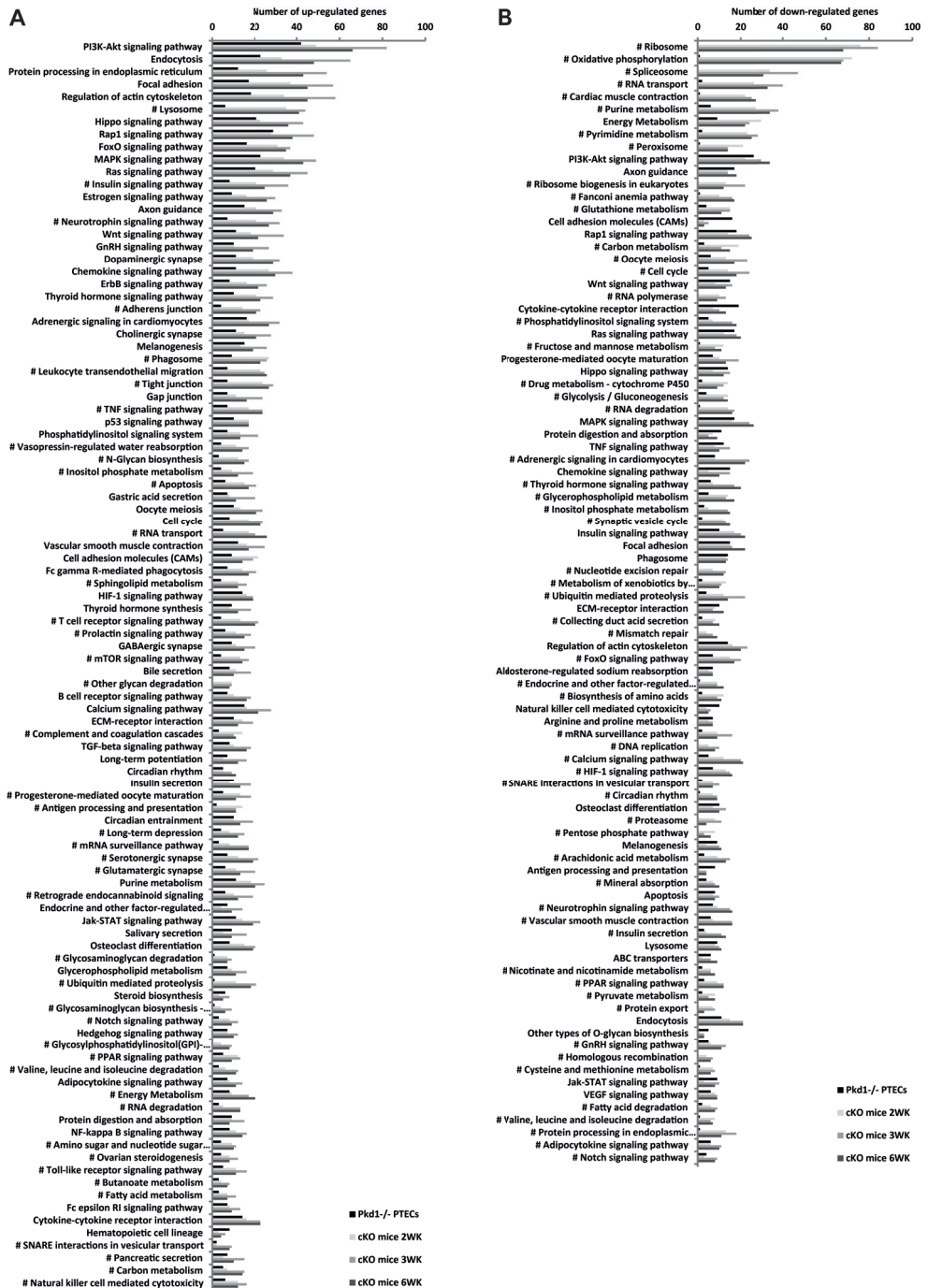
Venn diagrams of up-regulated (A) and down-regulated (B) genes in core signaling pathways (KEGG) showing the number of genes in overlap between *Pdk1*^{-/-} PTEC cells and *iKsp-Pkd1*^{del} (cKO) mice at 2, 3 or 6 weeks (WK) upon *Pkd1* gene disruption. (%) means the percentage of genes of all up-regulated or down-regulated genes.



Supplementary Figure S4. Comparison of altered pathways and processes upon *Pkd1* gene disruption in cells and mice - significant in *Pkd1*^{-/-} cells.

Number of differentially expressed genes, which were annotated to up-regulated (A) or down-regulated (B) signaling pathways and cellular processes (KEGG) for *Pkd1*^{-/-} PTECs or iKsp-*Pkd1*^{del} (cKO) mice at 2, 3 or 6 weeks (WK) upon *Pkd1* gene disruption. Significantly (FDR < 0.01) enriched pathways and processes in *Pkd1*^{-/-} PTECs are shown and compared to iKsp-*Pkd1*^{del} (cKO) mice. Pathways are ordered by lowest false discovery rate (FDR) in *Pkd1*^{-/-} PTECs. Only annotations from the KEGG database were included, without disease related pathways.

COMPARATIVE TRANSCRIPTOMICS OF SHEAR STRESS TREATED *PKD1*^{-/-} CELLS AND PRE-CYSTIC KIDNEYS

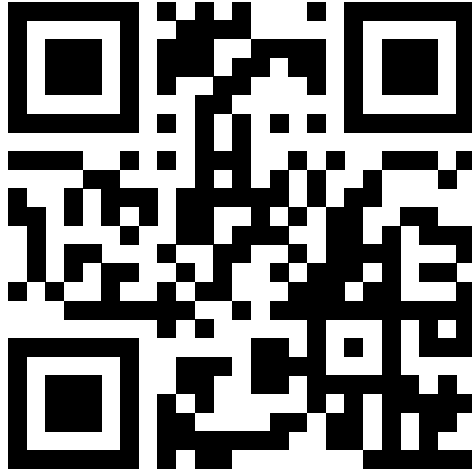


◀ **Supplementary Figure S5. Comparison of altered pathways and processes upon *Pkd1* gene disruption in cells and mice - significant in *Pkd1^{del}* mice.**

Number of differentially expressed genes, which were annotated to up-regulated (A) or down-regulated (B) signaling pathways and cellular processes (KEGG) for *Pdk1^{-/-}* PTECs or iKsp-*Pkd1^{del}* (cKO) mice at 2, 3 or 6 weeks (WK) upon *Pkd1* gene disruption. Significantly (FDR < 0.01) enriched pathways and processes in iKsp-*Pkd1^{del}* (cKO) mice are shown and compared to *Pkd1^{-/-}* PTECs. Pathways are ordered by lowest false discovery rate (FDR) in any of the four groups shown. Only annotations from the KEGG database were included, without disease related pathways. # = Not significantly enriched pathways in *Pdk1^{-/-}* PTECs from functional enrichment analysis (FDR >= 0.01).

SUPPLEMENTARY TABLES

<https://goo.gl/yRe32v>



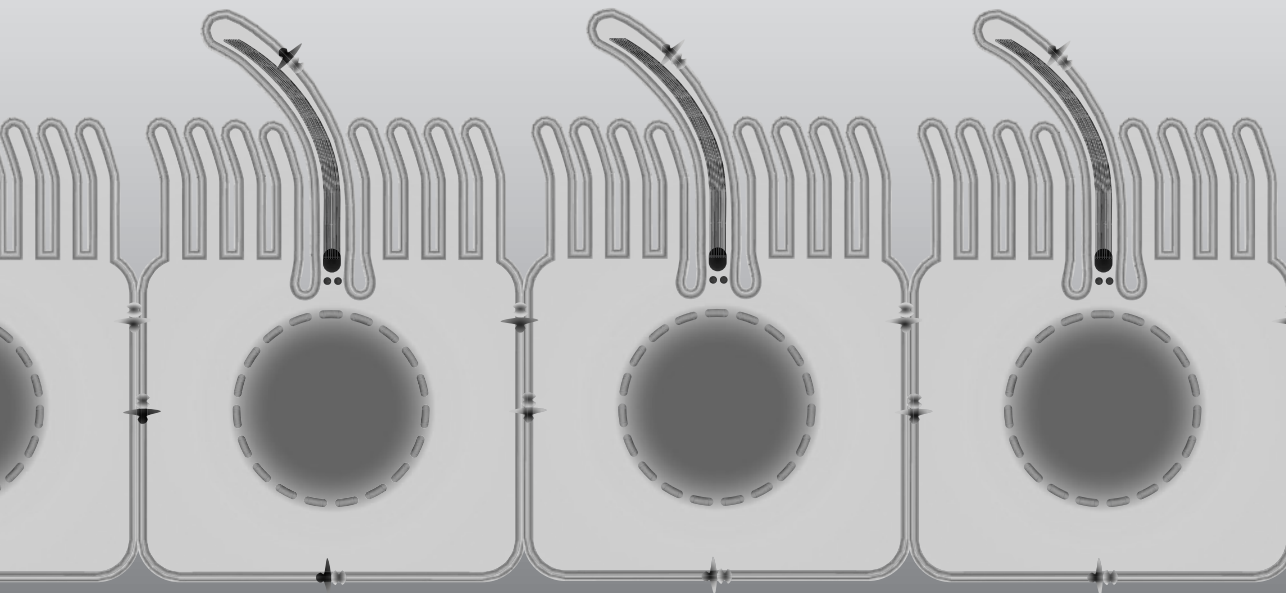
CHAPTER 5

Inhibition of Activin signaling slows progression of Polycystic Kidney Disease in mice.

Wouter N. Leonhard¹, Steven J. Kunnen¹, Anna J. Plugge¹, Arja Pasternack⁴, Sebastian B.T. Jianu¹, Kimberley Veraar², Fatiha el Bouazzaoui¹, Willem M.H. Hoogaars⁵, Peter ten Dijke³, Martijn H. Breuning¹, Emile De Heer², Olli Ritvos⁴, Dorien J.M. Peters¹.

¹Dept. of Human Genetics, ²Pathology and ³Molecular Cell Biology and Cancer Genomics Centre Netherlands at the Leiden University Medical Center. ⁴Dept of Bacteriology and Immunology, Haartman Institute, University of Helsinki, Finland. ⁵Department of Human Movement Sciences, Faculty of Behavior and Movement Sciences, Vrije Universiteit Amsterdam, MOVE Research Institute Amsterdam, The Netherlands.

J Am Soc Nephrol. 2016; 27(12): 3589-3599



ABSTRACT

Autosomal Dominant Polycystic Kidney Disease (ADPKD), characterized by the formation of numerous kidney cysts, is caused by *PKD1* or *PKD2* mutations and affects 0.1% of the population. Although recent clinical studies indicate that reduction of cAMP levels slows progression of PKD, they have not yet led to an established safe and effective therapy for patients, indicating the need to find new therapeutic targets. The role of transforming growth factor β (TGF β) in PKD is not clearly understood but nuclear accumulation of pSMAD2/3 in cyst-lining cells suggests the involvement of TGF β signaling in PKD. In this study we ablated the TGF β type I receptor (also termed activating receptor-like kinase 5 (ALK5)) in renal epithelial cells of PKD mice, which had little to no effect on the expression of SMAD2/3 target genes, or on the progression of PKD. These data suggest that alternative TGF β superfamily ligands may account for SMAD2/3 activation in cystic epithelial cells. Activins are members of the TGF β superfamily and drive SMAD2/3 phosphorylation via Activin receptors and have not yet been studied before in the context of PKD. Already in mice with early PKD, we found increased expression of Activin ligands. In addition, treatment with a soluble Activin receptor IIB fusion protein (sActRIIB-Fc), which acts as a soluble trap to sequester Activin ligands, effectively inhibited cyst formation in three distinct mouse models of PKD. These data point to Activin signaling as a key player in PKD, and as a promising target for therapy.

INTRODUCTION

Autosomal Dominant Polycystic Kidney Disease (ADPKD) is a frequent disorder affecting 1 in 1000 individuals and involves the *polycystic kidney disease 1 (PKD1)* gene, which is mutated in 85% of the cases, and the *PKD2* gene, which is mutated in 15% of the cases¹⁻³. Besides extra-renal manifestations such as liver cysts, pancreas cysts, hypertension, cardiovalvular abnormalities and cerebral aneurisms, the kidney is the most severely affected organ⁴. Patients develop thousands of renal cysts causing anatomically distorted, enlarged and fibrotic kidneys, which ultimately leads to renal failure around the age of 60 years^{5,6}. When the levels of functional Polycystin 1 (PC1) or Polycystin 2 (PC2), the gene-products of *PKD1* and *PKD2*, deviate too much from the normal levels the likelihood of cyst formation increases⁷⁻¹². In addition, the context of the renal tissue is crucial in determining whether or not cyst formation occurs and at what growth rate this process takes place. Under normal conditions the adult kidney is relatively resistant to cyst formation but during renal development, renal injury or during continuous stress on renal tissue imposed by existing cysts, cells are prone to take part in cyst formation once they have lost Polycystin function¹³⁻¹⁸.

Multiple signaling pathways, such as mTOR, cAMP, Ca²⁺, Wnt, STAT3 and Src/Ras/Raf/MEK/ERK, among others, seem to be involved in driving cyst formation¹⁹. In addition, we showed in a previous study that transforming growth factor- β (TGF β) signaling may also play a role in PKD²⁰. Following binding of the TGF β ligands (TGF β 1, 2 or 3) to the TGF β type II receptor II (TGFBR2), TGF β type I receptor (also termed Activin Receptor-like Kinase 5: ALK5) is recruited and phosphorylated, which then phosphorylates SMAD2 and SMAD3. These phosphorylated SMAD2 and SMAD3 (pSMAD2/3) proteins form a complex with SMAD4 and this complex can enter the nucleus to initiate the transcription of various genes²¹. In pathological conditions TGF β signaling is known to drive fibrosis in various end-stage renal diseases²²⁻²⁵. In cancer, TGF β can either inhibit tumor formation or promote metastasis depending on the specific conditions in the tumor microenvironment. We previously found increased levels of nuclear pSMAD2 also in cystic epithelial cells, suggesting a possible role for TGF β in these cells²⁰. Although TGF β inhibited cyst formation in 3D-cyst cultures of ADPKD cells²⁶, the pleiotropic actions of TGF β renders it difficult to predict the exact role of TGF β in the context of the polycystic kidney.

To better understand the role of TGF β signaling in cyst formation, and to assess whether TGF β signaling can be used as a therapeutic target to inhibit disease progression, we crossbred kidney-specific tamoxifen-inducible *Pkd1* deletion mice (iKsp-*Pkd1*^{del}) with mice in which exon 3 of the *Alk5* gene is flanked by Lox-P sites^{13,27}. This allowed us to simultaneously knock-out *Pkd1* and *Alk5* specifically in the renal epithelium and to study the role of TGF β signaling in cyst formation. However, we show here that the additional inactivation of

Alk5 did not affect the progression of PKD and only mildly affected SMAD2/3 dependent signaling, suggesting that alternative pathways are accountable for these changes. We previously showed increased expression levels of *Inhibin* β A²⁸. The different subtypes of *Inhibin* β chains are able to form hetero- or homodimers with other *Inhibin* β chains to form different Activins, or they can dimerize with *Inhibin* α to form Inhibins, which antagonize the activity of Activins²⁹. Activins are members of the TGF β superfamily that bind to Activin type II receptors, which results in recruitment of Activin type I receptor (ACVR1B, or ALK4) and subsequent phosphorylation of SMAD2/3²⁹. The soluble Activin receptor IIB fusion protein (sActRIIB-Fc) has been used to enhance muscle growth by antagonizing Myostatin, which is a member of the TGF β superfamily that signals through the ActRIIB receptor and is a negative regulator for muscle growth³⁰. Like Myostatin, also Activin A and Activin B signal through Activin II receptors and can be sequestered by sActRIIB-Fc. We show here that treatment with sActRIIB-Fc markedly slows progression of PKD in three different mouse models for PKD. Taken together, our results suggest that the role of TGF β in renal epithelial cells is limited in the context of PKD. Furthermore, Activins drive the progression of PKD and are highly promising targets for therapeutic intervention.

CONCISE METHODS

Mice and treatments

iKspCre-*Pkd1*^{lox} mice (*Pkd1*-cKO) have a homozygously bred kidney specific tamoxifen inducible Cre³⁶, and two *LoxP* sites that flank exons 2-11 of the *Pkd1* gene¹³. For some experiments, these mice were crossed with mice having exon 3 of the *Alk5* gene flanked by *LoxP* sites²⁷, to obtain the indicated genotypes. These mice were all on full C57BL6/J genetic background. Oral tamoxifen administration to facilitate gene disruption was done as described previously³⁶. The mice received either 200 mg/kg tamoxifen at P40-P42, 150 mg/kg at P18-P20 or 6 mg/kg tamoxifen at P10-12. Tamoxifen administration at these dosages and ages are well tolerated based on careful assessment of behavior, but the P10-12 mice have reduced bodyweights due to the Tamoxifen treatments. Hypomorphic *Pkd1*^{nl,nl} mice have a PGK promoter-driven neomycin-resistance gene that is flanked by *LoxP* sites in intron 1 of the *Pkd1* gene. This neomycin resistance gene causes alternative splicing of the *Pkd1* gene, resulting in reduced expression of *Pkd1*-WT transcripts, which leads to rapid cyst formation starting around P7^{10,32}. Male *Pkd1*^{nl,wt} mice on 129Ola/Hsd genetic background were crossed with female *Pkd1*^{nl,wt} mice on C57BL6/J genetic background to generate *Pkd1*^{nl,nl} F1-hybrids having a fixed genetic background of exactly 50% C57BL6/J and 50% 129Ola/Hsd. These F1-hybrids were used in the experiments. Since PKD in male P18-*Pkd1*-cKO mice progresses faster compared to PKD in female P18-*Pkd1*-cKO mice, we only used male mice for the survival experiment to reduce the number of mice needed for the experiment. For the rapid PKD models, male and female mice have a comparable progression rate and both sexes were used.

The recombinant human sActRIIB-Fc protein is a fusion of a human Fc and the ActRIIB receptor and was produced in house in CHO-S cell suspension cultures using chemically defined serum free medium and the protein was purified by affinity chromatography as described in detail in Hulmi *et. al.* 2013⁴⁹. Mice were treated twice a week with intraperitoneal (IP) injections with sActRIIB-Fc either with 1, 3, or 10 mg/kg in PBS. As a control group, mice received IP injections twice a week with PBS.

Blood sampling and blood urea measurements were performed using Reflotron technology (Kerkhof Medical Service) as described previously¹⁶.

Local animal experimental committee of the Leiden University Medical Center and the Commission Biotechnology in Animals of the Dutch Ministry of Agriculture approved the experiments performed.

Gene expression analysis

Kidneys from sacrificed mice were removed, snap-frozen in liquid nitrogen and stored at -80°C until further processing. Kidneys were homogenized using Magnalyser technology (Roche Applied Science) and total RNA was isolated from kidney samples using Tri-Reagent

(Sigma-Aldrich). Gene expression was either measured by Reverse-Transcription-Multiplex-Dependent-Probe-Amplification (RT-MLPA), or by quantitative-PCR (qPCR) as described previously¹⁶. RT-MLPA: Briefly, 60-120 ng of RNA was used to synthesize cDNA with strand-specific oligonucleotides in a single reaction with Reverse Transcriptase (Promega). Forward probes (oligonucleotides with a universal sequence at the 5'end) and reverse probes (oligonucleotides with a universal sequence at the 3'end) were hybridized directly adjacent to each other onto the cDNA followed by a ligation step and PCR, using a single primer set (forward primer labeled with a 6-Carboxyfluorescein (FAM) or Hexachloro-fluorescein (*HEX*) fluorescent label) designed to simultaneously amplify all ligated probes (MLPA reagents were from MRC-Holland). The PCR fragments were run on a 3730 DNA analyzer (Applied Biosystems) and peak-heights were analyzed using Peak Scanner 2.0 software (Applied Biosystems). *Ywhaz* and *Hprt* served as reference genes and relative peak-ratios were calculated to determine relative gene expression. Probe sequences of the specific genes are available on request. qPCR: cDNA synthesis was done with Transcriptor First Strand cDNA Synthesis Kit (Roche Applied Science) according to the manufacturer's protocol. Quantitative PCR was done on the LightCycler 480 II (Roche Applied Science) using 2x FastStart SYBR-Green Master (Roche Applied Science) according to the manufacturer's protocol. Primer sequences are available upon request. Data was analysed with Lightcycler 480 Software, Version 1.5 (Roche Applied Science). Gene expression was calculated using LinRegPCR method as described previously⁵⁰. and normalized to *Hprt* expression, giving the relative gene expression. Mean gene expression and standard deviation of the treatment groups were calculated.

Histochemistry and cystic, fibrotic, proliferation and apoptotic indices

Kidneys were fixed in buffered 4% formaldehyde solution and embedded in paraffin. Kidney sections (4µm) were stained with standard hematoxylin and eosin (H&E). Total scans from H&E stained kidney sections were used to determine the cystic indices. The cystic index was determined using Image J software (public domain software; National Institutes of Health) and defined as the percentage of cystic area relative to total tissue. The fibrotic index was measured by staining sections with SiriusRed: After deparaffinization, sections were stained with 0.2% Phosphomolybdic acid (1 min.), 0.1% SiriusRed in Picric Acid (90 min.), and then with saturated Picric Acid, followed by standard ethanol/xylol washes and mounting. All sections were stained simultaneously to avoid inter-experimental variation, and all scanned images were processed exactly the same using Photoshop software. Specifically designed color palettes were used to first remove signal within cysts (leaving only the pixels from all tissue), and then that of the tissue except for the red SiriusRed signal (leaving only the SiriusRed signal). Large arteries were removed from the analysis. The ratio (SiriusRed_pixels vs Complete_tissue_pixels) of the number of pixels were calculated as a percentage and was defined as the fibrotic index. The proliferation index was determined on the basis of

immunohistochemical staining with Ki67 (NCL Ki67p; Nova Castra) as described previously³¹. The apoptotic index was determined in a similar fashion like the proliferation index, only then using Rabbit anti cleaved caspase 3 (9661; Cell Signaling). To determine from which segment of the nephron cysts originate in the kidneys of the P18-*Pkd1*-cKO mice, we performed marker staining with rabbit anti-megalin (1:500; Pathology LUMC, Leiden) to detect proximal tubular cysts, goat anti-Tamm Horsfall protein (uromodulin, 1:500; Organon Teknika-Cappel), to detect distal tubular cysts, or rabbit antiaquaporin-2 (1:4,000; Calbiochem) to detect collecting duct cysts, as described previously³¹.

Cell culture and Western blotting

For *in-vitro* analysis, primary cells were generated from the cortexes of kidneys of tamoxifen treated *iKspCre;Pkd1^{lox,lox}* and *iKspCre;Pkd1^{lox,lox},Alk5^{lox,lox}* mice. In addition, mouse *Pkd1^{-/-}* and *Pkd1^{+/+}* proximal tubular epithelial cells were cultured and processed as described previously³¹. Western blotting was performed on crude protein extracts using standard procedures and as described previously using an anti-phospho-SMAD2 antibody⁵¹, an anti- α Tubulin antibody (CP06, Calbiochem), and a total-SMAD2 antibody (3103 Cell Signaling Technologies)²⁰. For optimal performance using westernblot analysis of tissue extracts, TGX gradient gels were used from BioRad. Densitometric analysis was carried out using Odyssey technology (Licor-biosciences).

Statistical Analysis

Differences between survival curves were tested with the generalized Wilcoxon test. All other group comparisons were tested using two-tailed t tests.

RESULTS

TGFBR1 (ALK5) ablation in conditional Pkd1 deletion mice.

To better understand the role of TGF β signaling specifically in the renal epithelium during cystogenesis, we crossbred kidney-specific-tamoxifen-inducible-Cre-*Pkd1*^{lox} mice (iKspCre-*Pkd1*^{lox,lox}) with mice in which exon 3 of the *Alk5* gene is flanked by *LoxP* sites^{13,27}. As such, we generated iKspCre-*Pkd1*^{lox,lox} and iKspCre-*Pkd1*^{lox,lox};*Alk5*^{lox,wt} and iKspCre-*Pkd1*^{lox,lox};*Alk5*^{lox,lox} mice. Eleven weeks following tamoxifen administration at Post-Natal day (P) 40, 41 and 42 (i.e. these mice have mild tubular dilations), *Alk5* expression was reduced in iKspCre-*Pkd1*^{lox,lox};*Alk5*^{lox,wt} mice and was reduced more in iKspCre-*Pkd1*^{lox,lox};*Alk5*^{lox,lox} mice, indicating homozygous inactivation of *Alk5* (Figure 1A). Next, we followed mice until the onset of end-stage PKD (defined as Blood Urea (BU) concentration > 20 mmol/l). Both iKspCre-*Pkd1*^{lox,lox} (from now on referred to as *Pkd1*-cKO) and iKspCre-*Pkd1*^{lox,lox};*Alk5*^{lox,lox} mice (from now on referred to as *Pkd1*;*Alk5*-cKO) had a similar progression rate of PKD and although there was a trend that the *Pkd1*;*Alk5*-cKO mice had slightly higher 2KW/BW%, this was not significant. Also renal histology was not different, indicating that renal epithelial *Alk5* expression does not play a significant role in the progression of PKD (Figure 1B-D).

We next measured the expression of SMAD2/3-dependent target genes by Reverse-transcriptase-ligation-dependent-probe-amplification (RT-MLPA), which were massively upregulated in cystic kidneys of *Pkd1*-cKO mice compared to control mice (Figure 1E). Surprisingly, however, *Pkd1*;*Alk5*-cKO mice showed a similar upregulation, being only slightly less compared to *Pkd1*-cKO mice (Figure 1E). These results indicate that the role of renal epithelial *Alk5* expression on cystogenesis or SMAD2/3-dependent signaling is limited, and suggests the involvement of other pathways to account for these changes during cyst formation.

Activin expression is increased in PKD and kidney cells respond to Activin.

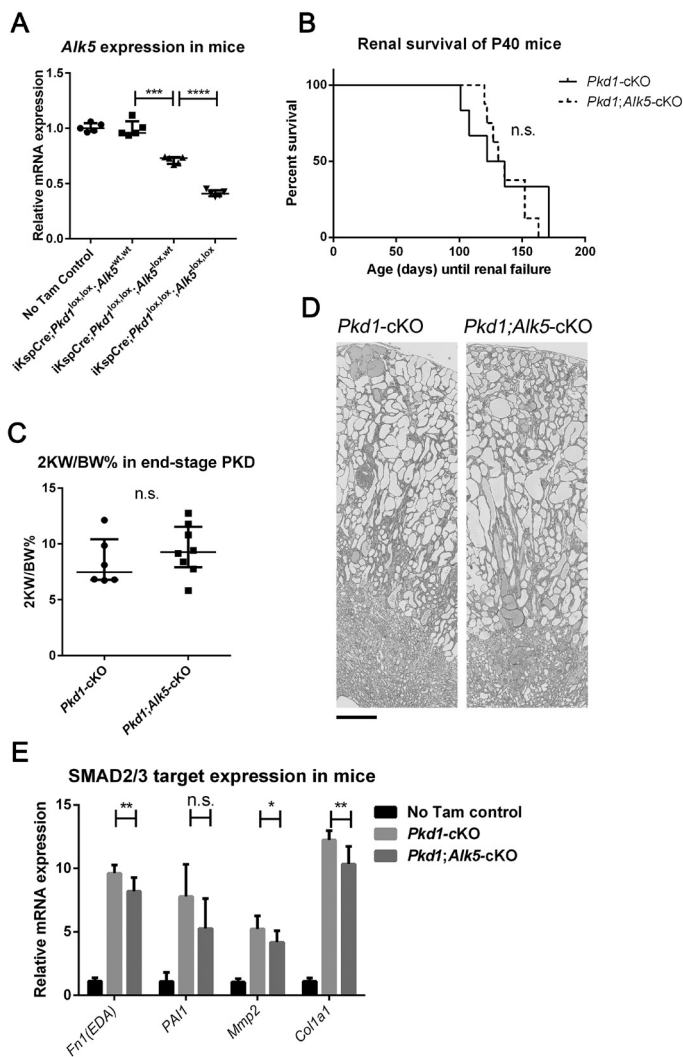
We previously found increased *Inhibin* β A expression in PKD samples, which is a member of the TGF β super family²⁸. Upon dimerization, Inhibin β chains can form different Activin subtypes, which can drive SMAD2/3 phosphorylation through the *ALK4* and *ACTRII* receptors²⁹. Here, we analyzed both *Inhibin* β A and *Inhibin* β B expression and found that the expression of both ligands were elevated at end-stage PKD (defined as BU > 20 mmol/L, which occurs approximately 16 weeks after Tamoxifen)³¹. but also at early-stage PKD (11 weeks after Tamoxifen administration, at which the mice have mild tubular dilations)³¹, suggesting a possible role for Activin signaling already at the early stages of cyst formation (Figure 2A and 2B).

Cultured primary cells isolated from total kidneys from tamoxifen treated *Pkd1*-cKO or *Pkd1*;*Alk5*-cKO mice, and cultured *Pkd1*^{+/+} or *Pkd1*^{-/-} immortalized proximal tubular epithelial cells were all capable to respond to ActivinA and TGF β by inducing SMAD2 phosphorylation

Figure 1. Conditional ablation of *Alk5* in the renal epithelium does not affect PKD.

(A) Renal expression of *Alk5* in mice of different genotypes (iKspCre;*Pkd1*^{lox,lox};*Alk5*^{wt,wt}, iKspCre;*Pkd1*^{lox,lox};*Alk5*^{lox,wt} and iKspCre;*Pkd1*^{lox,lox};*Alk5*^{lox,lox}) treated with Tamoxifen at P40, 41, 42 and euthanized 11 weeks after Tamoxifen. Adult iKspCre;*Pkd1*^{lox,lox};*Alk5*^{wt,wt} mice without Tamoxifen treatments served as a control (No Tam Control). Expression was measured by Reverse Transcriptase Multiplex Ligation-dependent Probe Amplification (RT-MLPA). *Hprt* and *ywhaz* served as housekeeping genes to correct for cDNA input ($n = 5$ mice per group). Error bars indicate interquartile range

(B) Renal survival analysis (a Blood Urea level (BU) of 20 mmol/L served as a cutoff point) of *Pkd1*-cKO ($n = 6$ mice) and *Pkd1*;*Alk5*-cKO ($n = 8$ mice) mice that were treated with Tamoxifen at P40, 41, 42. (C) The ratio of the kidney weight to body weight expressed as a percentage (2 KW/BW%) of the mice also depicted in Figure 1B. Error bars indicate interquartile range (D) Representative hematoxylin and eosin-stained kidney sections from end-stage polycystic kidneys of *Pkd1*-cKO and *Pkd1*;*Alk5*-cKO mice. Scale bar: 500 μ m. (E) Expression of the SMAD2/3 target genes the EDA splice form of fibronectin 1 (*Fn1*(EDA)), plasminogen activator inhibitor-1 (*PAI1*), matrix metalloproteinase-2 (*Mmp2*) and collagen, type I, $\alpha 1$ (*Col1a1*) from kidneys of P40 Tamoxifen treated *Pkd1*-cKO mice ($n = 5$) and *Pkd1*;*Alk5*-cKO mice ($n = 5$) that were euthanized at the onset of renal failure caused by severe PKD (defined as having BU levels above 20 mmol/L). Expression of the genes of *Pkd1*-cKO mice ($n = 5$) without Tamoxifen (No Tam Control) are also shown. Expression was measured by Reverse Transcriptase Multiplex Ligation-dependent Probe Amplification (RT-MLPA). *Hprt* and *ywhaz* served as housekeeping genes to correct for cDNA input. Error bars indicate standard deviations. (n.s. indicates Not Significant, * indicates $P < 0.05$, *** indicates $P < 0.001$, **** indicates $P < 0.0001$).



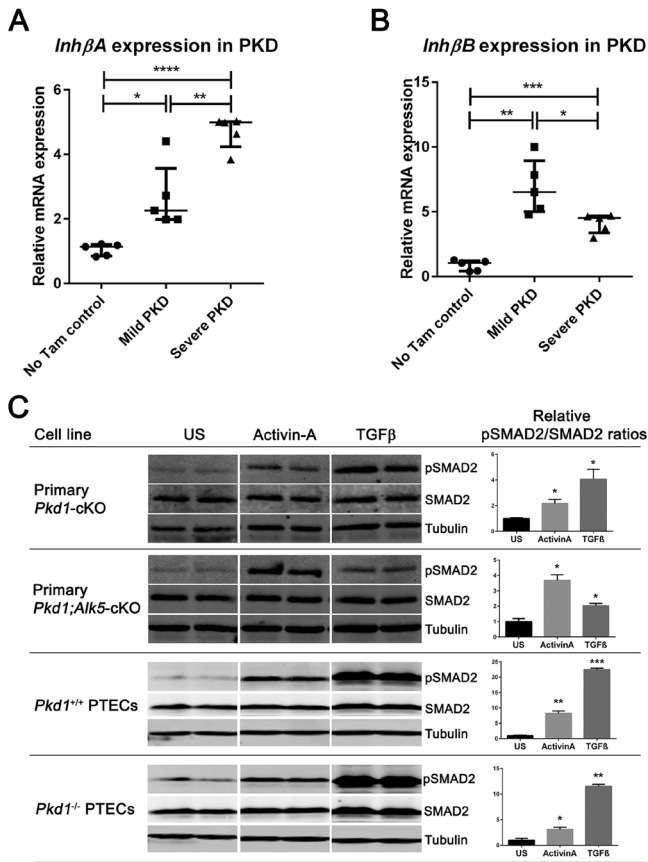


Figure 2. Activin expression in PKD kidneys and stimulation of cells.

(A-B) *InhbA* (A) and *InhbB* (B) mRNA expression in kidneys from P40 Tamoxifen treated *Pkd1*-cKO mice euthanized 11 weeks after Tamoxifen (Mild PKD) or at the onset of renal failure (defined as having BU levels above 20 mmol/L) (Severe PKD) ($n = 5$ mice per group). Expression of the genes of *Pkd1*-cKO mice without Tamoxifen (No Tam Control) served as a reference. The expression was measured by qPCR. *Hprt* served as a housekeeping gene to correct for cDNA input. Error bars indicate interquartile range. * indicates $P < 0.05$, ** indicates $P < 0.01$, *** indicates $P < 0.001$, **** indicates $P < 0.0001$. (C) Western blot and quantification of pSMAD2 and total SMAD2 on crude extracts from

primary cells from a kidney of one P40 Tamoxifen treated *Pkd1*-cKO (Primary *Pkd1*-cKO), and of one P40 Tamoxifen treated *Pkd1;Alk5*-cKO mouse (Primary *Pkd1;Alk5*-cKO). Also results of crude extracts of *Pkd1*^{+/+} (*Pkd1*^{+/+} PTECs) or *Pkd1*^{-/-} (*Pkd1*^{-/-} PTECs) mouse Proximal Tubular Epithelial Kidney cells (PTECs) are shown. All cell lines were either left unstimulated (US), or were stimulated with 5 ng/ml TGFβ1, or with 100 ng/ml Activin-A. Each stimulation experiment on the above mentioned cell lines was performed at least three times. A representative experiment with two replicates of the same cell line of each condition are shown in which tubulin served as a loading control. pSMAD2/SMAD2 ratios are shown and were normalized to the unstimulated cells that were set to 1. * indicates $P < 0.05$, ** indicates $P < 0.01$, *** indicates $P < 0.001$ compared with the unstimulated control.

(Figure 2C). The response pattern of the primary kidney cells from tamoxifen treated *Pkd1;Alk5*-cKO mice indicated reduced sensitivity to TGFβ, which is likely caused by the conditional ablation of *Alk5* in the majority of cells (Figure 1A and 2C). Although these *in vitro* experiments do not recapitulate the complex signaling in the context of a cystic kidney, these results indicate that renal epithelial cells can potentially be stimulated by Activins and TGFβ. To further assess the role of Activins in cystic kidneys we aimed to inhibit Activins in mouse models for PKD, using a soluble Activin ligand trap.

sActRIIB-Fc inhibits disease progression in two mouse models with rapid PKD progression.

To explore the role of Activin signaling in PKD and to determine whether Activins can be used as a therapeutic target for PKD, we used a soluble Activin ligand trap (*sActRIIB-Fc*). We first used the *Pkd1*-cKO model in which we inactivated *Pkd1* by tamoxifen administration at P10-12. *Pkd1*-inactivation before P14 results in rapid cyst formation as opposed to *Pkd1* inactivation after P14^{13,14}. As expected, at age P33, mice that received phosphate buffered saline (PBS) had increased 2-kidney to bodyweight ratios (2KW/BW%), cystic indices (CI) and increased Blood-Urea (BU) levels indicating deteriorating renal function (Figure 3A-C). By contrast, mice that also received biweekly intraperitoneal (IP) injections of 3 or 10 mg/kg *sActRIIB-Fc*, starting at P14 until the end of the experiment at age P33, showed improvement in all of these parameters and improvement of renal histology (Figure 3A-D and Supplemental Figure 1).

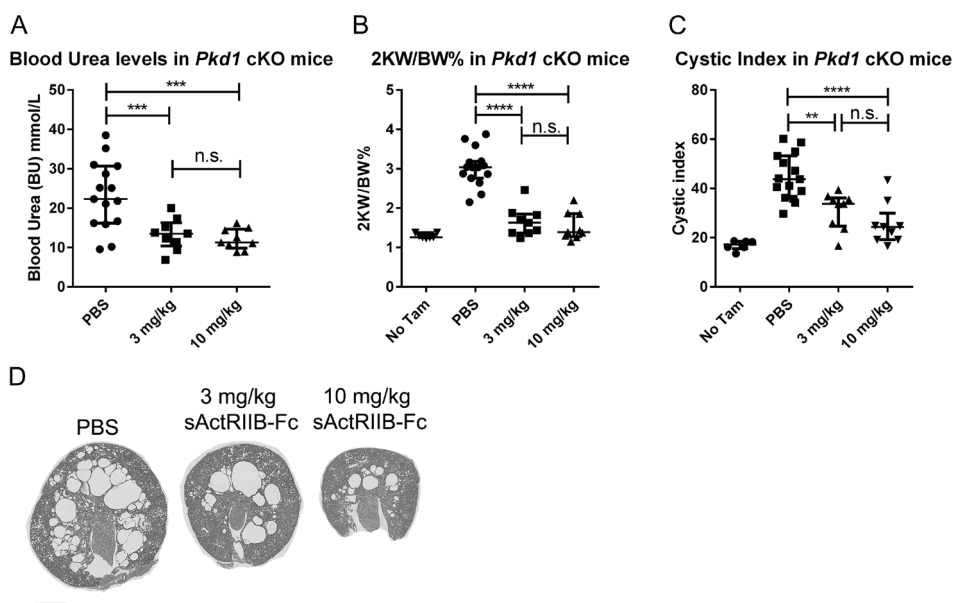


Figure 3. Antagonizing Activin signaling effectively inhibits cyst progression in conditional *Pkd1*-deletion mice.

(A-C) *Pkd1*-cKO mice ($n = 15$ mice; 8 males and 7 females) were treated with tamoxifen at P10,11,12 and euthanized at P33. Mice that were additionally treated with 3 ($n = 9$ mice; 4 males and 5 females) or 10 mg/kg ($n = 9$ mice; 4 males and 5 females) *sActRIIB-Fc* from P14-P33 had improved renal function (A), significantly lower kidney weights (B), and cystic indices (C). (D) Shown are representative images of the renal histology of the different treatment groups. The mice treated with 3 or 10 mg/kg *sActRIIB-Fc* had improved renal histology compared with PBS treated mice. Histology of all mice is shown in Supplemental Figure 1. Scale bar: 1 mm. (n.s. indicates Not Significant, ** indicates $P < 0.01$, *** indicates $P < 0.001$, **** indicates $P < 0.0001$, error bars indicate interquartile range).

To test if the cyst reducing properties of sActRIIB-Fc are not specific for just the conditional *Pkd1*-deletion model, we also used a different model for PKD. To this end, we tested the efficacy of sActRIIB-Fc also on hypomorphic *Pkd1*^{nl,nl} mice. These mice have in all of their cells only about 15-20% of normal *Pkd1* expression and have already small cysts at age P7 and by the age of P20 they have developed massive PKD^{10,32}. In addition, we bred these mice on a different genetic background (i.e. the *Pkd1*^{nl,nl} mice in this study were F1-hybrids having a fixed genetic background of exactly 50% C57BL6/J and 50% 129Ola/Hsd genetic background). We treated these mice with in total 4 IP injections of 0, 1 or 10 mg/kg sActRIIB-Fc between P10 and P21. Even this short treatment regimen showed significant improvements in renal function and size (Figure 4A-D and Supplemental Figure 2).

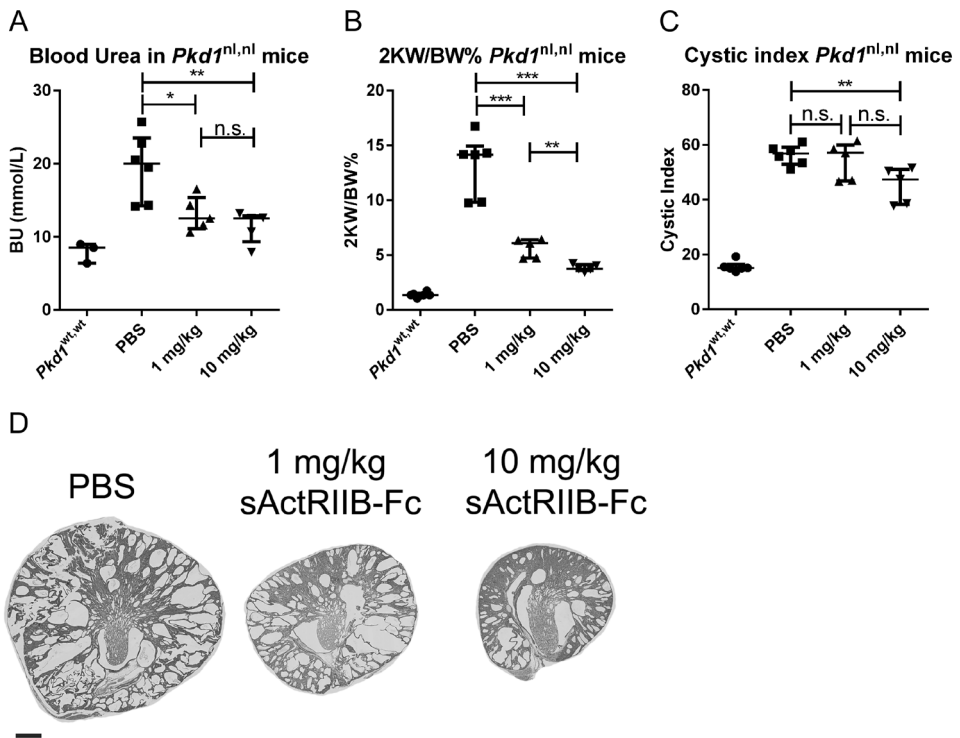


Figure 4. Antagonizing Activin signaling effectively inhibits cyst progression in hypomorphic *Pkd1* mice.

(A-C) Hypomorphic *Pkd1*^{nl,nl} mice bred on a mixed genetic background of C57BL6/J and 129Ola/Hsd were treated with in total 4 IP injections of 0 ($n = 6$ mice; 1 male and 5 females), 1 ($n = 5$ mice; 2 males and 3 females) or 10 ($n = 5$ mice; 2 males and 3 females) mg/kg sActRIIB-Fc between P10 and P21. Shown are BU levels (A), 2KW/BW% (B) and cystic indices (C). (D) Representative H&E stained kidney sections of the hypomorphic mice treated with the indicated dosages of sActRIIB-Fc. Histology of all mice is shown in Supplemental Figure 2. Scale bar: 1 mm. (n.s. indicates Not Significant, * indicates $P < 0.05$, ** indicates $P < 0.01$, *** indicates $P < 0.001$, error bars indicate interquartile range).

The improved renal health by sActRIIB-Fc treatment is associated with reduced fibrosis and SMAD2/3 dependent signaling.

The PKD phenotype is generally associated with increased proliferation and expression of SMAD2/3 target genes, which could be a reflection of increased fibrosis²⁰. We therefore measured the proliferation, apoptotic and fibrotic index of the P10-*Pkd1*-cKO mice. The proliferation indices were determined by taking the ratio of Ki67 positive and Ki67 negative nuclei of sections that were stained for this proliferation marker. The apoptotic index was measured in a similar fashion using sections stained for cleaved Caspase-3, which is a marker for apoptosis. The fibrotic index was measured by determining the amount of Collagen deposition in kidney sections using Sirius Red stainings. The number of apoptotic cells increased in mice with *Pkd1*-cKO compared to control mice without *Pkd1*-cKO, but the sActRIIB-Fc treatments did not significantly affect apoptosis and there were no statistically significant differences in proliferation between the tested groups (Figure 5A-B). However, the fibrotic index was clearly reduced in the 3 and 10 mg/kg sActRIIB-Fc treated mice, which correlated with reduced expression of *collagen, type I, $\alpha 1$ (Col1 $\alpha 1$)*, and *plasminogen activator inhibitor-1 (PAI1)*. However, compared to the PBS treated mice, the expression of the EDA splice form of *fibronectin 1 (Fn1(EDA))* was only significantly reduced in mice treated with 10 mg/kg sActRIIB-Fc (Figure 5C-D and Supplemental Figure 3). Since, pSMAD2 protein levels in kidney extracts of the P10-*Pkd1*-cKO mice, as assessed by western blotting, were below the detection limit, we were not able to connect the expression of these genes to the levels of pSMAD2/3 (data not shown). We therefore also immunoblotted kidney extracts of the *Pkd1*^{nl,nl} mice that were treated with PBS, 1 or 10 mg/kg sActRIIB-Fc. pSMAD2 was only detected in PBS treated *Pkd1*^{nl,nl} mice, and dropped below the detection limit in the sActRIIB-Fc treated mice (Figure 5E-F). Interestingly, also total SMAD2 levels were increased in *Pkd1*^{nl,nl} mice compared to WT-control mice, which were reduced in the sActRIIB-Fc treated mice (Figure 5E and 5G). Taken together, these results indicate that the reduced cystic load achieved by sActRIIB-Fc treatment, is associated with reduced SMAD2/3 dependent signaling and fibrosis.

sActRIIB-Fc treatment slows PKD in adult onset Pkd1-cKO mice.

To investigate if Activin inhibition could also slow disease progression in an adult onset model for PKD, we conducted a survival experiment. We first treated male *Pkd1*-cKO mice with Tamoxifen at P18, 19 and 20 to inactivate *Pkd1*. These mice have a young adult onset of PKD with cyst formation from all tubular segments (Supplemental Figure 4, and Leonhard W.N., Peters D.J.M.; manuscript in preparation). After randomization of the mice in the different groups, biweekly treatments with PBS (PBS control) or 3 mg/kg sActRIIB-Fc were started at P46 (long treatment). In addition, one group of mice that received PBS from P46, switched to 3 mg/kg sActRIIB-Fc treatment at P74 (late treatment). From approximately P78 the renal function of the mice was monitored weekly by measuring Blood Urea (BU) levels. BU of 20

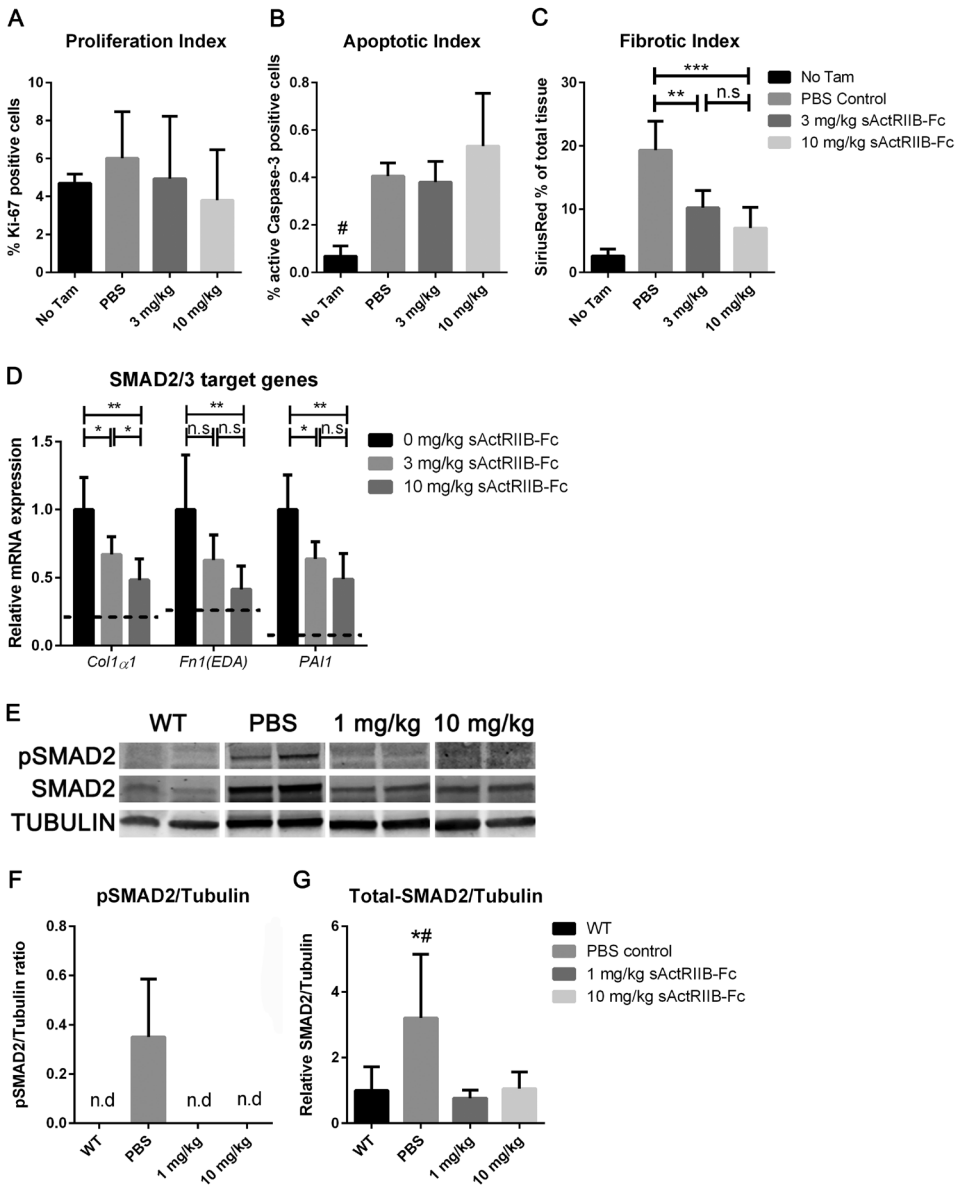


Figure 5. The improved renal phenotype by sActRIIB-Fc is associated with reduced SMAD2/3 signaling.

(A-B) The proliferation index and apoptotic index was measured in renal samples of the P10-*Pkd1*-cKO mice in the indicated groups. (C) Collagen deposition was measured by SiriusRed staining (example images are shown in Supplemental Figure 3) from renal sections of the P10-*Pkd1*-cKO mice in the indicated groups. (D) The expression of the EDA splice form of *fibronectin 1* (*Fn1(EDA)*), *plasminogen activator inhibitor-1* (*PAI1*), and *collagen, type I, α 1* (*Col1 α 1*) from kidneys of the P10-*Pkd1*-cKO mice that were treated with 0, 3 or 10 mg/kg sActRIIB-Fc was measured by qPCR. The dotted lines indicate the expression levels of genotype and age matched *Pkd1*-floxed mice without

mmol/L was used as a cutoff point to pinpoint the onset of renal failure. The median survival in days after the start of the long-treatment-regimen was 55 days in the PBS group and was significantly postponed to 97 days in the sActRIIB-Fc treated group (Figure 6). sActRIIB-Fc treatments starting at 74 days did not significantly slow PKD, suggesting that the effect of sActRIIB-Fc is more prominent during the milder stages of PKD (Figure 6). Collectively, the improvement in renal health in three distinct models for PKD by sActRIIB-Fc treatment, suggests that Activin inhibition is an attractive approach to inhibit ADPKD.

Additional effects of sActRIIB-Fc.

Several studies showed that sActRIIB-Fc treatment increases bodyweight, which is primarily caused by increased muscle size due to the ability of sActRIIB-Fc to antagonize Myostatin, which is a negative regulator for muscle growth. Since the 2KW/BW% is influenced by the bodyweight, we summarized the bodyweights, kidney weights, 2KW/BW% and cystic indices of all mice in Supplemental Figure 5. Whereas the bodyweights at the start of each experiment generally were comparable between the groups, at the end of the experiments the bodyweights of the sActRIIB-Fc treated mice tended to be slightly higher. This was more prominent in the long-term sActRIIB-Fc treated P18-*Pkd1*-cKO mice. Besides the effect on bodyweight, the data summary confirms that sActRIIB-Fc treatment reduced kidney weights and cystic indices, or delayed the onset of renal failure.

We measured the weight of the quadriceps's in the P10-*Pkd1*-cKO mice that were treated with 10 mg/kg sActRIIB-Fc and confirmed that muscle size was increased, which could explain the relative higher bodyweights of the sActRIIB-Fc treated mice in this study (Supplemental Figure 6A). Overall behavior and morphology was normal in sActRIIB-Fc treated mice, and there were no obvious changes in liver, spleen or pancreas tissues of the mice (data not shown). In addition, there was no sign of liver toxicity as the alanine aminotransferase (ALT) levels of the sActRIIB-Fc treated mice in the survival experiment were similar or slightly lower compared to PBS treated mice (Supplemental Figure 6).

◀ tamoxifen. *Hprt* served as a housekeeping gene to correct for cDNA input. (E-G) Renal extracts from *Pkd1*^{nl,nl} mice were immunoblotted and stained for phosphorylated SMAD2 (pSMAD2), total SMAD2 (SMAD2) or TUBULIN as a loading control. (E) a representative immunoblot of the indicated samples and protein expressions. (F-G) Quantification of pSMAD2/TUBULIN ratios (F) or SMAD2/TUBULIN ratios (G). pSMAD2 was only detected in *Pkd1*^{nl,nl} mice that were treated with PBS.

For all quantifications in this Figure: *n* = 5 mice for all groups. These mice were representative for the actual averages based on the 2KW/BW%. n.d. = not detected, n.s. = not significant, * indicates *P* < 0.05, ** indicates *P* < 0.01, *** indicates *P* < 0.001, # indicates: the 'No Tam' control group had significantly lower numbers of apoptotic cells compared to each of the other groups *P* < 0.05. *# indicates: PBS treatment compared to either 1 mg/kg or 10 mg/kg sActRIIB-Fc treated *Pkd1*^{nl,nl} mice, *P* < 0.05. Error bars indicate standard deviations).

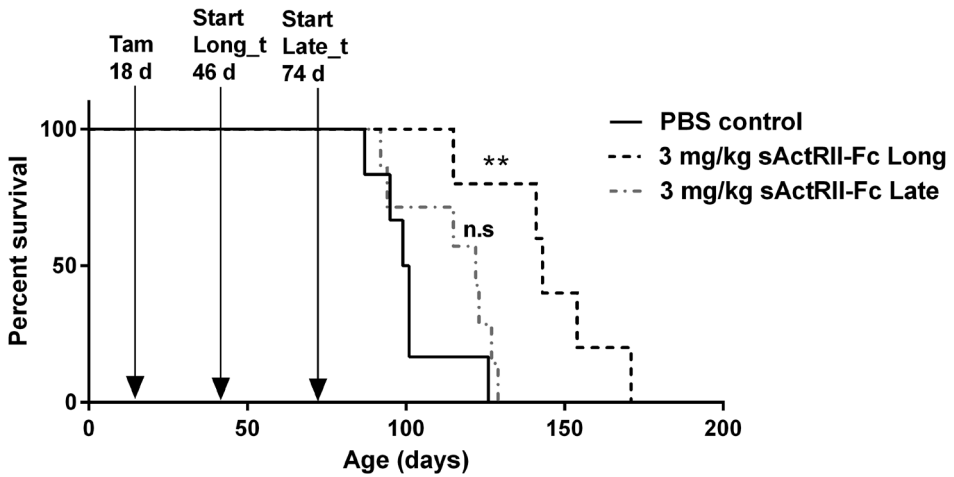


Figure 6. sActRIIB-Fc treatment slows PKD in an adult onset model for PKD.

Survival analyses of *Pkd1*-cKO mice treated with Tamoxifen at P18. PBS (PBS control) or sActRIIB-Fc (3 mg/kg sActRIIB long) treatment was started at 46 days of age. However, 7 mice switched from PBS treatment to sActRIIB-Fc treatment at 74 days of age (3 mg/kg sActRIIB Late). BU was measured weekly and the onset of renal failure was defined as having a BU > 20 mmol/L. From the start of the first treatment at age 46 days, the median survival of PBS treated mice (n = 6 mice) was 54 days (age 100 days), median survival of late treated mice (n = 7 mice) was 76 days (age 122 days) and median survival of long treated mice (n = 5 mice) was 97 days (age 143 days). ** indicates $P < 0.01$, n.s. indicates not significant.

DISCUSSION

The data presented in this study point to Activins as novel players in driving the progression of PKD. Treatment with sActRIIB-Fc, which is capable of sequestering Activins, inhibited cystogenesis in three distinct mouse models of PKD. At present there is not yet an approved, safe and effective therapy for the treatment of ADPKD, although a few completed and ongoing clinical trials with the primary focus of inhibiting cAMP have shown clinical benefit in ADPKD patients³³⁻³⁵. Many other PKD related signaling pathways are continued to be studied as potential targets for the treatment of ADPKD¹⁹.

In this study, we focused on TGF β and Activins, which are members of the TGF β superfamily that signal through their receptors and can drive SMAD2/3 phosphorylation. Increased expression of SMAD2/3 target genes and extracellular matrix remodeling enzymes, expansion of the interstitial space followed by fibrosis, and the accumulation of pSMAD2 in cystic epithelial cells, suggest their involvement in ADPKD^{20,25}. Since TGF β is involved in driving fibrosis in different chronic kidney diseases, its role likely has overlap with fibrosis in ADPKD²²⁻²⁵. The role of TGF β in driving cyst formation is less well studied, although in 3D-cyst cultures of ADPKD cells, TGF β inhibited cyst formation²⁶. To study the specific role of TGF β in renal epithelial cells in the context of a PKD phenotype, we ablated *TgfbRI* (*Alk5*) together with *Pkd1* using a previously developed renal epithelial specific and tamoxifen inducible Cre system^{13,27,36}. As expected, primary cells from *Pkd1*-cKO mice were capable to respond to TGF β , whereas this response was abrogated in primary cells from *Pkd1:Alk5*-cKO mice. By contrast, in the PKD context *in vivo*, additional ablation of *Alk5* only minimally affected the massive upregulation of SMAD2/3 target genes. We cannot exclude that other cell types may be involved in the increased expression of SMAD2/3 target genes in end-stage PKD. Another explanation could be that *Alk5* independent pathways contribute to these changes. Either way, our results indicate that renal epithelial expression of *Alk5* does not contribute significantly to cyst progression in adult *Pkd1*-cKO mice. These data and the observed increased *Inh β A* and *Inh β B* expression in PKD, pointed us to Activins, which, like the TGF β ligands, are members of the TGF β superfamily²⁹.

Activins are composed of two Inhibin β chains and can stimulate SMAD2/3 phosphorylation via the Activin type II receptors and ALK4²⁹. These ligands play key roles in cancer and in wound repair programs³⁷. Of interest, mutations in the von Hippel-Lindau tumor suppressor gene stimulates hypoxia-inducible factor (HIF)-dependent expression of Activin B, which promoted tumor growth³⁸. However, whether Activins stimulate or inhibit epithelial repair upon damage and how they are involved in fibrosis and cancer seems to differ among different tissues and also depends on the specific context of the tissue, the interplay between stromal and parenchymal cells, and on the expression of other members of the

TGF β superfamily³⁷. It is therefore difficult to predict the exact role of Activins in the context of PKD. Since cyst formation is suggested to be a state of chaotic repair³⁹, it is tempting to speculate that the increased Activin expression in PKD is in fact an underlying cause of this process. To test if blocking Activin signaling could be a therapeutic strategy to treat ADPKD, we treated three different PKD mouse models with sActRIIB-Fc, which can be used as a soluble Activin ligand-trap. In all of these models, sActRIIB-Fc treatment was associated with slower cyst progression compared to PBS treated littermates. Although in most analyses there was a trend towards a dose dependent response of the sActRIIB-Fc treatments, this did not reach statistical significance. The proliferation and apoptotic index varied between the animals and were not clearly different between PBS or sActRIIB-Fc treated P10-*Pkd1*-cKO littermates. Although these data suggest that sActRIIB-Fc treatment did not significantly affect these processes, we cannot exclude that sActRIIB-Fc affects proliferation and/or apoptosis during any other time-point throughout the course of the development of PKD. Whether this is the case, remains to be investigated. However, the slower onset of PKD by sActRIIB-Fc treatment, was associated with reduced SMAD2 expression, reduced SMAD2 phosphorylation, reduced SMAD2/3 target gene expression and reduced Collagen deposition, which is in line with the concept of the ability of sActRIIB-Fc to sequester Activin ligands, which are increased in PKD. However, sActRIIB-Fc is also known to sequester other ligands of the TGF β superfamily such as Myostatin, GDF11 and, with lower efficiencies, also a number of BMP's^{40,41}. In-house RNAseq data of mice with PKD, showed that Myostatin is not expressed in kidneys with or without PKD, and that GDF11 expression is low and unchanged throughout the course of PKD progression (Malas *et.al.* unpublished). BMP's primarily signal through SMAD1/5/8, which has been observed not to be significantly changed in two mouse models of PKD, suggesting that the cyst reducing properties of sActRIIB-Fc are not likely mediated by its limited ability to sequester BMP's²⁰. sActRIIB-Fc treatment indeed increased muscle mass and bodyweight, which is likely due to the ability of sActRIIB-Fc to sequester the negative regulator of muscle growth Myostatin. In addition, the ligand traps, including ActRIIA and ActRIIB variants, have been observed before to also prolong survival in cancer cachexia models, improve bone mineralization in models with established bone loss, suppress LPS-induced lung inflammation, improve obesity and obesity-linked metabolic disease, and to correct ineffective erythropoiesis in mice with beta-thalassemia by growth and differentiation factor (GDF11) inactivation⁴²⁻⁴⁶. We therefore cannot fully exclude that the renal cyst reducing property of sActRIIB-Fc is actually secondary to effects of sActRIIB-Fc on other organs such as the observed skeletal muscle hypertrophy. However, given the increase in the expression of Activins within the cystic kidney, the reduction of SMAD2/3 dependent signaling and collagen deposition upon sActRIIB-Fc treatment, our data point to a scenario in which the renal cyst reducing property of sActRIIB-Fc is caused by its ability to trap Activin ligands within the (pre)-cystic kidney. How Activins and their downstream signaling cascades are interconnected with other cyst inducing pathways, and how the

combined processes induce the development of cysts is not yet clearly understood and remains to be elucidated.

Currently, several soluble-receptor-ligand-traps are being tested in clinical trials for various purposes^{47,48}. One phase II trial to improve muscle function in Duchenne Muscular Dystrophy patients using a sActRIIB-Fc variant had to be terminated because of side effects, which included bleedings of the nose and gum (NCT01099761). However, another 4-month phase I trial assessing the safety of a sActRIIA variant in healthy postmenopausal women up to a dosage of 1 mg/kg, reported that the treatments were safe and well tolerated⁴⁸. A number of phase II trials are currently being undertaken to further assess the therapeutic potential of the sActRIIA variant, primarily in diseases involving anemia. These studies will shed more light on the tolerability of treatments with such ligand traps.

Since ADPKD patients likely require years of treatment, the treatment should have an excellent safety profile. The continuous improvements in the strategies to slow ADPKD are highly encouraging and will likely lead to a safe and effective therapy. Although it remains to be clarified if targeting Activins can be applied safely in humans for longer periods, the effective inhibition of PKD in three mouse models by sActRIIB-Fc points to Activins as potentially important targets for ADPKD treatment.

Acknowledgements

This research was funded by the Dutch Kidney Foundation grant NSN 14OI12 and IP11.34 (WNL, JP) and partially supported by the Netherlands Organisation for Scientific Research (Earth and Life Sciences-820.02.016) (SJK), NSN consortium project CP10.12 (Developing Interventions to hold progression of Polycystic Kidney Disease) (KV) and the Dutch Technology Foundation (Stichting Technische Wetenschappen) Project 11823 (WNL, FB) which is part of The Netherlands Organization for Scientific Research. We are grateful to Dr. Stefan Karsson for providing us with *Alk5* floxed mice.

Disclosures

None.

REFERENCES

1. Peters D.J.M. & Sandkuijl L.A. Genetic heterogeneity of polycystic kidney disease in Europe. *Contributions to Nephrology*. **97**, 128-139 (1992). *Polycystic Kidney Disease. 2nd International Workshop of the European Concerted Action Towards Prevention of Renal Failure Caused by Polycystic Kidney Disease, Parma, September 1991*. (eds: Breuning M.H., Devoto M., Romeo G.; Karger, Basel, 1992).
2. The European Polycystic Kidney Disease Consortium *et al.* The polycystic kidney disease 1 gene encodes a 14 kb transcript and lies within a duplicated region on chromosome 16. *Cell* **77**, 881-894 (1994).
3. Mochizuki T. *et al.* PKD2, a gene for polycystic kidney disease that encodes an integral membrane protein. *Science* **272**, 1339-1342 (1996).
4. Gabow P.A. Autosomal dominant polycystic kidney disease: More than a renal disease. *Am J Kidney Dis* **16**, 403-413 (1990).
5. Grantham J.J., Geiser J.L., & Evan A.P. Cyst formation and growth in autosomal dominant polycystic kidney disease. *Kidney Int*. **31**, 1145-1152 (1987).
6. Grantham J.J. *et al.* Detected renal cysts are tips of the iceberg in adults with ADPKD. *Clin. J. Am. Soc. Nephrol.* **7**, 1087-1093 (2012).
7. Qian F.J., Watnick T.J., Onuchic L.F., & Germino G.G. The molecular basis of focal cyst formation in human autosomal dominant polycystic kidney disease. *Cell* **87**, 979-987 (1996).
8. Wu G. *et al.* Somatic inactivation of Pkd2 results in polycystic kidney disease. *Cell* **93**, 177-188 (1998).
9. Pritchard L. *et al.* A human PKD1 transgene generates functional polycystin-1 in mice and is associated with a cystic phenotype. *Hum. Mol. Genet.* **9**, 2617-2627 (2000).
10. Lantinga-van Leeuwen I.S. *et al.* Lowering of Pkd1 expression is sufficient to cause polycystic kidney disease. *Hum. Mol. Genet.* **13**, 3069-3077 (2004).
11. Jiang S.T. *et al.* Defining a link with autosomal-dominant polycystic kidney disease in mice with congenitally low expression of Pkd1. *Am. J. Pathol.* **168**, 205-220 (2006).
12. Thivierge C. *et al.* Overexpression of PKD1 causes polycystic kidney disease. *Mol. Cell Biol.* **26**, 1538-1548 (2006).
13. Lantinga-van Leeuwen I.S. *et al.* Kidney-specific inactivation of the Pkd1 gene induces rapid cyst formation in developing kidneys and a slow onset of disease in adult mice. *Hum. Mol. Genet.* **16**, 3188-3196 (2007).
14. Piontek K., Menezes L.F., Garcia-Gonzalez M.A., Huso D.L., & Germino G.G. A critical developmental switch defines the kinetics of kidney cyst formation after loss of Pkd1. *Nat. Med.* **13**, 1490-1495 (2007).
15. Patel V. *et al.* Acute kidney injury and aberrant planar cell polarity induce cyst formation in mice lacking renal cilia. *Hum. Mol. Genet.* **17**, 1578-1590 (2008).
16. Happe H. *et al.* Toxic tubular injury in kidneys from Pkd1-deletion mice accelerates cystogenesis accompanied by dysregulated planar cell polarity and canonical Wnt signaling pathways. *Hum. Mol. Genet.* **18**, 2532-2542 (2009).
17. Takakura A. *et al.* Renal injury is a third hit promoting rapid development of adult polycystic kidney disease. *Hum. Mol. Genet.* **18**, 2523-2531 (2009).
18. Leonhard W.N. *et al.* Scattered Deletion of PKD1 in Kidneys Causes a Cystic Snowball Effect and Recapitulates Polycystic Kidney Disease. *J. Am. Soc. Nephrol.* **26**, 1322-1333 (2015).
19. Harris P.C. & Torres V.E. Genetic mechanisms and signaling pathways in autosomal dominant polycystic kidney disease. *J. Clin. Invest* **124**, 2315-2324 (2014).
20. Hassane S. *et al.* Elevated TGFbeta-Smad signalling in experimental Pkd1 models and human patients with polycystic kidney disease. *J. Pathol.* **222**, 21-31 (2010).
21. Ten Dijke P. & Arthur H.M. Extracellular control of TGFbeta signalling in vascular development and disease. *Nat. Rev. Mol. Cell Biol.* **8**, 857-869 (2007).
22. Yamamoto T., Noble N.A., Miller D.E., & Border W.A. Sustained expression of TGF-beta 1 underlies development of progressive kidney fibrosis. *Kidney Int.* **45**, 916-927 (1994).

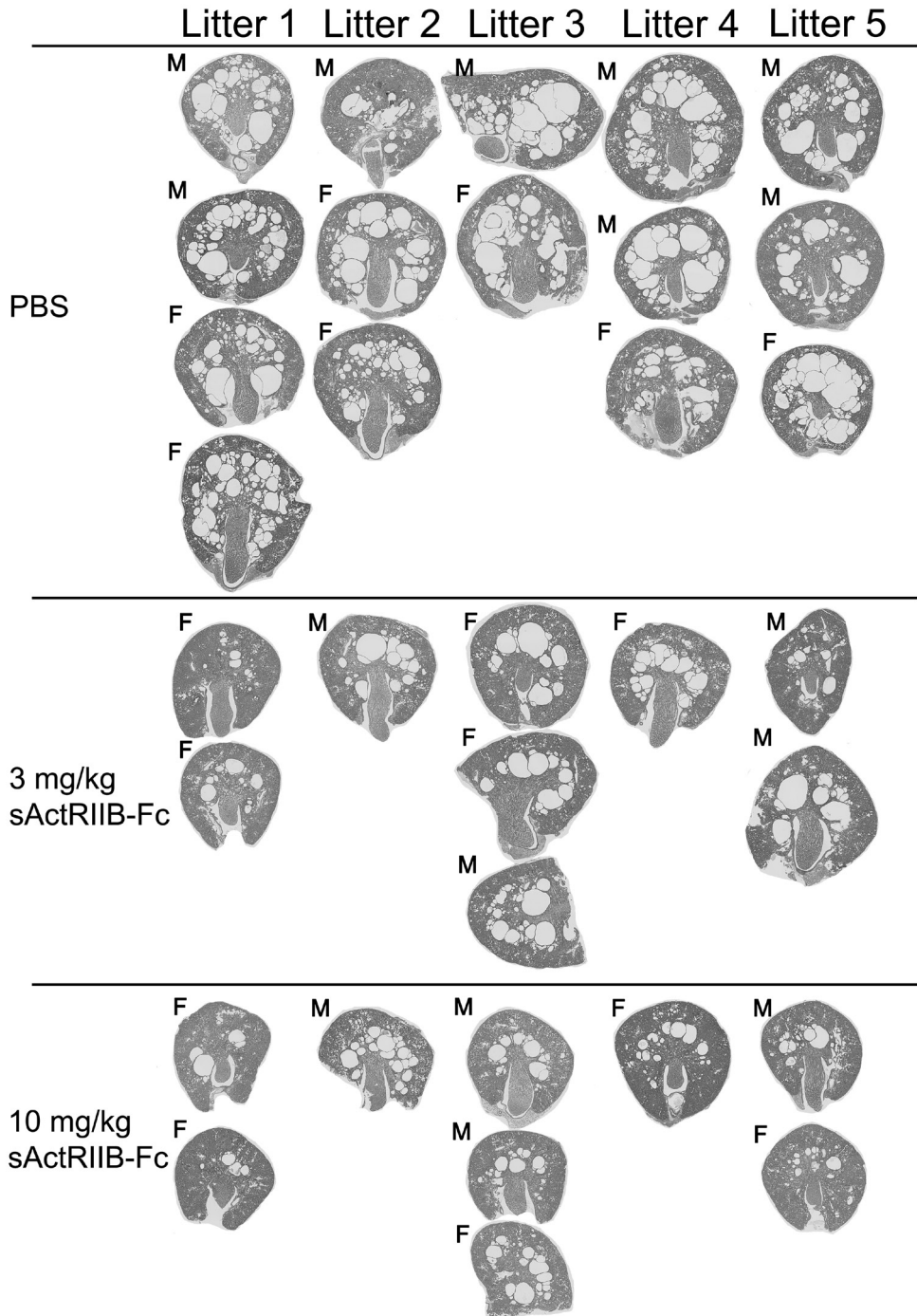
23. Ledbetter S., Kurtzberg L., Doyle S., & Pratt B.M. Renal fibrosis in mice treated with human recombinant transforming growth factor-beta2. *Kidney Int.* **58**, 2367-2376 (2000).
24. Moon J.A., Kim H.T., Cho I.S., Sheen Y.Y., & Kim D.K. IN-1130, a novel transforming growth factor-beta type I receptor kinase (ALK5) inhibitor, suppresses renal fibrosis in obstructive nephropathy. *Kidney Int.* **70**, 1234-1243 (2006).
25. Norman J. Fibrosis and progression of autosomal dominant polycystic kidney disease (ADPKD). *Biochim. Biophys. Acta* **1812**, 1327-1336 (2011).
26. Elberg D., Jayaraman S., Turman M.A., & Elberg G. Transforming growth factor-beta inhibits cystogenesis in human autosomal dominant polycystic kidney epithelial cells. *Exp. Cell Res.* **318**, 1508-1516 (2012).
27. Larsson J. *et al.* Abnormal angiogenesis but intact hematopoietic potential in TGF-beta type I receptor-deficient mice. *EMBO J.* **20**, 1663-1673 (2001).
28. Happe H. *et al.* Altered Hippo signalling in polycystic kidney disease. *J. Pathol.* **224**, 133-142 (2011).
29. Moustakas A. & Heldin C.H. The regulation of TGFbeta signal transduction. *Development* **136**, 3699-3714 (2009).
30. Hoogaars W.M. *et al.* Combined effect of AAV-U7-induced dystrophin exon skipping and soluble activin Type IIb receptor in mdx mice. *Hum. Gene Ther.* **23**, 1269-1279 (2012).
31. Leonhard W.N. *et al.* Curcumin inhibits cystogenesis by simultaneous interference of multiple signaling pathways: In vivo evidence from a Pkd1-deletion model. *Am. J. Physiol Renal Physiol* **300**, F1193-F1202 (2011).
32. Happe H. *et al.* Cyst expansion and regression in a mouse model of polycystic kidney disease. *Kidney Int.* **83**, 1099-1108 (2013).
33. Torres V.E. *et al.* Tolvaptan in patients with autosomal dominant polycystic kidney disease. *N. Engl. J. Med.* **367**, 2407-2418 (2012).
34. Caroli A. *et al.* Effect of longacting somatostatin analogue on kidney and cyst growth in autosomal dominant polycystic kidney disease (ALADIN): a randomised, placebo-controlled, multicentre trial. *Lancet* **382**, 1485-1495 (2013).
35. Meijer E. *et al.* Rationale and design of the DIPAK 1 study: a randomized controlled clinical trial assessing the efficacy of lanreotide to Halt disease progression in autosomal dominant polycystic kidney disease. *Am. J. Kidney Dis.* **63**, 446-455 (2014).
36. Lantinga-van Leeuwen I.S. *et al.* Transgenic mice expressing tamoxifen-inducible Cre for somatic gene modification in renal epithelial cells. *Genesis.* **44**, 225-232 (2006).
37. Antsiferova M. & Werner S. The bright and the dark sides of activin in wound healing and cancer. *J. Cell Sci.* **125**, 3929-3937 (2012).
38. Wacker I. *et al.* Key role for activin B in cellular transformation after loss of the von Hippel-Lindau tumor suppressor. *Mol. Cell Biol.* **29**, 1707-1718 (2009).
39. Weimbs T. Regulation of mTOR by polycystin-1: is polycystic kidney disease a case of futile repair? *Cell Cycle* **5**, 2425-2429 (2006).
40. Lee S.J. *et al.* Regulation of muscle growth by multiple ligands signaling through activin type II receptors. *Proc. Natl. Acad. Sci. U. S. A* **102**, 18117-18122 (2005).
41. Sako D. *et al.* Characterization of the ligand binding functionality of the extracellular domain of activin receptor type IIb. *J. Biol. Chem.* **285**, 21037-21048 (2010).
42. Zhou X. *et al.* Reversal of cancer cachexia and muscle wasting by ActRIIB antagonism leads to prolonged survival. *Cell* **142**, 531-543 (2010).
43. Pearsall R.S. *et al.* A soluble activin type IIA receptor induces bone formation and improves skeletal integrity. *Proc. Natl. Acad. Sci. U. S. A* **105**, 7082-7087 (2008).
44. Apostolou E. *et al.* Activin-A overexpression in the murine lung causes pathology that simulates acute respiratory distress syndrome. *Am. J. Respir. Crit Care Med.* **185**, 382-391 (2012).
45. Koncarevic A. *et al.* A novel therapeutic approach to treating obesity through modulation of TGFbeta

- signaling. *Endocrinology* **153**, 3133-3146 (2012).
46. Dussiot M. *et al.* An activin receptor IIA ligand trap corrects ineffective erythropoiesis in beta-thalassemia. *Nat. Med.* **20**, 398-407 (2014).
 47. Attie K.M. *et al.* A single ascending-dose study of muscle regulator ACE-031 in healthy volunteers. *Muscle Nerve* **47**, 416-423 (2013).
 48. Sherman M.L. *et al.* Multiple-dose, safety, pharmacokinetic, and pharmacodynamic study of sotatercept (ActRIIA-IgG1), a novel erythropoietic agent, in healthy postmenopausal women. *J. Clin. Pharmacol.* **53**, 1121-1130 (2013).
 49. Hulmi J.J. *et al.* Muscle protein synthesis, mTORC1/MAPK/Hippo signaling, and capillary density are altered by blocking of myostatin and activins. *Am. J. Physiol Endocrinol. Metab* **304**, E41-E50 (2013).
 50. Ruijter J.M. *et al.* Amplification efficiency: linking baseline and bias in the analysis of quantitative PCR data. *Nucleic Acids Res.* **37**, e45 (2009).
 51. Persson U. *et al.* The L45 loop in type I receptors for TGF-beta family members is a critical determinant in specifying Smad isoform activation. *FEBS Lett.* **434**, 83-87 (1998).

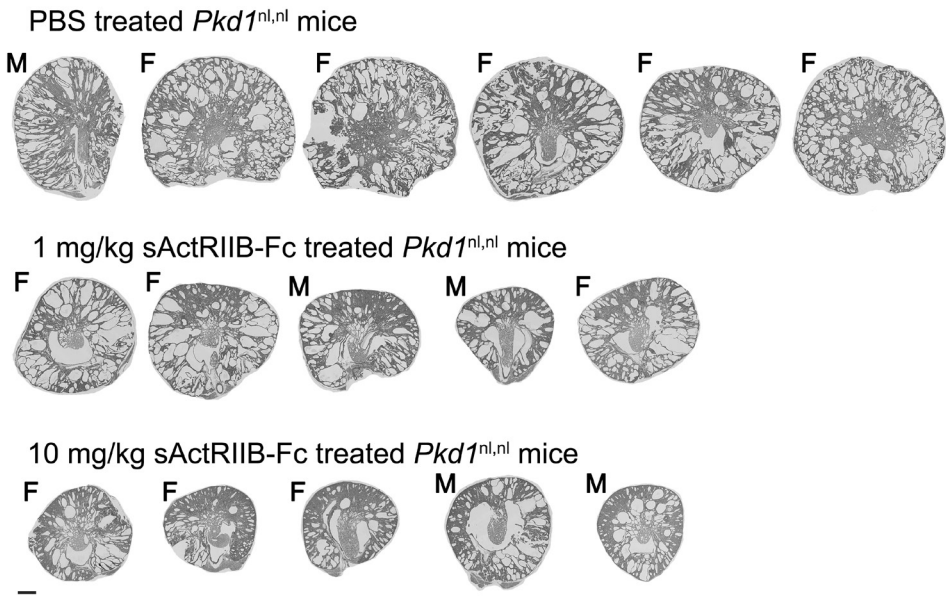
Supplemental Figure 1. Effect of sActRIIB-Fc on renal histology in Pkd1-cKO mice. 

Each litter was subdivided in a PBS, 3 mg/kg, or 10 mg/kg sActRIIB-Fc treatment group. Histology of all mice are shown. M; indicates male, F; indicates female. The mice on sActRIIB-Fc treatment had improved renal histology compared to the PBS treated mice.

SUPPLEMENTAL FIGURES

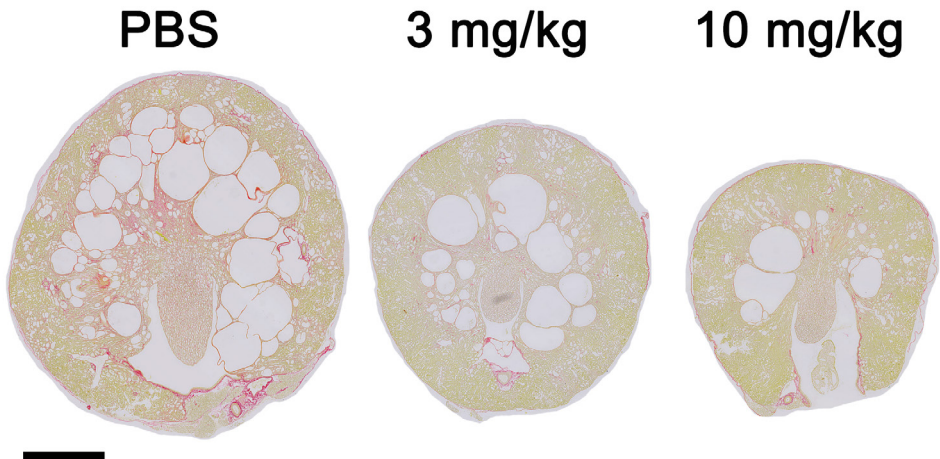


5

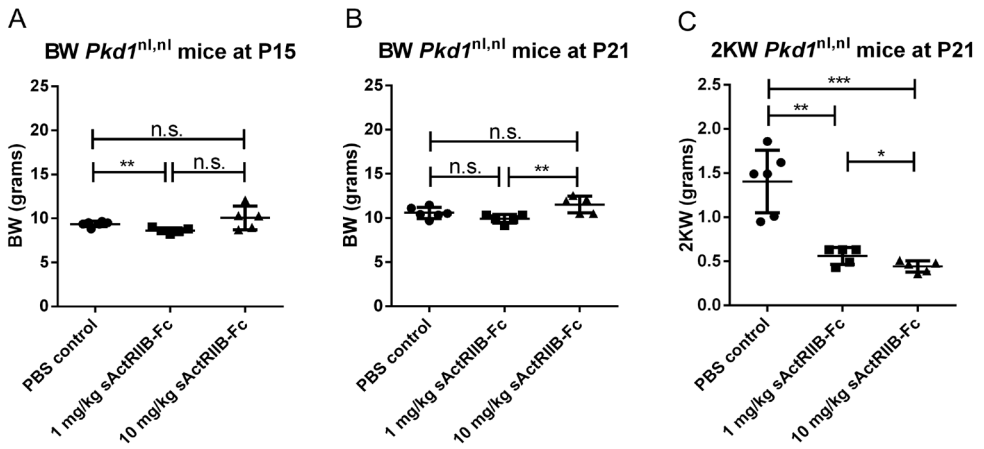


Supplemental Figure 2. Effect of sActRIIB-Fc on renal histology in *Pkd1^{nl,nl}* mice.

The mice were treated 4 times between P10-P21 with either PBS alone, 1 mg/kg, or 10 mg/kg sActRIIB-Fc. Renal histology of all mice are shown. M; indicates male, F; indicates female. The kidneys from mice on sActRIIB-Fc were smaller and generally appeared less cystic compared to the kidneys of the PBS treated mice. Scale bar: 1 mm

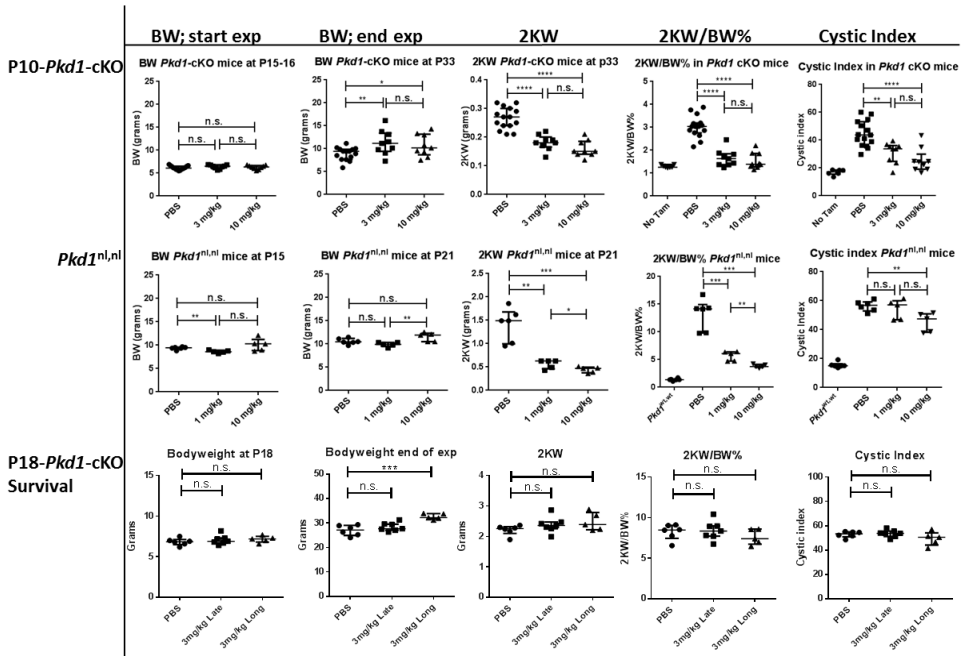


Supplemental Figure 3. Example images of SiriusRed stainings of renal sections of P10-*Pkd1*-cKO mice that were either treated with PBS, 3 mg/kg or 10 mg/kg sActRIIB-Fc. Quantification is shown in Figure 5C.



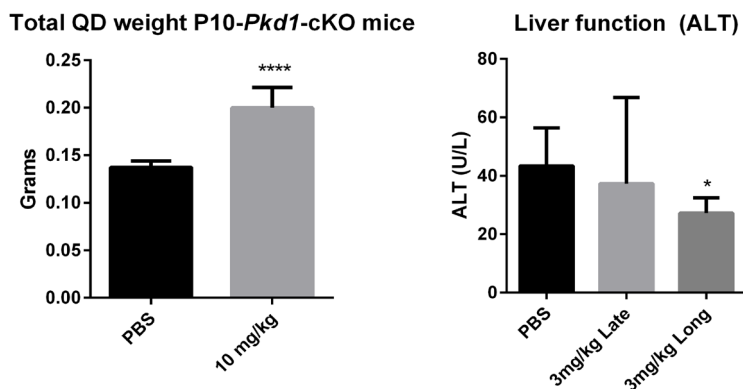
Supplemental Figure 4. Characteristics of the P18-*Pkd1*-cKO mouse model.

Pkd1-cKO mice were treated with 150 mg/kg Tamoxifen or left untreated. At 4 weeks after Tamoxifen ($n = 9$ mice), the 2KW/BW% had increased slightly compared to control mice without Tamoxifen ($n = 12$ mice). The mice were then followed until the onset of renal failure (indicated as having a BU > 20 mmol/L; $n = 6$ mice), which occurred approximately at 100 days of age (see also Figure 6), with 2KW/BW% of approximately 8%. Segmental marker staining using anti-Megalin (proximal tubular marker), anti-Tammhorskall protein (distal tubular marker), or Anti-Aqp2 antibodies (Collecting duct marker), revealed cyst formation from all tubular segments. Differences in 2KW/BW% between all groups: *** $P < 0.001$



Supplemental Figure 5. Summary of bodyweight (BW) and total kidney weights (2KW).

Summary of bodyweight (BW) at the beginning and at the end of the experiment, of the total kidney weights (2KW) and of the 2KW/BW%, and of the cystic indices of all mice in this study is shown. Of note, the sActRIIB-Fc treated mice that were euthanized at fixed time points (the P10-*Pkd1*-cKO and the *Pkd1*^{nl,nl} mice) had lower kidney weights and lower cystic indices compared to their PBS treated littermates. The kidney weights and cystic indices were not different between the groups of the P18-*Pkd1*-cKO mice but the progression was slower in the sActRIIB-Fc treated mice compared to their PBS treated littermates (see Figure 6). * indicates $P < 0.05$, ** indicates $P < 0.01$, *** indicates $P < 0.001$, **** indicates $P < 0.0001$. n.s. indicates Not significant

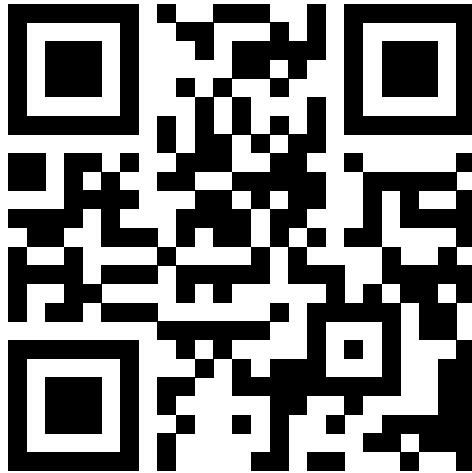


Supplemental Figure 6. Additional effects of sActRIIB-Fc.

The weight of the quadriceps's (QD) of sActRIIB-Fc treated P10-*Pkd1*-cKO mice (10 mg/kg) is higher than the QD weight of their PBS treated littermates. Alanine aminotransferase (ALT) blood levels were measured in the P18-*Pkd1*-cKO mice at the end of the experiment. Liver function was normal in all tested groups. * indicates $P < 0.05$, **** indicates $P < 0.0001$.

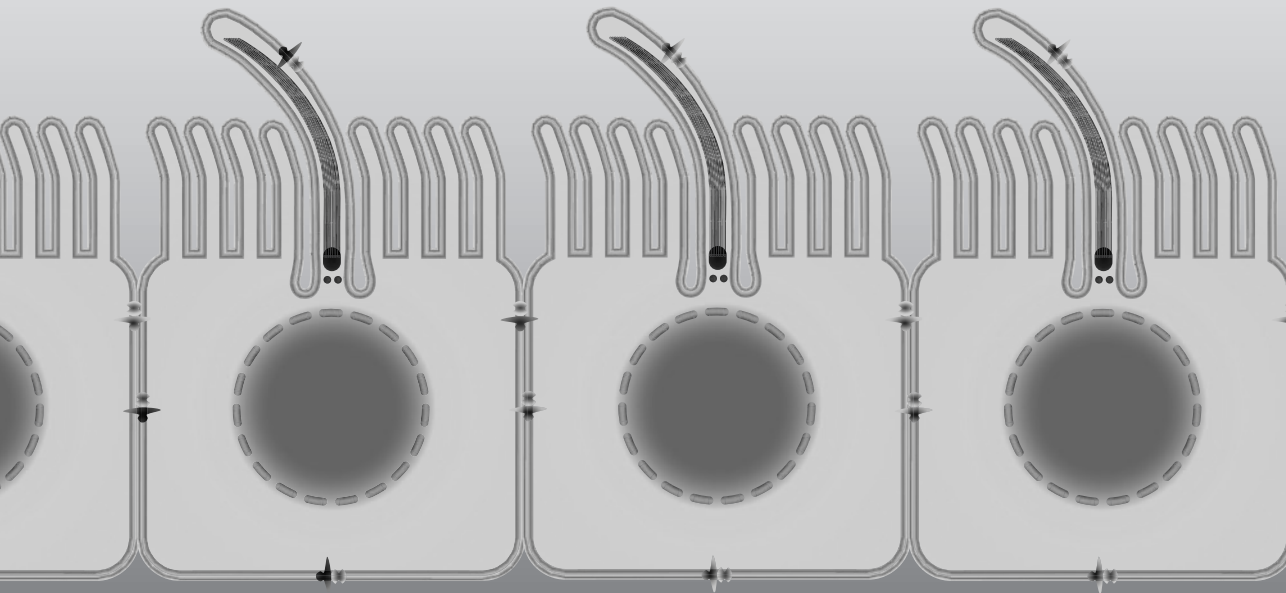
SUPPLEMENTARY MATERIALS CAN BE DOWNLOADED FROM

<https://goo.gl/693ao1>



CHAPTER 6

Summarizing discussion



Shear stress regulated signaling is essential during embryonic development, tissue homeostasis and cellular function. Defects in fluid shear sensing and mechanotransduction can cause or modulate a broad range of diseases including ciliopathies and ADPKD¹⁻⁷. In the last two decades, shear stress was more extensively investigated in renal epithelial cells to evaluate the role of mechano-sensing in cellular function and disease phenotypes⁸⁻¹⁰. However, cellular processes and signaling pathways that are altered by shear stress in renal epithelial cells are still not completely understood.

In this thesis, a comprehensive evaluation of shear stress regulated signaling in proximal tubular epithelial cells is presented, followed by a comparison of signaling pathways altered in ADPKD. Fluid flow within the lumen of nephrons exposes renal epithelial cells to mechanical forces like shear stress. Renal epithelial cells experience a relatively steady flow velocity and shear stress in a physiological range between 0.05 - 1 dyn/cm², where proximal tubular epithelial cells (PTECs) experience the highest range of shear stress¹⁰⁻¹⁴. However, variations in hydrodynamic forces and shear stress are common in kidney diseases, including ADPKD, due to hyperfiltration, tubular dilation and obstruction¹⁵. In this thesis, we applied a shear stress ranging from 0.25 to 2 dyn/cm², to mimic physiological and more pathological (hyperfiltration) levels of shear stress.

In **chapter 2** we presented fluid shear induced TGF- β /ALK5 signaling in both wild-type and *Pkd1*^{-/-} PTECs. This was evidenced by phosphorylation and nuclear accumulation of p-SMAD2/3, as well as altered expression of downstream target genes and EMT markers. ALK4/5/7 inhibitors blocked SMAD2/3 mediated signaling, indicating that autocrine signaling is involved, which was reported for endothelial cells as well¹⁶. This was further supported by shear induced mRNA expression of *Tgfb1* and *Tgfb3*. In addition, TGF- β neutralizing antibodies inhibited the flow response, while an activin ligand trap (sActRIIB-Fc) was ineffective, indicating that the flow response was TGF- β /ALK5 dependent. However, it still remains unclear how fluid shear activates TGF- β ligands, but a previous study suggests that TGF- β can be released from its latency-associated peptide (LAP) by shear stress, probably by forces exerted on $\alpha_v\beta_6$ -integrins via the actin cytoskeleton^{17,18}. In addition, a recent publication reported increased apical endocytosis upon shear stress exposure in PTECs¹⁹. Endocytosis may be important for the shear response in PTECs, since TGF- β /ALK5 signaling is mediated via clathrin dependent endocytosis^{20,21}.

In contrast to the ALK4/5/7 inhibitor, the MEK-inhibitor further enhanced shear induced expression of several SMAD2/3 target genes. Several studies report that TGF- β ligands can activate canonical (SMAD2/3) and non-canonical (MAPK/ERK) TGF- β pathways and the downstream responses can be modulated at several levels^{22,23}. Activated ERK proteins can both enhance and repress SMAD2/3 dependent gene transcription, depending on timing

and amount of ERK activation^{24,25}. Integration of TGF- β and MAPK/ERK signaling cascades is complex, biological context dependent and therefore difficult to predict.

The flow response appeared to be slightly but significantly stronger in *Pkd1*^{-/-} cells, suggesting that *Pkd1* restrains shear induced TGF- β /ALK5 signaling. Additionally, when comparing physiological (0.25-1 dyn/cm²) with pathological (2 dyn/cm²) levels of shear, we showed that flow induced target gene expression in PTECs was increased by the amount of shear stress. These data suggest enhanced TGF- β /ALK5 signaling upon *Pkd1* gene disruption and hyperfiltration, which might contribute to epithelial cell plasticity, fibrosis and kidney diseases progressions, where hyperfiltration is a common feature⁴⁵. In contrast, cilia ablation did not inhibit flow mediated SMAD2/3 signaling in *Pkd1*^{wt} cells. Even more, expression of early responsive SMAD2/3 target genes was enhanced upon deciliation, suggesting that to a certain extent primary cilia suppress TGF- β /ALK5 signaling. Additionally, our data indicate that fluid shear stress in PTECs is also regulated by other mechano-sensors, located at different locations of the cell membrane, which needs additional investigation in the future.

In **chapter 3** we further evaluated the cellular response of PTECs upon shear stress exposure, using RNA sequencing. In agreement with the previous chapter we showed that expression of numerous components of TGF- β and MAPK signaling pathways were up-regulated by shear stress. In addition, functional enrichment-analysis revealed shear induced Wnt and p53 signaling, as well as several other cytokine signaling pathways, including PDGF, FGF, HB-EGF and CXCL12. It needs more extensive investigation whether these increased cytokine signaling pathways are caused by autocrine or paracrine loops, as reported for TGF- β in this thesis. Nevertheless, increased expression of cytokines suggests activation of inflammatory cells upon shear *in vivo*. Inflammation is a common phenomenon during progression of kidney diseases, where shear stress is fluctuating due to changes in glomerular filtration rate, tubular hyperfiltration and obstruction²⁶. We further concluded that TGF- β and MAPK/ERK are master regulators of shear-induced gene expression, because inhibitors of these pathways modulate a wide range of mechanosensitive genes. This can be caused by several interactions between TGF- β and MAPK signaling^{23-25,27}. However, the main down-regulated pathway, *i.e.* JAK/STAT, is independent of TGF- β and MAPK/ERK.

What is clear from chapter 3 is that the cellular response to shear is modified at several levels. This is indicated by altered expression of genes involved in cell-matrix, cytoskeleton and glycocalyx remodeling, but also glycolysis and cholesterol metabolism are altered. Increased expression of cell-cell/cell-matrix interaction genes suggests reinforcement of epithelial cell morphology^{11,28,29}. However, high pathological shear stress of 5 dyn/cm² can result in loss of epithelial cell morphology³⁰, indicating that physiological relevant levels of shear are required to maintain epithelial integrity. Flow down-regulation of genes involved

in various metabolic pathways is mediated via AMPK, which was previously shown for endothelial cells³¹⁻³⁵. AMPK is an important kinase in energy metabolism and plays a central role in fluid flow induced down-regulation of mTORC1 activity in renal epithelial cells, which is dependent on bending of the primary cilium^{36,37}.

Our results revealed shear induced expression of genes involved in glycocalyx remodeling. This can be important for mechanotransduction of shear stress by amplifying the drag force exerted on renal epithelial cells. However, in this thesis we did not investigate if the glycocalyx itself is involved in mechano-sensing in PTECs. Nonetheless, we investigated the role of cilia in the shear stress response. Cilia ablation abolished shear induced expression of a subset of genes, but genes involved in TGF- β , MAPK and Wnt signaling were hardly affected, suggesting that other mechano-sensing structures or complexes play a prominent role in the shear stress response of renal epithelial cells. We finally showed that altered signaling due to increased fluid shear stress may be relevant for renal physiology and pathology, as indicated by elevated gene expression at pathological levels of shear stress compared to physiological shear.

RNA sequencing gene expression profiles of shear stress treated *Pkd1*^{-/-} PTECs were compared with *Pkd1*^{wt} controls in **chapter 4**. Functional enrichment analysis revealed that shear regulated genes in *Pkd1*^{-/-} and *Pkd1*^{wt} PTECs are involved in the same signaling pathways, including MAPK, PI3K-AKT, Hippo, Wnt, TNF, p53, FoxO, TGF- β , calcium, JAK-STAT and mTOR signaling. These data indicate that *Pkd1* is not directly involved in shear dependent activation of these pathways. However, expression of a number of genes was significantly more activated by shear stress in *Pkd1*^{-/-} PTECs, suggesting that *Pkd1* is partially restraining shear regulated signaling, which was shown for TGF- β /ALK5 related signaling in chapter 2 as well.

To study shear stress dependent signaling in ADPKD, we compared changes in gene expression in *Pkd1*^{-/-} PTECs during shear with *in vivo* transcriptome analysis of kidneys in *Pkd1*^{del} mice at three early pre-cystic time-points. *Pkd1* gene disruption was specifically induced in 40-50% of the renal epithelial cells, while there was still fluid flow present in *Pkd1*^{del} mice at pre-cystic stage³⁸⁻⁴⁰. Upon *Pkd1* gene disruption, there was a clear overlap in altered pathways and cellular processes between cells and mice, which was attributed to altered expression of identical or paralogous genes. A number of altered flow-induced pathways upon *Pkd1* gene disruption are also implicated in ADPKD, including PI3K-AKT, Hippo, MAPK, p53, calcium, Wnt, JAK-STAT and TGF- β signaling. This suggests that these pathways are already modified at pre-cystic stage and may contribute to the onset of disease. Several genes involved in endocytosis exhibited altered expression in *Pkd1*^{del} mice and *Pkd1*^{-/-} PTEC cells, while this process was also increased by *in vitro* fluid shear exposure, reported

in this thesis and previous publications^{19,41,42}. Enhanced endocytosis upon shear is mediated via cilium dependent Ca^{2+} increase, and subsequent calmodulin mediated activation of *Cdc42*⁴³. Increased endocytosis in ADPKD was recently published in transcriptomic analyses of ADPKD models as well⁴⁴. In addition, the involvement of endocytosis in several growth factor signaling cascades, like TGF- β and MAPK^{20,45}, makes this finding more interesting. Altered endocytosis by shear stress or *Pkd1* gene disruption suggests that this process may contribute to imbalanced cellular signaling or disease progression, although additional research is required to confirm the causality.

As discussed before, several cellular processes are affected by fluid shear stress and *Pkd1* gene disruption, including TGF- β signaling. Furthermore, the TGF- β pathway is proposed to be the initiator of fibrosis, which is a common clinical feature of ADPKD⁴⁶⁻⁴⁸. This is supported by a study showing nuclear translocation of p-SMAD2 in cyst lining epithelial cells of *Pkd1* mutant mice⁴⁹. Therefore, we focused on different interventions to target the TGF- β signaling pathway in **chapter 5**. Genetic disruption of TGF- β type I receptor (*Alk5*) in *Pkd1*^{del} mice only showed minor to no reduction of SMAD2/3 target gene expression or cyst progression. In contrast, primary cells from *Pkd1*-*Alk5* conditional knock-out (cKO) mice showed attenuated SMAD2 phosphorylation upon TGF- β stimulation compared to single *Pkd1* cKO mice. This may suggest that renal epithelial TGF- β /ALK5 signaling is not the driving factor during cyst progression *in vivo*, although it cannot be excluded that several other renal cell types contribute to PKD phenotype via TGF- β signaling. Alternatively, ALK5-independent pathways may be involved in disease progression.

One of these alternative TGF- β pathways is activin signaling via the activin type I (ALK4) and type II receptors⁵⁰. Activin ligands are formed by two homo- or heterodimers of inhibin- β subunits of which four are characterized in mammals (βA , βB , βC , βE). We found that *Inhba* and *Inhbb* gene expression was increased in *Pkd1*^{del} mice. The protein products of these genes are important for embryonic development, injury repair and tissue homeostasis, while inhibin- βC or βE knockout mice didn't display any phenotype⁵¹. However, activin C might have an antagonistic function to compete with activin A signaling. Activins are implicated in several diseases and can stimulate cell migration, differentiation and fibrosis. Therefore, activin inhibition was proposed as possible therapeutic strategy to retard disease progression⁵².

In our study we used a soluble activin receptor type II B fusion protein (sActRIIB-Fc), which is a ligand trap to sequester activins. We treated two young and one adult PKD mouse model with sActRIIB-Fc to assess if inhibition of activin signaling could be a therapeutic strategy for PKD. Overall cyst progression was significantly reduced in sActRIIB-Fc treated PKD mice compared to PBS treated littermates. The highest dose of sActRIIB-Fc treatment was in most

analyses not significant compared to the lower dose, although there was a dose dependent trend visible. This suggests that the lower dose of sActRIIB-Fc is already sufficient to reduce cyst progression in PKD mouse models. In addition, we found decreased SMAD2 expression and phosphorylation, as well as reduced SMAD2/3 target gene expression and collagen deposition, indicating that sActRIIB-Fc is sequestering SMAD inducing ligands, like activins. However, other TGF- β superfamily ligands can also be sequestered by sActRIIB-Fc, but with lower affinity, including GDF11 and myostatin^{53,54}. RNA sequencing data from our lab showed that myostatin (*Mstn*) is not expressed in kidneys of the PKD mouse models and *Gdf11* is low expressed and not changed in PKD mice (chapter 4 and Malas *et al.*)⁵⁵. In addition, the same data showed clearly higher expression of *Inhbb* compared to *Inhba* in PKD kidneys, while *Inhbc* and *Inhbe* were not expressed. This suggests that reduced cyst formation upon sActRIIB-Fc treatment might act by sequestering activin B. However, subtype specific activin type II receptor ligand traps or antibodies needs to be used in the future to confirm this hypothesis. In conclusion, activin inhibition showed promising results to slow PKD progression in three ADPKD mouse models. In addition, clinical trials assessing the safety of soluble activin receptor ligand traps reported that these compounds are well tolerated⁵⁶⁻⁵⁸, although some clinical trials were discontinued due to safety or efficacy concerns^{59,60}. Nevertheless, future research needs to address if the use of soluble activin receptor ligand traps is safe and effective during long term treatment of ADPKD patients.

GENERAL DISCUSSION

In the first chapters of this thesis we presented various cellular processes and signaling pathways that were altered by shear stress and we revealed that several factors can modify the fluid shear response in PTECs. Clearly, pathological shear can enhance the flow induced response in PTECs, but *Pkd1* gene disruption can also elevate shear induced expression of several genes involved in MAPK, TGF- β and Wnt signaling. It has been hypothesized that critical polycystin-1 levels are required to restrain cellular and cilia- or shear-related signaling in order to prevent polycystic kidney disease⁶¹. Moreover, strong variations in hydrodynamic forces and fluid shear are common in kidney diseases, including ADPKD, due to cyst growth, tubular dilation, obstruction and hyperfiltration, which occur to compensate for lost glomeruli and tubules¹⁵. Furthermore, shear stress is increased after unilateral nephrectomy^{40,62}, which can accelerate cyst progression in *Pkd1*^{del} mice³⁹. In addition, long-term pathological shear exposure can result in tubulointerstitial lesions and fibrotic deposition, which is commonly seen after renal mass reduction or during progression of renal diseases^{8,63-65}. Overall, this leads to the hypothesis that pathological shear stress and *Pkd1* gene disruption can both lead to imbalanced cellular signaling, which probably contribute to renal cyst formation and fibrosis. This hypothesis is supported by results in this thesis, showing that several processes

and pathways are cooperating to regulate the shear stress response in PTECs and to maintain cellular physiology. TGF- β , MAPK and Wnt signaling are elevated upon pathological shear or *Pkd1* gene disruption, while these pathways are associated to fibrosis, differentiation and uncontrolled cell proliferation in kidney diseases. Furthermore, several of these pathways are also perturbed in pre-cystic *Pkd1*^{del} mouse models (shown in chapter 4), indicating that imbalanced signaling is already occurring early upon *Pkd1* disruption at pre-cystic stage. In addition, a recent study by our group revealed clustered cyst formation in an adult slow onset PKD mouse model, which resembles the human ADPKD phenotype³⁹. Renal tubules are compressed and PKD-related signaling is increased in nephrons near existing cysts⁶⁶. Tubular compression or obstruction will likely affect local mechanical forces and shear stress on epithelial cells and may lead to altered signaling and local cyst formation. Of course, cellular processes and signaling pathways that drive cyst formation will depend on many factors in addition to functional PKD protein levels, including shear stress, renal injury, inflammation and cellular metabolism.

To date, it is still not completely clear which mechano-sensing structures and complexes are involved in fluid shear response of renal epithelial cells or several other cell types. In the last two decades, the function of the primary cilium was extensively investigated, but we lack knowledge about the role of the microvilli and glycocalyx in renal epithelial cells⁴². The glycocalyx is particularly important for the shear stress response in endothelial cells, but in renal epithelial cells the glycocalyx can also amplify the frictional force on the cell membrane and the microvilli. In this thesis, we revealed that shear altered expression of a number of genes was cilium dependent, while several other genes were still induced by fluid shear after cilia disruption. This indicates that additional mechano-sensing structures or complexes are involved in the shear stress response of renal epithelial cells. However, the involvement of other mechano-sensors, *i.e.* microvilli, the glycocalyx, tight junction proteins and integrin's, and possible interactions between these complexes were not addressed in this thesis, which needs more extensive investigation in future research.

Obviously, the broad range of human ciliopathies and the diversity of their phenotypes, including polycystic kidneys, have focused the research on the primary cilium function. Several studies have proposed that fluid flow bending of primary cilia induces a rapid Ca²⁺ influx, mediated by the polycystin1-2 complex, followed by release of intracellular Ca²⁺ stores and subsequent cytosolic Ca²⁺ increase⁶⁷⁻⁷¹. This process modulates several signaling cascades, including cAMP signaling. In ADPKD, aberrant ciliary polycystin function is the proposed mechanisms leading to reduced Ca²⁺ signaling, which induces cAMP, trans-epithelial fluid secretion and MAPK/ERK mediated cell proliferation⁷²⁻⁷⁴. However, recent studies question the direct role of primary cilia and polycystins in the Ca²⁺ response, since they show cytosolic calcium response prior to the ciliary calcium increase, whereas other

calcium transporters are involved⁷⁵⁻⁸⁰. In chapter 4, we showed shear altered expression of genes involved in Ca²⁺ signaling, while *Pkd1*^{wt} and *Pkd1*^{-/-} PTECs display both overlap and differences in Ca²⁺ signaling related gene expression. However, we did not detect differences in the shear induced cytoplasmic Ca²⁺ influx, when comparing *Pkd1*^{wt} and *Pkd1*^{-/-} PTECs using a Fura-2 AM reporter in a microscopic flow system (unpublished data). This suggests that polycystin-1 is not primarily involved in the shear stress induced Ca²⁺ response in renal epithelial cells. Moreover, a recent study reported that polycystin-2 is a monovalent cation channel within the primary cilium of renal epithelial cells, with a preference for K⁺ and Na⁺ over the divalent Ca²⁺ ions⁸¹. Ciliary localization of polycystin-2, nor its channel activity were altered in the absence of polycystin-1, although polycystin-1 and 2 may still interact at other cellular locations or via indirect mechanisms⁸¹. In this thesis, we lack data of *Pkd2*^{-/-} models, which is definitely required to refine the role of the polycystins in renal physiology and pathology, like ADPKD, whereas the molecular mechanisms of cyst formation may be distinct.

Despite numerous studies about fluid shear mediated Ca²⁺ influx, the mechanism of Ca²⁺ signaling is not entirely clear and still under debate, whereas the direct involvement of cilia and the polycystins is being criticized^{75-79,81,82}. Therefore, it is of indisputable importance to further investigate the role of primary cilia, polycystins and other mechano-sensing complexes in the shear response of renal epithelial cells. It is likely that shear stress sensing and mechanotransduction are different during development and cellular repair or tissue homeostasis, emphasizing the importance to select appropriate cellular models. This will hopefully reveal the complex mechanism of mechano-sensing and the relevance for disease progression, including ciliopathies and ADPKD. However, the cellular mechanism that initiate cyst formation might be distinct between ciliopathies and ADPKD, since a study by Ma *et al.* revealed that cilia disruption suppressed cyst growth in ADPKD models⁸³. They proposed that functional polycystin levels are essential to restrain cilia-dependent cyst activation, although additional research is required to refine this mechanism⁷⁹. Our results can support this hypothesis, since cilia ablation partially suppressed shear induced signaling, while *Pkd1* disruption seems to enhance specific shear induced signaling pathways, including TGF- β and Wnt signaling. Recent data, including data in this thesis, suggest that *Pkd1* has the function to restrain shear regulated signaling instead of being a mechano-sensing activator. Accordingly, Ma *et al.* previously proposed a role for *Pkd1* in restraining an unknown cilia-dependent signaling pathway involved in cyst formation⁷⁹. Therefore, it is of utmost importance to further elucidate the functions of cilia and ciliary located proteins, like the polycystins and IFT proteins, as well as their role outside the cilia. This is needed to establish a definite mechanism of cyst formation and disease progression, including ADPKD and other ciliopathies. Additionally, this should be supported by future research to identify the mechanism of mechanotransduction and the involved mechano-sensors using

PKD and ciliopathy models. In chapter 4 we showed a broad overlap in cellular processes and pathways that were altered upon *Pkd1* gene disruption, between *in vitro* and *in vivo* experiments. Despite the overlap there were clearly some differences. The most notable divergence was presented in chapter 5, which showed that inhibition of activin signaling was able to reduce cyst formation in *Pkd1^{del}* mice, but *in vivo* *Alk5* ablation was ineffective. This seems in contrast with the *in vitro* situation, where shear stress induced signaling is (partially) TGF- β /ALK5 dependent and is increased at pathological shear or upon *Pkd1* disruption. Obviously, the *in vitro* study is not fully representative for the *in vivo* situation, where several other cells types and cytokines in the nephrons are involved and cellular signaling will depend on the overall biological context. In chapter 5, genetic disruption of *Pkd1* and *Alk5* in mice was specifically induced in renal epithelial cells. So, TGF- β /ALK5 signaling can still be present in other cell types of *Pkd1-Alk5* cKO mice, like fibroblasts or inflammatory cells. Activin expression can be induced in macrophages and other inflammatory cells by several cytokines, like TGF- β , EGF, PDGF, TLRs, TNF α , INF- γ and interleukins^{84,85}. In addition, macrophages are found to accumulate near cysts and can stimulate cyst growth, while macrophage depletion inhibited cyst growth⁶⁶. So, this suggests that different cell-types may be involved during cyst formation and PKD-progression is biological context dependent.

In this thesis, we found several processes and pathways that were altered both by fluid shear stress and *Pkd1* gene disruption. Many of these signaling pathways are implicated in ADPKD as well and numerous potential therapies are targeting these pathways⁸⁶. However, more than 20 years after the discovery of *PKD1* and *PKD2* as genetic cause of ADPKD, the exact cellular function of the polycystins still remains unclear. Our data indicate that polycystin-1 is not a direct mechano-sensor, but it restrains shear stress induced gene expression via an unknown mechanism. Additional research is required to identify the cellular function of polycystins and the mechanism of mechanotransduction. This is needed to refine the mechanism of cyst formation in ADPKD and other ciliopathies, which could identify potential targets for therapy. Nevertheless, we showed that inhibition of activin signaling is a promising therapy to slow cyst progression in *Pkd1^{del}* mice. Although other treatment strategies have been tested successfully to reduce PKD progression in pre-clinical studies, the efficacy in human patients is sometimes minimal or absent, which was reported for several mTOR inhibitors⁸⁷⁻⁸⁹. Therefore, it has been suggested to combine therapies and target multiple signaling pathways affected in ADPKD^{66,90,91}. These combined therapies should reestablish the balance in cellular signaling of renal epithelial cells and maintain cellular homeostasis within physiological boundaries. However, additional research is required to evaluate the safety and efficacy of combined therapies, which will be challenging because ADPKD patients will require life-time treatment to postpone end-stage renal disease.

REFERENCES

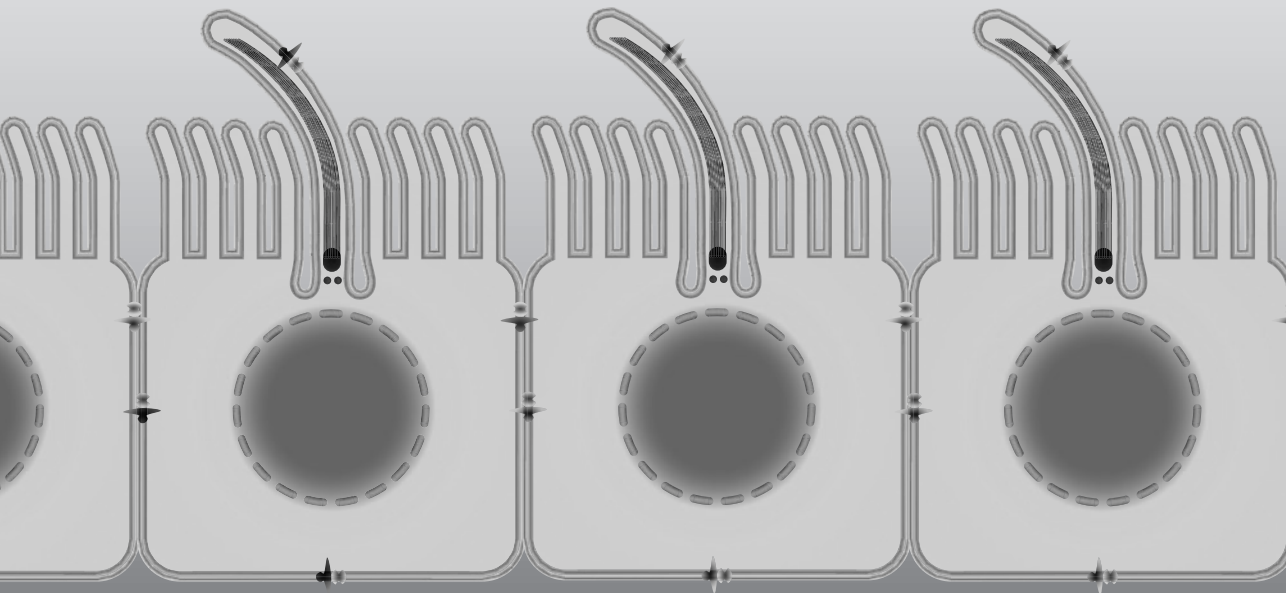
1. Bisgrove B.W. & Yost H.J. The roles of cilia in developmental disorders and disease. *Development* **133**, 4131-4143 (2006).
2. Quinlan R.J., Tobin J.L., & Beales P.L. Modeling ciliopathies: Primary cilia in development and disease. *Curr. Top. Dev. Biol.* **84**, 249-310 (2008).
3. Wozniak M.A. & Chen C.S. Mechanotransduction in development: a growing role for contractility. *Nat. Rev. Mol. Cell Biol.* **10**, 34-43 (2009).
4. Goetz S.C. & Anderson K.V. The primary cilium: a signalling centre during vertebrate development. *Nat. Rev. Genet.* **11**, 331-344 (2010).
5. Kolahi K.S. & Mofrad M.R. Mechanotransduction: a major regulator of homeostasis and development. *Wiley. Interdiscip. Rev. Syst. Biol. Med.* **2**, 625-639 (2010).
6. Freund J.B., Goetz J.G., Hill K.L., & Vermot J. Fluid flows and forces in development: functions, features and biophysical principles. *Development* **139**, 1229-1245 (2012).
7. Arts H.H. & Knoers N.V. Current insights into renal ciliopathies: what can genetics teach us? *Pediatr. Nephrol.* **28**, 863-874 (2013).
8. Essig M. & Friedlander G. Tubular shear stress and phenotype of renal proximal tubular cells. *J. Am. Soc. Nephrol.* **14**, S33-S35 (2003).
9. Piperi C. & Basdra E.K. Polycystins and mechanotransduction: From physiology to disease. *World J. Exp. Med.* **5**, 200-205 (2015).
10. Weinbaum S., Duan Y., Satlin L.M., Wang T., & Weinstein A.M. Mechanotransduction in the renal tubule. *Am. J. Physiol Renal Physiol* **299**, F1220-F1236 (2010).
11. Essig M., Terzi F., Burtin M., & Friedlander G. Mechanical strains induced by tubular flow affect the phenotype of proximal tubular cells. *Am. J. Physiol Renal Physiol* **281**, F751-F762 (2001).
12. Weinbaum S., Duan Y., Thi M.M., & You L. An Integrative Review of Mechanotransduction in Endothelial, Epithelial (Renal) and Dendritic Cells (Osteocytes). *Cell Mol. Bioeng.* **4**, 510-537 (2011).
13. Grabias B.M. & Konstantopoulos K. Epithelial-mesenchymal transition and fibrosis are mutually exclusive responses in shear-activated proximal tubular epithelial cells. *FASEB J.* **26**, 4131-4141 (2012).
14. Grabias B.M. & Konstantopoulos K. Notch4-dependent antagonism of canonical TGF-beta1 signaling defines unique temporal fluctuations of SMAD3 activity in sheared proximal tubular epithelial cells. *Am. J. Physiol Renal Physiol* **305**, F123-F133 (2013).
15. Sharma A., Mucino M.J., & Ronco C. Renal functional reserve and renal recovery after acute kidney injury. *Nephron Clin. Pract.* **127**, 94-100 (2014).
16. Egorova A.D. *et al.* Tgfbeta/Alk5 signaling is required for shear stress induced kif2 expression in embryonic endothelial cells. *Dev. Dyn.* **240**, 1670-1680 (2011).
17. Dong X. *et al.* Force interacts with macromolecular structure in activation of TGF-beta. *Nature* **542**, 55-59 (2017).
18. Ha T. Structural biology: Growth factor rattled out of its cage. *Nature* **542**, 40-41 (2017).
19. Raghavan V., Rbaibi Y., Pastor-Soler N.M., Carattino M.D., & Weisz O.A. Shear stress-dependent regulation of apical endocytosis in renal proximal tubule cells mediated by primary cilia. *Proc. Natl. Acad. Sci. U. S. A* **111**, 8506-8511 (2014).
20. Clement C.A. *et al.* TGF-beta signaling is associated with endocytosis at the pocket region of the primary cilium. *Cell Rep.* **3**, 1806-1814 (2013).
21. Pedersen L.B., Mogensen J.B., & Christensen S.T. Endocytic Control of Cellular Signaling at the Primary Cilium. *Trends Biochem. Sci.* **41**, 784-797 (2016).
22. Chapnick D.A., Warner L., Bernet J., Rao T., & Liu X. Partners in crime: the TGFbeta and MAPK pathways in cancer progression. *Cell Biosci.* **1**, 42 (2011).

23. Muthusamy B.P. *et al.* ShcA Protects against Epithelial-Mesenchymal Transition through Compartmentalized Inhibition of TGF-beta-Induced Smad Activation. *PLoS. Biol.* **13**, e1002325 (2015).
24. Kretzschmar M., Doody J., Timokhina I., & Massague J. A mechanism of repression of TGFbeta/ Smad signaling by oncogenic Ras. *Genes Dev.* **13**, 804-816 (1999).
25. Hough C., Radu M., & Dore J.J. Tgf-beta induced Erk phosphorylation of smad linker region regulates smad signaling. *PLoS. One.* **7**, e42513 (2012).
26. Akchurin O.M. & Kaskel F. Update on inflammation in chronic kidney disease. *Blood Purif.* **39**, 84-92 (2015).
27. Lee M.K. *et al.* TGF-beta activates Erk MAP kinase signalling through direct phosphorylation of ShcA. *EMBO J.* **26**, 3957-3967 (2007).
28. Duan Y. *et al.* Shear-induced reorganization of renal proximal tubule cell actin cytoskeleton and apical junctional complexes. *Proc. Natl. Acad. Sci. U. S. A* **105**, 11418-11423 (2008).
29. Jang K.J. *et al.* Human kidney proximal tubule-on-a-chip for drug transport and nephrotoxicity assessment. *Integr. Biol.* **5**, 1119-1129 (2013).
30. Maggiorani D. *et al.* Shear Stress-Induced Alteration of Epithelial Organization in Human Renal Tubular Cells. *PLoS. One.* **10**, e0131416 (2015).
31. Fisslthaler B., Fleming I., Keseru B., Walsh K., & Busse R. Fluid shear stress and NO decrease the activity of the hydroxy-methylglutaryl coenzyme A reductase in endothelial cells via the AMP-activated protein kinase and FoxO1. *Circ. Res.* **100**, e12-e21 (2007).
32. Fisslthaler B. & Fleming I. Activation and signaling by the AMP-activated protein kinase in endothelial cells. *Circ. Res.* **105**, 114-127 (2009).
33. Yamamoto K. & Ando J. Endothelial cell and model membranes respond to shear stress by rapidly decreasing the order of their lipid phases. *J. Cell Sci.* **126**, 1227-1234 (2013).
34. Yamamoto K. & Ando J. Vascular endothelial cell membranes differentiate between stretch and shear stress through transitions in their lipid phases. *Am. J. Physiol Heart Circ. Physiol* **309**, H1178-H1185 (2015).
35. Carling D. The AMP-activated protein kinase cascade--a unifying system for energy control. *Trends Biochem. Sci.* **29**, 18-24 (2004).
36. Boehlke C. *et al.* Primary cilia regulate mTORC1 activity and cell size through Lkb1. *Nat. Cell Biol.* **12**, 1115-1122 (2010).
37. Zhong M. *et al.* Tumor Suppressor Folliculin Regulates mTORC1 through Primary Cilia. *J. Biol. Chem.* **291**, 11689-11697 (2016).
38. Leonhard W.N., Roelfsema J.H., Lantinga-van Leeuwen I.S., Breuning M.H., & Peters D.J. Quantification of Cre-mediated recombination by a novel strategy reveals a stable extra-chromosomal deletion-circle in mice. *BMC. Biotechnol.* **8**, 18 (2008).
39. Leonhard W.N. *et al.* Scattered Deletion of PKD1 in Kidneys Causes a Cystic Snowball Effect and Recapitulates Polycystic Kidney Disease. *J. Am. Soc. Nephrol.* **26**, 1322-1333 (2015).
40. Lenihan C.R. *et al.* Longitudinal study of living kidney donor glomerular dynamics after nephrectomy. *J. Clin. Invest* **125**, 1311-1318 (2015).
41. Raghavan V. & Weisz O.A. Flow stimulated endocytosis in the proximal tubule. *Curr. Opin. Nephrol. Hypertens.* **24**, 359-365 (2015).
42. Raghavan V. & Weisz O.A. Discerning the role of mechanosensors in regulating proximal tubule function. *Am. J. Physiol Renal Physiol* **310**, F1-F5 (2016).
43. Bhattacharyya S. *et al.* Cdc42 activation couples fluid shear stress to apical endocytosis in proximal tubule cells. *Physiol Rep.* **5**, e13460 (2017).
44. Chatterjee S., Verma S.P., & Pandey P. Profiling conserved biological pathways in Autosomal Dominant Polycystic Kidney Disorder (ADPKD) to elucidate key transcriptomic alterations regulating cystogenesis: A cross-species meta-analysis approach. *Gene* **627**, 434-450 (2017).
45. Tomas A., Jones S., Vaughan S.O., Hochhauser D., & Futter C.E. Stress-specific p38 MAPK activation is sufficient to drive EGFR endocytosis but not its nuclear translocation. *J. Cell Sci.* **130**, 2481-2490 (2017).

46. Norman J. Fibrosis and progression of autosomal dominant polycystic kidney disease (ADPKD). *Biochim. Biophys. Acta* **1812**, 1327-1336 (2011).
47. Liu Y. *et al.* Rosiglitazone inhibits transforming growth factor-beta1 mediated fibrogenesis in ADPKD cyst-lining epithelial cells. *PLoS. One.* **6**, e28915 (2011).
48. Happe H. & Peters D.J. Translational research in ADPKD: lessons from animal models. *Nat. Rev. Nephrol.* **10**, 587-601 (2014).
49. Hassane S. *et al.* Elevated TGFbeta-Smad signalling in experimental Pkd1 models and human patients with polycystic kidney disease. *J. Pathol.* **222**, 21-31 (2010).
50. Moustakas A. & Heldin C.H. The regulation of TGFbeta signal transduction. *Development* **136**, 3699-3714 (2009).
51. Sideras P. *et al.* Activin, neutrophils, and inflammation: just coincidence? *Semin. Immunopathol.* **35**, 481-499 (2013).
52. Marino F.E., Risbridger G., & Gold E. The therapeutic potential of blocking the activin signalling pathway. *Cytokine Growth Factor Rev.* **24**, 477-484 (2013).
53. Lee S.J. *et al.* Regulation of muscle growth by multiple ligands signaling through activin type II receptors. *Proc. Natl. Acad. Sci. U. S. A* **102**, 18117-18122 (2005).
54. Sako D. *et al.* Characterization of the ligand binding functionality of the extracellular domain of activin receptor type IIb. *J. Biol. Chem.* **285**, 21037-21048 (2010).
55. Malas T.B. *et al.* Meta-analysis of Polycystic Kidney Disease expression profiles defines strong involvement of injury repair processes. *Am. J. Physiol Renal Physiol* **312**, F806-F817 (2017).
56. Attie K.M. *et al.* A single ascending-dose study of muscle regulator ACE-031 in healthy volunteers. *Muscle Nerve* **47**, 416-423 (2013).
57. Sherman M.L. *et al.* Multiple-dose, safety, pharmacokinetic, and pharmacodynamic study of sotatercept (ActRIIA-IgG1), a novel erythropoietic agent, in healthy postmenopausal women. *J. Clin. Pharmacol.* **53**, 1121-1130 (2013).
58. Bendell J.C. *et al.* Safety, pharmacokinetics, pharmacodynamics, and antitumor activity of dalantercept, an activin receptor-like kinase-1 ligand trap, in patients with advanced cancer. *Clin. Cancer Res.* **20**, 480-489 (2014).
59. Jimeno A. *et al.* A phase 2 study of dalantercept, an activin receptor-like kinase-1 ligand trap, in patients with recurrent or metastatic squamous cell carcinoma of the head and neck. *Cancer* **122**, 3641-3649 (2016).
60. Campbell C. *et al.* Myostatin inhibitor ACE-031 treatment of ambulatory boys with Duchenne muscular dystrophy: Results of a randomized, placebo-controlled clinical trial. *Muscle Nerve* **55**, 458-464 (2017).
61. Lee S.H. & Somlo S. Cyst growth, polycystins, and primary cilia in autosomal dominant polycystic kidney disease. *Kidney Res. Clin. Pract.* **33**, 73-78 (2014).
62. Srivastava T. *et al.* Fluid flow shear stress over podocytes is increased in the solitary kidney. *Nephrol. Dial. Transplant.* **29**, 65-72 (2014).
63. Rohatgi R. & Flores D. Intratubular hydrodynamic forces influence tubulointerstitial fibrosis in the kidney. *Curr. Opin. Nephrol. Hypertens.* **19**, 65-71 (2010).
64. Grabias B.M. & Konstantopoulos K. The physical basis of renal fibrosis: effects of altered hydrodynamic forces on kidney homeostasis. *Am. J. Physiol Renal Physiol* **306**, F473-F485 (2014).
65. Venkatachalam M.A. *et al.* Acute kidney injury: a springboard for progression in chronic kidney disease. *Am. J. Physiol Renal Physiol* **298**, F1078-F1094 (2010).
66. Leonhard W.N., Happe H., & Peters D.J. Variable Cyst Development in Autosomal Dominant Polycystic Kidney Disease: The Biologic Context. *J. Am. Soc. Nephrol.* **27**, 3530-3538 (2016).
67. Praetorius H.A. & Spring K.R. Bending the MDCK cell primary cilium increases intracellular calcium. *J. Membr. Biol.* **184**, 71-79 (2001).
68. Praetorius H.A., Frokjaer J., Nielsen S., & Spring K.R. Bending the Primary Cilium Opens Ca(2+)-sensitive

- Intermediate-Conductance K⁺ Channels in MDCK Cells. *J. Membr. Biol.* **191**, 193-200 (2003).
69. Nauli S.M. *et al.* Polycystins 1 and 2 mediate mechanosensation in the primary cilium of kidney cells. *Nat. Genet.* **33**, 129-137 (2003).
 70. AbouAlaiwi W.A. *et al.* Ciliary polycystin-2 is a mechanosensitive calcium channel involved in nitric oxide signaling cascades. *Circ. Res.* **104**, 860-869 (2009).
 71. Jin X. *et al.* Cilioplasm is a cellular compartment for calcium signaling in response to mechanical and chemical stimuli. *Cell Mol. Life Sci.* **71**, 2165-2178 (2014).
 72. Yamaguchi T. *et al.* Calcium restriction allows cAMP activation of the B-Raf/ERK pathway, switching cells to a cAMP-dependent growth-stimulated phenotype. *J Biol. Chem.* **279**, 40419-40430 (2004).
 73. Torres V.E. & Harris P.C. Mechanisms of Disease: autosomal dominant and recessive polycystic kidney diseases. *Nat. Clin. Pract. Nephrol.* **2**, 40-55 (2006).
 74. Tran P.V., Sharma M., Li X., & Calvet J.P. Developmental signaling: does it bridge the gap between cilia dysfunction and renal cystogenesis? *Birth Defects Res. C. Embryo. Today* **102**, 159-173 (2014).
 75. DeCaen P.G., Delling M., Vien T.N., & Clapham D.E. Direct recording and molecular identification of the calcium channel of primary cilia. *Nature* **504**, 315-318 (2013).
 76. Delling M., DeCaen P.G., Doerner J.F., Febvay S., & Clapham D.E. Primary cilia are specialized calcium signalling organelles. *Nature* **504**, 311-314 (2013).
 77. Delling M. *et al.* Primary cilia are not calcium-responsive mechanosensors. *Nature* **531**, 656-660 (2016).
 78. Norris D.P. & Jackson P.K. Cell biology: Calcium contradictions in cilia. *Nature* **531**, 582-583 (2016).
 79. Ma M., Gallagher A.R., & Somlo S. Ciliary Mechanisms of Cyst Formation in Polycystic Kidney Disease. *Cold Spring Harb. Perspect. Biol.* **9**, a028209 (2017).
 80. Mohammed S.G. *et al.* Fluid shear stress increases transepithelial transport of Ca(2+) in ciliated distal convoluted and connecting tubule cells. *FASEB J.* **31**, 1796-1806 (2017).
 81. Liu X. *et al.* Polycystin-2 is an essential ion channel subunit in the primary cilium of the renal collecting duct epithelium. *Elife.* **7**, e33183 (2018).
 82. Praetorius H.A. The primary cilium as sensor of fluid flow: new building blocks to the model. A review in the theme: cell signaling: proteins, pathways and mechanisms. *Am. J. Physiol Cell Physiol* **308**, C198-C208 (2015).
 83. Ma M., Tian X., Igarashi P., Pazour G.J., & Somlo S. Loss of cilia suppresses cyst growth in genetic models of autosomal dominant polycystic kidney disease. *Nat. Genet.* **45**, 1004-1012 (2013).
 84. Yamashita S., Maeshima A., Kojima I., & Nojima Y. Activin A is a potent activator of renal interstitial fibroblasts. *J. Am. Soc. Nephrol.* **15**, 91-101 (2004).
 85. de Kretser D.M., O'Hehir R.E., Hardy C.L., & Hedger M.P. The roles of activin A and its binding protein, follistatin, in inflammation and tissue repair. *Mol. Cell Endocrinol.* **359**, 101-106 (2012).
 86. Harris P.C. & Torres V.E. Genetic mechanisms and signaling pathways in autosomal dominant polycystic kidney disease. *J. Clin. Invest* **124**, 2315-2324 (2014).
 87. Serra A.L. *et al.* Sirolimus and Kidney Growth in Autosomal Dominant Polycystic Kidney Disease. *N. Engl. J. Med.* **363**, 820-829 (2010).
 88. Walz G. *et al.* Everolimus in Patients with Autosomal Dominant Polycystic Kidney Disease. *N. Engl. J. Med.* **363**, 830-840 (2010).
 89. He Q., Lin C., Ji S., & Chen J. Efficacy and safety of mTOR inhibitor therapy in patients with early-stage autosomal dominant polycystic kidney disease: a meta-analysis of randomized controlled trials. *Am. J. Med. Sci.* **344**, 491-497 (2012).
 90. Saigusa T. & Bell P.D. Molecular pathways and therapies in autosomal-dominant polycystic kidney disease. *Physiology* **30**, 195-207 (2015).
 91. Rysz J., Gluba-Brzozka A., Franczyk B., Banach M., & Bartnicki P. Combination drug versus monotherapy for the treatment of autosomal dominant polycystic kidney disease. *Expert. Opin. Pharmacother.* **17**, 2049-2056 (2016).

APPENDIX



LIST OF ABBREVIATIONS

ACVR1	Activin A Receptor Type 1
ADPKD	Autosomal dominant polycystic kidney disease
ANOVA	Analysis of variance
ALK	Activin receptor like kinase
AS	Ammonium sulfate
BBS	Bardet-Biedl syndrome
BMP	Bone morphogenetic proteins
cAMP	Cyclic adenosine monophosphate
cKO	Conditional knock-out
CPM	Counts per million
CDH1	Cadherin-1
COL1A1	Collagen, type I, alpha 1
COX2	Cyclo-oxygenase-2
DEG	Differentially expressed genes
DPBS	Dulbecco's phosphate-buffered saline
ECM	Extracellular matrix
EGFR	Epidermal growth factor receptor
ELISA	Enzyme-linked immunosorbent assay
EMT	Epithelial-to-mesenchymal transition
ERK	Extracellular signal-regulated kinase
ESRD	End stage renal disease
FDR	False discovery rate
Fn1	Fibronectin 1
GFR	Glomerular filtration rate
GPCR	G-protein coupled receptors
Hh	Hedgehog
HPRT	Hypoxanthine-guanine phosphoribosyltransferase
IFT	Intraflagellar transport
LAP	Latency-associated peptide
MAPK	Mitogen-activated protein kinase
MEK	MAPK/ERK kinase
MKS	Meckel syndrome
mTOR	Mechanistic Target Of Rapamycin
MVID	Microvillus inclusion disease
NGS	Next generation sequencing
NO	Nitric oxide
OFD	Oral-Facial-Digital Syndrome

PAI1	Plasminogen activator inhibitor 1
PC	Polycystin
PCP	Planar cell polarity
PI3K	Phosphoinositide 3-kinase
PKD	Polycystic kidney disease
PKD1	Polycystic kidney disease 1 gene
PKD2	Polycystic kidney disease 2 gene
PKHD1	Polycystic kidney and hepatic disease 1 (fibrocystin / polyductin)
NPHP	Nephronophthisis
PTEC	Proximal tubular epithelial cell
PTGS2	Prostaglandin-endoperoxide synthase 2
qPCR	Quantitative polymerase chain reaction
RIPA	Radioimmunoprecipitation assay
sActRIIB-Fc	Soluble Activin receptor-IIB fusion protein
SDS-PAGE	Sodium dodecyl sulfate polyacrylamide gel electrophoresis
SERPINE1	Serpin Peptidase Inhibitor, Clade E, Member 1
SMAD	Mothers against decapentaplegic homolog
TBS	Tris-buffered saline
TGF	Tubuloglomerular feedback
TGFBRI	Transforming growth factor β receptor I (ALK5)
TGF- β	Transforming growth factor β
TGF- β Ab	TGF- β neutralizing antibody
VIM	Vimentin
YAP	Yes-associated protein

NEDERLANDSE SAMENVATTING

Voor cellen in het lichaam is het van essentieel belang om signalen uit de omgeving waar te kunnen nemen, zodat ze hun functie daarop kunnen aanpassen. Dit doen cellen onder andere met behulp van mechano-sensoren. Dit zijn eiwitten op het celmembraan of in de cellen die vervormen of geactiveerd worden door krachten uit de omgeving en hierdoor kunnen ze een signaal aan de cellen doorgeven. Dit proces wordt mechanotransductie genoemd. Mechanotransductie is dus de biochemische reactie op fysische krachten waaraan cellen voortdurend worden blootgesteld, zoals druk, vloeistof beweging (shear stress), rek van het celmembraan of actine cytoskelet. Deze processen spelen een zeer belangrijke rol in de embryonale ontwikkeling en bij normale weefsel homeostase. Defecten in de mechanotransductie kunnen dan ook resulteren in veel verschillende soorten ziekten.

Onderzoek naar mechanotransductie is al begonnen in de jaren 60 van de vorige eeuw, met als doel het onderzoeken van de water reabsorptie in nierbuisjes (tubulus). Vanaf de jaren 80 en 90 werd het onderzoek toegespitst op de bloedvatcellen en botcellen, omdat deze cellen ook veel worden blootgesteld aan mechanische krachten. Pas vanaf de eeuwwisseling gingen onderzoekers specifiek kijken naar het effect van vloeistofstroming (shear stress) op nier epitheelcellen. Dit zijn de cellen in de wand van de nierbuisjes, waar voorurine door stroomt en water en voedingsstoffen worden teruggewonnen. Het is echter nog steeds niet geheel duidelijk hoe het nier-epitheel reageert op shear stress en welke eiwitten, complexen en processen daarbij een rol spelen. Naast structuur eiwitten in het celmembraan en cytoskelet, hebben het primaire cilium en mogelijk de microvilli daar een belangrijke functie in. Cilia en microvilli en zijn uitstulpingen van het celmembraan van epitheelcellen uit de proximale tubulus (nierbuisjes), die kunnen bewegen door invloed van vloeistofstroming. Primaire cilia komen in bijna elk celtype voor, terwijl microvilli alleen aanwezig zijn in gespecialiseerde cellen, zoals proximaal tubulaire epitheelcellen. Mutaties in eiwitten die een functie hebben in het cilium kunnen leiden tot erfelijke ziekten, ciliopathieën genaamd, waarbij vaak ook nieren zijn aangedaan. Eén van die erfelijke nierziekten is ADPKD (autosomal dominant polycystic kidney disease = autosomaal dominant polycysteuze nierziekte), waarbij de patiënten veel vochtblazen (cysten) ontwikkelen in de nieren. Uiteindelijk leidt dit tot verslechtering van de nierfunctie en nierfalen bij 50% van de patiënten op 50-60-jarige leeftijd, waardoor de patiënten nierdialyse of niertransplantatie moeten ondergaan.

ADPKD-patiënten hebben een mutatie in een van de twee DNA-kopieën van het *PKD1* of *PKD2* gen. Tijdens hun leven ondervinden ze een "somatische" mutatie in de tweede functionele kopie van het PKD gen, waardoor de gen-activiteit onder een minimum zakt en de ziekte zich kan ontwikkelen. De twee PKD-genen bevatten de genetische code voor de eiwitten polycystine-1 en 2 (PC-1 en PC-2), die gelokaliseerd zijn in het celmembraan en in

het cilium. De precieze cellulaire functie van de polycystine-eiwitten is niet geheel duidelijk, maar PC-1 lijkt op een receptoreiwit en PC-2 is een ion-kanaal. Inmiddels wordt al zeker 15 jaar aangenomen dat de polycystine-eiwitten een rol spelen bij mechanotransductie en de detectie van shear stress, maar de exacte rol van deze eiwitten in dit proces blijft nog onduidelijk. In dit proefschrift is daarom de rol van shear stress onderzocht in nier-epitheelcellen van de proximale tubulus. Daarbij is ook gekeken naar de rol van het cilium en de relevantie voor de erfelijke nierziekte ADPKD.

In hoofdstuk 2-4 is gekeken naar invloed van shear stress ten gevolge van vloeistofstroming op proximaal tubulaire (nier)-epitheelcellen (PTEC) en de rol van primaire cilia en *Pkd1* activiteit. In hoofdstuk 2 lag de focus op de processen TGF- β (SMAD2/3) en MAPK/ERK signalering. Deze signaleringsroutes spelen een rol bij herstel van cellulaire schade, celproliferatie, migratie en differentiatie. Echter in ziekteprocessen zijn deze routes vaak te sterk geactiveerd, waardoor er te veel celdeling plaatsvindt en bindweefsel (fibrose) kan vormen, wat een kenmerk is van ADPKD. We laten zien dat de TGF- β route wordt geactiveerd door shear stress en dat dit afhankelijk is van actief TGF- β en het receptoreiwit ALK5, waaraan het signaal eiwit TGF- β kan binden. Daarnaast bleek uit het onderzoek dat inactivatie van het *Pkd1* gen ertoe leidt dat de SMAD2/3 gereguleerde expressie van de target genen werd versterkt. Dit houdt feitelijk in dat de TGF- β pathway sterker wordt geactiveerd in *Pkd1* geïnactiveerde cellen, die worden blootgesteld aan shear stress. Remming van een belangrijke component in de MAPK/ERK signaleringsroute, MEK1/2, liet zien dat deze route ook invloed heeft op de door shear stress geactiveerde TGF- β route. Echter, het verwijderen van cilia zorgde niet voor een verandering van de activiteit van de TGF- β signalering. Dit suggereert dat niet het cilium maar andere celstructuren en complexen ook een rol spelen bij mechanotransductie in nier epitheelcellen.

In hoofdstuk 3 hebben we veel uitgebreider gekeken naar de processen die een rol spelen bij shear stress in proximaal tubulair nier-epitheel door gebruik te maken van RNA-sequencing. Deze techniek brengt alle messenger RNA (mRNA) moleculen in kaart, wat een goede indicatie geeft van de activatie van processen en functies in de cellen. Veel verschillende signaleringsroutes zijn veranderd door shear stress, waaronder verhoogde activatie van de TGF- β , MAPK, Wnt en andere cytokine signalering, maar componenten van de JAK/STAT route zijn verlaagd door shear stress. Ook zijn er cellulaire processen veranderd die betrokken zijn bij de celstructuur (cel-matrix, cytoskelet, glycocalyx) en metabolisme (glycolyse en cholesterol). We laten zien dat de TGF- β en MAPK/ERK signaleringsroutes een belangrijke rol spelen bij veel van de shear stress geactiveerde signaleringsroutes en processen, omdat de remmers van deze routes (ALK4/5/7 en MEK1/2) veelal vermindering laten zien van de shear response. Net als voor de eerdergenoemde TGF- β en MAPK/ERK signaleringsroutes concluderen we dat er naast cilia ook andere complexen een rol spelen

bij mechanotransductie in nier epitheelcellen, omdat veel processen na verwijdering van de cilia nog steeds geactiveerd werden door vloeistofstroming. Tenslotte constateren we dat verhoogde pathologische levels van shear stress zorgen voor een sterkere activatie van de door stroming geïnduceerde processen. Daarom concluderen we dat pathologische vloeistofstroming mogelijk kan bijdragen aan het ontstaan van het ziektebeeld doordat specifieke processen te sterk geactiveerd worden.

Vervolgens hebben we in hoofdstuk 4 gekeken naar de grootschalige veranderingen in genexpressie ten gevolge van shear stress in *Pkd1* geïnactieveerde cellen (*Pkd1*^{-/-}) en hebben dit vergeleken met cellen met een functioneel *Pkd1* gen (*Pkd1*^{wt}). We concluderen dat dezelfde processen worden geactiveerd in *Pkd1*^{-/-} en *Pkd1*^{wt} nier-epitheelcellen. Echter, in *Pkd1*^{-/-} PTEC werden verschillende signaleringsroutes sterker geactiveerd door shear stress dan in *Pkd1*^{wt} cellen, waaronder de MAPK, PI3K-AKT, Hippo, Rap1, Wnt, TNF, Ras en TGF-β routes, zoals al eerder beschreven was voor de TGF-β route in hoofdstuk 2. Gebaseerd op deze resultaten trekken we de hypothese dat het *Pkd1* gen mogelijk de functie heeft om de shear stress geïnduceerde processen te remmen, zodat deze onder controle blijven. Als het *Pkd1* minder of niet meer functioneel is, zoals bij ADPKD-patiënten, dan kan deze controle wegvallen, waardoor bepaalde processen te sterk geactiveerd worden en de ziekte zich mogelijk kan ontwikkelen.

Ook hebben we de veranderde processen tijdens shear stress in *Pkd1*^{-/-} nier-epitheelcellen vergeleken met een *Pkd1*^{-/-} muis-model, waarbij nog geen cysten zijn gevormd. In deze fase is er nog normale vloeistofstroming in de nieren van de muizen en daarom is dit te vergelijken met veranderingen in *Pkd1*^{-/-} proximale tubulaire epitheelcellen tijdens shear stress. In beide *Pkd1*^{-/-} modellen zijn vergelijkbare processen veranderd ten opzichte van de *Pkd1*^{wt} controles, waaronder de PI3K-AKT, MAPK, JAK-STAT, Hippo, p53, calcium, Wnt en TGF-β signaleringsroute. Deze routes zijn ook veranderd in ADPKD-patiënten en andere *Pkd1*^{-/-} modellen tijdens cystegroei. Deze resultaten suggereren dat deze signaalroutes al zijn veranderd in de pre-cyste fase van ADPKD en dat deze cellulaire veranderingen mogelijk kunnen bijdragen aan cyste vorming.

Voor de behandeling van ADPKD-patiënten is het belangrijk dat de cystegroei wordt verminderd of geremd, zodat nierfalen in een later stadium of helemaal niet optreedt. In hoofdstuk 5 hebben we daarom in een *Pkd1* knock-out (*Pkd1*^{del}) muis-model verschillende therapieën getest, die gericht zijn op de TGF-β signaleringsroute, omdat deze een belangrijke rol speelt bij fibrosevorming in nieren van ADPKD-patiënten. Genetische inactivatie van een TGF-β receptoreiwit (*Alk5*) leidde echter niet tot verminderde cystegroei in *Pkd1*^{del} muizen. Daarom concluderen we dat er mogelijk andere, ALK5 onafhankelijke, routes een rol spelen bij cystegroei in *Pkd1*^{del} muizen. Een van de alternatieve TGF-β routes is via de ALK4

receptor, die specifiek is voor activine cytokines. In dit onderzoek hebben we daarom een oplosbaar activine receptor type IIB-fusie eiwit (sActRIIB-Fc) gebruikt, wat activine-liganden kan wegvangen. *Pkd1*^{del} muizen die behandeld waren met sActRIIB-Fc lieten duidelijk een verminderde activatie van de TGF- β /activine route zien, wat gepaard ging met verminderde cystegroei. Verder onderzoek zal nodig zijn om vast te stellen via welk mechanisme en welke subtypes van de TGF- β /activine cytokines de cystevorming wordt gestimuleerd. Aangezien er naast de TGF- β /activine route verschillende signaleringsroutes een rol spelen in ADPKD, verwachten we dat het nodig zal zijn om meerdere processen te remmen die een rol spelen bij de cystegroei. Klinische studies lieten namelijk al zien dat remming van alleen de mTOR route niet voldoende is om PKD progressie te verminderen in patiënten. Gecombineerde therapieën kunnen daar mogelijk een uitkomst bieden. Daarvoor moeten de effectiviteit van de therapie en de veiligheidsaspecten beter onderzocht worden, omdat ADPKD patiënten levenslange behandeling moeten ondergaan om nierfalen uit te stellen. Mechanistisch onderzoek naar de functie van de *Pkd1* en *Pkd2* genen en de rol van shear stress zullen hier zeker aan bij kunnen dragen. Daarnaast kan een verfijnd mechanisme van cystegroei in ADPKD ook bijdragen aan onderzoek en mogelijke behandeling van andere ciliopathieën.

CURRICULUM VITAE

Steven Jeffrey Kunnen is geboren op 24 oktober 1984 in Rotterdam als de jongste van een tweeling. Van 1997 tot 2003 heeft Steven het Gymnasium succesvol doorlopen aan het Melanchthon College in Rotterdam met als profiel “Natuur en Techniek” en Biologie als keuzevak. Vanwege zijn fascinatie voor de biologie en natuurwetenschappen begon Steven in 2003 aan de opleiding Life Science & Technology aan de Universiteit Leiden en de Technische Universiteit Delft. In 2006 werd het Bachelor programma succesvol afgerond met als afstudeeropdracht een stage bij de afdeling Moleculaire Celbiologie van het LUMC. Na een bedrijfsstage bij Crucell (tegenwoordig Janssen) en een afstudeerstage bij de afdeling Humane Genetica van het LUMC behaalde Steven zijn Master diploma in 2009.

Vervolgens begon hij in 2010 aan zijn promotieonderzoek bij dezelfde groep als waar hij zijn masterstage doorliep onder begeleiding van zijn promotor prof. dr. Dorien Peters. Het onderzoek was gericht op het mechanistisch effect van vloeistofstroming op nier epitheelcellen en de relevantie voor de nierziekte ADPKD. Tijdens zijn promotie heeft Steven zijn onderzoek gepresenteerd op meerdere congressen en heeft hij meeholpen bij de organisatie van een congres voor PhD studenten in Düsseldorf. De resultaten van zijn promotieonderzoek zijn beschreven in dit proefschrift met als titel “Shear stress regulated signaling in renal epithelial cells and polycystic kidney disease”. Tijdens de afrondende fase van zijn proefschrift is Steven in 2017 begonnen aan een postdoc functie bij het LACDR in de groep van prof. dr. Bob van de Water. Daar doet hij onderzoek naar de schadelijke effecten van medicijnen op de nieren en lever om zo het cellulaire mechanisme van de schade te ontrafelen en dit te gebruiken voor een model om mogelijke schade van nieuwe medicijnen te voorspellen.

LIST OF PUBLICATIONS**Comparative transcriptomics of shear stress treated *Pkd1*^{-/-} cells and pre-cystic kidneys reveals pathways involved in early Polycystic Kidney Disease**

Kunnen SJ, Malas TB, Formica C, Leonhard WN, 't Hoen PAC, Peters DJM.
Biomedicine & Pharmacotherapy 2018; *in press*

Comprehensive transcriptome analysis of fluid shear stress altered gene expression in renal epithelial cells

Kunnen SJ, Malas TB, Semeins CM, Bakker AD, Peters DJM.
J Cell Physiol. 2018; 233(4): 3615-3628. DOI: 10.1002/jcp.26222

High-Throughput Phenotypic Screening of Kinase Inhibitors to Identify Drug Targets for Polycystic Kidney Disease.

Booij TH, Bange H, Leonhard WN, Yan K, Fokkelman M, Kunnen SJ, Dauwerse JG, Qin Y, van de Water B, van Westen GJP, Peters DJM, Price LS.
SLAS Discov. 2017; 22(8): 974-984. DOI: 10.1177/2472555217716056

Fluid shear stress-induced TGF- β /ALK5 signaling in renal epithelial cells is modulated by MEK1/2.

Kunnen SJ, Leonhard WN, Semeins C, Hawinkels LJAC, Poelma C, Ten Dijke P, Bakker A, Hierck BP, Peters DJM.
Cell Mol Life Sci. 2017; 74(12): 2283-2298. DOI: 10.1007/s00018-017-2460-x

Inhibition of Activin signaling slows progression of Polycystic Kidney Disease in mice.

Leonhard WN, Kunnen SJ, Plugge AJ, Pasternack A, Jianu SB, Veraar K, El Bouazzaoui F, Hoogaars WM, Ten Dijke P, Breuning MH, De Heer E, Ritvos O, Peters DJ.
J Am Soc Nephrol. 2016; 27(12): 3589-3599. DOI: 10.1681/ASN.2015030287

Altered Hippo signalling in polycystic kidney disease.

Happé H, van der Wal AM, Leonhard WN, Kunnen SJ, Breuning MH, de Heer E, Peters DJ.
J Pathol. 2011; 224(1): 133-42. DOI: 10.1002/path.2856

Curcumin inhibits cystogenesis by simultaneous interference of multiple signaling pathways: in vivo evidence from a *Pkd1*-deletion model.

Leonhard WN, van der Wal A, Novalic Z, Kunnen SJ, Gansevoort RT, Breuning MH, de Heer E, Peters DJ.
Am J Physiol Renal Physiol. 2011; 300(5): F1193-202. DOI: 10.1152/ajprenal.00419.2010

DANKWOORD

Mijn proefschrift is dan eindelijk een feit, na een lange weg met veel hobbels. Om dit mogelijk te kunnen maken ben ik veel mensen dank verschuldigd. Ten eerste wil ik alle collega's van het PKD-lab bedanken voor hun hulp en steun bij mijn onderzoek. Wouter en Hester bedankt voor al jullie interesse, hulp en goede discussies die ik met jullie had, wat heeft geleid tot een aantal mooie gezamenlijke publicaties. Chiara, Sandra, Julie en Hans wil ik ook graag bedanken voor alle steun op het lab en gezelligheid op de kamer. Luuk, Tareq, Peter-Bram, Peter, Beerend, Martijn, Silvere, Christiaan, Janne, Fatiha, Daniëlle, Lin en Tijmen, bedankt voor jullie samenwerking, adviezen en hulp. Mijn studenten, Maaïke, Aliesa en Melanie, wil ik bedanken voor hun inzet en enthousiasme. Tenslotte, ben ik Dorien ook zeer dankbaar voor haar begeleiding tijdens mijn promotieonderzoek. Bedankt voor alle interessante discussies, die vaak langer duurden dan gepland, maar zeker ook bedankt voor al je adviezen, steun en geduld die je hebt gehad tijdens mijn promotie.

Verder wil ik alle collega's van de afdeling Humane Genetica van het LUMC bedanken. Peter, Richard, Marlinde, Maartje, Bianca, Maurice, Barry, Melvin, Lodewijk, Mattijs, Maaïke, Marc, Robin, Lisa, Sam, Amanda, Remco, Christiaan, Patrick, Ludo, Cor, en iedereen die ik nog vergeet, bedankt voor jullie gezelligheid tijdens borrels, uitjes en MGC PhD workshops. Ook wil ik Maarten, Angela, Annelieke, Dave, Loes, Ivo, Joost, Zhe, Mohsin en Madeleine bedanken voor de mooie momenten die we mee hebben gemaakt tijdens de organisatie van de MGC PhD workshop naar Düsseldorf in 2012.

Mijn proefschrift was er niet gekomen als ik niet de mogelijkheid had gekregen om een deel van mijn onderzoek te doen bij het Academisch Centrum voor Tandheelkunde Amsterdam (ACTA). Ten eerste ben ik Willem dankbaar voor het leggen van de initiële contacten met de afdeling Orale Celbiologie. Daar werd ik welkom ontvangen om shear stress proeven te doen na overleg met Astrid en Jenneke. Tenslotte ben ik iedereen van de afdeling dankbaar voor hoe ze me hebben opgevangen en met name Cor en Jolanda, die me altijd wilden helpen met problemen. Mede dankzij jullie zijn meerdere papers tot stand gekomen door deze samenwerking.

Lieve vrienden, Patrick, Edwin, Elena, Angélique, Wouter, Merel, Stefan, Dorien, Mariska, Davey, Erik, Leonore, Johan, Wilbert, Ben en Lydi-Anne, bedankt voor al jullie hulp en vriendschap. Ik kon bij jullie altijd terecht met mijn zorgen, problemen en zeker voor de gezelligheid en een BBQ. Beste "DOT" studievrienden, Steven, Joost, Oscar, Chantal, Ingeborg en Marscha, ook jullie wil ik heel erg bedanken voor de gezellige tijd tijdens de studie en zeker ook daarna. Jullie begrepen de inhoud van mijn promotieonderzoek het beste en dank voor jullie adviezen en steun. Ook wil ik mijn voetbalvrienden en andere

vrienden bedanken voor de gezelligheid en de afleiding die ik kon vinden in het voetbal en de gezellige borrels en feesten.

Uiteraard ben ik mijn broers en Amber, Shuo en Eloi erg dankbaar voor hun steun. Lennart, jij bent er al mijn hele leven en dat we samen zijn opgegroeid heeft ons mede gemaakt tot wie we nu zijn. Dank je voor alle hulp en de mooie momenten, vakanties en hobby's die we samen deelden. Brent, je bent dan wel mijn 'kleine' broertje, maar in geen enkel opzicht lijkt dat nog zo, want je hebt altijd je mening klaar en bent altijd bereid om me te helpen. Mijn ouders kunnen zeker niet in dit dankwoord ontbreken, omdat ze altijd voor me klaar stonden als ik ze nodig had. Bedankt voor jullie opvoeding, steun, vertrouwen, bemoedigende woorden en geduld. Verder wil ik zeker mijn overige familie en schoonfamilie niet vergeten. Opa Jan en oma Nel, opa Jo (en oma Betty), bedankt voor het oppassen, jullie hulp bij de opvoeding en voor alle mooie en leuke momenten samen. Jullie maken onze familie altijd tot een gezellige en vertrouwde eenheid. Herman, Nannie, Ivette, Christiaan, Eline, Iris, Stieneke en Wim, ik ben jullie dankbaar hoe jullie me hebben opgenomen in jullie familie. Het voelde al meteen vertrouwd en ik ben erg blij met jullie gezelligheid en steun.

En tot slot, lieve Gerrien, ik ben zeer blij en dankbaar dat jij mijn partner bent. We hebben al zoveel leuke en mooie momenten samen meegemaakt en ik hoop graag in de toekomst nog veel meer moois mee te maken. Ondanks dat je mij met de inhoud van mijn onderzoek en proefschrift niet zoveel kon helpen, was je in alle andere opzichten een geweldige steun voor me. Zonder jou had ik mijn promotieonderzoek niet volgehouden. Zeer veel dank daarvoor en op naar een geweldige toekomst samen!

